ЖУРНАЛ
ЭКСПЕРИМЕНТАЛЬНОЙ И ТЕОРЕТИЧЕСКОЙ
ФИЗИКИ
АКАДЕМИЯ НАУК СССР

SOVIET PHYSICS

JETP

VOLUME 5 **NUMBER 3**

A Translation

of the

Journal of Experimental and Theoretical Physics

of the

Academy of Sciences of the USSR

Volume 32

OCTOBER, 1957

Published by the

AMERICAN INSTITUTE OF PHYSICS
INCORPORATED

SOVIET PHYSICS
JETP

A translation of the Journal of Experimental and Theoretical Physics of the USSR.

A publication of the

AMERICAN INSTITUTE OF PHYSICS

Governing Board

Frederick Seitz, *Chairman*
Allen V. Astin
Walter S. Baird
Jesse W. Beams
Hans A. Bethe
Raymond T. Birge
Richard H. Bolt
Franklin D. Dexter
Irvine C. Gardner
Samuel A. Goudsmit
Charles Kittel
Hugh S. Knowles
Winston E. Kock
R. Bruce Lindsay
William F. Meggers
Walter C. Michels
R. Ronald Palmer
Robert F. Paton
Joseph B. Platt
Ralph A. Sawyer
Henry D. Smyth
Mark W. Zemansky

Administrative Staff

Elmer Hutchisson
Director
Henry A. Barton
Associate Director
Mark W. Zemansky
Treasurer
Wallace Waterfall
Executive Secretary
Theodore Vorburger
Advertising Manager
Ruth F. Bryans
Publication Manager
Alice Mastro
Circulation Manager
Kathryn Setze
Assistant Treasurer
Eugene H. Kone
Director of Public Relations

American Institute of Physics Advisory Board on Russian Translations

Robert T. Beyer, *Chairman*
Dwight Gray, Morton Hamermesh, Vladimir Rojansky,
Freeman Dyson

Editor of Soviet Physics—JETP

J. George Adashko, Department of Electrical Engineering,
The City College of New York, Convent Avenue and
139th Street, New York, New York.

Soviet Physics is a monthly journal published by the American Institute of Physics for the purpose of making available in English reports of current Soviet research in physics as contained in the Journal of Experimental and Theoretical Physics of the Academy of Sciences of the USSR. The page size of Soviet Physics will be 7⅛" x 10½", the same as other Institute journals.

Transliteration of the names of Russian authors follows the system employed by the Library of Congress.

This translating and publishing project was undertaken by the Institute in the conviction that dissemination of the results of researches everywhere in the world is invaluable to the advancement of science. The National Science Foundation of the United States encouraged the project initially and is supporting it in large part by a grant.

The American Institute of Physics and its translators propose to translate faithfully all the material in the Journal of EXPERIMENTAL AND THEORETICAL PHYSICS OF THE USSR appearing after January 1, 1955. The views expressed in the translated material, therefore, are intended to be those expressed by the original authors, and not those of the translators nor of the American Institute of Physics.

Two volumes are published annually, each of six issues. Each volume contains the translation of one volume of the Journal of EXPERIMENTAL AND THEORETICAL PHYSICS OF THE USSR. New volumes begin in February and August.

Subscription Prices:

Per year (12 issues)	
United States and Canada	$60.00
Elsewhere	64.00
Back Numbers	
Single copies	$ 6.00

Subscriptions should be addressed to the American Institute of Physics, 335 East 45th Street, New York 17, New York.

Copyright by American Institute of Physics 1957

SOVIET PHYSICS

JETP

A translation of the Journal of Experimental and Theoretical Physics of the USSR.

SOVIET PHYSICS—JETP VOL. 5, NO. 3, PP 345-525 OCTOBER, 1957

ANNOUNCEMENT

ABOUT two and one half years ago, the American Institute of Physics began the translation of the *Journal of Experimental and Theoretical Physics* under a grant from the National Science Foundation. At the time, this was a pioneering effort, as far as scientific societies in the United States were concerned. It was then estimated that the number of Russian pages would run to approximately 1600 per year.

Since that time, the Russian journal has twice expanded, and is now publishing at a rate of 4000 pages per year. At the same time, The American Institute of Physics has undertaken the translation of three other journals *(Journal of Technical Physics, Acoustics Journal* and the physics portion of the *Proceedings of the Academy of Sciences),* so that approximately 8000 pages are being translated annually. All of these journals are finding steadily increased support from subscribers.

Beginning with the next issue, *Soviet Physics JETP* will have a new editor, Prof. J. George Adashko of the City College of New York. It is my hope that the new editor will have the same generous support from translators and subscribers that was the good fortune of the retiring editor.

Robert T. Beyer

Grigorii Samuilovich Landsberg

J. Exptl. Theoret. Phys. (U.S.S.R.) 32, 409-412 (March 1957)

THE outstanding Soviet physicist Grigorii Samuilovich Landsberg died in his 68th year on February 2, 1957 after a painful illness.

Physical science suffered an irreparable loss. G. S. Landsberg's great physical discoveries and his fruitful pedagogical and scientific activities, spanning more than 40 years, made him widely known in our country and abroad. A highly educated person, a scientist with most varied interests, Grigorii Samuilovich contributed much to the theory and practical application of physical optics, molecular physics, and atomic and molecular spectroscopy.

G. S. Landsberg was born on January 22 (new calendar), 1890 in the city of Vologda. He was graduated from the Moscow University in 1913, where he remained to prepare for a teaching career. This marked the beginning of his scientific and pedagogical activity.

In 1915 Grigorii Samuilovich was drafted into the army, and in 1917 he was assigned to the Laboratory of the Agricultural Union, where he first worked as a scientist, and then as deputy chief of this laboratory.

After teaching two years in the Omsk Agricultural

Institute (1918-1920) and after three years' work at the Institute of Physics and Biophysics in Moscow, Grigorii Samuilovich started his long scientific and pedagogical association with the Moscow State University. At the same time, during 1923-1931, he also lectured in general physics also at the Second Moscow University (now V. I. Lenin Pedagogical Institute). Grigorii Samuilovich worked more than 25 years at the Moscow State University. There he founded the optical laboratory and made many of his remarkable investigations.

When the Academy of Sciences moved to Moscow, Grigorii Samuilovich organized the Optical Laboratory of the P. N. Lebedev Physic Institute, to which most of his scientific activity shifted gradually. He headed this laboratory until his death. In recent years Grigorii Samuilovich taught at the Moscow Mechanical Institute, and then in the Moscow Physico-Technical Institute, where he established and headed the optics division.

Grigorii Samuilovich published his first scientific work in 1915. When L. I. Mandel'shtam, who influenced G. S. Landsberg greatly, moved to Moscow in 1925 the two started their joint prolonged work on molecular optics. This work led to fundamental discoveries.

The first great series of investigations was devoted to the study of molecular scattering of light in solids (quartz). This was before even the existence of such scattering in crystals was established. The experimental difficulties involved seemed insurmountable because the stray light was hundreds of times stronger than the molecularly-scattered light. Grigorii Samuilovich first succeeded in observing and measuring molecular scattering of light in solids because of his outstanding experimental skill in devising clever and elegant techniques that lead to success. This phenomenon was exhaustively studied quantitatively in subsequent works by G. S. Landsberg and his students. G. S. Landsberg, L. I. Mandel'shtam and their students created the theory of molecular scattering of light in solids. They observed and studied the anisotropy of the scattered light in crystals. All their experimental results were in full agreement with theory. Thanks to these investigations, scattering of light in crystals can now be considered a closed discipline, *i.e.*, one fairly well developed from both the experimental and theoretical aspects.

Immediately after the first reliable observations of molecular scattering of light in crystals, G. S. Landsberg and L. I. Mandel'shtam started a search for the fine line structure of the classical (Rayleigh) scattering, predicted by L. I. Mandel'shtam as early as 1918. This fine structure (splitting) is due to modulation of the scattered light by elastic thermal waves (hypersound). This line splitting was too fine to be observable with the apparatus available to Grigorii Samuilovich at that time. The experiments were therefore performed with extreme precision. The systematic investigation of the spectral composition of scattered light in crystals has led G. S. Landsberg and L. I. Mandel'shtam to the discovery in 1928 of an entirely new phenomenon of tremendous scientific and practical significance—the combination scattering of light (Raman effect). This discovery was destined to play an outstanding role in the history of science. The investigation of the new phenomenon distracted G. S. Landsberg somewhat from the initial problem, to which he returned only in 1930, when the modulation of scattered light by hypersound was indeed observed. This effect was studied subsequently in many laboratories in the world. It became evident in the course of this investigation in G. S. Landsberg's laboratory that precise measurements of the speed and absorption of ultrasound in liquids were necessary. Although such measurements were new and unusual for an optical laboratory, Grigorii Samuilovich included them in his laboratory's program without hesitation.

It was generally typical of Grigorii Samuilovich to have a broad and versatile approach to a solution of a problem. His study of all the problems connected with classical scattering of light led to results of great scientific significance. Grigorii Samuilovich retained interest in this topic, and continued to develop these investigations to his last days.

An investigation of certain aspects of resonant fluorescence led G. S. Landsberg and L. I. Mandel'shtam to the discovery of an entirely new phenomenon — selective scattering in mercury vapor. Grigorii Samuilovich displayed here a particular experimental virtuosity, leading to an unmistakable observation and to a thorough study of the effect not only qualitatively but also quantitatively.

The second great subject in which Grigorii Samuilovich engaged was the study and practical application of combination scattering of light. Combination scattering of light (Raman scattering) discovered by him jointly with L. I. Mandel'shtam in quartz crystals and discovered independently by Raman in liquids, is one of the greatest physical discoveries. G. S. Landsberg and L. I. Mandel'shtam grasped immediately the true nature of this phenomenon. Many of their investigations and those of their associates were devoted to exhaustive experimental and theoretical studies of this scattering. They developed the classical and quantum theories of the phenomenon and studied the temperature behavior of the long-wave and short-wave satellites. The great significance of this phenomenon to physical and chemical problems was immediately appreciated. A new path was blazed in scientific research and many practical applications were found. Thus, G. S. Landsberg and his school used combination scattering to study exhaustively the so-called "hydrogen bond," which plays a particularly important role in many problems of molecular physics and chemistry. They performed the difficult investigation of second-order combination-scattering lines that characterize the nonlinearities of the intramolecular forces, and were the first to measure by interference the widths and the contours of the combination-scattering lines. The work by Grigorii Samuilovich and his students on the analytic application of conbination scattering of light has made this method a powerful precision tool for quantitative and qualitative analysis of complex organic mixtures. Shortly before his death, Grigorii Samuilovich and his students summarized the results of their research in this field in a special monograph.

G. S. Landsberg's all-around scientific activity was by no means limited to a study of the above scientific problems. His outstanding accomplishment is the development of the scientific foundations and methods for the application of emission analysis to metallurgy and to other branches of industry. Grigorii Samuilovich proceeded to develop and introduce spectral analysis at the very same time when some of the greatest spectroscopists in the world thought it impossible to apply spectral analysis to production. The persistent work by Grigorii Samuilovich and his school led to a solution of this problem, which he clearly understood to be important to the government, and now spectral analysis is widely used in many plants and enterprises of the country to the great benefit of the national economy.

Grigorii Samuilovich was also most influential in training of an entire army of spectroscopists and in launching a domestic industry of spectral instruments. He was the permanent head of the Commission on Spectroscopy, Academy of Sciences, USSR, and guided the policies of its important work.

As already mentioned, Grigorii Samuilovich's pedagogical activity began in 1918. He taught courses in general physics, in "Experimental Foundations of Atomic Theory," in "Scattering of Light," *etc.* His masterful lectures inspired in the listeners great interest in physics and love for science. His lectures were a creative process. Grigorii Samuilovich believed teaching to be his unswerving duty. He has trained many generations of Soviet physicists, who remember their teacher with respect and gratitude.

Grigorii Samuilovich's qualities as scientist and teacher are shown in his excellent *Optics*, which went through four editions, and in the three-volume *Elementary Textbook of Physics*, produced under his leadership, to which he devoted much of his labor. These books occupy an outstanding place in our physics literature.

Grigorii Samuilovich's tremendous scientific accomplishments, his scientific-organizational merits, and his activity as a Soviet patriot were highly esteemed. On November 30, 1946, G. S. Landsberg was elected an active member of the Academy of Sciences, USSR. He was awarded the Stalin prize for outstanding services in the development of spectral analysis. He was awarded two orders of Lenin and medals.

Grigorii Samuilovich was a man with a sense of duty, both as a scientist and a citizen. He never compromised with his conscience. His high principles, consistency, and courage in defending his point of view gained him universal respect. He was generous and responsive, but was feared by climbers and grabbers. Everyone who was genuinely devoted to science gained his support and unselfish aid.

The glowing memory of Grigorii Samuilovich will long be indentified with the idea of what a scientist's basic human qualities should be.

G. S. LANDSBERG'S PRINCIPAL WORKS

Molecular Scattering of Light in Solids: 1. Scattering of Light in Crystalline Quartz and its Temperature Dependence, Z. Physik 43, 773 (1927). – II. Temperature Dependence of Intensity of Scattered Light, Z. Physik 45, 442 (1927). – III. Intensity of Light Scattered by Crystalline Quartz (with K. S. Vul'fson), Z. Physik 58, 95 (1929). – IV. Intensity of Light Scattered by Rock Salt (with L. I. Mandel'shtam) Z. Physik 73, 502 (1931).

Discovery and Investigation of Combination Scattering of Light (with L. I. Mandel'shtam): Sixth Congress of Russian Physicists, Moscow, Gosizdat (1928); Journal of Russian Physical and Chemical Society, Physics Part 60, 335 (1928); Compt. rend. 187, 109 (1928); Z. Physik 50, 769 (1928); Naturwiss 16, 57 (1928); Uspekhi Fiz. Nauk 9 (1931).

Contributions to the Theory of Molecular Scattering of Light (with L. I. Mandel'shtam). Zh. prikl. fiz. 6, 155 (1929).

Concerning the Intensity and Temperature Dependence of Combined Scattering (with M. A. Leontovich), Z. Physik 53, 439 (1929).

Scattering of Light in Crystals at High Temperature (with L. I. Mandel'shtam), Z. Physik 58, 250 (1929); Z. Physik 60, 364 (1930).

On the Theory of Molecular Scattering of Light in Crystals (with L. I. Mandel'shtam and M. A. Leontovich), Z. Physik 60, 334 (1930).

Combination Scattering in Absorption and Fraunhoffer Lines (with F. S. Baryshanskaia), Naturwiss 18, 183 (1930).

Combination Scattering of Light and its Significance to Chemical Problems, Uspekhi Khimii 1, 464 (1932).

Absorption of Light by Ammonia (with A. S. Predvoditelev), Z. Physik 31, 594 (1925).

Fundamental Works on Spectral Analysis of Metals: J. Tech. Phys. (U.S.S.R.) 3, 771 (1933) (with S. L. Mandel'shtam and S. M. Raiskii); Uch. zap. Moscow State Univ. 1, 26 (1933) (with S. L. Mandel'shtam and S. M. Raiskii); Liteinoe delo 5, 9 (1933); J. Techn. Phys. U.S.S.R. 2, 574 (1935); Zavodskaia laboratoriia 4, 1220 (1935) (with L. I. Mandel'shtam, S. V. Tuliankin, and V. V. Tseiden).

Selective Scattering of Light in Mercury Vapor (with L. I. Mandel'shtam) Phys. Z. Sowjetun. 8, 378 (1935).

Second-Order Lines in Combined Scattering (with V. L. Malyshev). Dokl. Adad. Nauk SSSR 3, 365 (1936).

Frequency of Hydroxyl Group of Methyl Alcohol and its Dependence on Density (with S. A. Ukholin), Dokl. Akad. Nauk SSSR 16, 399 (1937).

Intermolecular Forces in Combination Scattering of Light. Izv. Akad. Nauk SSSR, Ser. Fiz 3, 373 (1938).

Combination Scattering of Heavy-Water Solutions (with V. I. Malyshev and V. E. Solov'ev), Dokl. Akad. Nauk SSSR 24, 873 (1939).

Scattering of Light in Unevenly Heated Crystal (with A. A. Shubin), J. Exptl. Theoret. Phys. (U.S.S.R.) 9, 1309 (1939).

Concerning the Heat Conduction of Crystals (with A. A. Shubin), J. Exptl. Theoret. Phys. (U.S.S.R.) 10, 247 (1940).

Combination Scattering of Light in Crystalline Hydroxides and the Hydrogen Bond (with F. S. Baryshanskaia), Izv. Akad. Nauk SSSR, Ser. Fiz. 10, 509 (1946). J. Phys. 11, 101 (1947).

Scattering of Light in KH_2PO_4 and $(NH_4)H_2PO_4$ and its Use in the Theory of Ferroelectrics (with F. S. Baryshanskaia), Dokl. Akad. Nauk SSSR 61, 1027 (1948).

The Doppler-Fizeau Phenomenon and Molecular Motion, Uspekhi Fiz. Nauk 36, 284 (1948).

Effect of Temperature on the Scattering Spectrum of Crystals Containing OH-Groups (with F. S. Baryshanskaia), Memorial Collection to S. I. Vavilov, Moscow, Academy of Sciences, USSR 1952, Page 147.

Basic Work on Molecular Spectral Analysis of Organic Mixtures: Transactions of All-Union Conference on Chemistry and Processing of Petroleum, Baku, Azerbaydzhan SSR Academy of Sciences, 7 (1953); Transactions of Committee on Hydrocarbons, Moscow (1944); Izv. Adad Nauk SSSR, OKhN 1, 9 (1941) (with N. D. Zelinskii); Izv. Akad Nauk SSSR, Ser. Fiz 4, 158 (1940) (with P. A. Bazhulin, U. V. Rozenberg, and A. S. Eliner).

Fluctuating Spectra of Diphenyl and Deka-Deutorodiphenyl (with A. I. Shatenshtein, G. V. Perogudov, E. E. Izrailevich, and L. A. Novikova), Optika i spektroscopiia 1, 34 (1956).

Basic Parameters of Spectra of Combination Scattering of Hydrocarbons (with P. A. Bazhulin and and M. M. Sushchinskii), Moscow, Academy of Sciences, USSR (1956).

Translated By J. G. Adashko
105

SOVIET PHYSICS JETP VOLUME 5, NUMBER 3 OCTOBER, 1957

Spectrum and Positive Excess of the Hard Component in the (9.3 – 17) x 10^9 ev/c Momentum Range at an Altitude of 3250 Meters

A. I. ALIKHANIAN AND A. O. VAISENBERG
Physical Institute, Academy of Sciences, Armenian SSR

(Submitted to JETP editor, October 6, 1956)
J. Exptl. Theoret. Phys. (U.S.S.R.) 32, 413–416 (March, 1957)

The spectral distribution of the positive excess in the hard component was measured in the (0.3 – 17) × 10^9 ev/c momentum range. The measurements were performed on the large spectrograph of the Alagez Laboratory at an altitude of 3.25 km.

THE purpose of the present work is to continue into a region of significantly greater momenta, up to 1.7 × 10^{10} ev/c, the measurements of the momentum spectrum and positive component which were carried out in Ref. 1 in the region (0.1 – 2.5) × 10^9 ev/c. At the present time interest in this problem has increased in connection with the fact that the study of the production of K-mesons in cosmic rays and especially in accelerators has disclosed a sharp asymmetry in the number of positively and negatively charged mesons produced. By this same fact, the proton character of the primary cosmic rays has ceased to be the only possible explanation of the positive component. Measurements were carried out in 1952 in the large magnetic spectrometer of the Alagez Laboratory at a magnetic field of magnitude 13,700 oe. At such a field the probable error in the measurement of a momentum of 1.7 × 10^{10} ev/c is close to 50%. The construction of the magnetic spectrometer and the methods of treating the data have been described briefly[2,3], and we will limit ourselves here to introducing only a sectional drawing of the distribution of the counters in the telescope and of the absorbers (Fig. 1).

A layer of lead of 7 cm thickness was placed over the entire apparatus. The total thickness of all the lead absorbers over the rows of counters $VI - X$ was equal to 5.8 cm. Under the row of counters X

TABLE Distribution of the particles of the hard component by momentum intervals.

Momentum interval in units of 10^8 ev/c		3–5	5–6	6–8	8–10	10–15
$R>5,8$ см	n_+	83	140	382	436	898
	n_-	88	114	261	318	667
	$k=n_+/n_-$	0,94±0,14	1,23±0,14	1,46±0,09	1,37±0,08	1,35±0,07
$R>19,8$ см	n_+	32		99	152	490
	n_-	30		101	123	395
	$k=n_+/n_-$	1,07±0,25		1,12±0,10		1,24±0,08

(continuation of the table)

		15–20	20–30	30–50	50–90	90–170	>170	3–170
$R>5,8$ см	n_+	611	880	765	582	309	211	5082
	n_-	431	616	546	418	220		3669
	$k=n_+/n_-$	1,42±0,08	1,43±0,07	1,40±0,07	1,39±0,08	1,47±0,09		1,39±0,02
$R>19,8$ см	n_+	371	588	551	422	224	141	2929
	n_-	288	424	405	329	176		2271
	$k=n_+/n_-$	1,29±0,09	1,39±0,08	1,36±0,08	1,28±0,08	1,27±0,12		1,29±0,03

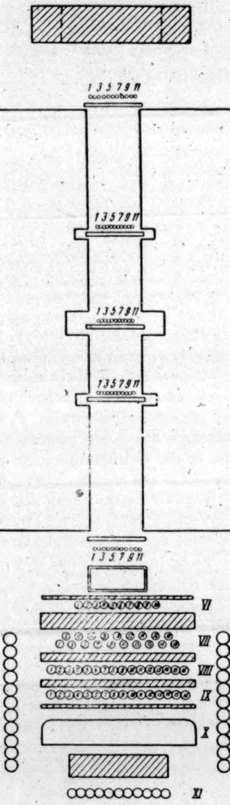

FIG. 1. Distribution of the counters in the telescope and of the absorbers.

was located a layer of lead of 14 cm thickness, under which was placed the row of counters *XI*. Particles which passed through all the rows of counters up to the tenth inclusively, and did not undergo multiplication, as determined by coordinated counters, were considered to belong to the hard component. The path of these particles was greater than 5.8 cm of lead. The path of those particles of the hard component which also passed through the row of counters *XI* was greater than 19.8 cm of lead.

The Table gives the experimental results — the number of positively and negatively charged particles (n_+ and n_-) the momenta of which lie within the indicated intervals (the tabulated numbers being given without correction for the magnetic aperture ratio of the apparatus). These data were obtained as a result of measurements of the momenta of 8966 particles. They give the momentum spectrum and the distribution of the positive component in this spectrum. The last column of the table gives the values of the positive excess for the entire momentum interval investigated, this excess is $k = 5082/3666 = 1.39 \pm 0.08$ for the particles with path length $R > 5.8$ cm of lead. In order to explain how an excess of this magnitude is concerned with mesons, let us consider the average value of the excess for particles with a path greater than 19.8 cm of lead. Because of ionization braking, protons of momentum less than 1.05×10^9 ev/c do not occur among these particles. Protons of greater momenta must be strongly absorbed in the supplementary 14 cm block of lead, the thickness of which is equivalent to a single "geometrical" nuclear absorption path. The positive excess for particles with a path greater than 19.8 cm of lead is given by $k = 2929/2271 = 1.29 \pm 0.03$.

The spectrum of the positive excess was measured in Ref. 1 up to 2.5×10^9 ev/c. It is of interest to obtain the value of the positive excess for larger momenta. From the data of the table it follows that for momenta greater than 3×10^9 ev/c the positive component is equal to:
$k = 1656/1174 = 1.41 \pm 0.05$ for particles with path $R > 5.8$ cm; $k = 1197/910 = 1.31 \pm 0.5$ for particles with path $R > 19.8$ cm.

These results, in agreement with Ref. 1, indicate that in each measured spectrum as well as in the region of larger momenta a significant part of the positive excess is produced by μ mesons. Since a part of the protons of high energy produces penetrating particles in the lead and thus "passes" into the hard component, it follows from the results introduced that the positive excess arising from the meson component itself is, in any event, less than 1.30.

The spectral distribution of the positive excess is shown in the table and in Fig. 2. In these results it is to be noted that the positive excess in the region of small momenta, where protons are known to be absent (momenta less than 0.6×10^9 and 1.0×10^9 ev/c for mesons with paths greater than 5.8

and 19.8 cm of lead, respectively), is near unity. This fact, which appears as a consequence of the local generation of slow mesons by the neutron component, is well known at the present time[4,5].

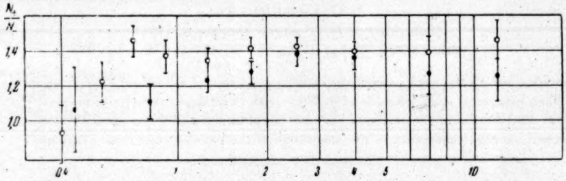

FIG. 2. o— positive excess for particles with $R > 5.8$ cm Pb; o—the same with $R > 19.8$ cm Pb. Momenta in units Bev/c are plotted as abscissa.

The separation of the positive excess into a proton part and a meson part which has been carried out in this and the preceding work[1] allows the possibility of determining the vertical intensity of the proton component under the conditions of our experiment, that is, under a layer of lead of 7 cm thickness. Subtracting the spectrum of the negative particles, increased by the magnitude of the mesonic positive excess, from that of the positive particles, and carrying out a summation over the momentum intervals, we obtain the number of protons with momenta of interest to us. The results obtained above show that the upper limit of the positive excess for mesons is near 1.30. On the other hand, measurements at sea level, where the intensity of the proton component is of a smaller order than at a height of 3250 m, show that the positive excess of the mesonic part of the spectrum, k_μ, in our momentum interval, measured with high statistical accuracy[6], is near 1.25. Just such a value of k_μ was obtained in Ref. 1 for the mesonic part of the spectrum in the momentum region $(2.4 - 7.7) \times 10^8$ ev/c at a height of 3250 m. Taking $k_\mu = 1.25$, therefore, we find the intensity of the proton share of the hard component by the formula

$$N_p = \sum_i (n^i_+ - 1{,}25\, n^i_-) \Big/ \sum_j \left(n^j_+ + n^j_-\right).$$

The summation in the numerator is carried out beginning with the fifth momentum interval ($p > 10^9$ ev/c), while that in the denominator is carried out over all the tabulated momentum intervals. Thus, from the intensity of the total hard component registered by the apparatus, we obtain $N_p = 4.8 \pm 0.05\%$.

In conclusion we note that in the region of momenta greater than 5×10^9 ev/c the integral μ meson spectrum, constructed according to the table for paths greater than 19.8 cm of lead, is satisfactorily described by a power function $\sim p^{-\gamma}$ with exponent $\gamma = 2.45 \pm 0.05$.

LITERATURE

[1] A. O. Vaisenberg, J. Exptl. Theoret. Phys. (U.S.S.R.) **32**, 417 (1957).

[2] Alikhanian, Dadaian and Shostakovich, Dokl. Akad. Nauk SSSR **82**, 693 (1952).

[3] V. M. Kharitonov, Dissertation, Moscow, 1955.

[4] G. Poiani and G. Salvatori, Nuovo cimento **4**, 503 (1956).

[5] H. A. Morewitz and M. H. Shamos, Phys. Rev. **92**, 134 (1953).

[6] Beretta, Filosofo and Sommacal, Nuovo cimento **10**, 1354 (1953).

Translated by M. G. Gibbons
106

Momentum Spectrum of the Cosmic Radiation and the Positive Excess in the (0.1–2.5) x 10^9 ev/c Range at an Altitude of 3250 m

A. O. VAISENBERG

(Submitted to JETP editor October 6, 1956)
J. Exptl. Theoret. Phys. (U.S.S.R.) 32, 417-422 (March, 1957)

The spectrum of the hard component and the spectrum of unfiltered cosmic radiation have been measured at an altitude of 3.25 km with the aid of magnetic analysis. The spectral distribution of the positive excess was obtained and the contributions of the proton and meson components to the magnitude of the excess have been evaluated.

IN recent years the spectrum of the charged part of the cosmic radiation at mountain altitudes has been studied in a number of works[1-4]. In the present article, momentum spectra of the cosmic radiation which were measured during 1949-52 in the small magnetic spectrograph of the Alagez Cosmic Ray Laboratory are considered. A detailed description of the apparatus and of other similar spectrographs has already been given briefly elsewhere[5,6], so that we can limit ourselves to a schematic diagram showing the arrangement of the counters in the telescope and of the absorbers (Fig. 1).

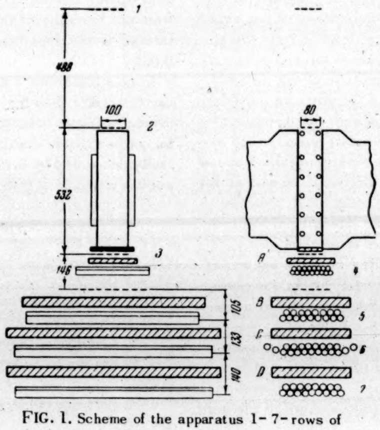

FIG. 1. Scheme of the apparatus 1- 7- rows of counters: A, B, C, D- absorbers, measured in millimeters.

In our apparatus the total error in a momentum measurement due to the geometrical dimensions of the counters of groups 1, 2 and 3 (indicated by dashed lines in Fig. 1) and scattering in their walls is such that momenta in the range (0.1–0.2) x 10^9 ev/c is measured with a relative error of about 25%.

In what follows we shall consider spectra of the unfiltered rays, consisting of electrons, mesons and protons, and spectra of the hard component, from which electrons are excluded.

1. SPECTRA OF THE UNFILTERED RAYS

The spectra of the unfiltered rays were obtained in experiments where no special absorbers were used over the magnetic spectrograph or between the counter trays of its telescope.

Let us consider the spectra of the unfiltered rays (Table 1 gives the distribution of particles according to intervals of deviation in the magnetic field. The deviation distance δ (cm) for a momentum pc (ev) is obtained from the formula $\delta = 1.7 \times 10^9/pc$, where 1.7×10^9 ev-cm is a constant of the apparatus.

TABLE I

Deviation interval δ in cm	Average momentum in 10^8 ev/c	Correction for the "aperture ratio"	Spectrum of the infiltered rays		Spectrum of the hard component	
			N_+	N_-	N_+	N_-
$\delta < 0{,}5$			949		2273	
0,5— 1,0	22,7	1,00	669	409	1569	999
1,0— 1,5	13,6	1,02	500	301	188	747
1,5— 2,0	9,7	1,03	367	207	785	508
2,0— 2,5	7,6	1,05	303	152	538	313
2,5— 3,0	6,2	1,06	218	121	321	246
3,0— 3,5	5,2	1,09	163	89	256	197
3,5— 4,0	4,5	1,11	133	58	140	134
4,0— 5,0	3,8	1,17	165	101	216	166
5,0— 6,0	3,1	1,25	120	69	94	82
6,0— 8,0	2,4	1,46	121	99	89	64
8,0—10,0	1,9	1,85	70	77	14	7
10,0—12,0	1,5	2,44	52	49	4	4
12,0—14,0	1,3	3,40	30	31	5	2
14,0—15,0	1,2	4,60	7	9	2	0
$\delta > 15{,}0$			12	16	0	2

The third column of the table gives the correction for the "aperture ratio" of the apparatus. The momentum spectrum obtained after the momentum interval is shown in Fig. 2.

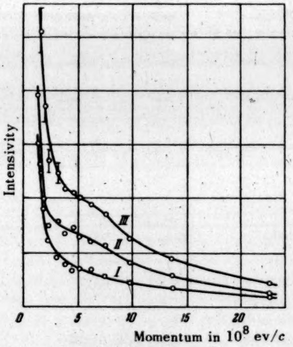

FIG. 2. Momentum spectra:
I—negatively charged
II—positively charged,
III—sum of both spectra.

From the spectra shown it is clearly evident that the spectrum of the negatively charged particles has two components, an electron component, which decreases rapidly with increasing momentum, and a meson component extending to the end of the spectrum, while the spectrum of the positively charged particles differs sharply from it by the presence of a bulge in the momentum region $(3\text{–}10) \times 10^8$ ev/c which occurs because of the presence of a third component. It is natural to suppose that this component consists of protons. The difference just described in the spectra of the positively and negatively charged particles was noted also in Ref. 2, where the work was carried out at an altitude of 3.4 km.

The difference between the two spectra can be described in terms of the magnitude of the positive excess $k = N_{\pm}/N_-$ in the various regions of the spectrum. In order to obtain the magnitude of k with sufficient statistical accuracy, it was determined for eight rather large intervals of momentum. The distribution of the positive excess through the spectrum is shown in Fig. 3 (curve A). From a consideration of this curve we may make the following conclusions:

1. For momenta of less than 2×10^8 ev/c the positive excess, to with the limits of the statistical accuracy of the observations, does not occur. That is, $k \approx 1$. Just such a value of k

would, in fact, be expected for the electron-positron part of the spectrum.

2. The positive excess arises in the neighborhood of a momentum of 2×10^8 ev/c and increases rapidly, reaching a maximum value, approximately $k = 2$, near a momentum value of 5×10^8 ev/c. An approximate result was obtained in Ref. 1, where the positive excess in the momentum region $(0.3–0.7) \times 10^9$ ev/c was found to be equal to 2.50 ± 0.14 at an altitude of 3.4 km. We note that the emergence and rapid growth of the positive excess begins in the neighborhood of the minimum momentum of the protons stopped by the apparatus (the total thickness of the walls of the counters, equal to 0.2 mm of Cu, corresponds to a proton momentum of 2.4 × 2.4×10^8 ev/c). This indicates that in the region of small momenta the positive excess arises as soon as protons begin to appear among the particles counted.

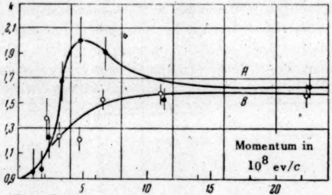

FIG. 3. Distribution of the positive component
A–unfiltered radiation
B–hard component.

3. With a further increase in momentum ($p > 5 \times 10^8$ ev/c) the positive excess decreases slowly, approaching a constant value of about 1.5–1.6. This is in agreement with the date of Ref. 1 and 2, where, under conditions analogous to ours, it is found that $k = 1.50 \pm 0.05$ and $k = 1.68 \pm 0.06$, respectively.

2. ABSORPTION OF THE POSITIVE EXCESS

A series of measurements was made in an attempt to determine whether all of the positive excess observed in the spectrum could be explained in terms of the presence of protons. The experiments carried out consisted of the measurement of the magnitude of the positive excess when lead and graphite absorbers which should have cut off a significant part of the proton component (experiments 3, 4 and 5, see Table 2) were placed over the entire apparatus. In experiment 3, a 10 cm layer of lead was placed over the apparatus, in experiment 4, a 20 cm layer of lead was used, and in experiment 5, a 40 cm layer

TABLE II. Absorption of the positive excess

1	Scheme of the experiment	**1** **2** **3** **4** **5**	**1** **2** 0,8 см Pb — **3** 1,1 см Pb — **4** — **5**	10 см Pb — **1** **2** 0,8 см Pb — **3** 1,1 см Pb — **4** — **5**	20 см Pb — **1** **2** 0,8 см Pb — **3** 1,1 см Pb — **4** — **5**	40 см C — **1** **2** 2,4 см Pb — **3** 3,0 см Pb — **4** — **5**
2	Number of the Experiment	1	2	3	4	5
3	$P_{\min}$ (10^8 eV/c)	—	—	8,3	10,8	8,5
4	N_+	1870	11914	3260	1295	1673
5	N_-	1288	8411	2350	948	1256
6	$k = N_+/N_-$	1,45±0,05	1,42±0,02	1,39±0,03	1,37±0,06	1,33±0,05

Note. The boldface numbers indicate the rows of counters in the apparatus. The horizontal bars signify absorbers placed over the counters. The first column gives the number of the line in the table.

or graphite was used. In order to pass through these absorbers, the protons must possess minimum momenta of 8.3, 10.8 and 8.5 × 10^8 ev/c, respectively. Hence the protons having smaller momenta before their entrance into the absorber must disappear from the spectrum. As for the protons with larger momenta, nuclear interactions in the upper filters must lead to a significant weakening in their intensity. Hence if the entire positive excess is composed of protons, then one would expect it to decrease strongly in experiments 3, 4 and 5.

For an inspection of the results of the experiments, let us turn to Table 2, which gives the scheme of the experiments and its number (lines 1 and 2), the minimum momentum of a proton passing through the upper filter (line 3), the number of positively and negatively charged particles in the complete spectrum which pass through the apparatus without multiplication (lines 4 and 5), and the magnitude of the positive excess (line 6).

Consideration of the data of Table 2 allows us to make the following conclusions:

1. The positive excess has much greater value in the spectrum of the filtered rays ($k = 1.45 \pm 0.05$).
2. As the layer of material above the apparatus is the magnitude of the absorption of the positive component decreases correspondingly from the value $k = 1.42 \pm 0.02$, when there is no material above the apparatus, to a minimum value 1.33 ± 0.05, when a 40 cm layer of graphite is placed over the apparatus.

The results obtained serve as an argument to show that the observed positive excess cannot be explained by protons alone, and that the positive excess occurs also in the meson part of the spectrum. The measurement of the spectrum of the hard component has allowed the separation of the mesonic and protonic parts of the positive excess.

3. SPECTRUM OF THE HARD COMPONENT

In the measurement of the spectrum of the hard component, measures were taken, as carefully as possible, to get rid of electrons. The arrangement of the absorbers in this experiment is shown in Fig. 4. The hard component consists of particles which have passed without multiplaction (recorded by rows of counters 3 and 4) through absorbers A, B, C, and D, the total thickness of which is equivalent to 8.6 cm of lead. The number of electrons among such particles must be very small: the probability of cascade multiplication is near unity, but the electrons which have not undergone multiplication will be absorbed in the layers A, B, C and D and will not enter into the hard component. The measured spectrum of the hard component is shown in Table 1 and Fig. 4. A comparison of this spectrum with the spectrum of the unfiltered radiation (Fig. 2) shows that the electron component, the principal part of which belongs to the momentum region below (3–4) (3–4) × 10^8 ev/c, is actually missing from it.

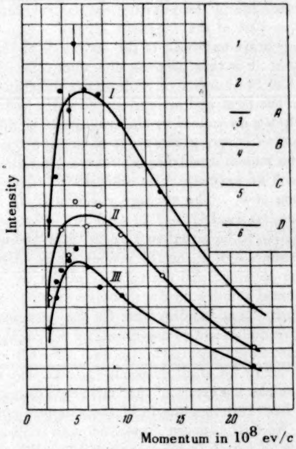

FIG. 4. Spectra of the hard component. I—total radiation, II—positively charged particles, III—negatively charged particles. A = 1.5 cm Pb, B = 5.1 cm Pb, C = 4 cm C, D = 4 cm C.

Considering the spectrum from the point of view of the presence of protons, it should be kept in mind that protons whose path lenghts are less than 8.6 cm of lead, (i.e., protons with momenta less than 7.7 × 10^8ev/c) are absent from it. In connection with this, it is of interest to consider the positive excess for this spectrum, and to compare it with the positive excess for the spectrum of the unfiltered radiation. The positive excess in the spectrum of the hard component is shown in Fig. 3 (curve B). A comparison of curves A and B shows clearly that a significant part of the positive excess in the spectrum of the unfiltered radiation in the momentum region (2.4–7.7) × 10^8 ev/c is connected with protons. Since protons in the momentum interval (2.4 × 10^8 ev/c are not present in the spectrum of the hard component ($R > 8.6$ cm Pb), then the positive excess in this momentum interval is composed only of mesons. The magnitude of the purely mesonic part of the positive excess can be determined. 1105 positively charged particles and 883 negatively charged particles were counted in the interval (2.4–7.7 × 10^8 ev/c. This corresponds to a positive excess $k_\mu = 1105/883 = 1.25 \pm 0.06$.

4. INTENSITY OF THE PROTON COMPONENT

A knowledge of the positive excess inherent in the meson part of the spectrum allows one to make a rather accurate estimate of the intensity of the proton component. For this purpose one must take as a measure of the number of protons the difference between the first and second spectra, the ordinates of which are increased by the magnitude of the positive excess at any given point of the spectrum where the meson spectrum is present. In order to make such an estimate it is necessary to know the magnitude of k_μ. The average value of k_μ in the momentum interval (2.4–7.7) × 10^8 ev/c was determined above to be equal to 1.25 ± 0.06. Although the dependence of k_μ on the momentum is unknown, the value obtained and the totality of the known experimental results on the positive excess in the meson component indicate that for the momentum interval in question the magnitude of k_μ changes very little, being within the limits 1.2 to 1.3 and close to 1.25. We shall determine the number of protons in the spectrum of the unfiltered radiation, starting from this magnitude of the mesonic positive excess. We will concern ourselves with protons the momentum of which is greater than 3.4 × 10^8 ev/c, that is, protons which are deviated less than 5 cm in the magnetic field. The number of such protons is given by the formula

$$N_p = \sum_i N_+^i - k_\mu N_-^i,$$

where the summation is taken over all deviations less than 5 cm (Table 1). Values of N_p calculated for k_μ assumed equal to 1.00, 1.25 and 1.30, respectively, are given below in percent of the total intensity registered by the apparatus.

k_μ	N_p
1,00	22 ± 1
1,25	14 ± 1
1,30	11 ± 1

We see that the intensity of the proton component lies within the limits of 11–14% of the total intensity. In order to obtain the intensity of the protons in the hard component it is necessary to increase these numbers by 18%. Thus the proton intensity lies within the limits of 13–17% of the intensity of the hard component. This result is very close to that obtained in Ref. 1–4.

CONCLUSIONS

1. From the form of the spectra of the unfiltered radiation, it follows that, besides the electron and meson components, a notable amount of proton component is also present at an altitude of 3250 m. The existence of an intense proton component manifests itself in the measured spectra first of all in the fact that the positive excess for the total radiation is equal to 1.50 ± 0.02, while at sea level, where the intensity of the proton component if less by an order of magnitude, the positive excess lies within the limits 1.2–1.3.

2. In the region of momenta greater than 8 × 10^8 ev/c, where the main portion of the particles counted by the apparatus are located, the positive excess changes very little with momentum, and its magnitude is close to 1.5. The positive excess is close to unity in the region of small momenta in the spectrum of the unfiltered rays. This is explained by the fact that the overwhelming majority of particles in this region of the spectrum are electrons and positrons.

3. In the intermediate region of momenta, from 2 to 8 × 10^8 ev/c, the positive excess increases rapidly, reaching a maximum of about 2 at $k \sim 5 \times 10^8$ ev/c, and then decreases to 1.5. The large value of the positive excess in this region is explained by the presence of a significant number of protons.

4. The influence of the protons on the magnitude of the positive excess is clearly manifested in the spectrum of the hard component from which all protons with momenta (2.4–7.7) × 10^8 ev/c have been removed. Thus it has been possible to determine the purely mesonic positive excess in this region of the spectrum. It turns out to be equal to 1.25 ± 0.06.

5. Knowing the positive excess of the meson component, we may estimate the number of protons in the momentum interval (3.4–25) × 10^8 ev/c, which we are investigating. It lies within the limits of 13–17% of the total intensity of the hard component.

The author wishes to convey his gratitude to M. I. Daion and V. M. Kharitonov for their assistance in a considerable part of the measurements and to A. I. Alikhanian for a discussion of the results.

---

[1] W. L. Whittemore and R. P. Shutt, Phys. Rev. **86**, 940 (1552).

[2] Miller, Henderson, Potter, Todd and Wotring, Phys. Rev. **19**, 459 (1950).

[3] N. M. Kocharian, Dissertation, Moscow, Physical Institute, Academy of Sciences, 1954.

[4] Becker, Chanson, Nageotte and Treille, J. Phys. radium **16**, 191 (1955).

[5] A. O. Vaisenberg, J. Exptl. Theoret. Phys. (U.S.S.R.) **19**, 727 (1949).

[6] Alikhanian, Dadaian and Shostakovich, Dokl. Akad. Nauk SSSR **82**, 693 (1952).

Translated by M. G. Gibbons
107

SOVIET PHYSICS JETP VOLUME 5, NUMBER 3 OCTOBER, 1957

Energy and Angular Distribution of Neutrons Emitted in the Be^9 (d, n) B^{10} Reaction

A. I. SHPETNYI
Physical-Technical Institute, Academy of Sciences, Ukrainian SSR

(Submitted to JETP editor July 9, 1956)
J. Exptl. Theoret. Phys. (U.S.S.R.) **32**, 423-431 (March, 1957)

The energy spectra and angular distributions of neutrons from the $Be^9\,(d,n)\,B^{10}$ reaction have been investigated at deuteron energies of 0.5, 0.8, 1.0, 1.2, 1.4 and 1.6 Mev. The excitation curve for this reaction indicates a resonance at 1 Mev in the compound nucleus, B^{11}. The angular distribution corresponding to an excited state in B^{10} with excitation energy $E_x = 3.62$ Mev points to the existence of a stripping mechanism. The angular distributions of reactions involving the formation of compound nuclei are appreciably distorted on passage through a resonance.

1. INTRODUCTION

THE experimental study of spectra and of angular distributions of neutrons emitted when light nuclei are bombarded by charged particles, for instance by deuterons, yields useful information on the excited states of the residual nucleus and on the mechanism of the nuclear transmutation. In this work*, the reaction $Be^9\,(d,\,n)\,B^{10}$ was investigated. Lately a number of authors[1-3] have published results on the investigation of this reaction for deuteron energies less than 1 Mev. Five energetic neutron groups were observed. The angular distributions indicate a stripping mechanism only for the fourth excited state of B^{10}, for the other states a substantial contribution from the formation of the compound nucleus is presented.

This work is believed to be more detailed investigation of the energy spectra and the angular distributions of the neutrons from the reaction $Be^9\,(d,\,n)\,B^{10}$ as a function of the incident deuterons in the range of 9.5 to 1.6 Mev.

2. EXPERIMENTAL SET-UP

A beam of fast deuterons, obtained from the tube of an electrostatic generator, hit a thin metallic beryllium foil after magnetic analysis. The energy of the incident deuterons had values of 0.5, 0.8, 1.0, 1.2, 1.4 and 1.6 Mev. The voltage of the electrostatic generator was determined with the help of a generating voltmeter, calibrated with the reaction $F^{19}\,(p\,\alpha\gamma)\,O^{16}$. The voltage stabilization was carried out with the help of a corona triode for which the signal was the beam passing through the magnetic analyzer.

The focussed deuteron beam falling on the target had a diameter of about 5 mm. The neutrons from the reaction were detected by means of proton recoil tracks in photoemulsions. The surface of the photoemulsions was placed parallel to the direction of the incoming neutrons coming out of the target. The NIKFI photographic plates with 200 μ thick emulsions were placed at various angles to the direction of the incident deuteron beam in a ring-like hermetically closable duraluminum chamber (Fig. 1). The inside diameter of the chamber was 140 mm, the outside diameter was 170 mm. The

---

*This work was carried out in 1950-1952

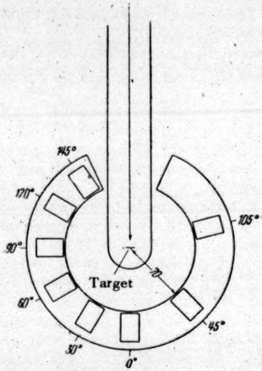

FIG. 1. Experimental Set-Up.

chamber was fastened at the end of the pipe through which the deuteron beam was brought, in such a way that the beryllium target was at the center of the chamber. The thickness of the chamber (wall) was 4 mm which excluded the possibility of charged particles reaching the photoplates.

The photoplates had dimensions of 20 × 30 mm. At each angle, two plates were placed with the emulsions one on top of the other and separated by a 0.1 mm aluminum foil (this was done in case one of the plates was spoiled during development and use). It was checked that the average number of proton recoil tracks was the same on both plates. The distance beteeen the forward edge of the plate and the center of the target was 70 mm for all angles.

The current of the incident beam was measured with a current integrator consisting of a Faraday cup and electronic equipment. The number of deuterons falling on the target at each energy was 1.1×10^{17} (that is, $26.3 \times 10^3\ \mu\ Q$) which gave a sufficient number of proton recoil tracks in the photoemulsions. The target was prepared from pure beryllium (99.99% pure) by evaporation in vacuum and its deposition onto a platinum disk of 16 mm diameter and of 0.2 mm thickness. The target had a glossy metallic finish. The weight of the target was 0.1 mg/cm^2 which corresponded to an energy loss for 1-Mev deuterons of approximately 30 kev.

After exposure, all the photoplates are processed at the same time with an amidol developer. The simultaneous processing of all the plates assured obtaining the same shrinkage of the emulsion layer after drying. The dried photoplates were examined with a microscope. We used binocular microscopes of the "Liuminan" and MBI-2 types, working with a magnification of 7 × 1.5 × 90.

Only those proton recoil tracks were measured which were entirely within the emulsion and which made with the assumed direction of the neutrons (leaving the target under a given angle) a horizontal angle not larger than 5° to the right or to the left and also a dip angle in the emulsion not larger than 5°.

Thirty three plates were examined by us. At each plate the same surface of 36 mm^2 was examined in 3000 fields of view. On the average 400 to 800 proton recoil tracks were measured on each photoplate.

3. NEUTRON ENERGY SPECTRA

The energy spectra are presented in Figs. 2 to 4. They show the number of tracks, counted at each angle and collected as a function of energy in 100-kev intervals (the spectra for deuteron energies of 0.8, 1.2 and 1.4 Mev are not shown, since their appearance is similar to the spectra shown on Figs. 2 to 4). The experimentally obtained number of neutrons was corrected for the neutron-proton scattering cross section according to the formula of Smorodinskii[4] to take into account neutron-proton scattering in the emulsion, and it was also corrected for the probability of the proton leaving the emulsion.

Five groups of neutrons, corresponding to five states of the residual nucleus B^{10}, are well resolved at all angles. The reaction energy Q, was calculated for each maximum on all plates. The average values of Q, are given below in the table for the determined values of the deuteron energies, E_d. The table also shows the corresponding values of the excitation energies E_x for five states of B^{10}.

The results of our measurements are in good agreement with the results published earlier[1-3]. The values of the errors shown for Q were determined from the deviations at various angles and the uncertainly in the range-energy determination connected with the determination of the average values of E_d. For the determination of the neutron yields for each group and also of the total yield of neutrons in a given deuteron energy region, spectra were constructed for each bombarding energy in the center of mass system by summing the data obtained at all angles. These spectra are shown in Fig. 5 for energies of 0.5, 1.0 and 1.6 Mev (the data for 0.8, 1.2 and 1.4 Mev are not presented because they do not differ appreciably from those presented on Fig. 5). On the basis of these spectra, curves were plotted showing the yield for each of the five neutron groups (Fig. 6) and the total yield (Fig. 7).

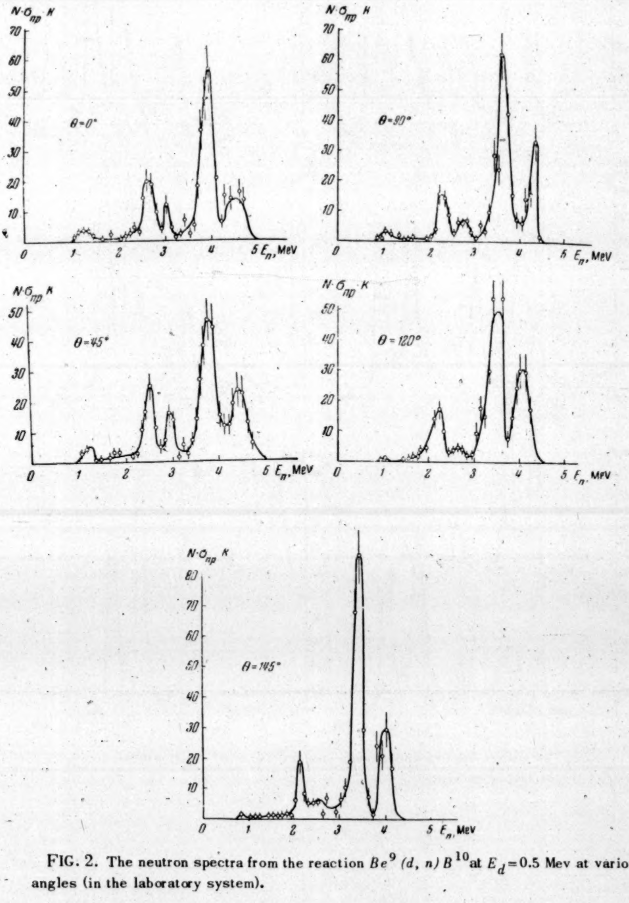

FIG. 2. The neutron spectra from the reaction Be^9 (d, n) B^{10} at $E_d = 0.5$ Mev at various angles (in the laboratory system).

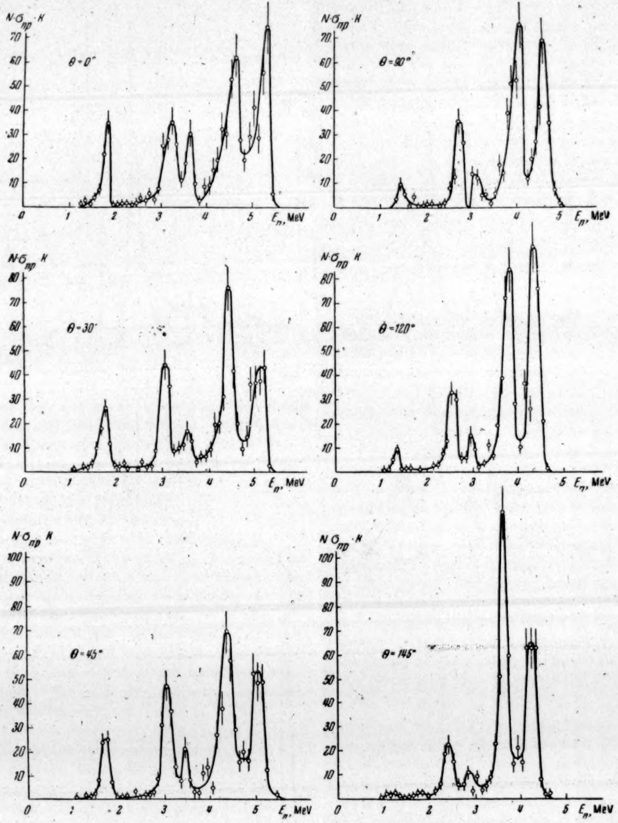

FIG. 3. The neutron spectra from the reaction $Be^9\,(d,\,n)\,B^{10}$ at $E_d = 1$ Mev at various angles (in the laboratory system).

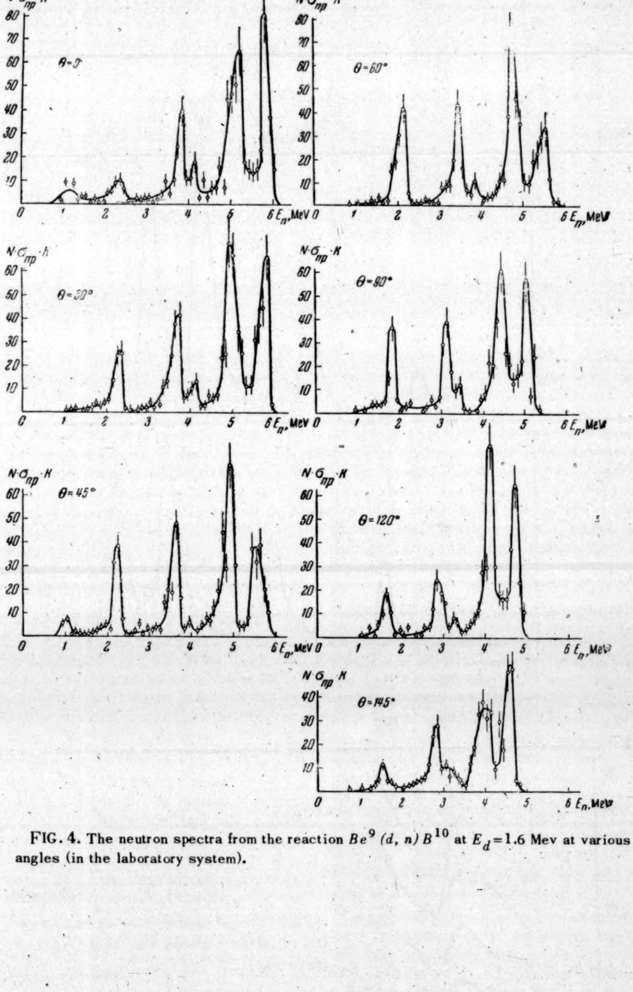

FIG. 4. The neutron spectra from the reaction $Be^9\ (d,\ n)\ B^{10}$ at $E_d = 1.6$ Mev at various angles (in the laboratory system).

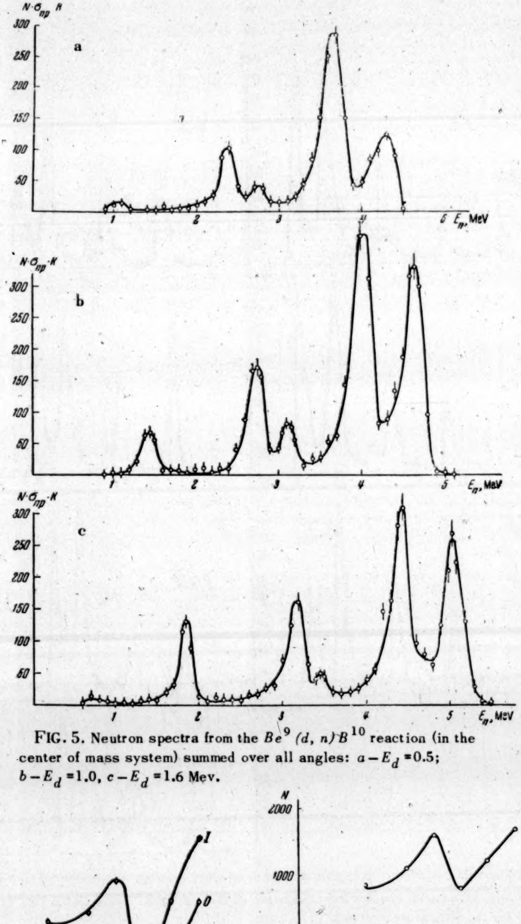

FIG. 5. Neutron spectra from the Be^9 (d, n) B^{10} reaction (in the center of mass system) summed over all angles: a – E_d = 0.5; b – E_d = 1.0, c – E_d = 1.6 Mev.

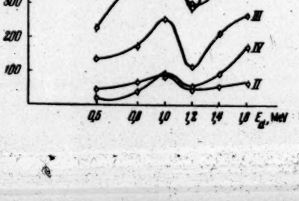

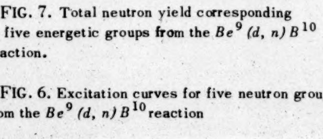

FIG. 7. Total neutron yield corresponding to five energetic groups from the Be^9 (d, n) B^{10} reaction.

FIG. 6. Excitation curves for five neutron groups from the Be^9 (d, n) B^{10} reaction

E_d, MeV	Q	E_x	E_d, MeV	Q	E_x
0,5	4,33±0,04	0,00	1,2	4,32±0,07	0,00
	3,56±0,04	0,77±0,06		3,55±0,06	0,77±0,09
	2,57±0,03	1,76±0,05		2,56±0,05	1,76±0,08
	2,13±0,03	2,20±0,05		2,12±0,05	2,20±0,08
	0,71±0,03	3,62±0,05		0,70±0,05	3,62±0,08
0,8	4,31±0,05	0,00	1,4	4,38±0,07	0,00
	3,54±0,05	0,77±0,07		3,61±0,07	0,77±0,10
	2,55±0,04	1,76±0,07		2,62±0,06	1,76±0,09
	2,11±0,04	2,20±0,07		2,18±0,06	2,20±0,09
	0,69±0,04	3,62±0,07		0,76±0,06	3,62±0,09
1,0	4,37±0,06	0,00	1,6	4,33±0,09	0,00
	3,60±0,06	0,77±0,09		3,56±0,08	0,77±0,12
	2,61±0,05	1,76±0,08		2,57±0,07	1,76±0,11
	2,17±0,05	2,20±0,08		2,13±0,06	2,20±0,10
	0,75±0,05	3,62±0,08		0,71±0,06	3,62±0,10

As can be seen from the results which were obtained, a maximum is observed for a deuteron energy of 1 Mev, which indicates the presence of a resonance for the compound nucleus, B^{11}, at 1 Mev. Evidence on the presence of this resonance has been obtained in work published earlier[5-6] on γ-ray yields. Comparison of the neutron yield curve, shown in Fig. 7, with the results obtained earlier[7-8], does not appear to be possible, because it was not possible by our method to register neutrons of low energy (lower than 1 Mev).

4. THE ANGULAR DISTRIBUTIONS OF THE NEUTRONS

The angular distributions for five states of B^{10} are shown on Fig. 8 (where for the first four states the angular distributions are not shown for the 1.2 and 1.4-Mev energies because they are similar to the angular distribution at 1.6 Mev; for the same reasons, the angular distribution at the 0.5-Mev energy is not shown for the fifth state).

It is seen from the curves that only the fourth excited state with $E_x = 3.62$ Mev is formed as the result of a stripping mechanism. The angular distributions of this group of neutrons have an appreciable maximum in the forward direction, for example at 50°, which is characteristic for an angular distribution in a stripping process. Comparison of these distributions with the Bhatia-Butler theory[9,10] gives good agreement. Results of theoretical calculations carried out with the formula of Bhatia and a nuclear radius $R = 6.2 \times 10^{-13}$ cm, for an $l = 1$ momentum, are shown on the diagrams as black dots.

The shapes of the angular distributions of the other four groups of neutrons are characteristic of processes involving the formation of the compound nucleus, but indicate interference with the stripping mechanism (to the extent that both these mechanisms are coherent). Moreover the angular distributions for these four groups of neutrons in the energy region to 1 Mev coincides with the angular distributions in (previous) work[1-3]. In passing through the maximum at about 1 Mev an appreciable deformation is observed in the angular distribution of these groups of neutrons, which is not detected for the group which is formed by the stripping mechanism.

5. DISCUSSION OF THE RESULTS AND CONCLUSIONS

The results of the investigation show convincingly the presence of the resonance for the compound nucleus B^{11} at an energy of 1 Mev. The angular distribution of the neutrons during passage through the resonance appreciably changes in the case of the formation of the compound nucleus. Such a change in the angular distribution is not observed in the case of a stripping mechanism. This can be seen in Fig. 8 and also in Fig. 9 were relative (with respect to the total neutron yield) yield curves are plotted for each group. As can be seen from the curves, the relative yield of neutrons from the fourth excited state of B^{10} smoothly increases with an increase in the deuteron energy.

Comparison of the curves for the other groups shows that the lower the excitation energy of the residual nucleus, the stronger is the influence of the resonance on the angular distribution. Analysis of the angular distributions in terms of a formula of the type $A + B\cos\theta + C\cos^2\theta$ shows that the

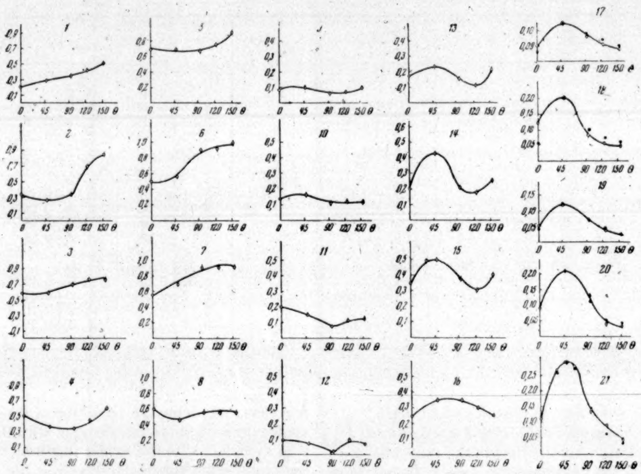

FIG. 8. Angular distributions of neutrons from the Be^9 (d, n) B^{10} reaction (the angles are in the c. of m. system). For 1, 2, 3, 4 $E_x = 0$; for 5, 6, 7, 8 $E_x = 0.76$ Mev; for 9, 10, 11, 12 $E_x = 1.76$ Mev; for 13, 14, 15, 16 $E_x = 2.2$ Mev; for 17, 18, 19, 20, 21 $E_x = 3.62$ Mev; for 1, 5, 9, 13 $E_d = 0.5$ Mev; for 2, 6, 10, 14, 17 $E_d = 0.8$ Mev; for 3, 7, 11, 15, 18 $E_d = 1.0$ Mev; for 19, $E_d = 1.2$ Mev; for 20, $E_d = 1.4$ Mev; for 4, 8, 12, 16, 21, $E_d = 1.6$ Mev.

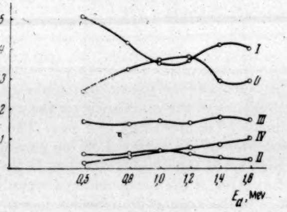

FIG. 9. Yield of individual neutron groups relative to the total yield (the total yield is taken to be unity).

experimental curves of the angular distributions for the ground state of B^{10} and for the first excited state are in good agreement with such a distribution. This calculation is more difficult for the case of the second and third excited states because of the interference process between the formation of the compound nucleus and the stripping reaction.

Spins and parities for this reaction are given in the review article[11].

---

[1] Pruitt, Hanna and Swartz, Phys. Rev. **92**, 1456 (1953)

[2] J. Genin, Comptes Rendus **240**, 2514 (1955)

[3] Green, Scamlon and Willmott, Proc. Phys. Soc. (London) **A68**, 386 (1955)

[4] Ia. A Smorodinskii, J. Exptl. Theoret. Phys. (U.S.S.R.) **17**, 94 (1947)

[5] Evans, Malich and Rigger, Phys. Rev. **75**, 1161 (1949)

[6] Hornyak, Lauritsen, Morrison and Fowler, Rev. Mod. Phys. **22**, 291 (1950)

[7] P. I. Vatset and V. S. Dementii, Ukrainian. Phys. J. (to be published).

[8] T. W. Bonner and J. W. Butler, Phys. Rev. **83**, 1091 (1951)

[9] S. T. Butler, Proc. Roy. Soc. (London) **A208**, 559 (1951)

[10] Bhatia, Huang, Huby and Newns, Phil. Mag. **43**, 485 (1952)

[11] F. Ajzenberg and T. Lauritsen, Rev. Mod. Phys. **27**, 77 (1955)

Translated by F. Ajzenberg-Selove
108

SOVIET PHYSICS JEPT VOLUME 5, NUMBER 3 OCTOBER 1957

Neutron Emission by Excited RaD Nuclei

A. V. KOGAN AND L. I. RUSINOV
Physico-Technical Institute, Academy of Sciences, USSR

(Submitted to JETP editor August 14, 1956)
J. Exptl. Theoret. Phys. (U.S.S.R.) 32, 432-439 (March, 1957)

Neutron emission from an active deposit of radium emanation on pure heavy metals was investigated. It is shown that the observed neutron activity is related to disintegration of the RaC″ isotope. The neutrons are apparently emitted by excited RaD nuclei produced as a result of β disintegration of RaC″. Control experiments have been carried out which permit one to estimate the contribution of other possible processes to the neutron radiation from the shortlived active radon deposit.

POLLARD[1] and Copeland and Lind[2] have mentioned the existence of a weak neutron background for sources prepared from radium, radiothorium, or radon. This background has been attributed to the interaction of α radiation, emitted by radium, radiothorium, or by their disintegration products, with the backing material or to the interaction of α radiation with the medium surrounding the source. Recently[3,4] it has been shown that the neutron radiation is mainly connected with the disintegration of the RaC″ isotope. It was shown that it is energetically possible for neutrons to be emitted by excited RaD nuclei produced as a result of the β disintegration of RaC″. Neutron activity with a corresponding life time has been observed.

1. EXPERIMENTAL METHOD

a) *Neutron Measurements*

This paper is devoted to an investigation of the neutron emission of preparations of RaC″, where one has about 3 neutrons per 1 millicurie/sec of radon, and also, to controlled measurements which permit an estimate of the possible contribution of the other processes to the neutron emission from the short-lived radium deposit.

A large volume ionization chamber, filled with boron trifluoride (Fig. 1a), and a set of proportional counters (Fig. 1 b) were used to measure the number of neutrons emitted by the sources under study. The chamber and source were placed in a large, carefully screened paraffin block; the γ activity of the sources amounted to as much as 400 millicuries. To reduce the γ background a lead disk 80 mm thick was placed between the chamber and the source. During maximum source activity the chamber did not register counts from fluctuations in the γ background.

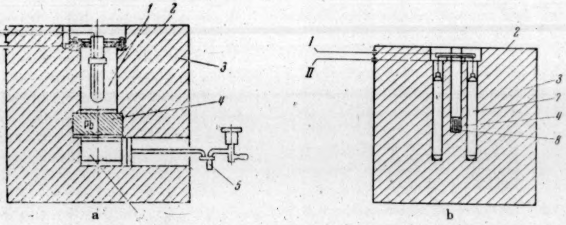

FIG. 1. Experimental arrangement for measuring neutron activity. I — lead to the linear amplifier, II — lead to the high voltage source; 1 — ionization chamber, 2 — screen, 3 — paraffin block, 4 — lead filter, 5 — trap, 6 — chamber with source, 7 — neutron counter, 8 — ampoule with source.

When the proportional counters were used for measurements, the sources had a γ activity of 1 millicurie or less and were situated at the center of a group of six counters. The diameter of the counter body was 30 mm, the diameter of the central filament was $56\,\mu$, and the length of the operational volume was 250 mm. The counters were operated at a voltage of 1800 v with a gas amplification of about 50; under these conditions, the γ ray pulses were not registered. The γ activity was measured by means of comparison with a 29.3 millicurie radium standard.

The neutrons were measured by comparison with (Ra-α-Be) neutron standards with activities from 0.5 to 1.5 millicuries (of radium). In the described apparatus the probability of neutrons being registered by the detector depends on their energy and the alignment of the detector and source in the paraffin block. The group of counters used had a stable intrinsic background of about three counts per minute and permitted the detection of radiation from constant sources emitting 2-3 neutrons per second.

Since the probabilities of registering neutrons of different energies emitted by the source and the standard are unknown, the obtained values of specific activity contain a systematic error, which could not be determined because of the low activity of the sources. With comparative measurements on sources of the same type, under standard conditions, this error is eliminated. Non-calculable errors enter in the comparison of data obtained under different geometric conditions or for sources with different neutron energies. For this reason, only the statistical errors of measurement will be shown henceforth.

b) *Preparation of the Radioactive Sources*

The neutron emission of ampoules containing radon and the neutron activity of a short-lived deposit of radium or of preparations of RaC enriched with the RaC″ isotope have been measured. In the first case the radon was inserted into lead ampoules with pressed tubes of various metals. In some cases the ampoules used had nickel seals, which made it possible to inject or withdraw the radon under pressure (Fig. 2).

The radon, which came in glass ampoules, was distilled into a system for further purification, and then was frozen with liquid air so that it could be inserted into a lead ampoule which had been evacuated and outgassed. The short-lived deposit was obtained by using an electric field to activate the foil of the investigated metal in a radon atmosphere. The foil, activated on one side, was placed near the center of the cylindrical vacuum chamber, whose walls were covered with the same foil material (Fig. 3). Measurements of the neutron activity of the short-lived deposit usually took 1.5-2 hours.

The RaC″ preparations were obtained by collecting recoil ions. The active deposit, precipitated onto nickel disks, was allowed to age for about 30 minutes so that the RaA isotope, which emits α ($T_{1/2} \sim 3$ min), would have essentially disappeared. After this time the deposit would contain mainly the isotopes RaB, RaC, RaC′ and RaC″.

Removable nickel plates 0.1 mm thick were placed opposite the disks. A positive voltage was applied to the disk with a field gradient as high as 6–7 *kv*/cm; this served to extract primarily the RaC″ ions produced by the α disintegration of RaC and in addition ions of the long-lived RaD isotope ($T_{1/2}$ = 22 yrs.) produced in the α disintegration of RaC′ (see Fig. 4). Besides these ions, RaC recoil ions

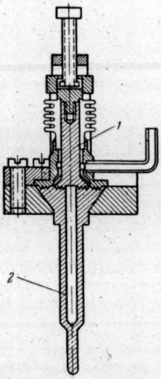

Fig. 2

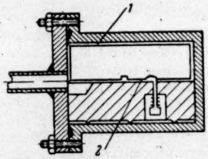

Fig. 3

FIG. 2. Lead ampoule for measuring the neutron activity of radon sources. 1—nickel, 2—insert, Pt foil

FIG. 3. Chamber for measuring the neutron activity of preparations of Ra(B + C + C′) in helium under pressure. 1—outer facing, Pt, 2—specimen

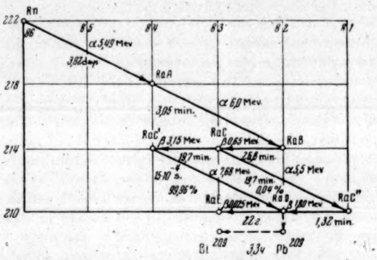

FIG. 4. Radioactive decay scheme for radon disintegration

produced in the β disintegration of RaB also strike the plate. However, the probability of the emission of ionized RaC recoil atoms from the surface of the source is comparatively small, because the recoil energy in a β disintegration is on the order of three times less than in an α disintegration, in spite of the fact that the number of RaB disintegrations exceeds that of RaC α disintegrations by more than three times. The activity of a RaC″ preparation increases with larger extracting fields, but at the same time a noticeable quantity of RaC (up to 0.5 millicuries) is collected on the plates.

Each nickel plate was activated for 4.5 minutes, after which its neutron activity was measured. During these measurements the next plate was activated, and so on.

During the measurements of neutron emission the plates were enclosed in nickel envelopes and placed in a small glass vessel which was pumped out to a pressure of 10^{-1} mm of mercury in order to prevent any (α, n) reaction by RaC′ α particles with the nitrogen and oxygen of the air.

2. DETERMINATION OF THE NEUTRON EMITTING ISOTOPE

In order to identify the isotope connected with the observed neutron emission, it was expedient to measure the neutron emission of the separate isotopes produced during radon disintegration. Sorting these by chemical methods requires considerable time (which lessens the activity of the preparations) and may lead to the appearance of contaminations by light elements, *i. e.*, an extraneous neutron background.

The change in neutron emission as a function of time was investigated with radon inserted in a clean ampoule and with it pumped out of the ampoule. A comparison of the computed curves for the time dependence of the concentration of different isotopes with the experimental data (Fig. 5) shows that the observed effect is due to RaC or to the short-lived products of its disintegration, RaC′ and RaC″. The divergence in the computed and experimental data for the neutron activity and α emission at the times when radon was inserted and pumped out is explained by the fact that an active radon deposit is partially carried off.

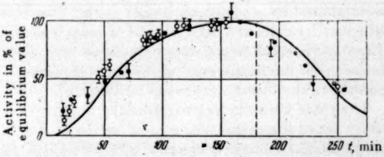

FIG. 5. Dependence of neutron and γ activity of radon on time. $t = 0$ — clean ampoule filled with radon; $t = 180$ min. — radon pumped out. o — Rn in glass tap (for γ rays). o — purified Rn in a Pt ampoule (for neutrons); solid curve as computed for RaC.

Neutron emission from an active radon deposit may be connected with the following processes: 1) an (α, n) reaction due to RaC′ α particles; 2) a (α, n) reaction due to α rays emitted after the β transitions in RaC″; 3) spontaneous fission of the nuclei of one of the isotopes RaC, RaC′, and RaC″, or RaD; 4) neutron emission by excited RaD nuclei formed during the β disintegration of the RaC″ ("delayed neutrons").

Control experiments, described in Sec. 3, showed that the first three processes cannot cause the major portion of the neutrons observed in the experiment. Thefore, there was good reason to measure the neutron activity of an isolated RaC″ preparation. When "delayed" neutrons are emitted, the activity should decrease with the half-life period of the β activity of the initial nucleus (the RaC″ isotope), *i. e.*, 1.33 min.

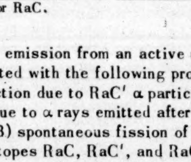

FIG. 6. Time dependence of the neutron actibity of preparations enriched with RaC″

It was possible to perform a series of measurements on 6 to 10 samples enriched with RaC" before the activity of the deposit had decreased to 50–30% of the initial activity. Figure 6 shows the data for one of the series of measurements. It should be remarked that after the first minute the measured signal exceeded the intrinsic background of the apparatus by less than 4 times. Therefore, the obtained date were summarized for all the samples, were processed for the series as a whole, and the results were plotted on a semi-logarithmic scale. The half life was determined by the method of least squares. The experimental errors were calculated with allowance for the background of the apparatus according to the formula proposed by Peierls[5].

The table below brings together the neutron activity data for measurements on 13 series of RaC" preparations. Column 5 shows the coefficient of the enrichment of the preparations with the RaC" isotope in comparison with its equilibrium content in the active radon deposit. The quantity of RaC" was determined from its neutron activity. In this connection it was assumed that the RaC" contained in 1 millicurie of radon would emit ~ 3 neutrons per second and that the efficiency of the detector in these measurements (whose geometric conditions varied from the standard) would not differ from the usual efficiency. The activity of the RaC was determined from its γ emission after disintegration of the RaC". The sixth column shows the "isolation coefficient"—the ratio of the average RaC" activity in the samples to its activity in the original active deposit. The isolation coefficient, as well as the enrichment coefficient, was determined to within a certain systematic error due to inaccuracy in measuring the number of neutrons emitted by the preparations. From the tabular data it is apparent that, within the limits of the (statistical) measurement errors, the average weighted value for the half life of neutron activity coincides with the half life of RaC" β activity. This coincidence confirms the assumption that the observed neutron activity is connected with the disintegration of the RaC".

In order to eliminate the possibility of instrumental effects, control experiments were carried out.

Neutron Activity of preparations enriched with RaC"

Series Number	Ratio of Signal to Background During First Minute	Number of Samples in Series	Half-Life in min. $T_{1/2}$	RaC" Enrichment Coefficient of Samples	Isolation Coefficient in %	Avg. Activity of Rac in Samples in Millicuries
1	1	8	1,4 ± 0,7	100	10	0,1
2	0,6	6	0,5 ± 1,9	50	5	0,5
3	0,8	10	1,1 ± 1,9	50	8	0,1
4	0,6	12	3,3 ± 1,9	150	5	0,03
5	0,3	5	2,6 ± 2,9	100	2	–
6	1,5	3	0,85 ± 0,4	—	3	–
7	1	7	1,7 ± 0,8	—	5	–
8	1	2	1,7 ± 1,1	—	7	—
9	0,5	4	0,7 ± 0,6	100	3	0,03
10	2	4	1,6 ± 0,6	1000	3	0,003
11	4	7	1,6 ± 0,4	100	15	0,01
12	3	4	1,15 ± 0,45	—	15	—
13	1	6	1,15 ± 0,95	300	15	0,01
Weighted average			1,50 ± 0,25			

a) The sign of the electric field that extracted the ions was altered in such a way that negatively charged particles were collected on the nickel plates. This done, the neutron activity of the plates fell below the sensitivity range of the apparatus.

b) To check the operation of the detecting system a series of measurements were made using the activity of the $(Po\text{-}\alpha\text{-}Be)$ source, which emitted ~ 10 neutrons per second. These measurements were made under exactly the same conditions as prevailed when the RaC" preparations were measured. The magnitude of the measured activity of this source did not depend on time.

The data given above and the control experiments show that neutrons are emitted when RaC" disintegrates.

3. CONTROL STUDIES

To clarify the role of other possible processes in the observed neutron activity a series of control experiments were conducted.

a) *The possibility of fission by excited nuclei in the Rn deposit.* An evaluation of the life time for the fission process, according to available empirical formulas and curves, indicates that this is hardly probable (the half-life periods are more than 10^{24} years). Nevertheless, the ionization chamber was used to carry out an experimental check* into the possibility of nuclear fission in the active deposit.

It was shown that the contribution of the fission process amounts to no more than 1% of the observed neutron activity, assuming that in the disintegration no more than three neutrons were released.

b) *The (γ, n) reaction.* The probability of this reaction for deuterium in paraffin may be estimated on the basis of the known energies of γ rays from RaC and RaC"; it amounts to $\sim 2.5\ 10^{-2}$ neutrons per 1 millicurie/sec. This estimate was checked experimentally. Around the radon source there was placed an additional lead absorber, which reduced the number of RaC and RaC" γ rays by 75%. Neutron activity decreased by 1.0%; with a statistical accuracy of 4.6% in the measurements. Obviously, γ radiation in this case could cause no more than 8% of the total neutron activity.

In order to provide a more exact determination of the role of γ radiation, experiments were conducted with a preparation enriched with RaC". Measurements were made alternately under ordinary circumstances and with the source surrounded by a layer of heavy water 2 mm thick. In this case the amount of deuterium that could participate in the reaction, in comparison with that contained in the paraffin, was increased by more than 100 times. The observed neutron activity approximately doubled, with an experimental error of ± 30%. From this it follows that no more than 1 – 1.5% of the neutrons emitted by the RaC" preparation were due to the (γ, n) reaction.

c) *An (α, n) reaction due to RaC' α particle.* An estimate of the probability of α particles penetration through the Coulomb barrier shows that for metals with $Z > 72$ (Ta, Pt, Pb), which are ordinarily used for preparing sources, the neutron yield must be less than 10^{-9} per 1 millicurie/sec. The actual neutron yield may increase over that calculated on account of the presence of light impurities, but their content would have to be considerable—greater than the total amount of impurities in the pure platinum used for preparing the sources.

The content of impurities in the platinum which would be necessary to explain the observed neutron yield on the basis of an (α, n) reaction is characterized by the following data:

Impurity	Li	Be	B	C	N	F	Na	Mg	Al	Cl	Fe
Amt. in % (by weight)	0,03	0,01	0,1	2	1	0,05	0,1	0,5	0,3	2	3,5

It should be remarked that filling the ampoules with spectrally pure porous platinum did not change the magnitude of the neutron yield. Nickel was also used in the preparation of the sources; the (α, n) reaction is energetically impossible for most of the isotopes of nickel. The neutron yield in this case should not exceed 0.1– 0.2 neutrons per 1 millicurie/sec. However, the averaged yield values for the most thoroughly investigated elements (Ni, Ta, Pt) do not differ, within a range of statistical error from 5 to 15%, which is apparent from the following table:

Backing material	Pt	Ta	Ni
Number of neutrons (per 1 millicurie/sec)	2,75±0,15	2,95±0,15	2,8±0,4

---

*Together with A. N. Baryshev.

The probability is small that the neutron yield for metals with such a great difference in their atomic numbers (from 28 to 78) would be constant if this yield was basically determined by an (α, *n*) reaction in the basic isotopes or chemical impurities. Gaseous helium was used for a more direct experimental check as to the role of the (α, *n*) reaction. About half of the α particles emitted by the source impinge on the metal backing bearing the sample, but the remaining 50% of the α particles may be stopped, either totally or partially in helium (in which the (α, *n*) reaction is energetically impossible), so it is impossible for this portion of the α particles to give rise to neutrons in any material. The range of RaC′ α particles in helium is ~ 35 cm, and therefore the gas used was under a pressure of 6 atm. The air content of the helium did not exceed 0.01% by particle density, *i. e.*, its partial pressure was less than 0.5 mm of mercury. The source was located in the central portion of a cylindrical chamber (Fig. 3) 60 mm in diameter. Platinum was used as the material for the backing of the source and the outer facing of the chamber. The control experiments showed that at this pressure the emission of no more than 0.1 neutron per 1 millicurie/sec could be due to an (α, *n*) reaction in the residual nitrogen. The energy of the RaC′ α particles falling on the outer facing was reduced by collisions in the helium to ~ 5.4 Mev. The data displayed in Fig. 5 show that for α particles from Rn and RaA (E_α = 5.5 and 6 mev), the (α, *n*) reaction is practically absent. Thus neutron emission would have been reduced by about 2 times if it were due to the (α, *n*) reaction.

In the experiment the neutron yield was 2.5 ±0.4 when the helium was absent, but when it was present, the yield was 2.7 ±0.5 neutrons per 1 millicurie/sec instead of a yield of 1.4 ±0.2 neutrons which might have been expected from an (α, *n*) reaction. Allowing for the experimental errors, one can consider that the contribution of the (α, *n*) reaction must amount to less than 50% of the observed effect. The same results were obtained at lower helium pressures.

The experiments with helium are conclusive in those cases where the reaction occurs either in the backing of the source or the facing of the chamber. If it occurred only on the surface of the source (in some impurity appearing during activization), the folding of the inner layer of the source upon itself would increase the neutron yield by about two times, since the layer can only be very thin, and the yield would show a linear increase with the width. In a test the activity of the sample did not vary within the limits of the statistical accuracy of measurement, ± 10%.

Another control experiment, which made it possible to evaluate the probability of the (α, *n*) reaction, was the measurement of the neutron background of Th(B + C + C′) sources on platinum. The disintegration pattern of ThB and its radioactive products eliminates the possibility of the formation of nuclei with sufficient excitation energy to emit neutrons. When ThC″) disintegrates, hard γ rays with an energy of 2.62 Mev are emitted, and these cause a (γ, *n*) reaction on the deuterium in paraffin. The energy of the basic group of ThC′ α particles is ~ 8.8 Mev. If the neutron emission from radon sources is due to the (α, *n*) reaction, then it should increase considerably in the change from RaC′ to ThC′, because the cross section of the (α, *n*) reaction near the threshold grows exponentially with the energy of the α particles. Measurements have shown that neutron radiation from a Th(B+C+C′) source on platinum is equal to 0.3 ±1.8, *i. e.*, fewer than 2 neutrons per 1 millicurie, which is less than for Ra(B+C+C′). A background of this order might be expected on account of the (γ, *n*) reaction in paraffin. The small degree of accuracy in the measurements is explained by the low activity of the radiothorium preparation used in the control experiments.

All of the described results show that neither the (α, *n*) reaction, (γ, *n*) reaction nor nuclear fission in the active deposit is the basic process responsible for neutron emission from radon sources. The possible total contribution of these reactions to the total neutron emission is difficult to estimate quantitatively because of the low absolute activity of the sources and the short life time of the active deposit.

CONCLUSIONS

The investigations carried out confirm the predictions[3] that the basic process responsible for the neutron activity of a short-lived active radon deposit will be neutron emission by excited RaD nuclei produced during the β disintegration of RaC″. It should be noted that this process is energetically possible. According to the data available on the thresholds of *(d, p)*, *(γ, n)*, and *(d, T)* reactions, the binding energy of the neutron in RaD is 5.2 or 4.8 Mev[6]. The low value for the binding energy in RaD is explained by the fact that in RaD there are only 2 neutrons outside the filled shell (*i. e.* Pb^{208}). In the Pb^{209} nucleus one has an even smaller binding energy—3.9 Mev. The total energy of the RaC″ – RaD transition has not been directly measured because it has not been possible to isolate a sufficient quantity of this comparably short-lived isotope. The transition energy can be determined from the known data on the α disintegration of RaC and RaC′ and the β disintegration of RaC by comparing the total energy of the conversion of RaC to RaD over two branches of the "radium fork" (see Fig. 4). Judging by the latest published decay scheme for RaC[7], the total energy of the RaC″ – RaD transition is 5.4 Mev. It is obvious that the sum of the energy of the partial β spectrum and the kinetic energy of a neutron is 0.2 or 0.6 Mev, if the magnitude of the binding energy is respectively 5.2 or 4.8 Mev.

According to our data, the probability of neutron emission due to the β disintegration of RaC″ is $\sim 2\times10^{-2}$%. A partial β spectrum is also predicted with an end-point energy of $\sim$ 100 kev and a relative transition probability of $10^{-1} - 10^{-2}$%. When the energy of the basic β transition is $\sim$ 2 Mev, the existence of this transition is possible. The neutron kinetic energy in this case should be no more than 0.5 Mev.

The authors are deeply grateful to the now deceased Academician P. I. Lukirskii for his fruitful discussion of this paper. We should also like to express our gratitude to M. I. Sergeev for his help in taking the measurements and preparing the apparatus and to V. M. Permiakov and O. M. Nechaeva for their help in obtaining and purifying the radon.

---

[1] E. Pollard and W. L. Davidson, Phys. Rev. **53**, 351 (1938)

[2] C. S. Copeland and S. C. Lind, J. Phys. Chem. **42**, 567 (1939)

[3] A. V. Kogan, Dokl. Adad. Nauk SSSR **108**, 817 (1956)

[4] A. V. Kogan, Dissertation, Leningrad, Leningrad Physico-Technical Institute, Academy of Sciences, USSR, 1952.

[5] H. Peierls, Proc. Roy. Soc. (London) A**149**, 467 (1935)

[6] Kinsey, Bartolomew, and Walker, Phys. Rev. **82**, 380 (1952)

[7] S. A. E. Johansson, Arkiv f. Fysik **9**, 561 (1955)

Translated by A. Skumanich
109

SOVIET PHYSICS JETP VOLUME 5, NUMBER 3 OCTOBER, 1957

Elastic and Quasi-elastic Scattering of 660 Mev Protons by Deuterons *

G. A. LEKSIN
Joint Institute for Nuclear Research

(Submitted to JETP editor October 20, 1956)
J. Exptl. Theoret. Phys. U.S.S.R. **32**, 440-444 (March, 1957).

The differential elastic *p–d* scattering cross sections at angles of 40° to 150° and the differential quasi-elastic *p–p* scattering cross sections at angles of 50 to 90° of the two nuclei were measured in the center of mass system by the ganged-telescope method. The experimental data point to the existence of a predominant interaction between the incident proton and the separate nucleons in the deuteron and also to the existence of collective interactions between the three nucleons. The energy dependence of the differential cross section of quasi-elastic *p–n* scattering into an angle of 90° in the c. m. s. of the two nucleons was also measured in the 460 to 660 Mev range.

1. A study of the interaction of fast protons with the simplest nucleus–the deuteron–leads to several conclusions concerning the elementary nucleon-nucleon interactions and concerning the character of the motion of the nucleons in the deuteron, and also permits an approach to the study of the collective interaction of nucleons at high energies.

This article describes the experimental results of *p–d* elastic and of *p–p* and *p–n* quasi-elastic scattering of 657 ± 2 Mev protons by deuterons. The proton beam was generated in the synchrocyclotron of the Institute for Nuclear Problems of the Academy of Sciences of the U.S.S.R. The method of ganged telescopes[1] was used to separate the above processes from the variety of meson-producing proton–deutron interactions. The twice-collimated proton beam from the accelerator passed through a monitor, before striking the target. An ionization chamber filled with helium was used as a monitor in the present experiments. Aluminum cylindrical containers filled with equal numbers of nuclei of heavy and ordinary water were used throughout as targets. The targets enveloped the beam and the errors caused by scattering in the side walls of the containers were thus eliminated. Two telescopes were used to detect the charged particles, each telescope consisting of three scintillation counters (photomultiplier and toluene crystal). The dimensions of the toluene crystals were selected so that the system registered coincidence if a scattered proton passed throught the crystal which determined the solid angle. To decrease the background count the crystals of the photomultipliers were chosen to be only 3 to 6 mm thick. The resolution time of the coincidence counts from the scintillation counters in the telescope was 4 x 10^{-8} sec. The resolution time of the coincidence counts from the telescopes was 8 × 10^{-8} sec. The number of accidental coincidences was measured by including a delay line of suitable length in one of the coincidence channels and also by uncoupling the telescopes. The individual telescopes and the entire system had a counting plateau 200 to 300 V wide at a working voltage on the photomultipliers of 1500 V.

---

*This work was reported at the All-Union Conference on the Physics of High Energy Particles, May 1956 and at the Geneva Conference in June, 1956.

2. The laws of conservation of momentum and energy make it possible to distinguish between the scattering processes of the two particles in accordance with the angle $\theta = \theta_1 + \theta_2$ subtended by the two particles for given divergence angle θ_1 of one of the particles. To distinguish elastic and quasi-elastic scattering of protons by deuterons, the dependence of the coincidence counting rate N on the angle θ subtended by the telescopes was therefore studied for three values of angle θ_1 of the fixed telescope relative to the direction of the proton beam. The three "divergence curves" obtained for the angles of the scattered protons in the laboratory coordinate system $\theta_1 = 24$, 36 and 41° are given in Figure 1 (all three curves *a*, *b*, *c* are plotted in a single

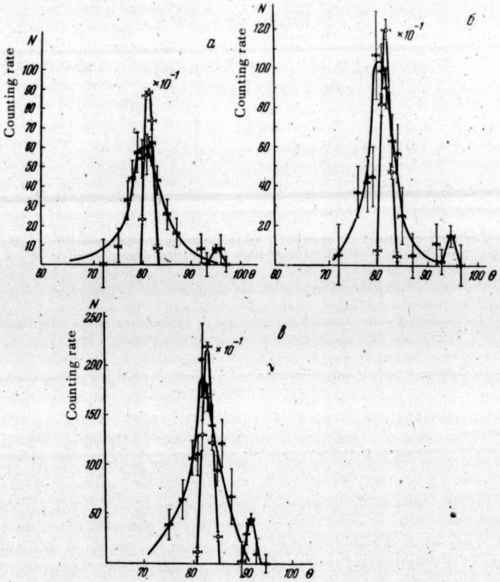

FIG. 1. Dependence of the coincidence count rate on the evergence of particles; $\theta = \theta_1 + \theta_2$, curve *a* for $\theta_1 = 41°$, *b* for $\theta_1 = 36°$, *c* for $\theta_1 = 24°$ in the laboratory system of coordinates.

scale). Each point on a divergence curve represents the difference between the counting rates obtained with D_2O and H_2O targets, after a correction for chance coincidence counts. The effect of the H_2O target, measured by the ganged telescopes, made it possible to determine, the contribution from processes originating from the oxygen nuclei outside the narrow range of angles comprising the peak of elastic *p–p* scattering. It also made possible measurement of the peak of the elastic scattering of protons by protons under identical conditions. To evaluate the magnitude of the cross section, and to show the characteristic resolution of the apparatus, the peak of elastic *p–p* scattering is shown in Figure 1 with the ordinate scale reduced by ten times.

The comparatively small cross section of the studied processes and the differential character of the experiment resulted in large statistical errors in the determination of the divergence curves. However, the divergenge curves obtained for deuterium and their comparison with the peak *p–p* elastic scattering permit the following conclusions:

a) Each divergence curve has two maxima. The position of the smaller of these two maxima corresponds to a divergence angle for elastic proton-deuteron scattering. The width of this maximum, as well as the equal width of the peak for elastic *p–p* scattering, is not connected with the properties of the nuclear interaction and characterizes the angular resolution of the apparatus. Thus the presence of a smaller maximum in the divergence curves points to the existence of elastic scattering of protons by deuterons in the range of angles studied.

b) The existence and the position of the second maximum near the peak of the elastic proton-proton scattering allows this maximum to be considered as the result of quasi-elastic scattering of the bombarding proton by individual protons in the deuteron.

c) The motion of protons in deuterons leads to a blurring of the maximum of the quasi-elastic scattering. The width and the shape itself of the maximum can be calculated from one of the momentum distributions of the nucleons in the deuteron. Ryndin[2] calculated the scattering of 460 Mev protons by deuterons assuming Hulthen and Bethe-Peierls deuteron wave functions. The shape of the maximum depends weakly on the energy of the bombarding nucleon at very high energies. Therefore the calcuations agree well with the available experimental data.

d) The maximum of the quasi-elastic *p–p* scattering is observed to be shifted relative to the peak of elastic *p–p* scattering. This shift is explained by the effect of the binding of proton in deuteron.

The "divergence curves" obtained in the present work do not differ significantly from those obtained previously for lower energies of bombarding protons[3,4], and show the predominance of the interaction of the bombarding nucleon with one of the nucleons in deuteron. More detailed quantitative comparisons of the parameters of the maximum of *p–p* quasi-elastic scattering with theory[2] do not allow, within the present experimental accuracy, to shed any light on the character of the wave function of the deuteron at small distances.

3. Principal attention was paid in this work to the measurement of the differential elastic scattering cross section of protons by deuterons in the range of proton emission angles 40 to 150° in the center of mass system (c. m. s.) of the colliding particles. The elastic *p–d* scattering was separated by ganged telescopes set at the elastic-scattering divergence angles of the proton and deuteron. An additional selection of the elastic *p–d* scattering events and a decrease in the number of counts in the deuteron-counting telescope were accomplished by placing behind the telescope a deuteron-absorbing copper filter together with a scintillation counter set for anti-coincidence. Except for accidental coincidences, this system registered only elastic *p–d* scattering events. This was verified for each proton scattering angle by uncoupling the telescopes. The number of accidental coincidences varied together with the number of total counts, ranging from 5 to 40% of the measured effect and reaching 40% in the measurement of the cross section of elastic scattering of protons by deuterons at angles $\geq 90°$ in the laboratory system of coordinates. Therefore, as a control experiment filters absorbing protons of the corresponding energy were inserted in the path of protons scattered into these angles and caused complete cessation of the counting of the elastic *p–d* scattering events. The presence of elastic *p–d* scattering was thus verified over the entire range of emission angles of the scattered protons in which the present measurements were carried out.

To obtain the absolute values of the differential cross sections of elastic *p–d* scattering in the range of angles 40 to 70° in the c. m. s., the counting rates at the peaks of elastic *p–d* and *p–p* scattering were measured under identical conditions and compared. The comparative character of the measurement allowed elimination of a series of errors connected with the absolute measurements.

The values of the differential cross sections of elastic scattering of 660 Mev protons by protons were reported previously[5]. The measured differential cross sections for elastic *p–d* scattering are shown in Table I in units of 10^{-27} cm^2/sterad for 10 values of the proton emergence angle θ^* in the c. m. s. The last line of the table shows the standard statistical deviations.

TABLE I.

θ^*	40.5°	49°	59.5°	67°	78.5°	92.5°	111.5°	126.5°	139.5°	150°
$d\sigma_{pd}^{el}/d\omega$	0,124	0,067	0,035	0,030	0,033	0,011	0,000	0,034	0,047	0,063
$\pm\Delta$	0,015	0,013	0,012	0,008	0,016	0,009	0,025	0,017	0,016	0,027

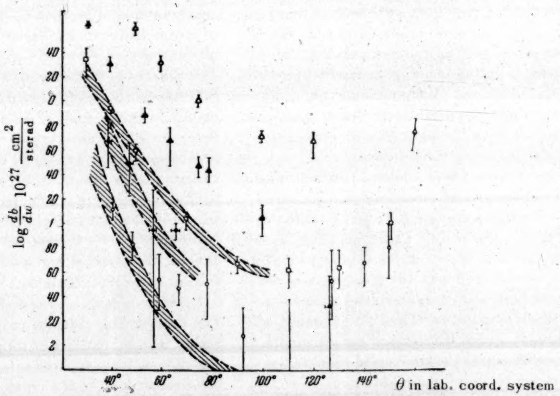

FIG. 2. Differential elastic *p–d* scattering cross section at various energies. Δ – 146, ▲ – 240, □ – 340, ● – 460, ○ – 660 Mev.

Figure 2 compares the data obtained in the present work with the results of previous experiments[3,4,6-8] on elastic *p–d* scattering at lower energies of the bombarding protons. The abscissa gives the proton emission angle in the c. m. s. of the colliding particles while the ordinate gives, on a logarithmic scale, the differential cross section in units of 10^{-27} cm^2/sterad. The angular dependence of the differential elastic scattering cross section of 660 Mev protons by deuterons is given by an asymmetrical curve with a minimum in the range of angles 100 to 110° in the c. m. s. The differential cross sections increase, starting with 110° in the c. m. s. of the colliding proton and deuteron.

For all of the studied energies, a decrease in the differential cross section was observed with an increase in the emission angle of the scattered protons. In the range of angles $\theta^* < 100°$ in the c. m. s. a decrease in the cross section of the elastic *p–d* scattering is observed with an increase in the energy of the bombarding proton.

The concept of independent interaction between the bombarding proton and one of the nucleons in the deuteron makes it possible to correlate the peculiarities of the angular dependence of the differential cross section in elastic *p–d* scattering with the change in the partial proton-nucleon scattering cross sections and with the decrease in the probability of the deuteron remaining whole upon increase in the momentum transferred to the deuteron. This concept was the basis of the impulse approximation for the theoretical analysis of the elastic scattering of fast protons (energy $\geqslant$ 100 Mev) by deuterons[9,10]. Of course, the amplitudes of the proton interaction with the nucleons should agree with the experimental data on elastic p–p and p–n scattering. As a condition of applicability of the impulse approximation, the wave length of the bombarding particle must be small compared with the distance between nucleons in the deuteron. A condition connected with this requirement is that the time of the interaction of the nucleons is comparable with the characteristic "inversion" time of the system. Both conditions are satisfied in the case of elastic scattering of protons by deuterons in the range of angles studied herein ($<100°$ in the c. m. s.). Therefore, there is a qualitative and a definite quantitative agreement between the experimental data[3,4,6-8] and the theoretical calculations[9,10]. By way of an example, Figure 2 shows such a comparison for the 340 and 460 Mev bombarding protons.

A comparison of the results of the present experiment was carried out by calculations quite analogous to those made by Golovin[10] for 660 Mev protons. The differential elastic p–d scattering cross section $d\sigma^{pd}(\theta^*_{pd})/d\omega$ at an angle θ^*_{pd} in the c. m. s. of the colliding proton and deuteron was found from the expression

$$\frac{d\sigma^{pd}(\theta^*_{dp})}{d\omega} = \frac{16}{9}(A+B)T_1^2 + \frac{16}{9}CT_1^2. \qquad (1)$$

Here A, B and C are functions that can be evaluated from the data on elastic scattering of protons and neutrons by protons:

$$\frac{2}{3}\frac{d\sigma^{pp}(\theta^*_{pp})}{d\omega} \leqslant A \leqslant \frac{d\sigma^{pp}(\theta^*_{pp})}{d\omega};$$

$$\frac{2}{3}\frac{d\sigma^{pn}(\theta^*_{pn})}{d\omega} \leqslant B \leqslant \frac{d\sigma^{pn}(\theta^*_{pn})}{d\omega};$$

$$|C| \leqslant \frac{d\sigma^{pp}(\theta^*_{pp})}{d\omega} + \frac{d\sigma^{pn}(\theta^*_{np})}{d\omega}.$$

T_1 is the same as the "sticking" factor evaluated by Chew[9] and depends on the momentum transferred to the deuteron and on the deuteron wave function.

The scattering angle θ^*_{pd} of the protons in the p–d center of mass coordinate system is related to the scattering angles $\theta^*_{pp} = \theta^*_{pn}$ of protons in the center of mass system of two nucleons by the expression

$$\sin\frac{\theta^*_{pp}}{2} = \frac{4}{3}\sin\frac{\theta^*_{pd}}{2}.$$

The coefficient C and the corresponding second terms of Eq. (1), expressing the interference of the waves scattered by the proton and the neuteron in deuteron, was set equal to zero in the calculations. Discarding this term is in agreement with the results of previous calculations[6-10]. The calculated curve obtained in this manner describes well the angular dependence of the differential cross section of elastic p–d scattering at angles $<100°$ in the c. m. s. It is evident from Figure 2 that the qualitative agreement is as good as could be expected with the calculation method employed.

In agreement with the results analogous experiments, the deuteron wave function for lower proton energies is written in the form $\varphi_0(r)=A(e^{-\alpha r}-e^{-\beta r})/r$, where $\beta=6\alpha$. This function (proposed by Hulthen) describes the deuteron better than the wave function $e^{-\alpha r}/r$. The presence of protons scattered at angles 60 to 100° in the c. m. s. already shows that at the moment of collision the nucleons in the deuteron are closely packed. This observation was previously made by Bogachev and Vzorov[5]. However, particular attention should be given to the group of protons elastically scattered backward at angles $>110°$ in the c. m. s. The forward scattered deuterons assume thereby the greater part of the momentum and acquire an energy 100 times greater than the binding energy of the nucleons in deuteron. Such transfer of momentum and energy (up to 560 Mev) can take place only at the instant when the neutron and proton are separated by a distance on the order of the wavelength of the bombarding nucleon. This circumstance may mean that scattering of protons by deuterons at large angles takes place through the interaction of the bombarding proton with both nucleons in the deuteron.

A simultaneous interaction of three particles centered in a region having linear dimensions on the order of the wave length of the bombarding particle or smaller makes the impulse approximation inapplicable. At the present time there is no other theory applicable to a calculation involving a strong interaction of three particles, and capable of determining how much the non-additive terms due to the collective interaction of particles contribute to the scattering.

The experiment shows that following features of three-nucleon interaction manifest themselves in elastic backward scattering of protons by deuterons: a) An increase in the differential elastic p–d scattering cross section is observed with an increase in the proton emission angle from 110 to 150° in the

c. m. s., i.e., with an increase in the momentum of the scattered deuteron; b) A relative increase in the magnitude of the cross section of elastic backward *p–d* scattering is observed with an increase in the incident proton energy from 100 to 660 Mev.

A comparison of elastic *p–d* backward scattering with the know facts about the emission of "fast" (with energy exceeding the repulsion energy of a particle in the Coulomb field of the remaining nucleus) deuterons, α-particles, Li, Be etc. from nuclei interacting with high-energy nucleons[11-13] shows a close relationship between these phenomena. In particular, the emission of fast fragments from nuclei can be considered a result quasi-elastic interactions between the bombarding nucleon with a group of nucleons in the nucleus that are strongly bound at the time of the collision. The question concerning the mechanism of the collective interaction still remains open. True, a hypothesis has been advanced[14] concerning the presence of multiple forces, apparently connected with a simultaneous exchange of the nucleons with several mesons. If such forces do exist and are responsible for the large transfer of momentum to the forward deuteron emitted in elastic *p–d* scattering, then the radius of interaction of the multiple forces should be small compared with the radius of ordinary nuclear forces. The facts and comparisons given above are necessarily skethy and skimpy, and therefore it is necessary to emphasize the necessity of a more detailed experimental and theoretical study of this interesting phenomenon.

4. A comparison of the yield of protons elastically scattered by free protons and quasi-elastically scattered by protons bound in deuterons permits determination of the differential cross section of the latter process. The resultant date are given in Table II. The differential quasi-elastic *p–p* scattering cross sections differs only slightly from the differential cross section of elastic scattering of protons by free protons at the corresponding angles. This fact again gives evidence that for a given energy *p–d* scattering results fundamentally in an interaction of the bombarding nucleon with individual nucleons in the target deuteron. More accurately, the differential cross section of elastic *p–p* scattering should be compared with the quantity

$$d\sigma_{pp}^{ge}(\Phi)\,/\,d\omega + d\sigma_{pd}^{el}\,(\Phi)\,/\,d\omega,$$

since the elastic scattering of protons by deuterons is a process competing with the quasi-elastic scattering of protons by nucleons. Figure 3 is a plot the quantity

$$\{d\sigma_{pp}^{ge}(\Phi)\,/\,d\omega + d\sigma_{pd}^{el}\,(\Phi)\,/\,d\omega\}\,/\,d\sigma_{pp}^{el}\,(\Phi)\,/\,d\omega$$

as a function of the angles Φ of the emission of protons in the laboratory system of coordinates. Disregarding the large statistical errors, a systematic deviation of the curve from unity can be noticed with a decrease in the proton scattering angle. Analogous results were obtained in a study of scattering of deuterons by 460 Mev protons[4]. These data are also shown in Figure 3. It is evident that the deviation should be attributed to the unaccounted competing process, namely non-coplanar scattering, in which all three nucleons assume large energies, again giving evidence of the presence of collective interaction.

TABLE II.

θ	54,5°	67,5°	80,5°	90°
$d\sigma_{pp}^{ge}/d\omega\cdot 10^{27}\,cм^2$/ sterad $\pm\,\Delta$	3,05 0,55	2,51 0,58	2,19 0,35	2,09 0,17

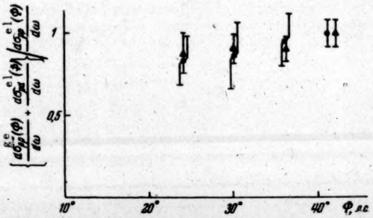

FIG. 3. Dependence of the quantity $[d\sigma_{pp}^{ge}(\Phi)\,/\,d\omega + d\sigma_{pd}^{el}\,(\Phi)/d\omega]/d\sigma_{pp}^{el}\,(\Phi)\,/\,d\omega$ on the scattering angle of proton in the lab. system of coordinates. ● — 660, ▲ — 460 MeV

5. The present experiments show that the differential quasi-elastic and elastic *p–p* scattering cross section at an angle of 90° in the c. m. s. are approximately equal to each other. Therefore, it should be expected that the differential elastic and quasi-elastic *p–n* scattering cross sections at a 90° angle would also be equal to each other. If this is so, measurement of the quasi-elastic *p–n* scattering at 90° in the c. m. s. can yield some evidence on the differential elastic scattering cross section of protons by free neutrons at that angle.

Great interest is centered about the comparison of the $p-n$ scattering cross sections measured under the same conditions for different energies. The measurement of the quasi-elastic $p-n$ scattering with a single telescope by counting the scattered protons is impossible for energies exceeding 600 Mev because of the large contribution of processes connected with meson production. Therefore, method of the ganged-telescope method was used to solve such a problem with one telescope employed as a highly effective neutron detector[14]. The energy of the protons was reduced with a series of polyethylene filters placed in the path of the proton beam. The beam intensity was maintained constant for all energies The cross sections measured at 460, 560, 590, and 660 Mev were in the ratios of 1.2 : 1.1 : 1.1 : 1. The relative statistical measurement error was 15%.

The data on the elastic $n-p$ scattering cross sections at 580 Mev[15], and also the corresponding data on elastic $p-p$ scattering[16], permit determination of the cross section connected with $p-n$ interaction in states with isotopic spin $T=0$. The data obtained are:

E (MeV) =	460	560	590	660
$\sigma_{T=0}(90°) =$	$0{,}8\pm0{,}6$	$0{,}8\pm0{,}4$	$0{,}8\pm0{,}4$	$1{,}3\pm0{,}4$

6. The experimental results and their evaluation lead to the following conclusions:

1. At 660 Mev, the most important process in proton-deuteron collisions is the elementary nucleon-nucleon interaction between the bombarding proton and one of the nucleons in the deuteron.

2. The observed elastic $p-n$ scattering cross section at the proton-emission angles $<110°$ in the center of mass system of the colliding particles agrees with the cross section calculated in the impulse approximation using the Hulthen deuteron wave function for the ground state of the deuteron.

3. The differential $p-n$ quasi-elastic scattering cross section at 90° in the c. m. s. decreases slightly with increasing energy. That part of the cross section due to interaction in the state $T=0$ remains unchanged in the energy interval of 460 to 660 Mev within the limits of experimental error.

4. The elastic forward scattering of deuterons with energy up to 560 Mev can apparently be considered as evidence that in some cases a proton-deuteron collision at energies of 660 Mev results in an interaction between all three nucleons.

5. The presence of such collective interaction between nucleons agrees with many other experimental data, but any detailed determination of the properties of collective interaction necessitates new experimental and theoretical investigations.

The author takes this opportunity to express deep gratitude to Professor M. G. Meshcheriakov for his constant interest in this work and for discussion of the experimental results, and to A. S. Kuznetsov for his help in constructing and adjusting the apparatus.

---

[1] Meshcheriakov, Bogachev, Piskarev, and Neganov, Dokl. Akad. Nauk. SSSR **99**, 655 (1954)

[2] R. M. Ryndin, Report of institute for Nuclear Research, Acad. of Science, U.S.S.R. (1953).

[3] R. D. Schamberger, Phys. Rev. **85**, 424 (1952)

[4] Meshcheriakov, Bogachev, Leksin, Neganov, and Piskarev, Proc. of CERN Symposium **2**, 124 (1956).

[5] N. P. Bogachev and I. K. Vzorov, Dokl, Akad. Nauk SSSR **99**, 931 (1954).

[6] O. Chamberlain and D. B. Clark, Bull. A. Phys. Soc. **29**, 48 (1954).

[7] Cassels, Stratford, and Pickavance, Nature **168**, 556 (1951).

[8] M. O. Stern and A. L. Bloom, Phys. Rev. **83**, 178 (1951).

[9] G. F. Chew, Phys. Rev **74**, 809 (1948); **84**, 1057 (1951).

[10] B. M. Golovin, Report of Inst. for Nuclear Research, Acad. of Sciences (U.S.S.R.) (1954). B. M. Golovin And V. P. Dzelepov, J. Exptl. Theoret. Phys. **31**, 194 (1956).

[11] S. O. C. Sorensen, Phil Mag **40**, 947 (1949); **42**, 188 (1951).

[12] D. H. Perkins, Proc Roy. Soc. **A203**, 399 (1950).

[13] A. Alikh[illegible]nian and G. Marikian, Dokl. Akad. Nauk SSSR **87**, 191 (1952).

[14] Akimov, Kuznetov, and Leksin, Pribory i Tekh, Eksperim. **2**, 70 (1956).

[15] Iu. M. Kazarinov and Iu. N. Simonov, J. Exptl. Theoret. Phys. **31**, 169 (1956).

[16] Meshcheriakov, Neganov, Soroko, and Vzorov, Dokl. Akad. Nauk SSSR **99**, 959 (1954).

[17] V. I. Veksler, Dokl. Akad. Nauk SSSR **82**, 865 (1952); D. I. Blokhintsev and B. B. Kadomtsev, The Atomic Station of the Acad of Sciences, U.S.S.R., Survey (1952).

Translated by M. J. Stevenson
109

SOVIET PHYSICS JETP VOLUME 5, NUMBER 3 OCTOBER, 1957

Elastic Scattering of 360 Mev Positive π-Mesons by Protons

N. A. MITIN AND E. L. GRIGOR'EV
Joint Institute for Nuclear Research

(Submitted to JETP editor October 19, 1957)
J. Exptl. Theoret. Phys. (U.S.S.R.) 32, 445-452 (March, 1957)

Photographic plates were used to study the angular distribution of 360 ±10 Mev π^+ mesons elastically scattered by protons. The differential cross section derived from 218 scattering events has the form (1) for *SP* analysis and the form (2) for *SPD* analysis. The phase shifts which correspond to these distributions are (*A*) and (*B*).

EXPERIMENTS involving a measurement of differential cross sections for the elastic scattering of π mesons by protons make it possible to determine which states take part in the scattering. It is also possible to calculate the phase shifts which correspond to those states. A phase analysis of the data for the scattering of π^+ mesons was carried out recently for energies up to 310 Mev[1,2].

In the present work the angular distribution of π^+ mesons with energies of 360 ±10 Mev was measured using photographic plates. The mesons were scattered by hydrogen nuclei contained in the photographic emulsions. The experiments were carried out on the synchrocyclotron of the Joint Institute for Nuclear Research.

Electron-sensitive photographic plates with emulsions 400 μ thick were exposed in a beam of π^+ mesons emerging from a magnetic meson spectrometer[3]. π mesons were produced in a carbon target 5 cm thick by a beam of 657 Mev protons brought out from the synchrocyclotron chamber. Mesons emitted from the target at an angle of 8.5° were deflected by the magnetic field of the spectrometer after preliminary collimation. The narrow converging beam of measons then passed through a 4 meter collimator at whose exit the photographic plates were placed. A copper shield 3 cm thick was used to protect the plates from protons. The energy of the mesons passing through this filter was measured to be 360 ±10 Mev. The intensity of the meson beam was about 4 mesons/cm^2 sec. The search for events was carried out by examination of photographic plates in sections by using immersion lenses, with about half the area examined at a magnification 630 times and the remainder at a magnification of 450 times. A significant fraction of the area of photographic plates was subjected to a careful second examination by various observers. This second examination disclosed a total of 8 previously-overlooked scattering events, evidencing a very high degree of efficiency in the examination of photographic plates.

The criteria used in the identification of the elastic scattering events were the angular correlation between the scattered mesons and the proton recoil, and co-planarity. Those events in which the deviation from co-planarity and the calculated angular correlation exceeded 1° were discarded.

A total of 218 scattering events were found in the angular interval of 10° to 170° in the center of mass coordinate system. The summation interval was 20°. A distribution of the number of scattering events with the angular intervals is given in the table.

Angular Intervals in center of mass system, in degrees	Corresponding angular intervals in the laboratory system of coordinates	Number of events in given interval	$\frac{d\sigma}{d\Omega}\cdot 10^{27}$ cm^2/sterad
10— 30	7— 21	42	11,2±1,7
30— 50	21— 36	64	9,2±1,2
50— 70	36— 52	49	5,2±0,7
70— 90	52— 70	24	2,2±0,5
90—110	70— 89	10	0,9±0,3
110—130	89—111	10	1,1±0,3
13[illegible]—150	111—138	13	1,9±0,5
150—170	138—166	6	1,6±0,6
	Total	218	

The angular distribution was normalized to satisfy the following equality

$$\sum_i \frac{d\sigma}{d\Omega}(\vartheta_i)\,\Delta\Omega_i = \sigma_t.$$

The total cross section of the elastic scattering σ_t

was chosen to be equal to 43.4×10^{-27} cm^{2}[4].

The experimental data is shown in Figure 1. Substitution of the experimental results into the series of Legendre polynomials

$$\frac{d\sigma}{d\Omega} = \sum_n A_n P_n(\cos\vartheta),$$

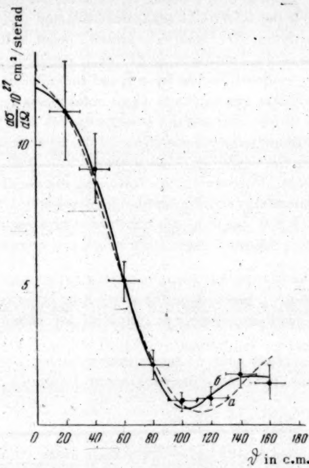

FIG. 1. Differential cross section for elastic scattering of mesons. Curves *a* and *b* are calculated from Eq. (1) and Eq. (2) respectively.

where A_n is computed from the equation

$$A_n = \frac{2n+1}{2} \sum_i \frac{d\sigma}{d\Omega}(\vartheta_i)\, P_n(\cos\vartheta_i)\, \Delta\cos\vartheta_i$$

leads to the following expression for the differential cross section:

$$d\sigma/d\Omega = [3{,}43P_0 + 4{,}63P_1 + 4{,}20P_2 + + 0{,}57P_3 - 0{,}81P_4]\cdot 10^{-27}\ \text{cm}^2/\ \text{sterad}$$

By writing out his expression it is possible to express the differential cross section in a power series in $\cos\vartheta$. This power series has the form:

$$d\sigma/d\Omega = [(1{,}33 \pm 0{,}20) + (4{,}63 \pm 0{,}62)\cos\vartheta + (6{,}30 \pm 1{,}42)\cos^2\vartheta]\cdot 10^{-27}\ \text{cm}^2/\text{sterad} \quad (1)$$

if only the first three terms are retained, and

$$d\sigma/d\Omega = [(1{,}02 \pm 0{,}16) + (3{,}78 \pm 0{,}48)\cos\vartheta + (9{,}35 \pm 1{,}31)\cos^2\vartheta + (1{,}42 \pm 0{,}86)\cos^3\vartheta - (3{,}56 \pm 1{,}64)\cos^4\vartheta]\cdot 10^{-27}\ \text{cm}^2/\text{sterad} \quad (2)$$

if the terms up to $n=4$ are included (see Fig. 1).

Owing to the low statistical accuracy of the obtained results it is difficult at first sight to find preference for one or the other expression for the differential cross section, even though it is evident from the figure that in the region of large angles curve *b* fits the experimental results better than curve a.

Scattering of π mesons by protons in *S, P* and *D* states with isotopic spin $T = 3/2$ is known to be characterized by five phase shifts α_3, α_{31}, α_{33}, δ_{33}, and δ_{35}, corresponding to the states *S*, $P_{1/2}$, $P_{3/2}$, $D_{3/2}$ and $D_{5/2}$ respectively. Ashkin and Vosko[5] have shown that the mathematical formulation of the problem of finding four solutions for the phase of π^+-p scattering by *SP* analysis. However, many physical considerations and the requirement of a continuous and smooth variation of the phase shifts with energies make it possible to select a solution in which α_{33} has a resonance character[6], i. e., passes through 90°. Taking this circumstance into account we have sought in our phase analysis of the experimental data only that solution corresponding to a resonance character of the phase α_{33}.

The optimum phase shifts can be determined in a general case only with electronic computers or special mechanical phase analyzers. However, under many simplifying conditions the phase analysis can be carried out in a sufficiently simple way. This happens for example, when a differential scattering cross section can be expressed in the form

$$d\sigma/d\Omega = a_0 + a_1\cos\vartheta + a_2\cos^2\vartheta.$$

If it is assumed that only the *S* and *P* states participate in the scattering, the phase shifts corresponding to these states can be determined in a given case graphically[5]. The phase shifts calculated graphically using Eq. 1 are:

$$\alpha_{33} = 146°;\ \alpha_{31} = -14°;\ \alpha_3 = -31°. \quad \text{(A)}$$

Phase analysis which takes into account contributions from *S, P* and *D* states (*SPD* analysis) was carried out with a mechanical phase analyzer[7].

The following phase shifts were obtained

$$\alpha_{33} = 143°;\ \alpha_{31} = -5°;\ \alpha_3 = -14°; \qquad \text{(B)}$$
$$\delta_{33} = 10°;\ \delta_{35} = -13°.$$

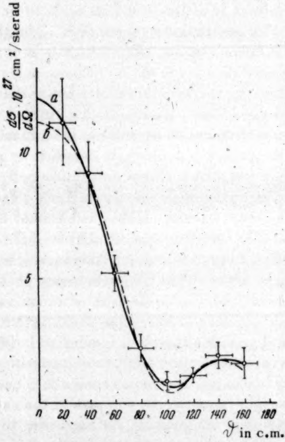

FIG. 2. Differential cross section for elastic scattering of mesons. Curves *a* and *b* are computed from phase sets *B* and *C*.

The differential cross sections calculated using the above set of phases are shown in Figure 2, curve *a*. From the quoted values of the phase shifts it is evident that the magnitudes of the phase α_{33} are practically equal both for *SP* and for *SPD* analyses. The dependence of this phase on the meson momentum

$$(\eta^3/\omega)\,\mathrm{ctg}\,\alpha_{33} = 9{,}3\,(1 - \omega/2{,}15),$$

as proposed by Chew and Low[8], does not hold at meson energies of 360 Mev (η is the momentum of the meson in the center of mass system in μc units; ω is the total energy in the center of mass system after subtracting the proton rest energy, in μc^2 units). A deviation from this dependence is already noticeable for meson energies above 240 Mev[2]; for 360 Mev mesons this deviation is approximately 20°. The values of the phase α_{33} given above agree well with the expression

$$\eta^3\,\mathrm{ctg}\,\alpha_{33} = 4{,}3 + 0{,}6\,\eta^2 - 0{,}8\,\eta^4,$$

proposed by Mukhin et al[2].

The magnitude of the phase α_3 depends strongly on whether the *D* state is taken into account in the phase analysis. *SPD* analysis yields almost half the value of $|\alpha_3|$ obtained by *SP* analysis. This observation evidently holds for a broad range of meson energies[2]. The quantity $\alpha_3 = -14°$ obtained in the analysis which included the *D* state agrees well with the linear dependence of α_3 on the meson momentum in the center of mass system: $\alpha_3 = -0.11\mu$[9].

Mukhin et al[2] proposed the following dependence of the phases δ_{33} and δ_{35} on the momentum:

$$\delta_{33} \approx -\delta_{35} = 0{,}20°\,\eta^5.$$

Taking these expressions into consideration and assuming that α_3 depends on the momentum linearly, $\alpha_3 = -6.3°\,\eta$, it is possible to calculate the phase shifts α_{33} and α_{31} from the condition that the total scattering cross section determined from the phase shifts must agree with the experimental value:

$$\sigma_t = 4\pi ƛ^2\,[\sin^2\alpha_3 + \sin^2\alpha_{31}$$
$$+ 2(\sin^2\alpha_{33} + \sin^2\delta_{33}) + 3\sin^2\delta_{35}].$$

The phase shifts calculated in this manner are:

$$\alpha_{33} = 148°;\ \alpha_{31} = -4°;$$
$$\alpha_3 = -15°;\ \delta_{33} = -\delta_{35} = 15°. \qquad \text{(C)}$$

The differential scattering cross sections corresponding to this set of phases is shown in Figure 2 (curve *b*). It is evident from the figure that curve *b* fits the experimental data as well as curve *a*. It must be noted, taking into account the statistical accuracy of the results, that both sets of phases are almost identical.

It is interesting to consider the results from the point in view of an application of the causality [illegible]ndition to the meson-nucleon scattering[10]. The energy dependence of the real part of the forward scattering amplitude was previously obtained[11, 12] from the data on the total meson-nucleon scattering cross section. It is possible to compare the magnitude of the real part of the forward scattering cross section obtained in this manner with the amplitude obtained by means of the above sets of phases (*A*, *B*, *C*). If we denote by D^+ the real part of the forward scattering amplitude in the laboratory system of coordinates and by $ƛ$ and $ƛ_{cm}$ the meson wavelengths in the laboratory and the center of mass systems respectively, the relationship between the real part of the forward scattering amplitude and its value in terms of the phase shifts assumes the form:

$$2\lambda\lambda_{\mathrm{cms}}^{-2}\,\mathrm{D}_{+} = \sin 2\alpha_{3} + \sin 2\alpha_{31} + 2\,(\sin 2\alpha_{33} + \sin 2\delta_{33}) + 3\sin 2\delta_{35} + \dots$$

Substituting into this expression the magnitudes of the phase shifts from sets *A*, *B*, *C*, we obtain -3.20, -3.22, and -2.96 for the right hand side and -3.16 for the left hand side. This result points out the good agreement between the real part of the forward scattering amplitude calculated from the causality condition and the values calculated using phase shifts obtained from angular distribution. A similar deduction was made in a study of the scattering of mesons in a broad energy range up to 310 Mev. The results obtained in the present work give grounds for assuming that this deduction can be extended to meson energies up to 360 Mev.

It is necessary to note in conclusion that the experimental data presented still do not afford a sufficiently strong proof that it is necessary to include *D* states in a phase analysis of the results. It is even less possible to make any conclusions concerning the dependence of the phase shifts δ_{33} and δ_{35} on the meson momentum. However, if it is assumed that the inclusion of the *D* states is justified, it is possible to deduce conclusively from the results of the *SPD* analysis for 307 and 360 Mev mesons that the phase shifts for the $D_{3/2}$ and $D_{5/2}$ states are approximately equal, opposite in sign, and have a tendency to increase with the meson energy.

The authors wish to express their gratitude to B. S. Neganov and V. P. Zrelov for assistance in the exposure of the plates, and also to L. I. Lapidus and N. P. Klepikov for discussion of the obtained results.

---

[1] E. L. Grigoriev and N. A. Mitin, J. Exptl. Theoret. Phys. (U.S.S.R.) **31**, 37 (1956). Soviet Physics JETP **4**, 10 (1957).

[2] Mukhin, Ozerov, Pontecorvo, Grigor'ev, and Mitin, Mitin, CERN Symposium, Geneva (1956).

[3] Meshcheriakov, Neganov, Zrelov, Vzorov, and Shabudin, J. Exptl. Theoret. Phys. **31**, 45 (1956). Soviet Physics JETP **4**, 60 (1957).

[4] Ignatenko, Mukhin, Ozerov, and Pontecorvo, Dokl. Akad. Nauk SSSR **103**, 209 (1955).

[5] J. Ashkin and S. H. Vosko, Phys. Rev. **91**, 1248 (1953).

[6] Bethe, Hoffman, Metropolis, and Alei, Phys. Rev. **95**, 1586 (1954).

[7] N. P. Klepikov, J. Exptl. Theoret. Phys. **30**, 1155 (1956). Soviet Physics JETP **3**, 981 (1957).

[8] G. Chew and F. E. Low, Proc. Fifth Annual Rochester Conference (1955).

[9] J. Orear, Phys. Rev. **96**, 176 (1954).

[10] Goldberger, Miyazawa, and Oehme, Phys. Rev. **99**, 986 (1955).

[11] Anderson, Davidon, and Kruse, Phys. Rev. **100**, 288 (1955).

[12] R. M. Sternheimer, Phys. Rev. **101**, 384 (1956).

Translated by M. J. Stevenson

111

SOVIET PHYSICS JEPT VOLUME 5, NUMBER 3 OCTOBER 1957

Loss of Two Electrons in Single Collisions Between Negative Hydrogen Ions and Molecules of Gases

IA. M. FOGEL, V. A. ANKUDINOV, AND R. E. SLABOSPITSKII
Physico-Technical Institute, Ukrainian Academy of Sciences.

(Submitted to JETP editor, October 22, 1956)
J. Exptl. Theoret. Phys. USSR, **32**, 453-462 (March, 1957)

The effective cross sections for the loss of two electrons in single collisions between negative hydrogen ions and He, Ne, A, Kr and Xe atoms and H_2, N_2, and O_2 molecules were measured. The measurements were carried out in a mass spectrometer in the energy range from 5 to 40 kev.

INTRODUCTION

THE measurements of effective cross sections for the loss of several electrons ("stripping") in single collisions between ions and gas molecules have been made recently in connection with the use of this phenomenon for the production of ions with multiple charges. Some of the studies dealing with this phenomenon investigate the loss of electrons by singly charged positive ions[1-5]. There are several investigations[6-12] devoted to the measurement of effective cross sections for the loss of a single electron in collisions of negative ions with gas molecules. There is only one paper[13] which cites the data on the loss of two electrons by ions Cl^-, Br^-, I^-, Na^-, Sb^-, Bi^-, Sb_2^-, in collisions with He and A atoms and with H_2 and N_2 molecules.

This paper deals with the measurement of effective cross sections σ_{-11}* for the loss of two electrons by the negative hydrogen ions with energies of 5 to 40 kev in single collisions with He, Ne, A, Kr, Xe atoms and with H_2, N_2, and O_2 molecules. The measurement of this cross section for the negative hydrogen ions is of considerable interest because these cross sections can be compared with electron loss cross sections for other particles with the same electron shell structure (He, Li^+). Furthermore, the knowledge of the cross section σ_{-11} enables one to compare it with the single electron loss cross section σ_{-10} as well as with the cross section σ_{-11} for the double electron capture by a proton.

DESCRIPTION OF THE EXPERIMENTAL SETUP AND THE MEASUREMENT METHODOLOGY

To obtain negative hydrogen ions, we used a previously developed method[14] for the transformation of positive hydrogen ions into negative ions by their passage through an ultrasonic stream of mercury vapor ("mercury vapor target").

The schematic diagram of the layout for the measurements described below is shown in Fig. 1. A detailed description of the apparatus for producing and shaping the beam of negative hydrogen atoms is given in Ref. 14.

By means of the magnetic analyzer *1*, the ion beam is separated from the protons and the neutral hydrogen atoms and is directed into the collision chamber *2*. The beam enters the collision chamber through a diaphragm 4 mm in diameter attached to the wall of a duct with an inner diameter of 5 mm and a length of 50 mm. The beam leaves the collision chamber through a duct having the same length and diameter as the inlet duct. The effective length of the collision chamber is 10 cm. The currents of the beam which entered and left the collision chamber were measured by means of Faraday cylinders 4 and 5, magnetically controlled. The current of the H_1^- ion beam entering the collision chamber was in the 10^{-10} to 5×10^{-9} A. range. The highest value of the current was obtained for the conversion $H_1^+ \rightarrow H_1^-$ with energies from 20 to 30 kev. To obtain H_1^- ions with energies of 5 kev, it was necessary to use the conversion $H_2^+ \rightarrow H_1^-$, because the ion gun focused poorly the primary beam of positive ions for this energy. The H_2^+ ion concentration was low in the primary beam of the high frequency ion source and, as a result, the H_1^- ion current passing through the collision chamber in this case did not exceed 10^{-10} A.

The separation of the beam leaving the collision chamber into neutral, positive, and negative components was achieved by means of the electric field in the parallel plate condenser *6* having plates 80 mm long at a distance of 28 mm from each other. The measurement of the currents of the positive and

---

*σ_{ik} is the effective cross section of the process in which a particle with a charge *ie* is converted into a particle with a charge *ke*.

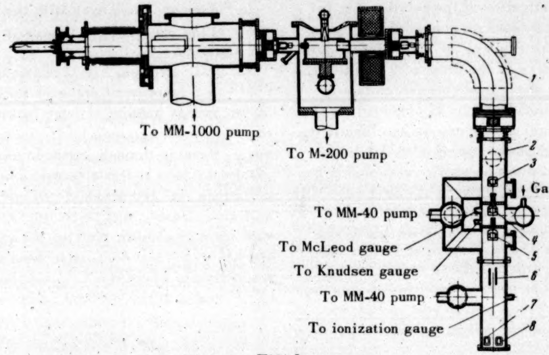

FIG. 1.

negative beam components was accomplished by means of two string electrometers connected to the Faraday cylinders *7* and *8*. The fibers of both electrometers were projected on two screens located one above the other so that the measurement of the beam component currents could be made simultaneously. This method eliminated the error due to random intensity fluctuations of the primary H_1^- ion beam. The pressure of the gas admitted into the collision chamber was measured with a Knudsen gauge, calibrated against a McLeod gauge. The calibration of the Knudsen gauge was made for all the gases in the investigation and was repeated several times during the measurements.

The collision and analyzer chambers were evacuated by separate MM-40 oil diffusion pumps. To freeze out the condensed vapors, liquid air traps were inserted into the collision chamber and into the space on either side of it. Besides, one more trap was located above the throat of the MM-40 pump which evacuated the collision chamber. The residual gas pressure in the collision chamber was 10^{-5} mm Hg.

The mass spectroscopic method fully described in Refs. 1, 15, 16 was applied to the determination of the effective cross sections σ_{-11}.

From the solutions of the differential equations [see Eq. (3) in Ref. 16), determining the beam composition produced as a result of the negative hydrogen ions passing through the gas in the collision chamber, (n = the number of gas atoms in 1 cm³, L = effective length of the collision chamber), the formula is

$$I^+ / I^- = \sigma_{-11} nL + \frac{1}{2} [\sigma_{-10} \sigma_{01} + \sigma_{-11} (\sigma_{-10} + \sigma_{-11} - \sigma_{10} - \sigma_{1-1})] (nL)^2, \quad (1)$$

where I^+ and I^- — the currents of the protons and negative hydrogen ions in the beam emerging from the collision chamber. The dependence of I^+/I^- on the gas pressure in the collision chamber can be written in the following form:

$$I^+ / I^- = \varkappa p + \Omega p^2, \quad (2)$$

where

$$\varkappa = \sigma_{-11} L / kT, \quad \Omega = \frac{1}{2} [\sigma_{-10} \sigma_{01} + \sigma_{-11} (\sigma_{-10} + \sigma_{-11} - \sigma_{10} - \sigma_{1-1})] (L / kT)^2. \quad (3)$$

During the investigation of the relationship between I^+/I^- and pressure we observed two cases: in the first case the graph of the I^+/I^- function is linear up to pressures on the order of $2+3\times10^{-4}$ mm Hg. and it is only above these pressures that a marked deviation from linearity is observed; in the second case, beginning with pressures close to p_Φ (p_Φ — the residual gas pressure in the collision chamber) one observes a parabolic relationship between I^+/I^- and p. Evidently, in the first case with pressures p 10^{-4} mm Hg the assumption $(\Omega/\kappa)p \ll 1$ is satisfied and formula (2) can be written in the form:

$$I^+ / I^- = \varkappa p. \tag{4}$$

In the second case even with the smallest pressures of the admitted gas the above condition is not satisfied.

As an illustration, Fig. 2 shows the graph of I^+/I^- as a function of pressure for H_1^- ions with 30 kev energy passing through hydrogen; fig. 3 — the corresponding graph for H_1^- ions with 20.6 kev energy passing through argon. In plotting these graphs the loss of two electrons by H_1^- ions during collisions with the residual gas molecules in the collision chamber was taken into account. This was accomplished by plotting the values of $p - p_\Phi$ and $(I^+/I^-) - (I^+/I^-)_\Phi$ abscissas and ordinates respectively, where $(I^+/I^-)_\Phi$ -is the value of the (I^+/I^-) ratio at the residual gas pressure.

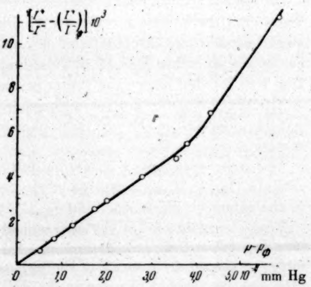

FIG. 2.

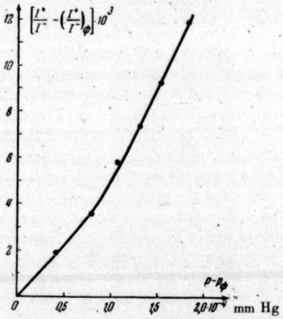

FIG. 3.

In the case where a linear portion was observed in the I^+/I^- graph, the cross section σ_{-11} was determined from this linear portion by the method of least squares. It is to be noted that if one determines σ_{-11} from all the points of the $I^+/I^- = f(p)$ curve which fit a parabola, then the calculated value of σ_{-11} does not differ significantly from the value calculated from the linear part of the graph.

If the linear portion was not present in the graph $I^+/I^- = f(p)$ over the range of measured pressures, then the cross section σ_{-11} was determined by the method of least squares according to formula (2). For the rapid selection of points satisfying this formula it is expedient to represent it in the form

$$(I^+/I^-)/p = \varkappa + \Omega\, p. \tag{5}$$

As can be seen from formula (5), the value $(I^+/I^-)/p$ is a linear function of p in the range of pressures for which formula (2) holds. The cross section σ_{-11} is determined from formula (5) by the method of least squares.

The method used by us for the measurement of cross sections σ_{-11} has inherent systematic errors associated with the effect of pressure and composition of the residual gas in the apparatus on the value of the measured cross section,* with the unequal scattering of negative hydrogen ions and protons in the collision chamber, and with the unequal weakening of the negative hydrogen ion and proton beams during their passage from the collision chamber to the Faraday cylinders of the analyzer. As for the error associated with the presence of residual gas in the path of the beam, we were able to show by investigating dependence of the measured value of σ_{-11} on the value of $(I^+/I^-)_\phi$ that for our conditions this error was small and was within the limits of random experimental errors. To clarify the effect of unequal scattering of ions and protons in a hydrogen-filled collision chamber, cross sections σ_{-11} were measured with a diaphragm 2 mm in diameter attached to the end of the exit duct, and without the diaphragm. The diaphragm decreased considerably the solid angle for the particles leaving the collision chamber. It turned out that the cross section values σ_{-11} measured with and without a diaphragm in the exit duct were the same within the limits of experimental errors. Thus, the effect under consideration, for the case investigated by us, can not materially alter the measurement results. The correction for the unequal weakening of the negative and positive beams in the analyzer chamber for the cases when it can be calculated* does not exceed several tenths of a percent and is consequently unimportant. The random error of the individual cross section σ_{-11} measurement was ±15%. To ascertain the most probable error, some of the cross sections were measured 5-7 times; this error was ±7%.

---

*This error was detected and discussed by us in Ref. 17.

The energy of the negative hydrogen ions was determined by the summation of the potential differential differences in the ion source and the accelerator tube. These potential differences were measured with electrostatic voltmeters, calibrated with a resistance voltmeter which was used in Refs. 15, 16. Such a method for determining the H_1^- ion energies could lead to an error if the protons lost an appreciable part of their energy in the mercury vapor stream while passing through it. Using the magnetic analyzer of our setup, we determined the proton energy loss during the passage through a beam of mercury vapor 2-3 × 10^{15} *atoms/cm²* thick, giving the optimum conversion $H_1^+ \rightarrow H_1^-$. It turned out that this energy loss was quite small and, as a consequence, the energy determination of the negative hydrogen ions by the above mentioned method is completely justified. The error associated with the measurement of the negative hydrogen ion energy was on the order of ±3%.

During the course of the present investigation, we obtained some information about the reliability of the steam-jet target. The steam-jet target worked more than 700 hours and during that time the boiler had to be taken apart only once in order to replace the nickel-constantan thermocouple, in which the constantan wire was corroded by the mercury vapor.

DATA AND DISCUSSION

The effective cross sections were measured for the loss of two electrons in collisions of H_1^- ions with energies of 5 to 40 kev with He, Ne, A, Kr, and Xe atoms, and with H_2, N_2 and O_2 molecules. The collision chamber was filled with palladium-filtered hydrogen, spectroscopically pure helium, neon, krypton, and xenon, oxygen with 0.9% impurities, argon with 0.3% impurities, and nitrogen with 0.3% impurities.

There are shown in Figs. 4 and 5 the curves of the relationship between the effective cross section σ_{-11} and the energy of the H_1^- ions for atomic and molecular gases. The value of σ_{-11} for each energy was obtained by averaging two measurements. As can be seen from Figs. 4 and 5, the effective cross section σ_{-11} for H_1^- ions in the investigated energy range grows with energy in neon, argon, xenon, nitrogen, and oxygen; in krypton the increase in σ_{-11} takes place up to an energy of 20.6 kev and thereafter remains constant to the end of the interval; in hydrogen, the cross section σ_{-11} remains constant over the entire interval; in helium, a maximum is indicated in the neighborhood of 10 kev, after which the cross section decreases monotonically with energy. The cross section σ_{-11} value varies from 3.3×10^{-17} cm² (in Kr, energy of 5.1 kev) to 1.8×10^{-16} cm² (in Xe, energy of 39.7 kev). One observes the dependence of the cross section σ_{-11} on the gas particle on colliding with which the H_1^- ion loses two electrons. In the case of molecular gases, the cross section σ_{-11} in oxygen and nitrogen is considerably greater than in hydrogen over the entire range of explored energies. In atomic gases, the cross section σ_{-11} is approximately the same at the beginning of the interval for all gases, but at the end of the interval the value is considerably greater for the heavy gases A, Kr, and Xe than for the light gases He and Ne.

As mentioned in the Introduction, there were no data in the literature on cross sections σ_{-11} for H_1^- ions. A comparison is only possible for the cross section data σ_{-11} of a number of heavy ions obtained by Dukel'skii and Fedorenko.[13] It is most expedient to compare the cross sections for the same ion velocities. Unfortunately, the data of Ref. 13 and ours differ widely with respect to the velocity intervals. The data on the cross sections σ_{-11} for Na$^-$ ions came closest to the interval of velocities investigated by us. The comparison of cross sections σ_{-11} for H_1^- and Na$^-$ ions is interesting also because, according to the most recent data[18], the electron affinity of for the sodium atom is equal to 0.84 ev, which is very close to that for hydrogen atoms (0.75 ev).

---

*To calculate this correction, it is necessary to know the cross section σ_{10} and σ_{-10} for the gas admitted to the collision chamber.

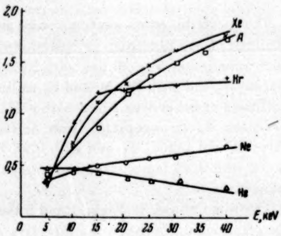

FIG. 4

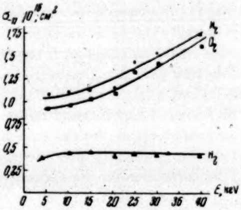

FIG. 5.

The curves of the relationship $\sigma_{-11} = f(v)$ for H$^-$ and Na$^-$ ions are shown in Fig. 6. By extrapolating the graph $\sigma_{-11} = f(v)$ for the H_1^- ion into the region of velocities where the corresponding curve of the Na$^-$ ion is located, the cross section of the process $\mathrm{H}_1^- \to \mathrm{H}_1^+$ should decrease. It follows therefrom that in this region of velocities the cross section of the process $\mathrm{Na}^- \to \mathrm{Na}^+$ should be larger than the cross section of the $\mathrm{H}_1^- \to \mathrm{H}_1^+$ process. It was established in Ref. 17 that the capture cross section of two electrons by a positive ion increases with a decrease in the binding energy of the electrons in the particle losing them. One can assume that the same relationship holds for the stripping of two electrons in collision of negative ions with gas molecules. The fact that the cross section σ_{-11} is larger for the process $\mathrm{Na}^- \to \mathrm{Na}^+$ than for the process $\mathrm{H}_1^- \to \mathrm{H}_1^+$ confirms the stated assumption, since the binding energy of the stripped electrons in the Na$^-$ ion is equal to the sum of the electron affinity and the first ionization energies of the Na atom, and is smaller than the corresponding quantity for the H_1^- ion. However, it is necessary to note that the paper gives data which contradict the assertion that the cross section σ_{-11} increases with a decrease in the binding energy of the stripped electrons. Evidently, an important role is played by the actual electron shell structure of the negative ion which is losing two electrons.

An opportunity presents itself to compare the cross sections for the loss of two electrons by H_1^- ions with the cross section σ_{-10} for the loss of a single electron by the same ions. The cross sections σ_{-10} for H_1^- ions in He, Ne, A, Kr, and Xe gases were measured by Stedeford and Hasted[10]. The corresponding measurements in hydrogen were made by Whittier[12]. The curves showing the relationship between cross sections σ_{-11} (solid curves) and σ_{-10} (dotted curves) and H_1^- ion energies are compared in Fig. 7. As can be seen from this figure, the effective cross section for the loss of two electrons in the investigated energy range is considerably smaller than the effective cross section for the loss of a single electron. The ratio σ_{-11}/σ_{10} for H_2, A, Kr, and Xe decreases with a decrease in energy, remains approximately constant over the entire energy range for Ne, and goes through a minimum for He at 15 kev. From this data given below, one can see the limits within which the ratio σ_{-11}/σ_{10} changes for various gases in passing from higher to lower energies of H_1^- ions.

The values cited in the Table show that in evaluating the intensity reduction of the H_1^- ion beam, it is sufficient (because of inelastic collisions with gas molecules) to account for the loss of a single electron only. Using these data, one can evaluate the errors which arise as a result of not taking into account the process of double electron loss by negative ions during the measurement of the effective cross section of a single electron loss by the method

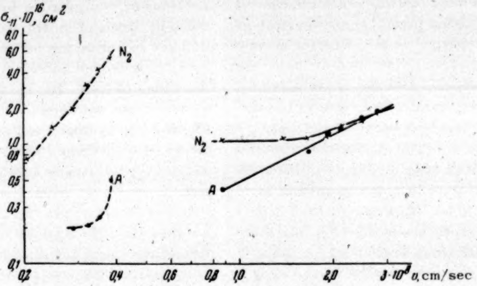

FIG. 6. Solid lines – H_1^- ions; dotted – Na^- ions.

of collecting slow ions and electrons produced in the gas by the passage through it of a beam of fast particles.*

Gas	σ_{-11}/σ_{10}
H_2	0.12-0.06
He	0.07-0.09
Ne	0.08
A	0.07-0.03
Kr	0.04-0.016
Xe	0.04-.02

By the method of collecting slow particles, one actually measures the cross section $\sigma = \sigma_{-10} + 2\sigma_{-11}$, from which the true cross section of a single electron loss $\sigma_{-10} = \sigma[1 - 2(\sigma_{-11}/\sigma_{-10})]$. The ratio $\sigma_{-11}/\sigma_{-10}$ was given above. As can be seen from the given data, the systematic error in Ref. 10 associated with the presence of the double electron loss is not large and in the worst case (He) does not exceed 20%. However, one must keep in mind that with the increase in ionic energies, because of the increase in the ratio $\sigma_{-11}/\sigma_{-10}$ with energy, this error may become quite considerable, and the use of the method of collecting slow particles for measuring cross sections σ_{-10} becomes inadmissible.

In spite of the large differences in the cross-section values of σ_{-11} and σ_{-10}, the nature of their dependence on the H_1^- ion energies is the same in the interval under study. This is particularly noticeable for the curves $\sigma = f(\varepsilon)$ in He and Ne. It is interesting to note that for single and double electron capture cross sections in hydrogen and helium (see Figs. 3 and 4 in Ref. 16), the curves $\sigma = f(\varepsilon)$ are different in approximately the same energy range.

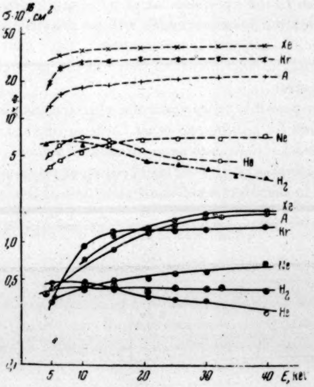

FIG. 7.

The experimental data for single [7, 10] and double electron [16, 17] capture cross sections are in definite agreement with the adiabatic hypothesis of Massey[19]. The sequence of maxima on the graphs of cross sections versus ion energy follows from the well-known Massey condition [see Eq. (8) in Ref. 16] with the assumption that the collision parameter differs little for different ion-molecule pairs, but that its value for a single electron exchange is considerably larger than for a double electron exchange. Assuming also that for double electron loss processes the collision parameter is approximately the same for different pairs, and having in mind that the resonance defect (the sum of the ionization potential and electron affinity of the hydrogen atom) is the same for all collision processes between H_1^- ions and atoms of inert gases, it is to be expected that the cross section maximum on the energy relationship graphs should be observed for all these processes at the same energy. As can be seen in Fig. 4, the cross section σ_{-11} maximum for helium is at an energy of about 10 kev, whereas for the other inert gases it is at an energy greater than 40 kev. In some contradiction with the adiabatic hypothesis is also the fact that for small energies the cross section σ_{-11} is quite large. Hasted [7,9] also points out the discrepancy between his data on the single electron loss cross sections and the adiabatic hypothesis. The paper by Bates and Massey [20] gives some reasons for the inapplicability of the adiabatic hypothesis to the processes for the single electron loss. A sounder judgment as to the existence of an adiabatic region in two electron loss processes will be possible after the cross section σ_{-11} measurements have been made with smaller energies than those in the present investigation.

---

*It was by this very method that Stedeford and Hasted[10] measured the cross section σ_{-10} in inert gases.

It is possible to compare the electron loss cross sections for helium and other "helium-like" particles (H^- and Li^+). As has been already mentioned, such a comparision is interesting because of the similarity in the electronic shell structure of these particles.

Krasner [21] measured the sums of effective cross sections $\sigma_{01} + \sigma_{02}$ for the loss of one and two electrons by atoms of helium with energies from 100 to 450 kev in collisions with helium atoms and molecules of hydrogen and air. Using the data of our work and those of Refs. 10, 12, the sum $\sigma_{-10} + \sigma_{-11}$ of effective cross sections for [illegible] loss of one and two electrons in hydrogen and helium can be calculated for negative hydrogen ions. For Li^+ the sum of cross sections in air can be calculated from the data of Ref. 2.

In Fig. 8 are shown the curves of the relationship between the $\sigma_{01} + \sigma_{02}$ cross sections and velocities for helium atoms and the corresponding graphs of the cross section sums $\sigma_{-10} + \sigma_{-11}$ for negative hydrogen ions and $\sigma_{12} + \sigma_{16}$ for Li^+ ions. As is seen from the drawing, for the same velocities, the electron loss cross sections by particles of the isoelectronic sequence H_1^-, He, Li^+ increase with a decrease in the binding energy of the lost electrons. A fact that calls attention to itself is that electron loss cross sections by these particles in the same velocity interval have a different dependence on velocity namely, the electron loss cross sections by H_1^- ions decrease; for helium atoms these cross sections increase slowly, and for Li^+ ions-increase rapidly with an increase of the particle velocities. One might suppose that the comparison of the electron loss cross sections by different particles would be accomplished most expediently for the same values of the parameter $\gamma_i = v_i/v$, where v_i – the orbital velocity of the stripped electron in the moving particle, calculated

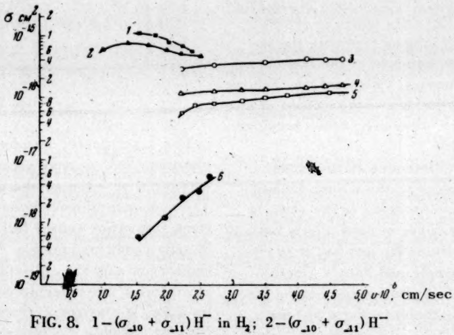

FIG. 8. 1 – $(\sigma_{-10} + \sigma_{-11})H^-$ in H_2; 2 – $(\sigma_{-10} + \sigma_{-11})H^-$ in He; 3 – $(\sigma_{01} + \sigma_{02})He^0$ in air; 4 – $(\sigma_{01} + \sigma_{02})He^0$ in He; 5 – $(\sigma_{01} + \sigma_{02})He^0$ in H_2; 6 – $(\sigma_{12} + \sigma_{13})L_7^+$ in air

from the formula ($v_i = 2V_i/m)^{1/2}$ (V_i – binding energy of the electron in the particle), and v – particle velocity.

Krasner[21] attempted to represent his results as well as those of Montague[22] and Kanner[23] as a function of the parameter γ_i. For the case of a moving helium atom the value of γ_i refers to either of the two 1s electrons. For this case, as can be shown easily, the electron binding energy is equal to the half-sum of the first and second ionization potentials of helium. In constructing the graph of the effective electron loss cross sections for helium and hydrogen as a function of the parameter γ_i, Krasner decreased the effective electron loss cross sections for helium atoms by a factor of two, because of the fact that an atom of helium has two 1s electrons. The points of the function $\sigma_{01} = f(\gamma)$ thus obtained for hydrogen and helium atoms moving in air and hydrogen fell on two smooth curves, from which Krasner drew the conclusion that the effective electron loss cross section, calculated for the equivalent removable electron, is a function of the parameter γ_i only. However, this conclusion has no general significance because, for other particles having only 1s electrons, the effective electrons loss cross section values do not lie on the curves plotted by Krasner; this is illustrated in Fig. 9 where, alongside the curves for the effective electron loss cross sections for hydrogen and helium atoms σ_{01} and $\frac{1}{2}\sigma_{01}$, the curves for $\frac{1}{2}\sigma_{-10}$ and $\frac{1}{2}\sigma_{12}$ are shown, corresponding to the cross sections from Refs. 2, 12 for H_1^- and Li^+ ions. In an article which appeared recently[24] it is stated that the data on the cross sections σ_{12} for He^+ ions do not fit the Krasner curve. Thus, it is impossible as yet to display a universal parameter which would determine the electron loss cross sections even for particles with the same electronic shell structure.

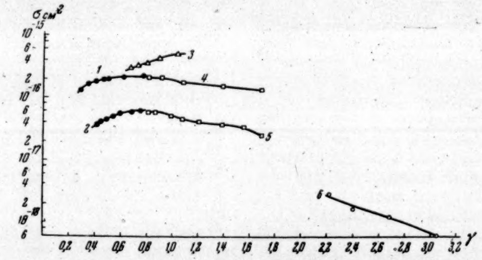

FIG. 9. 1 – $\sigma_{01}H^0$ in air; 2 – $\sigma_{01}H^0$ in H_2; 3 – $\frac{1}{2}\sigma_{-10}H^-$ in H_2; 4 – $\frac{1}{2}\sigma_{01}H^0$ in air; 5 – $\frac{1}{2}\sigma_{01}He^0$ in H_2; 6 – $\frac{1}{2}\sigma_{12}Li_7^+$ in air.

It is of some interest to compare the cross sections for the loss of two electrons by H_1^- ions measured in this investigation and the cross sections for the capture of two electrons by protons measured in Ref. 16. This comparison shows that the cross section σ_{1-1} is smaller than the cross section σ_{-11} for the entire investigated range of energies and for all investigated gases. For the gases He, Ne, A, N_2 and O_2 the ratio $\sigma_{1-1}/\sigma_{-11}$ does not exceed 7% and changes little with the energy of ions; for hydrogen the maximum value of this ratio is 30%.

The dependence of the ratio $\sigma_{1-1}/\sigma_{-11}$ on the parameter γ for Ne and H_2 is shown in Fig. 10 (the binding energy of either of the two electrons in the negative hydrogen ion was set equal to half the sum of the

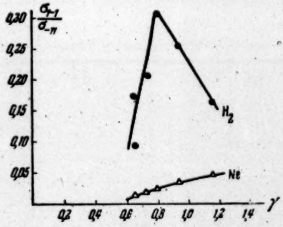

FIG. 10.

ionization potential and electron affinity of the hydrogen atom). The experimental data for the single electron exchange processes show (see Ref. 25) that the ratio σ_{10}/σ_{01} for hydrogen particles and the ratio σ_{21}/σ_{12} for helium particles is equal to one for $\gamma \approx 1$, *i.e.*, the cross sections for the capture and loss of a single electron are equal for a particle velocity equal to the orbital velocity of the electron. As is seen from Fig. 10, a similar situation does not take place for two-electron exchange processes.

D. V. Pilipenko participated in the investigation.

In conclusion the authors consider it a pleasant duty to express their thanks to prof. A. K. Val'ter for his constant interest in the investigation.

---

[1] N. V. Fedorenko, J. Tech. Phys. (U.S.S.R.) **24**, 769 (1954)

[2] Leviant, Korsunskii, Pivovar and Podgornii, Dokl. Akad. Nank SSSR, **103**, 403 (1955)

[3] Korsunskii, Piovar, Markus and Leviant, Dokl. Akad. Nank SSSR, **103**, 399 (1955)

[4] D. M. Kaminker and N. V. Fedorenko, J. Tech. Phys. (U.S.S.R.) **25**, 1843 (1955)

[5] Reynolds, Wyly and Zucker, Phys. Rev. **98**, 1825 (1955)

[6] V. M. Dukel'skii and E. Ia. Zandberg, J. Exptl. Theoret. Phys. (U.S.S.R.) **21**, 1270, (1951)

[7] J. B. Hasted, Proc. Roy. Soc. (London) **212A**, 235, (1952)

[8] V. M. Dukel'skii and E. Ia. Zandberg, J. Exptl. Theoret Phys. (U.S.S.R.) **24**, 339, (1953)

[9] J. B. Hasted, Proc. Roy. Soc. (London) **222A**, 74, (1954)

[10] J. B. H. Stedeford and J. B. Hasted, Proc. Roy. Soc. (London) **227A**, 446, (1955)

[11] J. B. Hasted and R. A. Smith, Proc. Roy. Soc. (London) **235A**, 349, (1956)

[12] A. C. Whittier, Canad. J. Phys. **32**, 275, (1954)

[13] V. M. Dukel'skii and N. V. Fedorenko, J. Exptl. Theoret. Phys. (U.S.S.R.) **29**, 473 (1955); Soviet Phys. J. Exptl. Theoret. Phys. (U.S.S.R.) **2**, 307 (1956)

[14] Fogel', Krupnik and Ankudinov, J. Tech. Phys. (U.S.S.R.) **26**, 1208, (1956)

[15] Ia. M. Fogel' and L. I. Krupnik, J. Exptl. Theoret. Phys. (U.S.S.R.) **29**, 209, (1955); Soviet Phys. J. Exptl. Theoret. Phys. (U.S.S.R.) **2**, 252 (1956)

[16] Ia. M. Fogel' and R. V. Mitin, J. Exptl. Theoret. Phys. (U.S.S.R.) **30**, 450, (1956); Soviet Phys. J. Exptl. Theoret. Phys. (U.S.S.R.) **3**, 334 (1957)

[17] Ia. Fogel', Mitin, and Koval', J. Exptl. Theoret. Phys. (U.S.S.R.) **31**, 397, (1956); Soviet Phys. J. Exptl. Theoret. Phys. (U.S.S.R.) **4**, 359 (1957)

[18] R. Gaspar and B. Molnar, Acta Phys. Hungar. **5**, 75, (1955)

[19] H. S. W. Massey, Rep. Progr. Phys. **12**, 248, (1949)

[20] D. R. Bates and H. S. W. Massey, Phil. Mag. **45**, 111, (1954)

[21] S. Krasner, Phys. Rev. **99**, 520, (1955)

[22] J. H. Montague, Phys. Rev. **81**, 1026, (1951)

[23] H. Kanner, Phys. Rev. **84**, 1211, (1951)

[24] Allison, Cuevas and Murphy, Phys. Rev. **102**, 1041, (1956)

[25] S. K. Allison and S. D. Warshaw, Rev. Mod. Phys. **25**, 779, (1953)

Translated by H. Kruglak
112

SOVIET PHYSICS JETP VOLUME 5, NUMBER 3 OCTOBER, 1957

Energy Spectrum of μ-Mesons in Extensive Atmospheric Cosmic Ray Showers

O. I. DOVZHENKO, B. A. NELEPO, AND S. I. NIKOL'SKII
P. N. Lebedev Physical Institute, Academy of Sciences, USSR

(Submitted to JETP editor November 3, 1956)
J. Exptl. Theoret. Physics (U.S.S.R.) 32, 463-466 (March, 1956)

The energy spectrum of μ-mesons in extensive atmospheric showers of varying primary energy was studied in the energy range from 0.3 to 3.5 Bev. The measurements were carried out at mountain altitudes. It was found that in the aforementioned energy range the energy spectrum of μ-mesons is independent of the energy of the primary particle which initiated the shower. The mean μ-meson energy decreases with the distance from the shower axis.

PREVIOUS experiments [1,2] on the absorption of the penetrating component of extensive atmospheric showers in a dense substance indicated that the energy spectrum of penetrating particles in extensive atmospheric showers near sea level can be represented by a law with an exponent ~ 0.6. This result was obtained by averaging the data over a wide interval of distances from the shower axis and over different energies of the primary particle. Nuclear passive (μ- mesons) as well as nuclear active particles of the penetrating component were recorded.

During the summer and fall of 1954, we carried out at Pamir (3,860 m above sea level) experiments to determine the nature of the energy spectrum of μ-mesons at three distances from the axis of an extensive atmospheric shower and made a comparison of μ-mesons spectra in showers of different primary energies. The energy of μ-mesons was determined from their absorption in lead and ground. The general experimental layout and the depth cross section of the pit are shown in Fig. 1. The control system (CS) consisted of three arrays of Geiger-Müller counters located above detectors of penetrating particles A, B and C, and also at 100 and 300 meters from them (Fig. 1). Above the detectors of penetrating particles there were placed a large number of hodoscopic counters for investigating the electron-photon component of the shower.[3]

The detector of penetrating particles A recorded μ-mesons with an energy $\geqslant 185$ Mev, detector B – μ-mesons with energy $\geqslant 1.7$ BeV, and detector C – μ-mesons with energy $\geqslant 3.5$ Bev. The area of the counters in detectors A, B, and C was 0.38, 2.4 and 2.4 m^2, respectively.

The use of detector counters connected to the hodoscopic arrangement permitted us to distinguish the passage of nuclear passive particles (μ-mesons) from the passage of nuclear active particles according to their shower producing ability. During the statistical treatment of the experimental data, we paid attention only to the cases of the recorded single

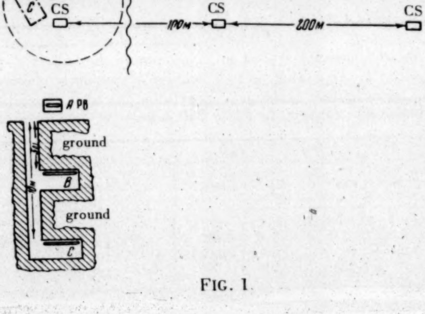

FIG. 1

penetrating particles not accompained by a shower under the dense absorber. The number of μ-mesons thus recorded is lowered, since μ-mesons initiating a δ-shower are excluded from the analysis. As shown by measurements, the number of such mesons constitutes 10 ±2%. The variation in this number with an increase in the thickness of the absorber above the setup does not exceed the experimental error. The high resolution of the apparatus used practically excluded random coincidence discharges in the counters.

The flux density of μ-mesons was determined from the formula

$$\rho_\mu = \frac{1}{\sigma} \ln \frac{N_1 N_2}{N_1 N_2 - N_3} .$$

Here σ = counter area of one hodoscopic group; N_3 = the number of recorded single μ-mesons; N_2 = the number of recorded extensive atmospheric showers; N_1 = the number of hodoscopic arrays of counters used during measurements.

The large system of hodoscopic counters located above the detectors of penetrating particles enabled us to determine the core location and the total number of charged particles in each recorded extensive atmospheric shower. The simultaneous determination of the core position, the total number of particles and the μ-mesons flux at various depth enabled us to determine the μ-meson energy spectrum for showers of varying energy. In all the cases investigated by us, the μ-meson energy spectrum can be represented by the law E_μ^{-n}, where E_μ – the energy of μ-mesons.

The value of the exponent n for showers with axes passing no farther than 8 m from detectors of penetrating particles are shown in Table 1. The energy of the shower-causing primary particle was assumed to be proportional to the total number of particles N in the shower ($E_0 \approx 2.5 \times 10^9 N$ ev)[5]. In the same table are shown the absolute values of the μ-meson flux density with the energy higher than that assigned to showers of a different primary energy.

As is seen from Table 1, the energy spectrum of μ-mesons in the interval 0.44 – 3.5 Bev near the core of extensive atmospheric shower does not depend on the energy of the primary particle. An analogous result is observed during the investigation of the periphery of an extensive atmospheric shower. In Table 2 are shown the values of the exponent n for extensive atmospheric showers with different primary energies, the axes of which are at a distance of 200-350 m from the detectors of penetrating particles.

Energy of the primary particle in 10^{14} ev	ρ_μ			Spectrum exponent n*
	$E_\mu \geqslant 0{,}185$ Bev	$E_\mu \geqslant 1{,}7$ Bev	$E_\mu \geqslant 3{,}5$ Bev	
1,25	0,23 ± 0,07	0,15 ± 0,03	0,16 ± 0,02	0,14 ± 0,17
1,75	0,27 ± 0,08	0,17 ± 0,03	0,16 ± 0,03	0,22 ± 0,10
2,6	0,38 ± 0,07	0,26 ± 0,03	0,18 ± 0,02	0,38 ± 0,07
4,2	0,36 ± 0,07	0,31 ± 0,03	0,25 ± 0,03	0,20 ± 0,05
6,2	0,50 ± 0,10	0,36 ± 0,05	0,31 ± 0,05	0,23 ± 0,07
10,0	0,65 ± 0,13	0,38 ± 0,05	0,36 ± 0,05	0,27 ± 0,12
15,0	0,55 ± 0,16	0,61 ± 0,08	0,42 ± 0,07	0,19 ± 0,25
20,0	1,00 ± 0,28	0,77 ± 0,11	0,62 ± 0,10	0,24 ± 0,02
35,0	1,21 ± 0,42	0,95 ± 0,18	0,76 ± 0,14	0,24 ± 0,02

---

*The value of the energy spectrum exponent was determined by the method of least squares.

Energy of the primary particle in 10^{14} ev	ρ_μ			n
	$E_\mu \geqslant 0{,}32$ Bev	$E_\mu \geqslant 1{,}7$ Bev	$E_\mu \geqslant 3{,}5$ Bev	
12	0,034±0,01	0,010 ±0,003	0,0044±0,0015	0,86±0,18
20	0,037±0,01	0,0084±0,0026	0,0056±0,0018	0,8 ±0,2
40	0,07 ±0,026	0,015 ±0,006	0,011 ±0,005	0,8 ±0,2

The comparison of the μ-meson energy spectrum at different distances from the axis of an extensive atmospheric shower gives:

Mean distance from the axis of a wide atmospheric shower, m	4	100	300
Mean value of the energy spectrum exponent, n	$0,25 \pm 0,02$	$0,32 \pm 0,03$	$0,82 \pm 0,11$

The cited data show that the μ-meson energy spectrum become softer with an increase in the distance from the axis of an extensive shower. Since a large part of μ-mesons in wide atmospheric showers is found at the shower periphery, then the energy spectrum of all μ-mesons in an extensive atmospheric shower at the observation level must be evidently still softer than the meson energy spectrum at a distance of 300 m from the shower axis. Actually, if one extrapolates to large distances, the observed change in the exponent of the energy spectrum with distance from the axis of an extensive atmospheric shower (see Fig. 2), and uses the experimentally obtained spatial distribution function for μ-mesons up to 1000 m in the form $\rho^{\mu} \sim R^{-2}$, then the value of the μ-meson energy spectrum exponent in an extensive atmospheric shower at the observation level is 1 ± 0.2 in the μ-meson energy range of $0.3 - 3.5$ Bev.

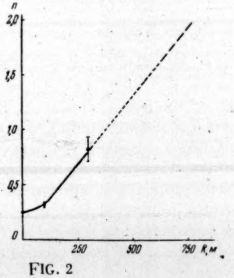

FIG. 2

In conclusion the authors wish to express their thanks to Professors N. A. Dobrotin and G. T. Zatsepin for their interest in the investigation.

Note added during proof-reading: After the paper has been submitted to the editor, we obtained supplementary data showing that in the energy interval $0.185 - 0.3$ Bev the μ-meson energy spectrum cannot be represented in the form E_{μ}^{-n}, where n – constant value for a given primary energy and given distance from the shower axis. This result is explained by the finite lifetime of μ-mesons.

---

[1] George, MacAnuff and Sturgess, Proc Phys. Soc. (London) A66, 346, (1953)

[2] E. L. Andronikashvili, *et al*, Izv. Akad Nauk SSSR, Fiz. Ser. 19, 681, (1955)

[3] Vavilov, Nikol'skii and Tukish, Dohl. Akad. Nauk SSSR, 93, 233, (1953)

[4] S. P. Dobrovol'skii, S. I. Nikol'skii, *et al*, J. Exptl. Theoret. Phys. (U.S.S.R.) 31, 939 (1956); Soviet Phys. JETP 4, 799 (1957)

[5] K. Greisen, *Progress in Cosmic Ray Physics*, vol. III, Amsterdam, (1956), pp. 1-141.

Translated by H. Kruglak
113

SOVIET PHYSICS JEPT VOLUME 5, NUMBER 3, OCTOBER 1957

Heat Capacity of Laminar Lattices at Low Temperatures

E. S. ITSKEVICH AND P. G. STRELKOV
Institute of Physico-technical and Radiotechnical Measurements

(Submitted to JETP editor November 3, 1956)
J. Exptl. Theoret. Phys. (U.S.S.R.) **32**, 467-477 (March, 1957)

The heat capacity of three anhydrous cadmium salts — CdI_2, $CdBr_2$, and $CdCl_2$ — which are classical laminar crystals has been measured in the temperature interval from 1.6 to 100° K. Possible thermal effects of sorption were excluded by carrying out the measurements on pressed preparations without heat exchanging gas. At helium temperatures, the heat capacities of all three salts obey a cubic law. In the 4-10° K range, the exponent in this relationship exceeded three for all three salts. Above 10° K, the exponent starts to [illegible]rease continuously and in a certain region the relation becomes quadratic; the region in which this relation holds decreases from the iodide to the chloride. Still higher, the relation is linear, the region of which increases from the iodide to the chloride. Attempts are made to compare the experimental results with theory.

THE study of the heat capacity of anisotropic crystals, in particular, laminar crystals, is of great value in the development of our representations of solid bodies. During the last ten years, a large quantity of theoretical work has been published on this question[1-7]. The conclusions arrived at by the various authors do not coincide. Very few experimental investigations of the heat capacity of laminar lattices below 50° K have been made; they have been carried out only up to hydrogen temperatures, and on a limited group of substances[8,9]. Quite recently, three articles appeared on the heat capacity of graphite in which measurements were also made at helium temperatures[10-12], and a communication appeared concerning measurements of the heat capacity of MoS_2 and BN at 5° K and higher[13].

We have studied the temperature dependence of the heat capacity of anhydrous iodide, bromide, and chloride of cadmium over the temperature range from 1.6 to 100° K. Measurements were also made above 100° K, but they cannot be used in the present article since we are interested in C_v which practically coincides with C_p at low temperatures, but begins to differ strongly above 100° K.

A short report concerning our results at temperatures above 11° K has been published[14]. $CdCl_2$, $CdBr_2$, and CdI_2 represent classical laminar crystals. Their layers are formed of two networks of closely packed halide atoms, and a network of cadmium atoms located in the octohedral vacancies between them. These triple layers are bound by Van der Waal forces, the bond in the layers is basically ionic. $CdCl_2$, $CdBr_1$, and CdI_2 form a series with regular varying properties, in particular, the binding forces between layers increases as we go from the iodide to the chloride[15,16].

The absence of free electrons allows us to attribute the entire measured heat capacity to the lattice (in distinction from graphite).

1. METHOD OF MEASUREMENT

We used preparations obtained from IONKH, Academy of Sciences, U.S.S.R.* The $CdCl_2$ and CdI_2 were marked "ChDA." According to analysis, the total impurity content was 0.18% for CdI_2, and 0.12% for $CdCl_2$. The $CdBr_2$ was marked "Ch" and contained 0.47% impurities. This preparation was purified by three recrystallizations in an aqueous solution.**

Measurements above 11° K and in the helium region were made on identical samples. The preparations were dehydrated and were guarded against moisture during the filling of the calorimeters. For measurements in the region above 11° K, we used 0.287 moles of CdI_2, 0.887 moles of $CdCl_2$, and 0.696 moles of $CdBr_2$. In the region of helium temperatures, we used 0.517, 0.830, and 0.843 moles, respectively.

To prevent possible sorption of heat-exchanging helium by the preparation during measurements at hydrogen temperatures, we selected large particles of the substance with linear dimensions of the order of 1 mm, comprising about 90% by weight. Furthermore, helium is adsorbed weakly at these temperatures. Deterioration of heat exchange in the caliometer, which would lead us to think of sorption, was not noted over the entire range of measurements. The effects of sorption at helium temperatures were avoided by the use of special measures, described below.

---

*The authors are grateful to E. I. Banashek and V. A. Sokolov for kindly giving them preparations.

**The authors thank T. N. Rezukhin (Professor of Physical Chemistry, Moscow State University) for his help in the purification of the $CdBr_2$.

Part of the preparation was in the form of a powder, and it was necessary to consider its possible influence. However, from the work of Dugdale, Morrison, and Patterson[17,18], it appears that the presence in the calorimeter of ~ 10% of crystals with mean dimensions of the order of 100μ will not alter the results.

For experiments above 11° K, we used an adiabatic vacuum calorimeter described in Refs. 19 and 20. The platinum resistance thermometer used in the measurements was calibrated at 10.7, 14.0, 20.4, and 90.19° K by direct comparison with a secondary reference thermometer made of the same kind of platinum. The temperature dependence of the latter was found by comparison with a gas thermometer[21].

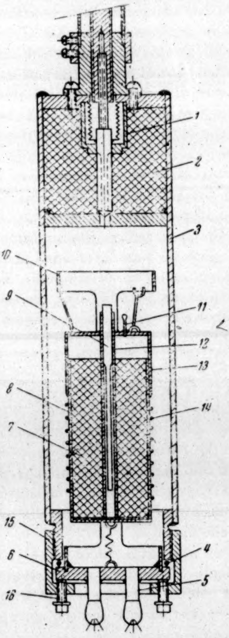

FIG. 1. Calorimeter for helium temperatures. 1 – carbon pump valve; 2 – activated carbon; 3 – body of the calorimeter vacuum jacket; 4 – sealing ring; 5 – copper-glass unions for leads; 6 – vacuum jacket cover; 7 – pressed preparation; 8 – glass calorimeter; 9 – thermometer; 10 – calorimeter holder; 11 – capillary for evacuating the calorimeter; 12 – tube with disc for the thermometer; 13 – calorimeter cover; 14 – heater; 15 – support ring for the jacket; 16 – sealing screws.

At 1.6° K and above, we used a vacuum system of the type accepted here, with a carbon pump[22] and a removable seal[19] (Fig. 1).

To avoid the effects of sorption, having in mind that the selected crystals of CdI_2, $CdBr_2$, and $CdCl_2$ have sufficiently developed surfaces, heat-exchanging gas was not introduced, and the preparation was located in a high vacuum. In order to provide proper thermal contact between the sample and the walls of the calorimeter, the heater, and the thermometer, without heat-exchanging gas, we used a modified type of calorimeter (Fig. 1). The salt being studied was pressed into the glass container *8*, which is 60 mm high, 30 mm in diameter, has a wall thickness of 0.2 mm, and in which a tube *12* is set for the thermometer. In order not to disturb the tube during pressing, a centering disc was soldered to it, restraining it at the bottom of the calorimeter, after which the tube was filled with Wood's metal. The pressed salt was in good thermal contact with the wall, the bottom, and the tube, and the particles of the salt were in good thermal contact with one another.

A special die and plunger were made for pressing the salt in the thin walled glass vessel. The pressing pressure was 300-400 kg/cm². Cover *13* with capillary *11* was put on the glass vessel with the salt pressed in it and the tube, and the place where they joined was soldered. All parts of the calorimeter were made of pure copper. Identical calorimeters were used for $CdCl_2$, $CdBr_2$, and CdI_2. The calorimeters were pumped out through the capillaries for about 10 hours at 120° C. Then the capillaries were pinched under vacuum and unsoldered.

The heater *14* was made of enameled constantan wire, 0.1 mm diameter, wound on the surface of the glass vessel which was first covered with polymerized adhesive BF. To ensure good thermal contact, the constantan windings were again covered with BF. To ensure good thermal contact, the constantan windings were again covered with BF and polymerized. The heater resistance was ~ 150 at liquid helium temperatures.

The calorimeters were suspended by nylon threads from girder *10*, soldered to the removable cover of the jacket *6*, which simplified the assembly. The leads to the heater and to the thermometer were made of tinned constantan. The wires entered the vacuum system through platinum lead-ins, fused into the glass of copper-glass unions *5*. The carbon pump was located in the upper part of the jacket and was controlled from the cover of the Dewar.

Two thermometers were used. For the range from 1.6-4.2° K, a bronze resistance thermometer was used, calibrated by the vapor pressure of liquid helium using a specially built condensation thermometer. The calibration was based on the 1948 scale. However, the final results were recalculated on the basis of the 1955 scale[23]. The thermometer was a copper tube with a bifilar-wound two-section wire of phosphor bronze with diameters of 40 and 70μ.

The carbon thermometer, made of a radio resistance from the firm of Allen Bradley, was mounted in a copper case, filled with heat exchanging helium and sealed. The electrical leads to the sensitive element of the thermometer were led in with the aid of a well sealing layer of polymerized BF[24].

The thermometers, lubricated with a thin layer of Ramsay coating, were inserted tightly into tube *12*. The carbon thermometer served mainly for measurements in the intermediate temperature range (4.2-11° K); therefore it was calibrated at one temperature in liquid helium, and at the temperatures of normal boiling and the triple point of hydrogen. For these temperatures, the coefficients in the formula $\lg R + k/\lg R = A + B/T$ proposed by Clement and Quinnell[25] were calculated.

2. MEASUREMENTS

The sequence of measurements in the range from 11° K and above was similar to that described in previous works[19]. The heat capacity of the empty calorimeter was determined over the temperature range from 10.67 to 302.92° K. The values were smoothed graphically. Individual experimental points deviated from the smoothed curve by no more than 1%. The magnitude of the heat capacity of the empty calorimeter compared with the measured value for CdI_2 went from ~ 20% at 10.7° K to 60% at 100° K, and for $CdBr_2$ and $CdCl_2$ went from ~ 15% at 10.9° K to ~ 37% at 83° K.

The measurements in the range 1.6-4.2° K were carried out in a bath of liquid helium boiling under reduced pressure. The calorimeter was cooled to the temperature of the bath by means of heat-exchanging helium let into the jacket by a special measuring valve. This gas was then pumped off by the carbon pump, providing a high vacuum. Opening the carbon pump was always accompanied by some pulsations which warmed the calorimeter. To cool the calorimeter to the bath temperature with an open pump, a portion of heat-exchanging helium was let into the jacket. Since the heat capacity of the calorimeter is very small ($2\text{-}3 \times 10^{-3}$ cal/deg), it is possible to cool it during the time the heat-exchanging helium is being absorbed by the carbon. We started the measurements at 1.48° K.

Measurements in the range 4.2-16° K were carried out in a bath of liquid helium boiling at normal pressure. Before the start of each experiment, the resistance of the carbon thermometer was determined. This was done by letting heat-exchanging gas into the jacket, and measuring the vapor pressure over the helium in the Dewar precisely. To compare data obtained with the bronze and with the carbon thermometers, we started some series of measurements with the carbon thermometer (at least one for each salt) at temperatures ~ 3° K, so that the intervals of measurements with the different thermometers overlapped.

At the conclusion of the measurements of heat capacity in the helium bath, the remaining helium evaporated. Liquid hydrogen was quickly poured into the cold apparatus and the resistance of the carbon thermometer was determined at the point of normal boiling and at the triple point. This was done in each experiment because the carbon thermometers showed inadequate reproducibility from test to test.

Near 6° K, the tinned constantan leads to the heater lost their super-conductivity and began to dissipate energy. However, because of the cold-flow from the liquid helium bath, the portion of the wire adjacent to the bath remained superconducting. To measure the resistance of the nonsuperconducting part, an auxiliary potentiometer arrangement was used. The data were corrected for the power dissipated in these parts.

Equilibrium was established quickly in the pressed sample. We noticed no difference in the variation of calorimeter temperature with time between the pressed sample and the sample with heat-exchanging gas.

Since we measured the sum of the heat capacities of the preparation and the calorimetric vessel, it was necessary to know the heat capacity of the empty calorimeter, all parts of which were made of pure copper. The heat capacity of the calorimeter was calculated. The weight of copper in the calorimeter was 63.97 g for CdI_2, 36.66 g for $CdCl_2$, and

T°K	Heat capacity in % of the measured value					
	for the copper			overall for the empty calorimeter		
	CdI_2	$CdBr_2$	$CdCl_2$	CdI_2	$CdBr_2$	$CdCl_2$
1.6	15.1	9.8	13.9	16.5	11.5	17.0
2.0	11.7	7.7	11,8	12.8	9.3	14.6
2.5	9.2	5.0	8.6	10.3	6.8	11.9
4.0	5.2	3.0	5.0	6.2	4.7	7.9
7.0	2.9	1.7	3.0	4.2	3.7	7.0
10.0	2.9	1.6	2.4	4.4	4.0	6.2
14.0	—	1.6	—	—	4.1	—
16.0	3.7	—	2,7	5.2	—	6.2

36.63 g for $CdBr_2$ (the copper in the latter two calorimeters weighed less because thinner parts were used). The contribution of the copper[26] to the calculated heat capacity is given in the table for each calorimeter. We feel that the error involved in this determination of the heat capacity of the copper parts is hardly greater than 1/10 of the tabulated values. Corrections for the heat capacity of the solder used were introduced by calculations based on published data. We also introduced a correction for the polymerized BF.* In the region of helium temperatures, these corrections were considerably smaller than the corrections for the heat capacity of the copper. The total contribution of the heat capacity of the empty calorimeter is also given in the table.

We estimate the possible error associated with this method of determination of the heat capacity of the empty calorimeter to be approximately 1% above 3° K and up to 2% below 3° K.

The satisfactory agreement between our hydrogen and helium data in the region where they join between 11 and 17° K confirms the reliability of the method used. The high vacuum maintained by the carbon pump allowed us to raise the temperature of the calorimeter up to 17° K at a bath temperature of 4.2° K with a small change of temperature paths.

3. RESULTS OF THE MEASUREMENTS

The measured heat capacities of CdI_2, $CdBr_2$, and $CdCl_2$ from 1.6 to 30° K are shown on a logarithmic scale in Fig. 2. It is clear that the results obtained in the helium region conform with the results obtained in the hydrogen region. Except for the article by Dworkin *et al*[27] concerning measurements of CdI_2 above 16° K, already considered in Ref. 14, no published data exist concerning the heat capacities of CdI_2, $CdBr_2$, and $CdCl_2$ in the low temperature region.

The results are presented in Fig. 2 in the form of points (1 cal = 4.185 abs. joules). The authors plan to publish the numerical data separately. The intervals from 1.6 to 100° K for CdI_2, from 1.6 to 60° K for $CdBr_2$, and from 1.6 to 80° K for $CdCl_2$ were covered by the measurements without gaps; phase transitions were not observed.

The heat capacities of all three salts exhibit a cubic temperature dependence at helium temperatures. The straight lines in Fig. 2, corresponding to the points in the helium region, show this cubic relation. Fig. 3 also confirms this.

The cubic dependence is maintained up to 4.0° K for CdI_2 and $CdBr_2$, and up to ~ 5.0° K for $CdCl_2$, and is described by the following formulas: for CdI_2, $C_p = 0.76\ T^3$ mcal/deg mole, for $CdBr_2$, $C_p = 0.470\ T^3$ mcal/deg mole, and for $CdCl_2$, $C_p = 0.275\ T^3$ mcal/deg mole.

At higher temperatures the dependence becomes stronger and the exponent increases. $CdCl_2$ deviates from the cubic dependence somewhat more than the other salts. The maximum deviation of the $CdCl_2$ curve (Fig. 2) corresponds to a temperature exponent equal to 3.4. The deviation from cubic dependence is outside the limits of experimental error, and amounts to more than 20% for CdI_2 and $CdBr_2$, and more than 30% for $CdCl_2$.

Around 10° K the temperature exponent begins to decrease, and in the region of hydrogen temperatures the relation becomes quadratic over a certain interval. The region of "quadraticity", as was noted in Ref. 14, decreases as we go from CdI_2 to $CdCl_2$. At higher temperatures there is a region of linear dependence (Fig. 4), which broadens strongly as we go

---

*The authors take this opportunity to thank I. N. Kalinkin for making available to them his measurements of the heat capacity of polymerized coatings of BF at helium temperatures.

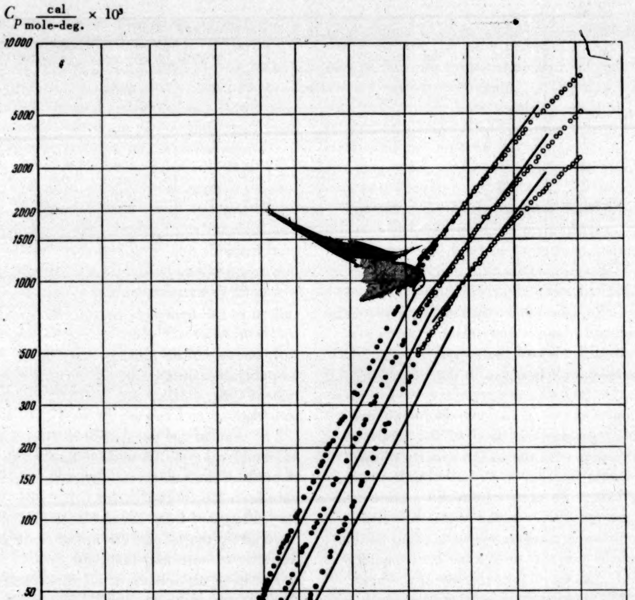

FIG. 2. Heat capacity of halide salts of cadmium from 1.6 to 30° K (● refers to the helium bath, ○ refers to the hydrogen bath[14]). 1 – $CdCl_2$, 2 – $CdBr_2$, 3 – CdI_2. The straight lines in the region 1.6-10° K correspond to a cubic relation. A series of points ●, coinciding with points ○, have been omitted in the region 10-20° K.

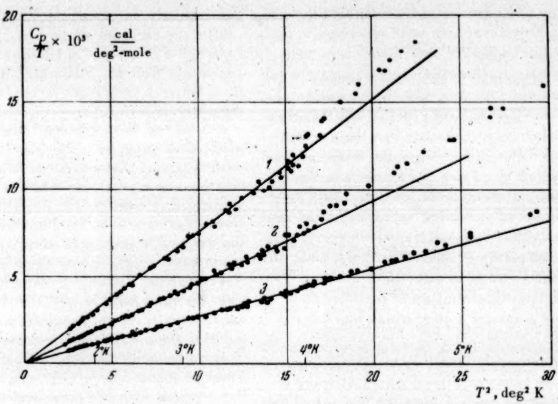

FIG. 3. The relation $C_p/T = f(T^2)$ for halide salts of cadmium at helium temperatures. 1 – CdI_2, 2 – $CdBr_2$, 3 – $CdCl_2$.

from the iodide to the chloride[14].

We estimate the mean experimental error to be generally 1% in the hydrogen region and 3% in the helium region. In the region 3.5-4.5° K, the error increases somewhat (up to 5%) due to the rough calibration of the carbon thermometer at one helium point between 3 and 4.2° K. However, this does not affect the conclusions, especially since the curve is rectified by the measurements with the bronze thermometer.

4. DISCUSSION OF THE RESULTS

During 1945-1950, Tarasov[1], in a series of articles, pointed out for the first time that the heat capacity of laminar lattices must have specific singularities, and cannot be described by the interpolated Debye formula. Using a method similar to that of Debye, he proposed interpolation formulas describing the heat capacity of laminar crystals at low temperatures. According to Tarasov, the heat capacity of a laminar crystal obeys a cubic law at very low temperatures, and at higher temperatures where the interaction energy between layers is less than kT, it becomes quadratic. Later Krumhansl and Brooks[4], Rosenstock[5], and others obtained relations similar to those of Tarasov based on models.

In 1952, Stepanov[3] criticized the basic assumptions used by Tarasov to obtain his formulas. At the same time, I. M. Lifshitz[2] examined the question again in detail, and constructed a completely phenomenological theory of the heat capacity of laminar crystals. He pointed out the specific contribution to the heat capacity of laminar structure of waves similar to bending waves in layers. He obtained a dispersion law (relation between the frequency and the wave vector) pertaining to laminar crystals with axial symmetry with respect to the elastic properties, in particular hexagonal properties for long waves, yielding a major contribution to the heat capacity at low temperatures. Lifshitz showed that in the temperature region in which the energy of interaction between layers may be neglected, the heat capacity depends linearly on temperature, which is determined by the bending waves. This differs significantly from the trend of Tarasov's ideas.

Lifshitz obtained an analytic expression for the heat capacity in the temperature region in which the interaction is significant. This expression was integrated which made it possible to tabulate heat capacity as a function of temperature[28]. It appeared possible to compare the heat capacity according to Lifshitz with experimental data without appealing to the unknown values of the elastic constants of a laminar lattice in this temperature region, because the elastic constants enter the formulas only in the form of determined combinations. The numerical values of these combinations may be determined if the heat capacity is known in the regions of pure cubic law, and pure quadratic law, and the expected values of the heat capacity may be calculated in the intermediate region between the cubic and the quadratic regions. We attempted to carry out such a comparison between theory and experiment for CdI_2, $CdBr_2$, and $CdCl_2$, whose heat capacities were measured in the regions of cubic, quadratic, and intermediate temperature dependence. However, the theoretically calculated values did not agree with the experimental values. This may be explained by the fact that the theoretical values were calculated on the assumption of a very large difference between the magnitudes of the elastic moduli in a layer and between layers[2], which apparently does not hold for CdI_2, $CdBr_2$, and $CdCl_2$. The anisotropy required[2] is such that the numerical values of the temperatures at which the purely cubic law and purely quadratic law hold, must differ by more than an order of magnitude. Judging from the published data, this relation is satisfied to a large extent by graphite; a comparison was carried out in Ref. 28.

It would be extremely laborious to obtain an expression for the heat capacity of a crystal using the complete dispersion law[2]. A possible way out of the situation was discussed in Ref. 28.

A quantitative comparison between theory and experiment is not possible in the region of linear temperature dependence. In addition to the fact that the Lifshitz theory deals with anisotropies which are not possessed by the real crystals investigated by us, a comparison would require further knowledge of the magnitude of the transverse rigidity of the layer. Qualitatively, however, the lengthing of the linear part of the curve as we go from the iodide to the chloride is contained in Lifshitz's theory[2], taking into account Ref. 15, from which it follows that the bond between the layers increases from the iodide to the chloride.

Newell[7] made an attempt to consider the question of the heat capacity of laminar lattices, based on models. Using the concept of two types of vibration in a laminar crystal, he obtained results agreeing qualitatively with Ref. 2. Newell shows that valence forces having a specific dispersion law (similar to the dispersion law for bending waves in Ref. 2) are responsible for the linear behavior of heat capacity. Nevertheless, Newell's conclusions remain qualitative. We agree with Newell that for almost isotropic substances, it is not possible, within the limits of existing theories, to obtain satisfactory information concerning molecular forces from heat capacity data, because almost all the data may be described by a Debye curve with one parameter θ_D. But data on the heat capacity of strongly anisotropic substances in the low temperature region may give some useful information concerning the forces of interaction in crystals—information which would be difficult to obtain directly.

The works of Lifshitz, Newell, and others show that to determine the vibratory spectrum of the lattice of a laminar crystal, at least four parameters

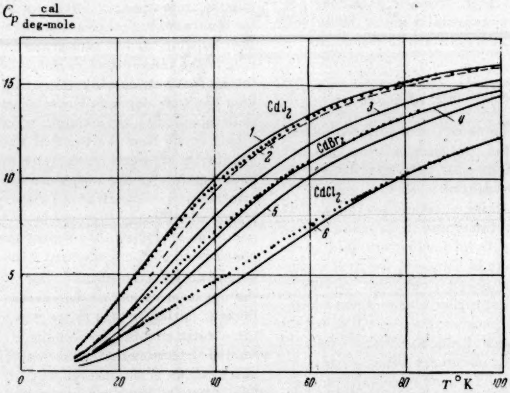

FIG. 4. Heat capacity of CdI_2, $CdBr_2$, and $CdCl_2$ in the region 11-100° K. The points represent the experimental results. The solid lines represent the value of heat capacity calculated according to Tarasov: 1 – CdI_2 with $\Theta_2 = 163$° K, $\Theta_3 = 32.6$° K; 3 – $CdBr_2$ with $\Theta_2 = 200$° K; 4 – $CdBr_2$ with $\Theta_2 = 223$° K; 5 – $CdCl_2$ with $\Theta_2 = 240$° K; 6 – $CdCl_2$ with $\Theta_2 = 320$° K. The dashed line 2 represents the heat capacity of CdI_2, calculated according to Debye ($\Theta_D = 155$° K).

must be known. Therefore it is doubtful *a priori* that Tarasov's functions with two parameters can be universal for the description of the heat capacity of laminar crystals. However, there are indications in the literature that the formulas proposed by Tarasov give a good representation of the temperature dependence of the heat capacities of a series of laminar crystals[1,9,29]. In view of this, we tried to use Tarasov's formulas with two parameters[1] to describe our data on CdI_2, $CdBr_2$, and $CdCl_2$.

In Fig. 4, the experimental results in the region 11-100° K are shown by points, and the solid lines show the values calculated according to Tarasov's formulas over the same interval. One-parameter curves are shown for $CdBr_2$ and $CdCl_2$ because the introduction of a second parameter does not change the calculated results above 16° K. We see that the experimental points for CdI_2 from 11 to 100° K are described well by the curve, with only a certain systematic deviation in the region 30-60° K (up to 4%). The deviation is stronger for $CdBr_2$ and is very sharply evident for $CdCl_2$. Their heat capacities are not at all well described by Tarasov's formulas in this temperature interval.

If the heat capacity curve calculated for CdI_2 according to Tarasov (Fig. 4) is extrapolated to lower temperatures, it diverges sharply from the experimental data. In the helium region it differs by a factor of two. If, in reverse, we determine the parameters in the Tarasov functions using experimental data in the helium region and in the neighborhood of 20° K, then there is a systematic divergence ~ 20% in the region 6-20° K. It should be noted that above 40° K, the heat capacity of CdI_2 is also satisfactorily described by the Debye function.

A comparison of the experimental data for $CdCl_2$ and $CdBr_2$ with Tarasov's curves below 11° K would have no meaning since the divergencies are already large in the hydrogen region. Thus, the Tarasov formula is not universal.

The experiment shows that for all three salts there is an interval in which the dependence of the heat capacity on temperature is greater than the third degree. It is possible that this is a consequence of the contribution of optical branches to the heat capacity. Optical branches corresponding to interlayer interactions may be sufficiently soft. The existence of such branches may be due to the fact that in our lattices the layers are not monatomic, and the surfaces of each layer, facing neighboring layers, are different[4]. In CdI_2 the iodide ions on one side of the layer are turned through an angle of 60° about the axis passing through the cadmium ions, with respect to the iodide ions on the other side of the layer. In $CdCl_2$ the picture is even more complicated: the triple layers of which it is formed repeat their configuration after two layers.

CONCLUSIONS

1. The heat capacities of anhydrous cadmium chloride, cadmium bromide, and cadmium iodide were measured over the range 1.6-100° K.

2. The heat capacity of all three salts obeys a cubic law in the interval 1.6-4° K.

3. The temperature exponent in the relation between heat capacity and temperature became greater than three between 4 and 10° K for all three salts. This is assumed to be due to the influence of the soft optical branches of interlayer interaction.

4. In the region of hydrogen temperatures a quadratic dependence occurs over an interval which decreases as we go from the iodide to the chloride.

5. At still higher temperatures a linear dependence occurs over an interval which increases as we go from the iodide to the chloride.

6. Our results do not qualitatively contradict the Lifshitz theory. A quantitative comparison was not possible because the particular case considered theoretically which led to tabulated results refers to lattices with sharply differing elastic constants in the layer and between layers, in any case, with far greater differences than occur in CdI_2, $CdBr_2$, and $CdCl_2$.

7. The two-parameter Tarasov functions cannot describe the experimental data referring to all three salts.

In conclusion, the authors consider it their pleasant duty to express their genuine gratitude to Academician P. L. Kapitza for making it possible for them to carry out measurements at helium temperatures at the Institute for Physical Problems, Academy of Sciences, U.S.S.R., and to Prof. I. M. Lifshitz for numerous and fruitful discussions on the questions considered in this article.

---

[1] V. V. Tarasov, Dokl. Akad. Nauk, U.S.S.R., **46**, 22 (1945); **54**, 803 (1946); **58**, 577 (1947); J. Phys. Chem. (U.S.S.R.) **24**, 111 (1950).

[2] I. M. Lifshitz, J. Exptl. Theoret. Phys. (U.S.S.R.) **22**, 471, 475 (1952).

[3] P. E. Stepanov, J. Phys. Chem. (U.S.S.R.) **26**, 1642 (1952).

[4] J. Krumhansl and H. Brooks, Chem. Phys. **21**, 1663 (1953).

[5] H. R. Rosenstock, Chem. Phys. **21**, 2064 (1953).

[6] K. Komatsu and T. Nagamiya, J. Phys. Soc. Japan **6**, 438 (1951); K. Komatsu, J. Phys. Soc. Japan **10**, 346 (1955).

[7] G. F. Newell, Chem. Phys. **23**, 2341 (1955).

[8] W. de Sorbo, Chem. Phys. **21**, 168 (1953); Am. Chem. Soc. **77**, 4713 (1955).

[9] Dworkin, Sasmor and van Artsdalen, Chem. Phys. **21**, 954 (1953); Smith, Brown, Dworkin, Sasmor and van Artsdalen, Chem. Phys. **78**, 1553 (1956).

[10] Bergenlid, Hill, Webb and Wilks, Phil. Mag. **45**, 367, 851 (1954).

[11] P. H. Keesom and N. Pearlman, Phys. Rev. **99**, 1119 (1955).

[12] W. de Sorbo, Chem. Phys. **23**, 1970 (1955).

[13] E. F. Westrum and J. J. McBride, Phys. Rev. **98**, 270 (1955).

[14] E. S. Itskevich, P. G. Strelkov, Dokl. Akad. Nauk, U.S.S.R. **106**, 805 (1956).

[15] Z. G. Pinskar, J. Phys. Chem. (U.S.S.R.) **15**, 599 (1951); **16**, 1 (1942); Izv. Akad. Nauk, U.S.S.R., ser. khim. **6**, 415 (1943); Z. G. Pinsker and L. I. Tatarinova, J. Phys. Chem. (U.S.S.R.) **15**, 1005 (1941).

[16] L. A. Smirnova, A. Kh. Breger, G. S. Zhdanov, J. Phys. Chem. (U.S.S.R.) **18**, 309, 425 (1944).

[17] J. S. Dugdale, J. A. Morrison, D. Patterson, Proc. Roy. Soc. (London) **224A**, 228 (1954).

[18] J. A. Morrison, D. Patterson, Trans. Farad. Soc. **52**, 764 (1956).

[19] Strelkov, Itskevich, Kostriukov, Mirskaia and Samoilov, J. Phys. Chem. **28**, 459 (1954).

[20] Astrov, Itskevich and Sharifov, J. Phys. Chem **29**, 424 (1955).

[21] Borovik-Romanov, Orlova and Strelkov, *Establishment of a low temperature scale between 90, 19 and 10° K by means of a graduated table of a group of standardized platinum resistance thermometers*, Moscow, 1954.

[22] M. O. Kostriukova and P. G. Strelkov, Dokl. Akad. Nauk, U.S.S.R. **90**, 525 (1953).

[23] H. van Dijk and M. Durieux, *Helium vapour pressure scale* T_L^{55}. Kamerlingh Onnes Laboratory, Leiden, 1955.

[24] B. N. Samoilov, J. Tech. Phys. (U.S.S.R.) **22**, 888 (1952).

[25] J. R. Clement and E. H. Quinnell, Rev. Sci. Instr. **23**, 213 (1952).

[26] Corak, Garfunkel, Satterthwaite and Wexler, Phys. Rev. **98**, 1699 (1955).

[27] Dworkin, Sasmor and van Artsdalen, Am. Chem. Soc. **77**, 1304 (1955).

[28] E. S. Itskevich and V. M. Kontorovich, J. Exptl. Theoret. Phys. (U.S.S.R.) **32**, 175 (1957).

[29] W. de Sorbo, Acta Metallurgica, **2**, 274 (1954).

Translated by D. Lieberman
114

SOVIET PHYSICS JEPT VOLUME 5, NUMBER 3 OCTOBER, 1957

Charge Invariance in Nuclear Reactions

A. I. BAZ'

(Submitted to JETP editor September 24, 1956)
J. Exptl. Theoret. Phys. (U.S.S.R.) 32, 478-490 (March, 1957)

It is shown that there exists a relation between the cross sections of the reactions $He^3(pp)He^3$, $He^3(nn)He^3$, $He^3(np)T$; $T(pn)He^3$; $T(pp)T$; $T(pp)T$. This relation is based on the hypothesis of charge invariance of nuclear forces; because of it we can reduce the number of independent parameters (phases) necessary for a complete description of these reactions. The cross sections of these reactions are all expressed by the same parameters $\delta(T)$ and $\epsilon(T)$ [the phases and mixture parameters in a state with isotopic spin T] and thus it is possible to carry out a phase analysis of all these reactions simultaneously. The method we have applied is a general one and is applicable, with only slight changes, to all reactions involving light nuclei.

---

1. INTRODUCTION

In the present work we have investigated the relation between the cross sections of certain nuclear reactions that follows from the assumption of charge invariance of nuclear reactions. We apply our considerations to reactions that are possible for a system of four nucleons [2 protons and 2 neutrons ($2p$, $2n$); 3 protons and 1 neutron ($3p$, n); 1 proton and 3 neutrons (p, $3n$)] at small energies:

$$T(pp)T;\quad He^3(pp)He^3;\quad T(nn)T;$$

$$He^3(nn)He^3;\quad T(pn)He^3;\quad He^3(np)T.$$

It will be evident from what follows, however, that our method is a general one and is applicable for reactions involving any type of light nuclei.

We divide the space in the center-of-mass system of the colliding particles into two parts: the internal, which is bounded by some radius r_0, and the external, which fills all the remaining space. The radius r_0 is so chosen that at distances $r > r_0$ there is no nuclear interaction between the colliding and outgoing particles. We know the exact wave functions of the particles in the external region for such a choice of r_0. In the case of uncharged particles, these are the ordinary wave functions of free motion, and in the case of charged particles, they are Coulomb functions.

In reactions involving light nuclei, the wave function in the internal region ought to satisfy the requirements of charge invariance. In order to understand to what they reduce, let us consider as a concrete case the reactions $T(pp)T$; $T(pn)He^3$; $He^3(pp)He^3$ for small energies, when other conceivable reactions, such as $T(pd)d$, are not possible. In a collision of a proton with a nucleus of tritium in the internal region ($r \leqslant r_0$), there is formed some sort of state of the system consisting of two protons and two neutrons ($2p$, $2n$). This state decays either to $T+p$ or to He^3+n, because the others are not possible for small energies.

For $r=r_0$, the wave function in a state with isotopic spin T is a combination of two terms $\varphi^{(1)}(T)$ and $\varphi^{(2)}(T)$:

$$\varphi^{(1)}(T) = \psi_T\psi_p\Psi^{(1)}(T) \equiv \psi(T+p)\Psi^{(1)}(T),$$
$$\varphi^{(2)}(T) = \psi_{He^3}\psi_n\Psi^{(2)}(T) \equiv \psi(He^3+n)\Psi^{(2)}(T), \tag{1.1}$$

where Ψ_T, Ψ_p, Ψ_{He^3} and Ψ_n are the wave functions of the internal state T, p, He^3 and n, while $\Psi^{(1)}(T)$ and $\Psi^{(2)}(T)$ are functions of the relative motion of the systems $T+p$ and $He+n$, respectively. It follows from charge invariance that $\varphi^{(1)}(T)$ and $\varphi^{(2)}(T)$ ought to change into one another for an exchange in the places of the neutron and the proton; consequently,

$$\Psi^{(1)}(T) = \Psi^{(2)}(T) \equiv \Psi(T).$$

The total wave function for $r \leqslant r_0$ is a superposition of states with isotopic spin $T=0$ and 1: $\varphi_{T=0}$ and $\varphi_{T=1}$. The wave function $\varphi_{T=1}$ ought to be symmetric for the substitution $\Psi_T \rightleftarrows \Psi_{He^3}$, $\Psi_p \;\; \Psi_n$ and therefore,

$$\varphi_{T=1} = \varphi^{(1)}(1) + \varphi^{(2)}(1). \tag{1.2}$$

The function $\varphi_{T=0}$ ought to change sign in such an exchange, i. e.,

$$\varphi_{T=0} = \varphi^{(1)}(0) - \varphi^{(2)}(0). \tag{1.3}$$

For the scattering $He^3(pp)He^3$ [the system ($3p$, n)], only the state with $T=1$ is possible, and for $r=r_0$, the wave function has the form

$$\Phi_{T=1} = \psi(He^3+p)\Psi^{(3)}(1), \tag{1.4}$$

where, as a consequence of charge invariance, $\Psi^{(3)}(1)=\Psi^{(2)}(1)=\Psi^{(1)}(1)\equiv\Psi(1)$.

It remains for us to determine the concrete form of the relative motion $\Psi(T)$ for $r=r_0$. First, let us consider the state with total momentum J and parity $P=(-)^l$ (l=orbital momentum). Since each particle in the system (T + p) and (He^3 + n) has spin ½, for any l (except $l=0$), there exist two states with given $J=l$ and $P=(-)^l$; states with total spin $s=0$ and $s=1$. If we denote the angular part of the wave function for given J, l, s by $Y^J_{l,s}$, and the radial part by $R^J_{l,s}$, then the total function $\Psi(T)$ in the states J, P has the form

$$\Psi^J_P(T)=R^J_{l1}(T)\,Y^J_{l1}+R^J_{l0}(T)\,Y^J_{l0}. \tag{1.5}$$

The angular parts are easily constructed with the help of the usual rules of momentum addition, while the radial functions for $r\sim r_0$ have the form

$$R^J_{ls}(T)=a^J_{ls}(T)\,R^{(-)}_{kl}(r)-b^J_{ls}(T)\,R^{(+)}_{kl}(r). \tag{1.6}$$

Here $a^J_{ls}(T)$ and $b^J_{ls}(T)$ are certain constants for each J, l, s and T, while $R^{(\pm)}_{kl}(r)$ are radial functions of the free motion

$$R^{(\pm)}_{kl}(r)=i\sqrt{\frac{\pi k}{2r}}\{\pm J_{l+1/2}(kr) \tag{1.7}$$
$$+\,iN_{l+1/2}(kr)\}\rightarrow\frac{1}{r}e^{\pm i\left(kr-\frac{\pi l}{2}\right)}.$$

Here $J_{l+1/2}$ and $N_{l+1/2}$ are Bessel functions of the first and second kind, the signs (±) referring to outgoing and ingoing waves, respectively, while k is the wave vector, in magnitude equal to the wave vector of the relative motion in the system He^3 + n, which is produced after the decay of the "intermediate" system.

Similarly, in states with total momentum J and $P=(-)^{l+1}$ ($l=J+1$), the function Ψ (T) has the form

$$\Psi^{J=l+1}_P(T)=R^{l+1}_{l1}(T)\,Y^{l+1}_{l1}+R^{l+1}_{l+2,1}(T)\,Y^{l+1}_{l+2,1}, \tag{1.8}$$

where the $R^J_{ls}(T)$ are defined by Eq. (1.6).

We can now write down the boundary values of the for wave function for $r=r_0$ as

$$\psi(r_0)=(\varphi_{T=1}+\varphi_{T=0})_{r=r_0}, \tag{1.9}$$

where the φ_T are determined from Eqs. (1.1)-(1.6).

All further calculations are similar, both those for the case $J=l$, $P=(-)^l$, and those for the case $J=l+1$, $P=(-)^l$. Therefore, we need carry out only the first of these.

2. BOUNDARY CONDITIONS

In this Section, we establish the form of the wave function of a system of two neutrons and two protons (2p, 2n) for such energies for which, as $r\to\infty$, only those states corresponding to the pairs (T + p) and (He^3 + n) are energetically allowed. The same general wave function of the system for $r\geqslant r_0$ has the form (we are at present interested only in a state with total angular momentum l and $l=J+1$):

$$\begin{aligned}\psi(r>r_0)={}&\psi(\mathrm{T}+p)\{[C_l\mathcal{R}^{(-)}_{k_1,l}(r)-D_l\mathcal{R}^{(+)}_{k_1,l}(r)]\,Y^{l+1}_{l,1}+\\&+[C_{l+2}\mathcal{R}^{(-)}_{k_1,l+2}(r)-D_{l+2}\mathcal{R}^{(+)}_{k_1,l+2}(r)]\,Y^{l+1}_{l+2,1}\}+\\&+\psi(\mathrm{He}^3+n)\{[A_l R^{(-)}_{k,l}(r)-B_l R^{(+)}_{k,l}(r)]\,Y^{l+1}_{l,1}+\\&+[A_{l+2}R^{(-)}_{k,l+2}(r)-B_{l+2}R^{(+)}_{k,l+2}(r)]\,Y^{l+1}_{l+2,1}\}.\end{aligned} \tag{2.1}$$

Here, as before, $\Psi(\mathrm{T}+p)$ and $\Psi(\mathrm{He}^3+n)$ denote the internal wave functions of the pairs T + p and He^3 + n, while the expressions in the curly brackets are functions of the relative motion of T and p, and He^3 + n, respectively. $\mathcal{R}^{(\pm)}_{k_1 l}(r)$ and $R^{(\pm)}_{kl}(r)$ are the Coulomb and ordinary free solutions; A, B, C, D are constants, about which we shall speak later, and k_1 and k are the wave vectors of the relative motion of the systems T + p and He^3 + n, respectively, and differ from each other only by the mass differences of $T+p$ and He^3 + n. The function (2.1) is divided in the usual way into two parts

$$\psi(r>r_0)=\psi_{r=1}+\psi_{r=0},$$

which at $r=r_0$ transform into the wave function $\delta_{T=1}$ and $\delta_{T=0}$, respectively. The functions $\Psi_{T=1}$ and $\Psi_{T=0}$ differ from each other by the different values of the constants A, B, C, and D, which we shall distinguish by the arguments 1 and 0: $A=A(1)+A(0)$; $B=B(1)+B(0)$, etc.

At $r=r_0$, the wave function (2.1) ought to join together with the internal wave function (1.9). We shall fist concern ourselves with states with isotopic spin $T=1$, and shall connect the function $\delta_{T=1}$ with the function $\delta_{T=1}$ which is defined by the values of the constants $A(1)$, $B(1)$, $C(1)$, $C(1)$. The boundary conditions are written in the following fashion:

$$\psi_{T=1}(r_0) = \varphi_{T=1}(r_0), \quad \psi'_{T=1}(r_0) = \varphi'_{T=1}(r_0). \tag{2.2}$$

Now, substituting the functions from (1.2, (1.6), (1.7), and equating terms with corresponding l, we get

$$\begin{aligned} a_{l1}^{l+1}\ (1) &= A_l(1);\ a_{l+2,1}^{l+1}(1) = A_{l+2}(1); \\ b_{l1}^{l+1}\ (1) &= B_l(1);\ b_{l+2,1}^{l+1}(1) = B_{l+1}(1), \end{aligned} \tag{2.2'}$$

$$\begin{aligned} &A_l(1)\,R_{kl}^{(-)}(r_0) - B_l(1)\,R_{kl}^{(+)}(r_0) \\ &\quad = C_l(1)\,\mathscr{R}_{k_1 l}^{(-)}(r_0) - D_l(1)\,\mathscr{R}_{k_1 l}^{(+)}(r_0); \\ &A_l(1)\,R_{kl}^{(-)'}(r_0) - B_l(1)\,R_{kl}^{(+)'}(r_0) \\ &\quad = C_l(1)\,\mathscr{R}_{k_1 l}^{(-)'}(r_0) - D_l(1)\,\mathscr{R}_{k_1 l}^{(+)'}(r_0), \\ &A_{l+2}(1)\,R_{k,\,l+2}^{(-)}(r_0) - B_{l+2}(1)\,R_{k,\,l+2}^{(+)}(r_0) \\ &\quad = C_{l+2}(1)\,\mathscr{R}_{k_1,\,l+2}^{(-)}(r_0) - D_{l+2}(1)\,\mathscr{R}_{k_1,\,l+2}^{(+)}(r_0), \\ &A_{l+2}(1)\,R_{k,\,l+2}^{(-)'}(r_0) - B_{l+2}(1)\,R_{k,\,l+2}^{(+)'}(r_0) \\ &\quad = C_{l+2}(1)\,\mathscr{R}_{k_1,\,l+2}^{(-)'}(r_0) - D_{l+2}(1)\,\mathscr{R}_{k_1,\,l+2}^{(+)'}(r_0) \end{aligned} \tag{2.2''}$$

(the primes denote differentiation with respect to r). We get directly from (2.2″):

$$\begin{aligned} C_l(1) &= \gamma_{11}^{(l)} A_l(1) + \gamma_{12}^{(l)} B_l(1), \\ D_l(1) &= \gamma_{21}^{(l)} A_l(1) + \gamma_{22}^{(l)} B_l(1) \end{aligned} \tag{2.3}$$

and corresponding equations for $l+2$. Here,

$$\begin{aligned} \gamma_{11}^{(l)} &= \frac{1}{G}\,[R_{kl}^{(-)'}(r_0)\,\mathscr{R}_{k_1,l}^{(+)}(r_0) - R_{kl}^{(-)}(r_0)\,\mathscr{R}_{k_1,l}^{(+)'}(r_0)], \\ \gamma_{12}^{(l)} &= -\frac{1}{G}\,[R_{kl}^{(+)'}(r_0)\,\mathscr{R}_{k_1,l}^{(+)}(r_0) - R_{kl}^{(+)}(r_0)\,\mathscr{R}_{k_1,l}^{(+)'}(r_0)], \\ \gamma_{21}^{(l)} &= \frac{1}{G}\,[R_{kl}^{(-)'}(r_0)\,\mathscr{R}_{k_1,l}^{(-)}(r_0) - R_{kl}^{(-)}(r_0)\,\mathscr{R}_{k_1,l}^{(-)'}(r_0)], \\ \gamma_{22}^{(l)} &= -\frac{1}{G}\,[R_{kl}^{(+)'}(r_0)\,\mathscr{R}_{k_1,l}^{(-)}(r_0) - R_{kl}^{(+)}(r_0)\,\mathscr{R}_{k_1,l}^{(-)'}(r_0)], \\ G &= -\frac{2ik_1}{r_0^2}, \end{aligned} \tag{2.4}$$

The $R_{rl}^{(\pm)}$ were determined earlier by (1.7), while the $\mathscr{R}_{r1,l}^{(\pm)}$ are functions of the motion in the Coulomb field

$$\mathscr{R}_{k_1,l}^{(\pm)}(r) = \frac{1}{r}\,[G_l(k_1 r) \pm iF_l(k_1 r)],$$

where F_l and G_l are the regular and nonregular Coulomb functions.* Carrying out the calculations for states with $T=0$, we get

$$\begin{aligned} C_l(0) &= -[\gamma_{11}^{(l)} A_l(0) + \gamma_{12}^{(l)} B_l(0)], \\ D_l(0) &= -[\gamma_{21}^{(l)} A_l(0) + \gamma_{22}^{(l)} B_l(0)] \end{aligned} \tag{2.5}$$

and corresponding equations for $l+2$.

We now consider the boundary conditions at infinity. Let the case of interest to us be the reactions T(pn) He^{3}and T(pp) T. In both these processes, the ingoing waves of the nuclei He^3 and n ought to be absent. Therefore, the condition below ought to be satisfied [see Eq. (2.1)]:

$$\begin{aligned} A_l &\equiv A_l(1) + A_l(0) = 0, \\ A_{l+2} &\equiv A_{l+2}(1) + A_{l+2}(0) = 0. \end{aligned} \tag{2.6}$$

The second pair of boundary conditions is connected with normalization of the ingoing waves of T and p. Actually, in the general problem, when we consider collisions of protons with the nucleus T, the amplitude of the ingoing (T + p)-wave is found by a simple expansion of plane waves (with consideration of the spins of the particles) in a series in the functions Y_{ls}^{J}. The corresponding formulas are ordered repeatedly[1], and the second pair of boundary conditions has the form:

$$\begin{aligned} C_l &\equiv C_l(1) + C_l(0) = \gamma_{11}^{(l)}(A_l(1) - A_l(0)) \\ &\quad + \gamma_{12}^{(l)}(B_l(1) - B_l(0)) = C_l^{(0)}, \\ C_{l+2} &\equiv C_{l+2}(1) + C_{l+2}(0) = \gamma_{11}^{(l+2)}(A_{l+2}(1) \\ &\quad - A_{l+2}(0)) + \gamma_{12}^{(l+2)}(B_{l+2}(1) - B_{l+2}(0)) = C_{l+2}^{(0)}. \end{aligned} \tag{2.7}$$

Here we have made use of Eq. (2.3), while the quantities on the right-hand side, $C_l^{(0)}$ and $C_{l+2}^{(0)}$, are the amplitudes (unknown from the statement of the problem) of the outgoing waves of T + p. The boundary conditions for the reactions He^3 (np)T and He^3 (nn) He^3 are formulated in a similar way. In these cases, the ingoing waves of T + p are absent.

---

*The coefficients $\gamma_{in}^{(l)}$ depend on the energy and on r_0. The value of r_0 is bounded above and below. Below, it is bounded by the condition that for $r > r_0$, nuclear interaction between the colliding and outgoing particles is absent. At the same time, r_0 cannot be too large, since the Coulomb interaction can be neglected only in the zone of action of the nuclear forces.

3. MATRIX OF THE REACTION FOR STATES WITH GIVEN *T*

In this Section, we shall study in detail the physical meaning and the structure of the amplitudes $A_l(T)$, $B_l(T)$, $C_l(T)$ and $D_l(T)$. It is evident from Eq. (2.1) that $A_l(T)$ and $C_l(T)$ are the amplitudes of the ingoing waves of ($\mathrm{He}^3 + n$), respectively, while $B_l(T)$ and $D_l(T)$ are the amplitudes of the outgoing waves. The amplitudes B and D are expressed by the amplitudes of the ingoing waves A and C:

$$\begin{aligned}
B_l(T) &= S^{(l+1)}_{l1,\,l1}(T)\,A_l(T) + S^{l+1}_{l1,\,l+21}(T)\,A_{l+2}(T) + \\
&+ \sqrt{\frac{k_1}{k}}\,[M^{l+1}_{l1,\,l1}(T)\,C_l(T) + M^{l+1}_{l1,\,l+21}(T)\,C_{l+2}(T)],\\
B_{l+2}(T) &= S^{l+1}_{l+21,\,l1}(T)\,A_l(T) + S^{l+1}_{l+21,\,l+21}(T)\,A_{l+2}(T) + \\
&+ \sqrt{\frac{k_1}{k}}\,[M^{l+1}_{l+21,\,l1}(T)\,C_l(T) + M^{l+1}_{l+21,\,l+21}(T)\,C_{l+2}(T)],\\
D_l(T) &= \sqrt{\frac{k}{k_1}}\,['M^{l+1}_{l1,\,l1}(T)\,A_l(T) + 'M^{l+1}_{l1,\,l+21}(T)\,A_{l+2}(T)] + \\
&+ \Omega^{l+1}_{l1,\,l1}(T)\,C_l(T) + \Omega^{l+1}_{l1,\,l+21}(T)\,C_{l+2}(T),\\
D_{l+2}(T) &= \sqrt{\frac{k}{k_1}}\,['M^{l+1}_{l+21,\,l1}(T)\,A_l(T) + 'M^{l+1}_{l+21,\,l1}(T)\,A_{l+2}(T)] + \\
&+ \Omega^{l+1}_{l+21,\,l1}(T)\,C_l(T) + \Omega^{l+1}_{l+21,\,l+21}(T)\,C_{l+2}(T).
\end{aligned} \tag{3.1}$$

The matrix of the coefficients S, M, $'M$, Ω is known as the reaction matrix. The element with indices $S^J_{ls,\,l's'}(T)$ describes the transition between the state ($Jl's'T$) and the state ($JlsT$). The indices for the other elements can be interpreted similarly. Since we assume the validity of the hypothesis of charge invariance, there are no transitions between states with different isotopic spins T and the amplitudes of the outgoing waves with given T are expressed in terms of the amplitudes of the ingoing waves with the same T. Inasmuch as the nuclear interaction depends on the isotopic spin, the reaction matrices for $T = 1$ and $T = 0$ will be different.

The matrix elements $S^J_{ls,\,l's'}(T)$ connect the amplitudes of the incident and outgoing waves of $\mathrm{He}^3 + n$. Therefore, this part of the matrix describes the elastic process of scattering $\mathrm{He}^3\,(nn)\,\mathrm{He}^3$. The elements $M(T)$ describe the reaction $\mathrm{T}\,(pn)\,\mathrm{He}^3$, the elements $'M(T)$, the reaction $\mathrm{He}^3\,(np)\,\mathrm{T}$, and the elements $\Omega(T)$, the elastic scattering $T\,(pp)\,\mathrm{T}$ (all these refer to states with given T).

It is not difficult to see that the matrix elements $M(T)$ and $'M(T)$ are identically equal to zero. We now show that this is a consequence of the assumed hypothesis of charge invariance. Actually, absorption of particles ought not to take place in the reaction process; therefore, the total particle flux incident on the sphere $r = r_0$ ought to be equal to the flux of outgoing particles on the sphere $r = r_0$. But the current through the sphere r_0 can be computed by using the wave functions (1.2) or (1.3), in which we must substitute the values for $\Psi^{(1)}$ and $\Psi^{(2)}$ from Eq. (1.8). In this case, use is made of the fact that the total number of particles ($\mathrm{He}^3 + n$), as also the total number of particles ($\mathrm{T} + p$) found in states with $J = l \pm 1$ and entering the sphere, is proportional to

$$|a^{l+1}_{l1}(T)|^2 + |a^{l+1}_{l+2,\,1}(T)|^2,$$

while the number of particles leaving the sphere is proportional to

$$|b^{l+1}_{l1}(T)|^2 + |b^{l}_{l+2,1}(T)|^2.$$

From the flux equality, it follows that

$$\begin{aligned}
&|b^{l+1}_{l1}(T)|^2 + |b^{l+1}_{l+21}(T)|^2 \\
&\qquad = |a^{l+1}_{l1}(T)|^2 + |a^{l+1}_{l+21}(T)|^2.
\end{aligned} \tag{3.2}$$

Making use of the conditions (2.2′), we rewrite (3.2′) in the form

$$|A_l(T)|^2 + |A_{l+2}(T)|^2 = |B_l(T)|^2 + |B_{l+2}(T)|^2. \tag{3.3}$$

Substituting $B_l(T)$ and $B_{l+2}(T)$ from (3.1) in (3.3), we get:

$$\begin{aligned}
&|A_l(T)|^2 + |A_{l+2}(T)|^2 \\
&\qquad = |A_l(T)|^2\,[\,|S^{l+1}_{l1,\,l1}(T)|^2 + |S^{l+1}_{l+21,\,l1}(T)|^2] \\
&+ |A_{l+2}(T)|^2\,[\,|S^{l+1}_{l+21,\,l+21}(T)|^2 + |S^{l+1}_{l1,\,l+21}(T)|^2]
\end{aligned}$$

$$
\begin{aligned}
&+[A_l(T)\,A^{*}_{l+2}(T)\,(S^{l+1}_{l1,\,l1}(T)\;S^{l+1*}_{l1,\,l+21}(T)\\
&\qquad + S^{l+1}_{l+21,\,l1}(T)\,S^{l+1*}_{l+21,\,l+21}(T)) + \text{c.c.}]\\
&+[\text{terms containing } C_l(T) \text{ and } C_{l+2}(T)]. \qquad (3.4)
\end{aligned}
$$

All the terms on the right-hand side of (3.4), except the first three, depend on the elements of M. Equation (3.4) ought to be satisfied for all values of $A_l(T)$, $A_{l+2}(T)$, $C_l(T)$ and $C_{l+2}(T)$. This is possible only if the matrix M is equal to zero, while the matrix

$$
S = \begin{vmatrix} S^{l+1}_{l1,\,l1}(T) & S^{l+1}_{l+21,\,l1}(T) \\ S^{l+1}_{l1,\,l+21}(T) & S^{l+1}_{l+21,\,l+21}(T) \end{vmatrix}
$$

is unitary, *i. e.*, if $S^{+}=S^{-1}$. Similarly, it can be shown that the matrix $'M$ is equal to zero. This also follows from the fact that, thanks to the invariance of the Hamiltonian relative to a time inversion, the total matrix of the reaction ought to be symmetric relative to the main diagonal[2]

$$
S=\widetilde{S};\quad \Omega=\widetilde{\Omega};\quad 'M=\widetilde{M}, \qquad (3.5)
$$

where ~ denotes the transposed matrix. It is not difficult to show that the most general form of the matrix S which satisfies all the above conditions is

$$
S(T)=\begin{vmatrix} \cos\varepsilon^{l+1}_{l}(T)\exp\{i\delta^{l+1}_{l}(T)\}; & i\sin\varepsilon^{l+1}_{l}(T)\exp\left\{\frac{i}{2}(\delta^{l+1}_{l}(T)+\delta^{l+1}_{l+2}(T))\right\} \\ i\sin\varepsilon^{l+1}_{l}(T)\exp\left\{\frac{i}{2}(\delta^{l+1}_{l}(T)+\delta^{l+1}_{l+2}(T))\right\}; & \cos\varepsilon^{l+1}_{l}(T)\exp\{i\delta^{l+1}_{l+2}T)\} \end{vmatrix} \qquad (3.6)
$$

the $\delta^{J}_{ls}(T)$ have the simple meaning of the scattering phases in states J, l, s, T, while the parameter $\epsilon^{J}_{l}(T)$ determines the amount of transitions $l\rightleftarrows(l+2)$. Frequently, $\epsilon^{J}_{l}(T)$ is known as the mixing parameter.

We shall now show that the matrices $S(T)$ and $\Omega(T)$ are expressible in terms of each other. For this purpose, we make use of the connection between C and D and A and B, which is given by the boundary conditions (2.3). Since $'M=0$, the latter two of Eqs. (3.1) connected the amplitudes C and D. Substituting in the right and left sides of these equations for C and D their values from (2.3), and expressing B in terms of A and $S^{J}_{ls,\,l's'}(T)$ by means of the first two of Eqs. (3.1), we get (upon equating terms with equal powers of A) four equations which connect $S(T)$ and $\Omega(T)$. Solving them for Ω, we find:

$$
\begin{aligned}
\Omega_0(T) &= \frac{1}{N}\{(\gamma^{(l)}_{21}+\gamma^{(l)}_{22}S_0(T))(\gamma^{(l+2)}_{11}\\
&\quad +\gamma^{(l+2)}_{12}S_2(T))-\gamma^{(l+2)}_{12}\gamma^{(l)}_{22}S^{2}_{1}(T)\},\\
\Omega_1(T) &= \frac{S_1(T)}{N}\{\gamma^{(l)}_{11}\gamma^{(l)}_{22}-\gamma^{(l)}_{12}\gamma^{(l)}_{21}\},\\
\Omega_2(T) &= \frac{1}{N}\{(\gamma^{(l+2)}_{21}+\gamma^{(l+2)}_{22}S_2(T))(\gamma^{(l)}_{11}\\
&\quad +\gamma^{(l)}_{12}S_0(T))-\gamma^{(l)}_{12}\gamma^{(l+2)}_{22}S^{2}_{1}(T)\},\\
N &= (\gamma^{(l)}_{11}+\gamma^{(l)}_{12}S_0(T))(\gamma^{(l+2)}_{11}\\
&\quad +\gamma^{(l+2)}_{12}S_2(T))-\gamma^{(l)}_{12}\gamma^{(l+2)}_{12}S^{2}_{1}(T),
\end{aligned} \qquad (3.7)
$$

where we have introduced the notation

$$
\begin{aligned}
&S_0(T)=S^{l+1}_{l1,\,l1}(T);\;\; S_1(T)\\
&\qquad = S^{l+1}_{l1,\,l+21}(T)=S^{l+1}_{l+21,\,l1}(T),\\
&S_2(T)=S^{l+1}_{l+21,\,l+21}(T),\;\; \Omega_0(T)=\Omega^{l+1}_{l1,\,l1}(T),\\
&\Omega_1(T)=\Omega^{l+1}_{l1,\,l+21}(T)=\Omega^{l+1}_{l+21,\,l1}(T);\\
&\Omega_2(T)=\Omega^{l+1}_{l+21,\,l+21}(T).
\end{aligned}
$$

Making use of Eqs. (3.7) and (7.1, it is not difficult to prove that the matrix Ω (T) is unitary and symmetric, *i. e.*, that it satisfies all those conditions which ought to be laid down for the scattering matrix. Thus the total scattering matrix of the system ($2p$, $2n$) which satisfies states with given J, T and P, is expressed by only three real parameters, for which we can choose, for example, $\delta^{l+1}_{l}(T)$, $\delta^{l+1}_{l+2}(T)$ and $\epsilon^{l+1}_{l}(T)$. We note here that we here that we could, with the same success, have expressed them all not by δ and ϵ but by three other parameters $\omega^{l+1}_{l}(T)$, $\omega^{l+1}_{l+2}(T)$ and $x^{l+1}_{l}(T)$ which would be related to the matrix $\Omega(T)$ in the same way as the first group were related with the matrix $S(T)$.

All the derivations of this Section apply with equal force to states with $T=1$ and with $T=0$. Since we deal experimentally with states which are superpositions of states with equal T, the total matrix of the reaction in states with momentum J are some combination of the scattering matrices which correspond to $T = 1$ and $T = 0$, and will therefore be determined by the same six real parameters. In the general case, where the hypothesis of charge invariance is invalid, the number of parameters in the reaction matrix is equal to 10^2.

4. THE REACTIONS T (pp) T, T (pn) He^3, He^3 (nn) He^3 AND He^3 (np) T

We begin by investigating the case of the collision of a proton with a tritium nucleus. The boundary conditions at infinity reduce in this case to the absence of ingoing waves of He^3 $+n$, *i. e.*, the conditions reduce to the four equations (2.6) and (2.7). Substituting in Eq. (2.7) the expressions for $C_l(T)$ and $C_{l+2}(T)$ [(2.3) and (2.5)], expressing the $B_l(T)$ and $B_{l+2}(T)$ therein in terms of $A_l(T)$ and $A_{l+2}(T)$, and taking Eq. (2.6) into account, we get the following equations for A_l (1) and A_{l+2}(1):

$$A_l(1)\,[2\gamma_{11}^{(l)} + \gamma_{12}^{(l)}S_0^{(+)}] + A_{l+2}(1)\,\gamma_{12}^{(l)}S_1^{(+)} = C_l^{(0)},$$

$$A_l(1)\,\gamma_{12}^{(l+2)}S_1^{(+)} + A_{l+2}(1)\,[2\gamma_{11}^{(l+2)} + \gamma_{12}^{(l+2)}S_2^{(+)}] = C_{l+2}^{(0)}, \tag{4.1}$$

$$S_i^{(+)} = S_i(1) + S_i(0) \qquad (i = 0,\ 1,\ 2).$$

Solving (4.1) for the various A, we get:

$$A_l(1) = -A_l(0) = \frac{1}{N_1}\{C^{(0)}[2\gamma_{11}^{(l+2)} + \gamma_{12}^{(l+2)}S_2^{(+)}] - C_{l+2}^{(0)}\gamma_{12}^{(l)}S_1^{(+)}\}.$$

$$A_{l+2}(1) = -A_{l+2}(0) = \frac{1}{N_1}\{-C_l^{(0)}\gamma_{12}^{(l+2)}S_1^{(+)} + C_{l+2}^{(0)}[2\gamma_{11}^{(l)} + \gamma_{12}^{(l)}S_0^{(+)}]\},$$

$$N_1 = [2\gamma_{11}^{(l)} + \gamma_{12}^{(l)}S_0^{(+)}].[2\gamma_{11}^{(l+2)} + \gamma_{12}^{(l+2)}S_2^{(+)}] - \gamma_{12}^{(l)}\gamma_{12}^{(l+2)}S_1^{(+)2}. \tag{4.2}$$

We can now compute the matrix elements of the total reaction matrix, which corresponds to the reactions T (pp) T and T (pn) He^3. The amplitude of the outgoing (T+ p) waves is equal to: in a state with orbital momentum l: $D_l \equiv D_l(1) + D_l(0)$; in states with orbital momentum $l+2$: $D_{l+2} \equiv D_{l+2}(1) + D_{l+2}(0)$. To begin with, we consider the first sum.

$$D_l = \gamma_{21}^{(l)}(A_l(1) - A_l(0)) + \gamma_{22}^{(l)}(B_l(1) - B_l(0))$$
$$= A_l(1)\,[2\gamma_{21}^{(l)} + \gamma_{22}^{(l)}S_0^{(+)}] + A_{l+2}(1)\,\gamma_{22}^{(l)}S_1^{(+)}$$

The first equation was written on the basis of Eqs. (2.3) and (2.5), and the second on the basis of Eq. (3.1). Replacing $A_l(T)$ and $A_{l+2}(T)$ by their values in (4.2), we get an expression of the following form for D_l:

$$D_l = \Omega_{l1,l1}^{l+1}C_l^{(0)} + \Omega_{l1,l+21}^{l+1}C_{l+2}^{(0)}; \tag{4.3}$$

$$\left.\begin{aligned} \Omega_{l1,l1}^{l+1} &= \frac{1}{N_1}\{(2\gamma_{21}^{(l)} + \gamma_{22}^{(l)}S_0^{(+)})(2\gamma_{11}^{(l+2)} + \gamma_{12}^{(l+2)}S_2^{(+)}) - \gamma_{22}^{(l)}\gamma_{12}^{(l+2)}S_1^{(+)2}\},\\ \Omega_{l1,l+21}^{l+1} &= \frac{1}{N_1}S_1^{(+)}2(\gamma_{11}^{(l)}\gamma_{22}^{(l)} - \gamma_{12}^{(l)}\gamma_{21}^{(l)}). \end{aligned}\right\} \tag{4.4}$$

According to the same interpretation of Eq. (4.3), which expresses the amplitude of the outgoing wave by the amplitudes of ingoing waves, the coefficients $\Omega_{l1,l1}^{l+1}$ and $\Omega_{l1,l+21}^{l+1}$ are the elements of the scattering matrix of the reaction T (pp) T.

Continuing similar calculations for D_{l+2}, we get

$$D_{l+2} = \Omega_{l+21,l1}^{l+1}C_l^{(0)} + \Omega_{l+21,l+21}^{l+1}C_{l+2}^{(0)}, \tag{4.5}$$

where

$$\Omega_{l+21,l1}^{l+1} = \Omega_{l1,l+21}^{l+1},$$

$$\Omega_{l+21,l+21}^{l+1} = \frac{1}{N_1}\{(2\gamma_{21}^{(l+2)} + \gamma_{22}^{(l+2)}S_2^{(+)})(2\gamma_{11}^{(l)} + \gamma_{12}^{(l)}S_0^{(+)}) - \gamma_{22}^{(l+2)}\gamma_{12}^{(l)}S_1^{(+)2}\}, \tag{4.6}$$

The matrix elements Ω completely describe the scattering T (pp) T in states with given J and P.

We now proceed to the reaction T (pn) He^3. In order to find the elements of the reaction matrix which describes this process, we proceed exactly as in the previous case, *i. e.*, we compute the amplitudes of the outgoing waves

$$B_l = B_l(1) + B_l(0); \qquad B_{l+2} = B_{l+2}(1) + B_{l+2}(0).$$

For brevity, we do not repeat the derivation, but merely write down the result:

$$B_l = \sqrt{k_1/k}\,\{M^{l+1}_{l1,l1}C^{(0)}_l + M^{l+1}_{l1,l+21}C^{(0)}_{l+2}\}, \quad (4.7)$$
$$B_{l+2} = \sqrt{k_1/k}\,\{M^{l+1}_{l+21,l1}C^{(0)}_l + M^{l+1}_{l+21,l+21}C^{(0)}_{l+2}\},$$

where the elements of the reaction matrix describing the process T (pn) He^3 are

$$M^{l+1}_{l1,l1} = \sqrt{\frac{k}{k_1}}\frac{1}{N_1}\{2\gamma^{(l+2)}_{11}S^{(-)}_0 + \gamma^{(l+2)}_{12}[S^{(+)}_2S^{(-)}_0 - S^{(+)}_1S^{(-)}_1]\},$$

$$M^{l+1}_{l1,l+21} = \sqrt{\frac{k}{k_1}}\frac{1}{N_1}\{2\gamma^{(l)}_{11}S^{(-)}_1 + \gamma^{(l)}_{12}[S^{(+)}_0S^{(-)}_1 - S^{(-)}_0S^{(+)}_1]\},$$

$$M^{l+1}_{l+21,l1} = \sqrt{\frac{k}{k_1}}\frac{1}{N_1}\{2\gamma^{(l+2)}_{11}S^{(-)}_1 + \gamma^{(l+2)}_{12}[S^{(+)}_2S^{(-)}_1 - S^{(-)}_2S^{(+)}_1]\}, \quad (4.8)$$

$$M^{l+1}_{l+21,l+21} = \sqrt{\frac{k}{k_1}}\frac{1}{N_1}\{2\gamma^{(l)}_{11}S^{(-)}_2 + \gamma^{(l)}_{12}[S^{(+)}_0S^{(-)}_2 - S^{(+)}_1S^{(-)}_1]\}.$$

$$S^{(-)}_i = S_i(1) - S_i(0) \quad (i = 0, 1, 2).$$

We can analyze the reactions He^3 (nn) He^3 and He^3, (np) T with the help of exactly the same considerations. In this case, only the waves of He$^3 + n$ with amplitudes $A^{(0)}_l$ and $A^{(0)}_{l+2}$ appear, while the waves of T $+p$ with amplitudes

$$D_l = \sqrt{k/k_1}\,\{'M^{l+1}_{l1,l1}A^{(0)}_l + {}'M^{l+1}_{l1,l+21}A^{(0)}_{l+2}\},$$
$$D_{l+2} = \sqrt{k/k_1}\,\{'M^{l+1}_{l+21,l1}A^{(0)}_l + {}'M^{l+1}_{l+21,l+21}A^{(0)}_{l+2}\} \quad (4.9)$$

and the waves of He$^3 + n$ with amplitudes

$$B_l = S^{l+1}_{l1,l1}A^{(0)}_l + S^{l+1}_{l1,l+21}A^{(0)}_{l+2},$$
$$B_{l+2} = S^{l+1}_{l+21,l1}A^{(0)}_l + S^{l+1}_{l+21,l+21}A^{(0)}_{l+2}. \quad (4.10)$$

both diverge.

The corresponding elements of the reaction matrix are:

$$'M^{l+1}_{l1,l'1} = M^{l+1}_{l'1,l1}; \quad (4.11)$$

$$S^{l+1}_{l1,l1} = \frac{1}{2}S^{(+)}_0 + \frac{1}{2N_1}\{2\gamma^{(l)}_{12}\gamma^{(l+2)}_{12}S^{(+)}_1S^{(-)}_1S^{(-)}_0 - \gamma^{(l)}_{12}S^{(-)2}_0(2\gamma^{(l+2)}_{11} + \gamma^{(l+2)}_{12}S^{(+)}_2) - \gamma^{(l+2)}_{12}S^{(-)2}_1(2\gamma^{(l)}_{11} + \gamma^{(l)}_{11}S^{(+)}_0)\},$$

$$S^{l+1}_{l1,l+21} = S^{l+1}_{l+21,l1} = \frac{1}{2}S^{(+)}_1 + \frac{1}{2N_1}\{\gamma^{(l)}_{12}\gamma^{(l+2)}_{12}S^{(+)}_1(S^{(-)}_0S^{(-)}_2 + S^{(-)2}_1) - \gamma^{(l)}_{12}S^{(-)}_0S^{(-)}_1(2\gamma^{(l+2)}_{11} + \gamma^{(l+2)}_{12}S^{(+)}_2) - \gamma^{(l+2)}_{12}S^{(-)}_2S^{(-)}_1(2\gamma^{(l)}_{11} + \gamma^{(l)}_{12}S^{(+)}_0)\}, \quad (4.12)$$

$$S^{l+1}_{l+21,l+21} = \frac{1}{2}S^{(+)}_2 + \frac{1}{2N_1}\{2\gamma^{(l)}_{12}\gamma^{(l+2)}_{12}S^{(+)}_1S^{(-)}_1S^{(-)}_2 - \gamma^{(l+2)}_{12}S^{(-)2}_2(2\gamma^{(l)}_{11} + \gamma^{(l)}_{12}S^{(+)}_0) - \gamma^{(l)}_{12}S^{(-)2}_1(2\gamma^{(l+2)}_{11} + \gamma^{(l+2)}_{12}S^{(+)}_2)\}.$$

We have thus computed the total reaction matrix of the system $(2p,\ 2n)$ in states with $s = 1$ and $J = l+1$, $P = (-)^l$.

$$\begin{array}{cc|cc|cc}
 & & \multicolumn{4}{c}{\text{Ingoing particles}} \\
 & & \multicolumn{2}{c|}{\mathrm{He}^3 + n} & \multicolumn{2}{c}{\mathrm{T} + p} \\
 & & l & l+2 & l & l+2 \\
\hline
\text{Outgoing particles: } \mathrm{He}^3 + n & l & S^{l+1}_{l1,l1} & S^{l+1}_{l1,l+21} & M^{l+1}_{l1,l1} & M^{l+1}_{l1,l+2} \\
 & l+2 & S^{l+1}_{l+21,l1} & S^{l+1}_{l+21,l+21} & M^{l+1}_{l+21,l1} & M^{l+1}_{l+21,l+21} \\
\hline
\mathrm{T} + p & l & M^{l+1}_{l1,l1} & M^{l+1}_{l+21,l1} & \Omega^{l+1}_{l1,l1} & \Omega^{l+1}_{l1,l+21} \\
 & l+2 & M^{l+1}_{l1,l+21} & M^{l+1}_{l+21,l+21} & \Omega^{l+1}_{l+21,l1} & \Omega^{l+1}_{l+21,l+21}.
\end{array} \quad (4.13)$$

where matrix elements are given by Eqs. (4.12), (4.8), (4.6) and (4.4). Direct verification shows that this matrix is unitary and symmetric, as was assumed for the reaction matrix. All its elements are expressed by $S_0(T)$, $S_1(T)$, $S_2(T)$, *i. e.*, by the six real parameters $\delta^{l+1}_l(T)$, $\delta^{l+1}_{l+2}(T)$, $\epsilon^{l+1}_l(T)$.

The reaction matrix for the states with $J = l$ is found by precisely the same method. Here two values of total spin are possible, $s = 0$ and $s = 1$. In this case the following four states are possible initially and finally:

$$\mathrm{T} + p : s = 0,\ s = 1; \quad \mathrm{He}^3 + n : s = 0,\ s = 1.$$

We omit the details and write down the result immediately. The complete reaction matrix has the form:

$$\begin{array}{lll|cc|cc}
 & & & \multicolumn{4}{c}{\text{Ingoing particles}}\\
 & & & \multicolumn{2}{c|}{\mathrm{He}^3+n} & \multicolumn{2}{c}{\mathrm{T}+p}\\
 & & & l,s=1 & l,s=0 & l,s=1 & l,s=0\\ \hline
\text{Outgoing particles} & \mathrm{He}^3+n & l,s=1 & S^l_{l1,l1} & S^l_{l1,l0} & M^l_{l1,l1} & M^l_{l1,l0}\\
 & & l,s=0 & S^l_{l0,l1} & S^l_{l0,l0} & M^l_{l0,l1} & M^l_{l0,l0}\\ \hline
 & \mathrm{T}+p & l,s=1 & M^l_{l1,l1} & M^l_{l0,l1} & \Omega^l_{l1,l1} & \Omega^l_{l1,l0}\\
 & & l,s=0 & M^l_{l1,l0} & M^l_{l0,l0} & \Omega^l_{l0,l1} & \Omega^l_{l0,l0}.
\end{array} \tag{4.14}$$

All the elements of this matrix are easily obtained from the corresponding (*i .e.*, located in the same box) elements of the matrix (4.13) with the help of the substitution

$$\gamma_{ik}^{(l+2)} \to \gamma_{ik}^{(l)}. \tag{4.15}$$

By $S_i(T)$ we now mean

$$S_0(T) = S^l_{l1,l1}(T); \tag{4.16}$$

$$S_1(T) = S^l_{l1,l0}(T)\,(= S^l_{l0,l1}(T)); \quad S_2(T) = S^l_{l0,l0}(T).$$

The matrix elements $S^l_{ls,l's'}(T)$ are expressed in terms of the corresponding real parameters $\delta^l_s(T)$ and $\epsilon^s_l(T)$ with the help of formulas similar to (3.6).

At present we are interested only in the wave functions of the system in states with given total momentum. The total scattering amplitude ought to be obtained by a summation over the various l and J. The corresponding formulas have already been derived[1].

5. THE REACTIONS $He^3(pp)He^3$ AND $T(nn)T$

In the foregoing Section, we investigated all reactions which are possible for the system of two protons and two neutrons at low energy. In this case, the system can be found both in states with $T=1$ and in states with $T=0$. In the present Section, we consider reactions in systems $(3p, n)$ and $(3n, p)$, where only states with $T=1$ are possible. States with isotopic spin $T=2$ will again not be taken into consideration, since they cannot be formed in reactions were there are (in the initial and final states) only particles with isotopic spin ½.

Let us look at the system $(3p, n)$. For low energies, such a system ought to have the form He^3+n at infinity and, consequently, only elastic scattering $He^3(pp)He^3$ is possible. In as much as only one value of T is possible ($T=1$), the scattering matrix $He^3(pp)He^3$ should coincide with the matrix $\Omega(T)$ computed in Sec. 3 for $T=1$ [Eqs. (3.7)]. However, we must take it into account that the charge of He^3 is twice that of T. This leads to a change of the function $R^{(+)}_{k1,l}(r)$ which describes the relative motion of He^3 and p for $r>r_0$, in comparison with the case $T+p$. The quantities $\gamma_{ik}^{(l)}$ are changed correspondingly. Equations (3.7) are introduced for the case $J=l+1$. The expressions for the scattering matrix in states with $J=l$ are obtained from (3.7) with the help of the substitution of (4.15) and (4.16) [here the element $\Omega^{l+1}_{l1,l1}(1)$ corresponds to $\Omega^l_{l1,l1}(1)$, the element Ω $\Omega^{l+1}_{l1,l+21}(1)$ to the element $\Omega^l_{l1,l0}(1)=\Omega^l_{l0,l1}(1)$ and the element $\Omega^{l+1}_{l+21,l+21}(1)$ to the element $\Omega^l_{l0,l0}(1)$]. Similarly, in the scattering case $T(nn)T$ [the system $(3n, p)$], where there is no Coulomb interaction between the colliding particles, the elements of the scattering matrix coincide with the matrices $S_{ls,l's'}(T)$ for $T=1$ [the form of this matrix for $J=l+1$ was given above in Eq. (3.6). The total scattering amplitudes for the reactions $He^3(pp)He^3$ and $T(nn)T$, which were obtained by summing over all J, can be obtained by using the equations of Ref. 1.

Thus, we could express the elements of the matrices of all the reactions which are possible for the systems $(2p, 2n)$, $(3p, n)$ and $(p, 3n)$ for small energies, by the parameters $\delta^J_{ls}(T)$ and $\epsilon^J_l(T)$. This greatly simplifies the problem of the experimental determination of the parameters δ and ϵ, since we can use (in finding them) the experimental data on all six reactions written down in the introduction, and not just any one, as usually was the case. It should be remembered that the parameters δ and ϵ depend on the form of the wave function inside the sphere $r \leqslant r_0$. For each of the systems $(2p, 2n)$, $(3p, n)$ and $(3n, p)$, the form of the wave function for $r=r_0$ is determined by that part of the energy of the system which is connected to the charge invariant nuclear interaction. Therefore, in the common analysis, we must select such energies for the incident particles in the systems $(2p, 2n)$, $(3p, n)$ and $(3n, p)$, that the energy of the nuclear interaction in all these systems were equal, and therefore the wave functions for $r \leqslant r_0$ likewise. This can be done approximately in the following way. The total energy of the system $(2p, 2n)$ is composed of the mass of the two neutrons and two protons $c^2(2m_n+2m_p)$, the Coulomb interaction of the two protons E_k and the energy of nuclear interaction E_n:

$$E(2p,\ 2n) = E_n + E_\text{K} + 2\,(m_n + m_p)\,c^2.$$

Similarly, the total energy of the system $(3p, n)$ is equal to

$$E(3p, n) = E_n + 3E_K + (3m_p + m_n)c^2. \quad (5b)$$

In the system $(3n, p)$, there is no Coulonb interaction, and

$$E(3n, p) = E_n + (3m_n + m_p)c^2. \quad (5c)$$

In order to carry out the common analysis, we must so choose the total energy of all systems that E_n will be the same in each. This is satisfied approximately if

$$E(2n, 2p) - E(3p, n) \approx 0, \quad (5d)$$
$$E(2n, 2p) - E(3n, p) \approx -0{,}4 \text{ MeV}.$$

We recall that here it is not a question of the total energy in the center-of-mass system.

6. BEHAVIOR OF THE ELEMENTS OF THE REACTION MATRIX AT THRESHOLD ENERGIES

In order to conclude the general investigation of the reaction matrix, it remains for us to study the behavior of the matrix elements for small energies of the incident particles and those generated during the reaction.

Let us consider the collision of T with p. At low energies, only elastic collisions are possible: T(pp) T. Beginning with the proton energy 1.019 Mev, (in the laboratory system), the reaction T(pp)He^3 becomes possible. Let us investigate the behavior of the elements of the reaction matrix in the neighborhood of 1.019 Mev. For this, we note that the boundary value of the radial wave function for $r=r_0$ [Eqs. (1.5) and (1.7)], must remain finite for all energies of the system; however, the functions entering into (1.5) and (1.7) of the free motion $R^{(+)}_{kl}(r)$ tend to infinity for $k\to 0$, *i. e.*, for energies which approach the threshold of He^3+n. In order that the wave function remain finite as $k\to 0$, the following rules for approach to zero of the phases (as $kr_0\to 0$) are necessary:

$$\delta^J_{ls}(T) \to \text{const}\,(kr_0)^{2l+1}; \quad \varepsilon^J_l(T) \to \text{const}\,(kr_0)^{2l+3}. \quad (6.1)$$

These laws are easily obtained by use of the expansion of $R^{(+)}_{kl}(r_0)$ in a power series in kr_0, and Eqs. (1.6)

With the help of the limiting law (6.1), we can easily determine the behavior of the elements of the reaction matrix (4.13) and (4.14) as $k\to 0$:

$$(S^J_{ls,l's'} - 1) \to \text{const}\,(kr_0)^{2l+1},$$
$$S^J_{l1,l+21} \to \text{const}\,(kr_0)^{2l+3}, \quad (6.2)$$
$$M^J_{ls,ls'} \to \mathfrak{M}_l\,(kr_0)^{l+1/2}; \quad M^J_{l1,l+21} \to \text{const}\,(kr_0)^{l+1/2},$$
$$M^J_{l+21,l1} \to \text{const}\,(kr_0)^{l+3/2}.$$

The constant coefficient $\mathfrak{M}_l$ entering into the formula for $M^J_{ls,ls'}$ is needed by us below. The elements $\Omega^J_{ls,ls'}$ remain finite for $k\to 0$, even though they have a break at $k=0$. We first consider the case $l=0$, *i. e.*, the element $\Omega^s_{0s,0s}$. It is evident from (4.4) and (4.6) that $\Omega^s_{0s,0s}$ depends only on $\gamma^{(l)}_{ik}$ and $S^{(l)}_i$. With the help of Eq. (3.7), we can express $S^{(+)}_i$, which, for $k\to 0$, ought to remain constant, since they are defined in the form of a wave function for $r<r_0$, and this function has no singularities for $k=0$. We can expand the coefficients $\gamma^{(0)}_{ik}$ in power series in k. Substituting these expansions in the formula for $\Omega^s_{0s,0s}$, we get, after lengthy but simple calculations, for the case $(kr_0)\to 0$,

$$\Omega^s_{0s,0s} \to (\Omega^s_{0s,0s})_{k=0}\left(1 - kr_0\,\frac{1}{2}\,|\mathfrak{M}_0|^2\right). \quad (6.3)$$

For energies lower than the threshold, only elastic scattering T(pp) T is possible; the modulus of $\Omega^s_{0s,0s}$ in this region must therefore be unity and, consequently, $|(\Omega^s_{0s,0s})_{k=0}|=1$ (this is also obtained upon direct computation). The wave vector k is positive above the threshold and becomes a pure imaginary below the threshold. It therefore follows from (6.3) that, in the neighborhood of the threshold (from below), $\Omega^s_{0s,0s}$ has a constant modulus and varies linearly in phase (with change in $|k|$), while in the neighborhood of the threshold from above, on the other hand, the phase is constant but the modulus varies linearly. Thus, for $k=0$, a break occurs in both the modulus and the phase of $\Omega^s_{0s,0s}$. Consequently, we also have a break in the cross section of T(pp) T, since the component $|\Omega^s_{0s,0s}-1|^2$ enters into the cross section. The cross section on both sides of $k=0$ must change linearly, while a break must be observed at $k=0$.

The elements $\Omega^J_{ls,ls}$ with $l \neq 0$ must behave in precisely the same way as $\Omega^s_{0s,0s}$ in the neighborhood of the threshold. The only difference lies in the fact the modulus and the phase will not depend linearly on kr_0, but on a much higher power of kr_0.

The break vanishes only when $\mathfrak{M}_l = 0$, and this, as is evident from (4.8), takes place only when $S_i\,(T=1) = S_i\,(T=0)$ *i. e.*, when the dependence of the reaction matrix on the isotopic spin vanishes, and when the cross section of the reaction $\mathrm{He}^3(np)\,\mathrm{T}$ is equal to zero.

7. CONCLUDING REMARKS

The results of the present research can be summarized as follows. We have succeeded in representing the elements of the reaction matrix (which correspond to possible reactions in the system of four nucleons) at low energies,

$$\mathrm{T}\,(pp)\,\mathrm{T};\;\; \mathrm{T}\,(pn)\,\mathrm{He}^3;\;\; \mathrm{T}\,(nn)\,\mathrm{T};\;\; \mathrm{He}^3\,(pp)\,\mathrm{He}^3;$$

$$\mathrm{He}^3\,(nn)\,\mathrm{He}^3;\;\; \mathrm{He}^3\,(np)\,\mathrm{T},$$

by the same parameters $\Omega^J_{ls}\,(T)$ and $\epsilon^J_l\,(T)$. The latter have the simple physical meaning of the scattering phases in a state with isotopic spin T. Thus, a common analysis of all six reactions is possible and this simplifies the problem of the experimental determination of the phases δ and ϵ.

Up to the present, we have expressed all the elements of the reaction matrix in terms of the phases δ and ϵ. This is not always useful. Sometimes it is more suitable to work with the parameters $\omega(T)$ and $x(T)$ which have the same connections with the matrix Ω as $\delta(T)$ and $\epsilon(T)$ have with the matrix $S(T)$. A corresponding calculation of all the formulas of the present work is easily carried out with the help of Eq. (3.7), which must be solved for $S_0(T)$, $S_1(T)$ and $S(T)$. The calculations here are trivial and we shall not carry them out. We must only consider that, as follows from (2.4),

$$\gamma^{(l)}_{11} = \gamma^{(l)*}_{22};\;\; \gamma^{(l)}_{12} = \gamma^{(l)}_{21}; \qquad |\gamma^{(l)}_{11}|^2 - |\gamma^{(l)}_{12}|^2 = \frac{k}{k_1} \quad \text{for } k<0, \tag{7.1}$$

and

$$\gamma^{(l)}_{11} = -\gamma^{(l)*}_{21};\;\; \gamma^{(l)}_{12} = -\gamma^{(l)*}_{22} \quad \text{for imaginary } k.$$

In conclusion I should like to thank Ia. A. Smorodinskii for his constant interest in the work.

---

[1] J. M. Blatt and L. C. Biedenharn, Rev. Mod. Phys. **24**, 258 (1052)

[2] J. Blatt and V. Weiskopf, *Theoretical Nuclear Physics.*

Translated by R. T. Beyer
115

SOVIET PHYSICS JETP VOLUME 5, NUMBER 3 OCTOBER, 1957

The Energy Spectrum of Cascade Electrons in Lead

I. P. IVANENKO
Moscow State University

(Submitted to JETP editor December 2, 1955)
J. Exptl. Theoret. Phys. (U.S.S.R.) 32, 491-497 (March, 1957)

Recursion formulas have been obtained for the nth moment of the distribution function of a shower containing particles with energies above a prescribed value. The first two moments of the electron distribution function in lead have been calculated. The moment method has been applied to compute the energy spectrum of cascade electrons in lead.

THE method of moments[1-7] has been applied to obtain a series of important characteristics of electron-photon cascade showers in heavy elements. This method is based on the computation of the distribution function $N(E_0, 0, t)$ at a depth t for the total number of particles in a shower initiated by a primary particle of energy E_0, by means of recursion formulas[2] for the moments $\overline{t^n}(E_0, 0)$. The moments are defined by the expression

$$\overline{t^n}(E_0, 0) = \int_0^\infty N(E_0, 0, t)\, t^n dt \Big/ \int_0^\infty N(E_0, 0, t)\, dt.$$

In Ref. 3 we suggested a method for computing cascade curves, including the energy dependence of the total absorption coefficient of photons, $\sigma(E)$, and the Rutherford scattering of charged particles, by means of a set of polynomials that are orthogonal in the interval $(0, \infty)$. It was shown in Ref. 3 that the use of the first two moments $\overline{t}$ and $\overline{t^2}$ allows one to compute cascade curves $N(E_0, 0, t)$ for heavy and light elements differing by less than 5 to 10% from the exact curves over a primary energy range of $0{,}1\beta$ to $\sim 1000\beta$. This method is easily generalized to allow computation of the energy spectrum of cascade particles in heavy elements. Carrying out a computation similar to that of Belen'kii and Maksimov,[4] one obtains recursion formulas for the moments of the distribution in depth for particles of energy greater than E^0, in showers initiated by primary particles of energy E_0:

$$\{\overline{t_p^n}(E_0, E^0)\}^p = n \int_{E^0}^{E_0} \Big[\{\overline{t_p^{n-1}}(E', E^0)\}^p \int_{E^0}^{E'} P_{p,0,0}$$

$$\times (E_0, E)\, dE \cdot P_{p,0,n}(E_0, E')$$

$$+ \{\overline{t_p^{n-1}}(E', E^0)\}^\Gamma \int_{E^0}^{E_0} P_{\Gamma,0,0}(E_0, E)\, dE \cdot \Gamma_{p,0,n}$$

$$\times (E_0, E')\Big] dE' \Big/ \int_{E^0}^{E_0} P_{p,0,0}(E_0, E)\, dE,$$

$$\{\overline{t_p^n}(E_0, E^0)\}^\Gamma = n \int_{E^0}^{E_0} \Big[\{\overline{t_p^{n-1}}(E', E^0)\}^p \int_{E^0}^{E'} P_{p,0,0}$$

$$(E_0, E)\, dE \cdot P_{\Gamma,0,n}(E_0, E')$$

$$+ \{\overline{t_p^{n-1}}(E', E^0)\}^\Gamma \int_{E^0}^{E'} P_{\Gamma,0,0}(E_0, E)\, dE \tag{1}$$

$$\times \Gamma_{\Gamma,0,n}(E_0, E')\Big] dE' \Big/ \int_{E^0}^{E_0} P_{\Gamma,0,0}(E_0, E)\, dE.$$

The upper indices p and Γ denote showers initiated respectively by primary electrons and photons of energy E_0, $P_{p,0,0}(E_0,E) = \int_0^\infty \int_{(\omega)} P_p(t, E, \theta)\, d\omega dt$, and $\Gamma_{p,0,0}(E_0, E) = \int_0^\infty \int_{(\omega)} \Gamma_p(t, E, \theta) d\omega dt$ are the "equilibrium" spectra for electrons and photons in showers caused by primary electrons; $P_p(t, E, \theta)$ and $\Gamma_p(t, E, \theta)$ are the distribution functions for electrons and photons at a depth $\overline{t}$, energy E, and angle θ in showers due to primary electrons. Analogous recursion formulas are easily obtained for the moments of the photon distribution function.

We list in Table I the moments $\overline{t}$ and $\overline{t^2}$ computed from Eq. (1) for various values of E_0 and E^0 including the energy dependence of the total absorption coefficient of photons $\sigma(E)$ (the dependence of $\sigma(E)$ upon E was taken from Ref. 8, and the Rutherford scattering of charged particles. In carrying out

TABLE I.

$\varepsilon_0 = 50$			$\varepsilon_0 = 90$			$\varepsilon_0 = 118{,}1$		
ε^0	$\{\overline{t}_p(\varepsilon_0, \varepsilon^0)\}^\Gamma$	$\{\overline{t^2_p}(\varepsilon_0, \varepsilon^0)\}^\Gamma$	ε^0	$\{\overline{t}_p(\varepsilon_0, \varepsilon^0)\}^\Gamma$	$\{\overline{t^2_p}(\varepsilon_0, \varepsilon^0)\}^\Gamma$	ε^0	$\{\overline{t}_p(\varepsilon_0, \varepsilon^0)\}^\Gamma$	$\{\overline{t^2_p}(\varepsilon_0, \varepsilon^0)\}^\Gamma$
0	6,30	58,5	0	7,08	70,3	0	7,43	74,6
0,183	6,12	54,9	0,183	6,89	66,6	0,183	7,25	70,9
0,738	5,59	45,4	0,932	6,22	53,6	0,838	6,57	59,5
1,292	5,18	40,2	1,680	5,74	45,4	1,493	6,12	50,8
2,402	4,66	31,8	2,428	5,40	38,9	2,476	5,67	43,9
3,511	4,30	26,7	4,674	4,79	31,6	4,114	5,19	36,3
5,175	3,90	22,0	6,919	4,33	27,5	6,734	4,54	29,1
6,839	3,61	18,6						

the numerical computations, we have used the expression for the "equilibrium" spectrum including scattering, $P_{p,0,0}(E_0, E), \ldots$, derived in Ref. 4. In that reference, the expressions for the "equilibrium" spectrum were obtained from an approximate solution, integrated over depth, of the basic equations of cascade theory including scattering. This approximation was shown in Ref. 5 to be within 6% of the exact value. Note that the expression for the "equilibrium" spectrum appears as the zero moment in the recursion formulas (1). An error in the zero moment will give rise to a growing error in higher moments, so that in adopting the moment method, it is important to have an accurate expression for the "equilibrium" spectrum.

We have used the values obtained for the moments $\{\overline{t}_p(E_0, E^0)\}^\Gamma$ and $\{\overline{t^2_p}(E_0, E^0)\}^\Gamma$, to calculate the distribution function for the number of electrons of energy greater than E^0, at a given depth t, in showers initiated by photons of energy E_0. We have approximated the function $\{N_p(E_0, E^0, t)\}^\Gamma$ by a sum of Laguerre polynomials $L^1_n(x)$:*

$$\{N_p(E_0, E^0, t)\}^\Gamma = (\gamma t)e^{-\gamma t}\sum_{n=0}^{K} A_n L^1_n(\gamma t),$$

$$L^1_0(x) = 1; \quad L^1_1(x) = 2 - x; \tag{2}$$

$$L^1_2(x) = 2 - 3x + x^2/2, \ldots$$

The orthogonality conditions on the polynomials yield the coefficients

$$A_n = \frac{\gamma}{n+1}\int_0^\infty N(E_0, E^0, t)\, L^1_n(\gamma t)\, dt. \tag{3}$$

These are simply related to the moments:

$$A_0 = \gamma K_\Gamma \frac{E_0}{\beta}; \quad A_1 = \frac{\gamma}{2} K_\Gamma \frac{E_0}{\beta}\{2 - \gamma\{\overline{t_p}(E_0, E^0)\}^\Gamma\};$$

$$A_2 = \frac{\gamma}{3} K_\Gamma \frac{E_0}{\beta}\{3 - 3\gamma\{\overline{t_p}(E_0, E^0)\}^\Gamma + \frac{\gamma^2}{2}\{\overline{t^2_p}(E_0, E^0)\}^\Gamma\}; \ldots$$

The coefficient γ is set equal to the minimum value of the total absorption coefficient of the most penetrating part of the radiation — the photons. $K_\Gamma(E_0, E^0)$ is defined by the expression

$$K_\Gamma(E_0, E^0) = -\frac{\varepsilon^0}{\varepsilon_0} e^{\varepsilon^0 - \varepsilon_0} + 1 + \varepsilon^0 e^{\varepsilon^0}(\mathrm{Ei}(-\varepsilon^0) - \mathrm{Ei}(-\varepsilon_0)) - \frac{\varepsilon^0}{\varepsilon_0^2}(1 - e^{-\varepsilon_0 + \varepsilon^0});$$

$$\varepsilon = \frac{Eq}{\beta}; \quad q = 2{,}29,$$

where β is the critical energy for a given substance.

The distribution function $\{N_p E_0, t, E^0)\}^\Gamma$ computed according to Eq. (2), is shown plotted in Fig. 1 to 3. The areas under the curve equal

$$\int_{E^0}^{E_0} P_\Gamma(E_0, E)\, dE = \frac{E_0}{\beta} K_\Gamma.$$

---

* Approximation (2) is obtained by generalizing the approximation obtained in Ref. 3 for the function $N(E_0, 0, t)$.

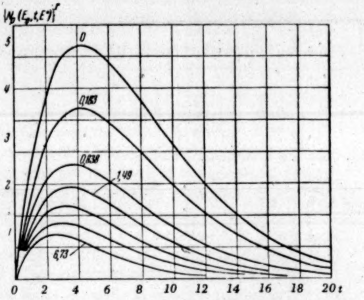

FIG. 1. Electron distribution functions in lead. The energy of the primary photon is $\varepsilon_0 = 118.1$. The values of ε_0 are indicated on the curves. The values of ε_0 for the second and the third curves from the bottom are respectively $\varepsilon_0 = 4.11$, and $\varepsilon^0 = 2.48$.

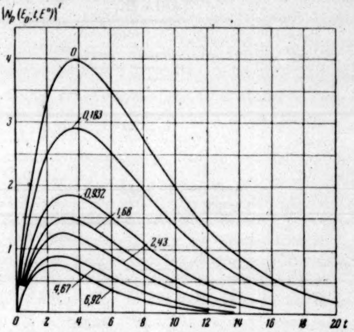

FIG. 2. Electron distribution functions in lead. The energy of the primary photon is $\varepsilon_0 = 90$. The values of ε^0 are indicated on the curves.

TABLE II.

$\varepsilon_0 = 50$		$\varepsilon_0 = 90$		$\varepsilon_0 = 118{,}1$	
ε^0	$K_\Gamma(\varepsilon_0, \varepsilon^0)$	ε^0	$K_\Gamma(\varepsilon_0, \varepsilon^0)$	ε^0	$K_\Gamma(\varepsilon_0, \varepsilon^0)$
0	1	0	1	0	1
0,023	0,924	0,023	0,924	0,023	0,924
0,072	0,836	0,072	0,836	0,072	0,836
0,107	0,790	0,107	0,790	0,107	0,790
0,183	0,715	0,183	0,715	0,183	0,715
0,738	0,413	0,932	0,417	0,838	0,438
1,292	0,354	1,680	0,307	1,493	0,329
2,402	0,246	2,428	0,245	2,476	0,242
4,511	0,190	4,674	0,155	4,114	0,171
5,175	0,142	6,919	0,114	6,734	0,117
6,839	0,113				

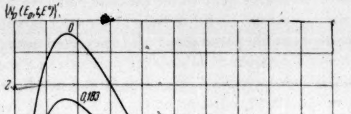

FIG. 3. Electron distribution functions in lead. The energy of the primary photon is $\varepsilon_0 = 50$. The values of ε^0 are indicated on the curves.

The values of $K_\Gamma(E_0, E^0)$ are listed in Table II for various values of E_0 and E^0. Note that for $E_0 \gg \beta$, the function $K_\Gamma(E_0, E^0)$ shows only slight dependence on E_0, and changes considerably as E^0 varies near zero. Fig. 4 shows the "equilibrium" spectrum obtained by Tamm and Belen'kii[9]; this figure also shows the energy spectra in the region of cascade maximum** constructed from the curves of Fig. 1 to 3. It may be seen in Fig. 4 that the energy spectra in the region of cascade maximum for $\epsilon_0 = 118.1$, 90, 50 agree with each other to within 2%, and agree within 10% with the "equilibrium" spectrum of Tamm and Belen'kii whose accuracy has been estimated several times.[10]

**As shown in cascade theory (see Ref. 13) the "equilibrium" energy spectrum resembles the spectrum found in the region of maximum spread of the cascade.

TABLE III.

t	1	2,6	4	6	8	10
$\varepsilon_0 = 118,1$	1,25	1,1	1,00	1,08	1,12	1,06
$\varepsilon_0 = 90$	1,11	1,00	1,01	0,98	1,08	1,22
$\varepsilon_0 = 50$	0,87	0,94	0,96	1,16	1,20	

TABLE IV.

	t	6	8	10	12
$\varepsilon_0 = 118,1$	S_{Pb}	1	1,1	1,2	1,3
	S_{light}	1,2—1,3	1,4—1,5	1,6—1,7	1,8—1,9
$\varepsilon_0 = 90$	S_{Pb}	1	1,1	1,2	1,3
	S_{light}	1,3—1,4	1,5—1,6	1,7—1,8	1,8—1,9

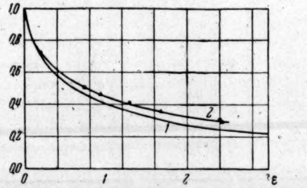

FIG. 4. Curve *1*: "equilibrium" energy spectrum; curve *2*: spectrum for maximum cascades initiated by primary photons of energy $\varepsilon_0 = 118.1$; the triangles give the spectrum for maximum cascades due to primary photons of energy $\varepsilon_0 = 90$, the squares, for maximum cascades due to primary photons of energy $\varepsilon_0 = 50$.

Let us assume that there are $N(E_0, 0, t_i)$ particles at a depth t_i; these particles have energy $E = \{1 - K(t_i)\} E_0$, where $K(t_i) = \frac{\beta}{E_0} \int_0^{t_i} N(E_0, 0, t) dt$ is determined by integrating $\{N_p(E_0, 0, t)\}^\Gamma$ (Fig. 1, 2, 3). We can therefore determine the average energy,

$$\overline{E}_{\text{area}} = \{1 - K(t_i)\} E_0 / N(E_0, t_i, 0),$$

of a particle at a depth t_i. On the other hand, we can use the curves $\{N_p(E_0, t, E^0)\}^\Gamma$ of Fig. 1 to 3 to determine the energy spectra of the particles and thus the average particle energy at a depth t_i.

Table III shows the value of the ratio of the average energies, $a = \overline{E}_{\text{spect}} / \overline{E}_{\text{area}}$, computed in these two ways; they agree within 20% for all values of the depth t_i. Obviously, damping is considerably faster in a light than in a heavy material at the cascade maximum. Therefore, at a given depth t_i, the energy spectrum of cascade particles will be softer in a light than in a heavy material at the cascade maximum. In order to verify whether this rule is fulfilled by the approximate curve *2*, we have evaluated the energy spectra for cascade particles according to Eq. (15.10) of Ref. 11 for various values of the cascade parameter.* We have then used these to determine the cascade parameter for the approximate curves *2*, Fig. 1 to 3, at a depth $t_i = 6, 8, 10, 12$ radiation units. We have also evaluated the cascade parameter s for a light material at the same depths t_i, by means of Eq. (15.15) of Ref. 11. The results of these calculations are presented in Table IV, from which it may be seen that for all depths, the cascade parameter s is larger in a light than in heavy material at the same depth. Therefore, in curves *2* the energy spectrum for cascade particles is softer in a light than in a heavy material. We conclude from this that the "equilibrium" spectrum of Tamm and Belen'kii appears correct.

---

*In cascade theory the parameter s characterizes the "softness" of the energy spectrum of cascade particles: the larger is s, the softer is the energy spectrum.

The "equilibrium" spectrum may be computed from the curves 2 appearing in Figs. 1 to 3, by integrating over the depth. It agrees to 1% with the expression obtained in Ref. 9, which permits us to judge the accuracy of the numerical computations. Thus the cascade curves $\{N_p E_0, t, E^0)\}^\Gamma$ obtained from Eq. (2) for lead, are accurate to 5 to 10%. We recall that the curves of Fig. 1 to 3 were obtained by including the energy dependence of the total absorption coefficient of photons and the Rutherford scattering of charged particles. The formula obtained by Fainberg[6] for the moments $\overline{t^n}(E_0,0)$ for an arbitrary spectrum of primary particles neglecting scattering, is easily generalized to include Rutherford scattering of charged particles for the moments $\overline{t^n}(E_0, E^0)$. Carrying out the corresponding calculation for the case when the photon spectrum in the boundary layer of the material has the form $\Gamma(E_0, 0, E, \theta) = \Phi_\gamma(E_0, E)\delta(\theta)$, where E_0 is the upper limit of the spectrum, we obtain the following formula:

$$\{\overline{t_p^n}(E_0, E^0)\}^{\Phi_\gamma} = \int\limits_{E^0}^{E_0} \Phi_\gamma(E_0, E)\{\overline{t_p^n}(E, E^0)\}^\Gamma \times$$

$$\times \int\limits_{E^0}^{E} P_{\Gamma, 0, 0}(E, E')\, dE' dE \Bigg/ \int\limits_{E^0}^{E_0} P_{0, 0}(E_0, E)\, dE;$$

$$\{\overline{t_\Gamma^n}(E_0, E^0)\}^{\Phi_\gamma} = \int\limits_{E^0}^{E_0} \Phi_\gamma(E_0, E)\{\overline{t_\Gamma^n}(E, E^0)\}^\Gamma \times$$

$$\times \int\limits_{E^0}^{E} \Gamma_{\Gamma, 0, 0}(E, E')\, dE'\, dE \Bigg/ \int\limits_{E^0}^{E_0} \Gamma_{0, 0}(E_0, E)\, dE. \tag{4}$$

The quantities $P_{0,0}(E_0, E)$ and $\Gamma_{0,0}(E_0, E)$ are determined from the formulas

$$P_{0, 0}(E_0, E) = \int\limits_{E}^{E_0} \Phi_\gamma(E_0, E')\, P_{\Gamma, 0, 0}(E', E)\, dE';$$

$$\Gamma_{0, 0}(E_0, E) = \int\limits_{E}^{E_0} \Phi_\gamma(E_0, E')\, \Gamma_{\Gamma, 0, 0}(E', E)\, dE'.$$

The remaining quantities are computed from our Eq. (1).* The moments $\{t_p(E_0, E^0)\}^{\Phi\gamma}$ and $\{\overline{t_p^2}(E_0, E^0)\}^{\Phi\gamma}$ were computed for lead in Ref. 7, including Rutherford scattering of charged particles and energy dependence of the total absorption coefficient of photons, from a spectrum of primary photons, $\Phi_\gamma(E_0, E)$, having the form:

$$\Phi_\gamma(E_0, E) = \begin{cases} 1/E & \text{for } E < 330 \text{ Mev,} \\ 0 & \text{for } E > 330 \text{ Mev.} \end{cases} \tag{5}$$

The results of these calculations were compared with the corresponding values computed from the experimental data of Blocker, Kenny and Panofsky,[12] assuming $E^0 = 0.5$ Mev; the computed and experimental values of $\{\overline{t_p^n}(E_0, E^0)\}^{\Phi\gamma}$ agree to 4%. However, the moments $\overline{t^n}(E_0, E^0)$ are very sensitive functions of E^0 in the neighborhood of zero. The correctness of the choice $E^0 \approx 0.5$ Mev may be verified as follows: The authors of Ref. 12 have measured the areas under the cascade curves for the photon spectrum (5) in various materials. They have obtained particularly accurate values for the cases of Cu and Pb as the cascade curves for these elements were measured to a distance of 20 and 40 "cascade" units respectively. According to the data of Ref. 12:

$$\int\limits_0^\infty N(E_0, t, E^0)\, dt = 0{,}946 \frac{E_0}{\beta} \text{ in Cu and}$$

$$\int\limits_0^\infty N(E_0, t, E^0)\, dt = 0{,}846 \frac{E_0}{\beta} \text{ in Pb.}$$

Making use of our results listed in Table II, both of these values for the areas may be satisfied with $E^0 = 0.2$ Mev.**Note that the results which have been obtained, apply to experiments in which the measuring apparatus is surrounded by absorbers on all sides,[13] thus excluding edge effects which we have neglected.

The author wishes to express his gratitude to Professor S. Z. Belen'kii for valuable advice.

---

*The formulas of Ref. 6 for the moments $\{\overline{t_p^n}(E_0, E)\}^{\Phi\gamma}$, $\{\overline{t}_p(E_0, E^0)\}^\Gamma$ and $\{\overline{t_p^2}(E_0, E^0)\}^\Gamma$ are in error.

** Note that the resulting spectra are somewhat uncertain in the region of such small energies; besides, the experimental value of $\{\overline{t_p^n}(E_0, E^0)\}^{\Phi\gamma}$ is 4% smaller than the theoretical value. Thus the actual value of E^0 lies between 0.2 and 0.5 Mev.

---

[1] G. T. Zatsepin, Dokl. Akad. Nauk SSSR 63, 243 (1948)

[2] S. Z. Belen'kii, J. Exptl. Theoret. Phys. (U.S.S.R.) 19, 940 (1949).

[3] I. P. Ivanenko, Izv. Akad. Nauk SSSR, ser. fiz. 19, 624 (1955).

[4] S. Z. Belen'kii and B. I. Maksimov, J. Exptl. Theoret. Phys. (U.S.S.R.) 22, 102 (1952).

[5] I. P. Ivanenko, Dokl. Akad. Nauk SSSR 107, 819 (1956); Sov. Phys. "Doklady" 1, 231 (1956).

[6] V. Ia. Fainberg, J. Exptl. Theoret. Phys. (U.S.S.R.) 22, 112 (1952).

[7] I. P. Ivanenko, J. Exptl. Theoret. Phys. (U.S.S.R.) 31, 86 (1956);

[8] W. Heitler, *The Quantum Theory of Radiation*, Clarendon Press, Oxford, 1954.

[9] J. Tamm and S. Belenky, J. Phys. (U.S.S.R.) 1, 177, (1939).

[10] B. Rossi, *High Energy Particles*, Prentice-Hall, Inc. New York, 1952.

[11] S. Z. Belen'kii, *Cascades in Cosmic Rays*, GITTL, 1948.

[12] Blocker, Kenney and Panofsky, Phys. Rev. 79, 419 (1950).

[13] S. N. Vernov and O. N. Vavilov, Phys. Rev. 70, 769 (1946).

Translated by M. A. Melkanoff
116

SOVIET PHYSICS JEPT VOLUME 5, NUMBER 3 OCTOBER, 1957

Characteristic Frequencies and Amplitudes of Free Normal Oscillations in KCl Crystals

T. I. KUCHER
Zhitomir Pedagogical Institute

(Submitted to JETP editor December 24, 1955)
J. Exptl. Theoret. Phys. (U.S.S.R.) 32, 498-505 (March, 1957)

Results are presented for a calculation of the characteristic frequencies and amplitudes of free normal oscillations of the ions of a KCl crystal. These calculations are carried out for values of the wave vector **k** which uniformly cover the cell of the reciprocal lattice by 729 points, with account taken of polarization deformation of the electron shells of the ions. A comparison is made with the results obtained by other authors.[1,2]

KNOWLEDGE of the characteristic frequencies and amplitudes of the free normal oscillations of the ions of a crystal is necessary in the solution of a number of problems, for example, in the determination of heat capacity, the interaction of a conduction electron with the vibrations of the lattice, the energy of interaction of point charges placed in a crystal, computation of the energy levels of the local states of an electron or hole with small radius of the state, etc.[3]

The frequencies $\omega_{\mathbf{k}}^{\alpha}$ for certain wave numbers **k** were found by Iona.[1] The amplitudes were not of interest since he computed the heat capacity. In determining the frequencies, Iona considered a model of a point lattice with ions of equal mass. Tolpygo and Zaslavskaia[2] computed the frequencies and amplitudes of the normal vibrations of a KCl crystal for 8 values of the vector **k** which, in particular, were obtained in Ref. 1 by considering the deformation of the electron shells of the ions, according to the method proposed earlier by Tolpygo.[4,5]

However, part of the exchange integral of the interaction of two (opposite) neighbors, which depends on the polarization, was thrown away in Ref. 2, without any justification. This can be avoided.[6] Moreover, knowledge of the frequencies for only 125 points of the reciprocal lattice is insufficient for the following quantitative analysis.

Let us consider an ideal crystal of KCl. We denote the dipole moment of the electron shell s, of the lth ion by $\mathbf{P}_s^l$, and the dipole moment, due to a shift $\mathbf{u}_s^l$ of this ion from its equilibrium position, by $\mathbf{p}_s^l = e_s \mathbf{u}_s^l$ (e_s = charge of the sth ion). For the

Characteristic frequencies and amplitudes of free normal oscillations of KCl crystals*

$\frac{k_x}{\pi}$; $\frac{k_y}{\pi}$; $\frac{k_z}{\pi}$	Ω^2	ω, sec^{-1}	$p_{1x}\vert\pi_{1x}$	$p_{1y}\vert\pi_{1y}$	$p_{1z}\vert\pi_{1z}$	$p_{2x}\vert\pi_{2x}$	$p_{2y}\vert\pi_{2y}$	$p_{2z}\vert\pi_{2z}$
1	2	3	4	5	6	7	8	9
0, 0, 1/4	5,7641	3,7209	0	0	4741	0	0	5259
			0	0	4195	0	0	1039
	2,9250	2,6506	4760	0	0	5240	0	0
			5378	0	0	5818	0	0
	2,9250	2,6506	0	4760	0	0	5240	0
			0	5378	0	0	5818	0
	0,5292	1,1274	0	0	—5008	0	0	4978
			0	0	—5102	0	0	5063
	0,0772	0,4305	—4991	0	0	4998	0	0
			—4952	0	0	4791	0	0
	0,0772	0,4305	0	—4991	0	0	4998	0
			0	—4952	0	0	4791	0
0, 0, 1/2	4,0051	3,1016	0	0	4632	0	0	5365
			0	0	4083	0	0	1419
	2,9918	2,6807	4767	0	0	5233	0	0
			5431	0	0	5885	0	0
	2,9918	2,6807	0	4767	0	0	5233	0
			0	5431	0	0	5885	0
	1,7459	2,0478	0	0	—5109	0	0	4864
			0	0	—5450	0	0	5281
	0,2424	0,7631	—4984	0	0	5005	0	0
			—4860	0	0	4326	0	0
	0,2424	0,7631	0	—4984	0	0	5005	0
			0	—4860	0	0	4326	0
1/4, 1, 1	2,8706	2,6259	4287	0	0	5672	0	0
			5025	0	0	5872	0	0
	0,3797	0,9550	0	0	4980	0	0	5009
			0	0	4782	0	0	3890
	0,3797	0,9550	0	4980	0	0	5009	0
			0	4782	0	0	3890	0
	2,2084	2,3032	—5402	0	0	4502	0	0
			—4945	0	0	0785	0	0
	3,0574	2,7100	0	0	—4770	0	0	5230
			0	0	—5482	0	0	5955
	3,0574	2,7100	0	—4770	0	0	5230	0
			0	—5482	0	0	5955	0
0, 0, 1	1,4696	1,8788	0	0	5029	0	0	4955
			0	0	4509	0	0	1395
	3,0840	2,7217	4771	0	0	5229	0	0
			5502	0	0	5985	0	0
	3,0840	2,7217	0	4771	0	0	5229	0
			0	5502	0	0	5985	0
	3,2821	2,8077	0	0	—4719	0	0	5281
			0	0	—5571	0	0	6016
	0,4296	1,0158	—4980	0	0	5010	0	0
			—4758	0	0	3716	0	0
	0,4296	1,0158	0	—4980	0	0	5010	0
			0	—4753	0	0	3716	0
0, 1/4, 1/4	5,7036	3,7013	0	3433	3433	0	3636	3636
			0	3051	3051	0	0824	0824
	2,9532	2,6633	4762	0	0	5238	0	0
			5399	0	0	5842	0	0
	2,5435	2,4717	0	3300	—3300	0	3770	—3770
			0	3620	—3620	0	3960	—3960
	0,7391	1,3324	0	—3463	—3463	0	3605	3605
			0	—3461	—3461	0	3397	3397

---

*ω in Column 3 has been multiplied by 10^{-13} and the components of the vectors **P** and $\pi = p + P$ in Columns 4-9 been multiplied by 19^4.

$\frac{k_x}{\pi}$; $\frac{k_y}{\pi}$; $\frac{k_z}{\pi}$	Ω^2	ω, sec^{-1}	p_{1x}/π_{1x}	p_{1y}/π_{1y}	p_{1z}/π_{1z}	p_{2x}/π_{2x}	p_{2y}/π_{2y}	p_{2z}/π_{2z}
1	2	3	4	5	6	7	8	9
	0,1742	0,6469	—4988	0	0	5000	0	0
			—4909	0	0	4558	0	0
	0,4545	1,0449	0	—3590	3590	0	3465	—3465
			0	—3667	3667	0	3536	—3536
0, $^1/_4$, $^1/_2$	4,3779	3,2428	0	3311	3627	0	3290	3876
			0	3238	3145	0	2033	0628
	3,0203	2,6934	4765	0	0	5235	0	0
			5448	0	0	5902	0	0
	2,2960	2,3484	0	—3419	2801	0	—4070	3786
			0	—3873	2718	0	—4639	2869
	1,8262	2,0944	0	0717	5007	0	—1283	—4752
			0	0616	5293	0	—0891	—4957
	0,3825	0,9585	—4985	0	0	5004	0	0
			—4814	0	0	4022	0	0
	0,7033	1,2997	0	—4938	1219	0	4838	—0712
			0	—4928	1362	0	4354	—1095
0, $^1/_4$, $^3/_4$	3,1463	2,7490	0	4446	1574	0	4725	2364
			0	4788	1247	0	4563	0485
	3,0864	2,7228	4765	0	0	5235	0	0
			5494	0	0	5964	0	0
	1,8225	2,0923	0	1360	—4621	0	2545	—4515
			0	1712	—4225	0	3007	—1804
	2,8694	2,6253	0	—0777	—4792	0	—0006	5144
			0	—0766	—5432	0	—0373	5748
	0,5583	1,1580	—4985	0	0	5004	0	0
			—4735	0	0	3522	0	0
	0,8675	1,4435	0	—5034	0882	0	4862	0073
			0	—4944	0972	0	3884	—0430
0, $^1/_4$, 1	2,8859	2,6328	0	4744	0	0	5256	0
			0	5241	0	0	5461	0
	3,1134	2,7347	4764	0	0	5236	0	0
			5512	0	0	5990	0	0
	1,3540	1,8034	0	0	5018	0	0	4967
			0	0	4530	0	0	1693
	3,2549	2,7961	0	0	—4730	0	0	5269
			0	0	—5564	0	0	6011
	0,6222	1,2225	—4986	0	0	5002	0	0
			—4706	0	0	3324	0	0
	0,9439	1,5057	0	—5006	0	0	4981	0
			0	—4861	0	0	3839	0
0, $^1/_2$, $^1/_2$	3,7106	2,9854	0	3677	3677	0	3364	3364
			0	3358	3358	0	1210	1210
	3,0886	2,7237	4759	0	0	5240	0	0
			5486	0	0	5944	0	0
	1,7309	2,0390	0	1289	—1289	0	4938	—4938
			0	1255	—1255	0	4826	—4826
	2,2163	2,3073	0	—3203	—3203	0	3861	3861
			0	—3287	—3287	0	3340	3340
	0,6820	1,2799	—4991	0	0	4998	0	0
			—4717	0	0	3334	0	0
	1,4946	1,8947	0	—4703	4703	0	1353	—1353
			0	—4965	4965	0	1718	—1718
$^1/_4$, $^1/_2$, 1	2,9320	2,6538	4761	1605	0	4819	1175	0
			5278	1555	0	5287	0714	0
	0,9330	1,4970	0	0	5000	0	0	4988
			0	0	4639	0	0	2703
	1,9385	2,1578	0825	—4072	0	1916	—5453	0
			1120	—4200	0	2211	—5104	0
	2,5349	2,4675	—2146	—4319	0	2878	4302	0
			—1816	—4263	0	1061	3155	0
	3,1558	2,7532	0	0	—4750	0	0	5250
			0	0	—5522	0	0	5986

$\frac{k_x}{\pi}$; $\frac{k_y}{\pi}$; $\frac{k_z}{\pi}$ 1	Ω^2 2	ω, sec^{-1} 3	$p_{1x}\|\pi_{1x}$ 4	$p_{1y}\|\pi_{1y}$ 5	$p_{1z}\|\pi_{1z}$ 6	$p_{2x}\|\pi_{2x}$ 7	$p_{2y}\|\pi_{2y}$ 8	$p_{2z}\|\pi_{2z}$ 9
0, $^1/_2$, 1	1,2385	1,7247	—4430	3079	0	4134	—1803	0
			—4228	3269	0	2434	—2003	0
	2,1061	2,2492	0	0	0	0	7242	0
			0	0	0	0	6344	0
	3,1837	2,7653	4746	0	0	5254	0	0
			5537	0	0	6003	0	0
	1,0246	1,5688	0	0	5004	0	0	4983
			0	0	4610	0	0	2457
	2,0117	2,1982	0	6896	0	0	0	0
			0	7039	0	0	0	0
	1,0246	1,5688	—5004	0	0	4983	0	0
			—4610	0	0	2457	0	0
	3,1837	2,7653	0	0	—4746	0	0	5254
			0	0	—5537	0	0	6003
$^1/_8$, $^1/_8$, $^1/_8$	6,2719	3,8814	2778	2778	2778	2995	2995	2995
			2460	2460	2460	0588	0588	0588
	2,8116	2,5987	1934	1934	—3868	2148	2148	—4296
			2165	2165	—4330	2346	2346	—4692
	2,8116	2,5987	3350	—3350	0	3721	—3721	0
			3751	—3751	0	4063	—4063	0
	0,2649	0,7977	—2852	—2852	—2852	2917	2917	2917
			—2834	—2834	—2834	2806	2806	2806
	0,1375	0,5747	—2046	—2046	4092	2031	2031	—4062
			—2053	—2053	4106	2020	2020	—4040
	0,1375	0,5747	—3544	3544	0	3518	—3518	0
			—3556	3556	0	3498	—3498	0
$^1/_4$, $^1/_4$, $^1/_4$	5,6541	3,6852	2886	2886	2886	2880	2880	2880
			2571	2571	2571	0745	0745	0745
	2,5586	2,4790	1907	1907	—3814	2175	2175	—4350
			2101	2101	—4202	2306	2306	—4612
	2,5586	2,4790	3303	—3303	0	3767	—3767	0
			3640	—3640	0	3994	—3994	0
	1,0171	1,5630	—2743	—2743	—2743	3031	3031	3031
			—2675	—2675	—2675	2590	2590	2590
	0,5149	1,1121	—2071	—2071	4142	2002	2002	—4004
			—2100	—2100	4200	1970	1970	—3940
	0,5149	1,1121	—3587	3587	0	3468	—3468	0
			—3638	3638	0	3412	—3412	0
$^3/_8$, $^3/_8$, $^3/_8$	4,7177	3,3662	3148	3148	3148	2561	2561	2561
			2838	2838	2838	0931	0931	0931
	2,1547	2,2750	1819	1819	—3638	2256	2256	—4512
			1961	1961	—3922	2308	2308	—4616
	2,1547	2,2750	3151	—3151	0	3908	—3908	0
			3397	—3397	0	3997	—3997	0
	2,1110	2,2518	—2438	—2438	—2438	3305	3305	3305
			—2316	—2316	—2316	2316	2316	2316
	1,0405	1,5809	—2149	—2149	4297	1910	1910	—3820
			—2214	—2214	4428	1872	1872	—3745
	1,0405	1,5809	—3722	3722	0	3309	—3309	0
			—3835	3835	0	3243	—3243	0
$^1/_2$, $^1/_2$, $^1/_2$	3,8645	3,0467	3982	3982	3982	0	0	0
			3643	3643	3643	0	0	0
	1,7171	2,0308	0	0	0	2956	2956	—5912
			0	0	0	2947	2947	—5894
	1,7171	2,0308	0	0	0	5121	—5121	0
			0	0	0	5104	—5104	0
	3,0358	2,7004	0	0	0	4181	4181	4181
			0	0	0	2404	2404	2404
	1,5274	1,9154	2815	2815	—5630	0	0	0
			2952	2952	—5905	0	0	0
	1,5274	1,9154	4876	—4876	0	0	0	0
			5114	—5114	0	0	0	0
$^1/_8$, $^1/_8$, $^3/_8$	5,2132	3,5386	1984	1984	3956	2004	2004	4298
			1898	1898	3444	1014	1014	0693

$\frac{k_x}{\pi}$; $\frac{k_y}{\pi}$; $\frac{k_z}{\pi}$ 1	Ω^2 2	ω, $\sec^{-1}$ 3	$p_{1x}\|\pi_{1x}$ 4	$p_{1y}\|\pi_{1y}$ 5	$p_{1z}\|\pi_{1z}$ 6	$p_{2x}\|\pi_{2x}$ 7	$p_{2y}\|\pi_{2y}$ 8	$p_{2z}\|\pi_{2z}$ 9
	2,6722	2,5335	—2745	—2745	2598	—3093	—3093	3042
			—3135	—3135	2656	—3548	—3548	2555
	2,8568	2,6196	3355	—3355	0	3716	—3716	0
			3781	—3781	0	4105	—4105	0
	1,1577	1,6676	0603	0603	4902	—0732	—0732	—4906
			0554	0554	5070	—0513	—0513	—4985
	0,3479	0,9141	—3456	—3456	1064	3479	3479	—0804
			—3403	—3403	1159	3132	3132	—1027
	0,2662	0,7996	—3539	3539	0	3523	—3523	0
			—3504	3504	0	3248	—3248	0
$^1/_8$, $^1/_8$, $^5/_8$	3,6436	2,9584	2762	2762	2833	2824	2824	3289
			2973	2973	2408	2690	2690	0488
	2,4466	2,4242	—1738	—1738	—0098	—1742	—1742	6301
			—2012	—2012	—0644	—2295	—2295	4862
	2,9195	2,6481	3358	—3358	0	3713	—3713	0
			3823	—3823	0	4168	—4168	0
	2,3509	2,3763	0900	0900	—6250	1693	1693	1358
			1071	1071	—1205	1701	1701	0469
	0,5538	1,1534	—3511	—3511	0680	3515	3515	—0180
			—3394	—3394	0779	2763	2763	—0519
	0,4206	1,0051	—3536	3536	0	3527	3527	0
			—3439	3439	0	2913	—2913	0
$^1/_8$, $^1/_8$, $^7/_8$	1,5740	1,9444	0208	0208	—5000	0621	0621	—4900
			0321	0321	—4508	0756	0756	—1530
	3,1454	2,7486	—3065	—3065	—2603	—3232	—3232	1833
			—3451	—3451	—2877	—3572	—3572	2727
	2,9626	2,6676	3359	—3359	0	3712	—3712	0
			3851	—3851	0	4214	—4214	0
	3,1730	2,7607	1393	1393	—3951	1687	1687	5025
			1595	1595	—4711	1719	1719	5310
	0,6889	1,2864	—3516	—3516	0397	3535	3535	0121
			—3352	—3352	0428	2518	2518	—0138
	0,5125	1,1095	—3535	3535	0	3527	—3527	0
			—3401	3401	0	2687	—2687	0
$^1/_8$, $^3/_8$, $^3/_8$	4,8928	3,4282	1762	3351	3351	1618	3289	3289
			1718	2990	2990	1046	0885	0885
	2,8394	2,6115	—4434	1156	1156	—4977	1235	1235
			—5059	1177	1177	—5603	1027	1027
	2,1521	2,2736	0	3151	—3151	0	3908	—3908
			0	3361	—3361	0	3905	—3905
	1,5453	1,9266	0873	3266	3266	—1010	—3679	—3679
			0789	3263	3263	—0548	—3216	—3216
	0,4866	1,0811	—4903	0740	0740	4902	—0590	—0590
			—4768	0794	0794	4035	—0695	—0695
	0,9646	1,5222	0	—3722	3722	0	3309	—3309
			0	—3879	3879	0	3442	—3442
$^1/_8$, $^3/_8$, $^5/_8$	3,6774	2,9720	1859	2366	1945	1825	2261	1858
			1998	2299	1687	1819	1469	0197
	2,8341	2,6091	—2692	1594	1052	—3331	1579	0816
			—3152	1636	0971	—3757	1411	0228
	1,7726	2,0634	—0027	1105	—2301	0522	3137	—3076
			0050	1317	—2139	0482	3292	—2284
	2,5126	2,4567	0432	0716	3038	—0321	—1196	—3728
			0397	0654	3328	0037	—0685	—3679
	0,7182	1,3134	—3334	0928	0229	3484	—0858	—0051
			—3164	0968	0258	2481	—0913	—0145
	1,3158	1,4778	0786	3447	—1776	—0750	—2808	0122
			0738	3512	—1912	—0354	—2363	0749
$^1/_8$, $^3/_8$, $^7/_8$	3,1397	2,7462	2359	0457	—3720	2761	1187	4667
			2724	0502	—4392	2904	0743	4930
	2,5648	2,4820	1453	—4425	—0903	1905	—4816	—0889
			1772	—4686	—0783	2278	—4621	—0055
	1,6012	1,9611	—1532	—4215	—0738	1715	4899	—1651

$\frac{k_x}{\pi}$; $\frac{k_y}{\pi}$; $\frac{k_z}{\pi}$ 1	Ω^2 2	ω, $\sec^{-1}$ 3	$p_{1x}\|\pi_{1x}$ 4	$p_{1y}\|\pi_{1y}$ 5	$p_{1z}\|\pi_{1z}$ 6	$p_{2x}\|\pi_{2x}$ 7	$p_{2y}\|\pi_{2y}$ 8	$p_{2z}\|\pi_{2z}$ 9
			−1365	−4102	−0501	0801	4004	−1211
	3,1397	2,7462	2359	0457	−3720	2761	1187	4667
			2724	0502	−4392	2904	0743	4930
	1,2614	1,7407	0466	2075	−4856	−0159	−0154	−4627
			0484	2207	−4489	0110	0331	−1953
	0,8487	1,4278	−4722	1770	0155	4687	−1548	0077
			−4450	1824	0159	2927	−1517	−0008
3/8, 3/8, 5/8	3,7399	2,9972	3679	3679	3289	2087	2087	1400
			3517	3517	2969	1659	1659	−0355
	1,4874	1,8901	−2791	−2791	5075	0140	0140	2614
			−2936	−2936	5163	−0529	−0529	1316
	2,1539	2,2745	3131	−3131	0	3926	−3926	0
			3430	−3430	0	4143	−4143	0
	2,8663	2,6239	−0886	−0886	−3252	3062	3062	4505
			−0690	−0690	−3486	1695	1695	3723
	1,8057	2,0826	1321	1321	−0715	−3538	−3538	4795
			1146	1146	−1112	−3095	−3095	4859
	1,1310	1,6482	−3738	3738	0	3288	−3288	0
			−3799	3799	0	2949	−2949	0
1/8, 5/8, 5/8	3,1991	2,7720	4600	1817	1817	4555	0734	0734
			5182	1696	1696	5235	−0089	−0089
	2,3842	2,3930	1363	−2530	−2530	2006	−4015	−4015
			1723	−2273	−2273	2430	−2484	−2484
	1,1830	1,6856	0	3763	−3763	0	3257	−3257
			0	3791	−3791	0	2730	−2730
	2,9024	2,6404	0118	3650	3650	−1947	−3103	−3103
			−0162	3754	3754	−1202	−2890	−2890
	1,0648	1,5993	−4951	0854	0854	4860	−0305	−0305
			−4619	0946	0946	2618	−0601	−0601
	2,1517	2,2734	0	−3102	3102	0	3951	−3951
			0	−3441	3441	0	4254	−4254
1/4, 1/4, 1/2	4,5714	3,3137	2858	2858	3218	2588	2588	3101
			2748	2748	2773	1562	1562	0328
	2,1637	2,2797	−1885	−1885	3504	−2609	−2609	4177
			−2201	−2201	3458	−2979	−2979	3348
	2,5941	2,4962	3307	−3307	0	3763	−3763	0
			3684	−3684	0	4076	−4076	0
	1,9810	2,1813	1141	1141	4421	−1523	−1523	−4835
			1022	1022	4626	−0865	−0865	−4673
	0,9540	1,5138	−3278	−3278	2352	3226	3226	−1389
			−3218	−3218	2560	2600	2600	−1943
	0,6453	1,2450	−3584	3584	0	3473	−3473	0
			−3575	3575	0	3122	−3122	0
1/4, 1/4, 3/4	3,4212	2,8666	3381	3381	1858	3219	3219	1645
			3554	3554	1596	3015	3015	−0168
	1,6900	2,0148	0047	0047	3983	−2528	−2528	4708
			−0250	−0250	3561	−2488	−2488	2599
	2,6263	2,5116	3302	−3302	0	3768	−3768	0
			3721	−3721	0	4166	−4166	0
	2,9038	2,6410	−0488	−0488	−4679	0734	0734	5167
			−0404	−0404	−5284	0212	0212	5584
	1,2642	1,7425	−3480	−3480	2522	2986	2986	0945
			−3388	−3388	2605	1797	1797	−0314
	0,7531	1,3449	−3588	3588	0	3468	−3468	0
			−3529	3529	0	2837	−2837	0
1/4, 1/4, 1	3,1006	2,7290	3447	3447	0	3622	3622	0
			3751	3751	0	3626	3626	0
	1,2417	1,7270	0	0	5015	0	0	4971
			0	0	4561	0	0	1971
	0,7931	1,3802	−3590	3590	0	3466	−3466	0
			−3511	3511	0	2723	−2723	0
	1,4699	1,8790	−3449	−3449	0	3620	3620	0
			−3232	−3232	0	2240	2240	0

$\frac{h_x}{\pi};\ \frac{h_y}{\pi};\ \frac{h_z}{\pi}$	Ω^2	ω, $\sec^{-1}$	$p_{1x}\vert\pi_{1x}$	$p_{1y}\vert\pi_{1y}$	$p_{1z}\vert\pi_{1z}$	$p_{2x}\vert\pi_{2x}$	$p_{2y}\vert\pi_{2y}$	$p_{2z}\vert\pi_{2z}$
1	2	3	4	5	6	7	8	9
	3,2249	2,7832	0	0	—4734	0	0	5266
			0	0	—5550	0	0	6005
	2,6400	2,5182	3300	—3300	0	3770	—3770	0
			3737	—3737	0	4203	—4203	0
$^1/_4,\ ^1/_2,\ ^1/_2$	3,9982	3,0990	3251	3286	3286	2438	2349	2349
			3229	2964	2964	2150	0639	0639
	2,3880	2,3950	3750	—0618	—0618	3230	—3582	—3582
			4169	—0583	—0583	4223	—2791	—2791
	1,7245	2,0352	0	0988	—0988	0	5014	—5014
			0	0966	—0966	0	4946	—4946
	2,5601	2,4798	—0499	3259	3259	—3891	—2609	—2609
			—0927	3248	3248	—3031	—1960	—1960
	0,9806	1,5347	—4765	1428	1428	4593	—0951	—0951
			—4640	1554	1554	3441	—1228	—1228
	1,5105	1,9048	0	—4775	4775	0	1037	—1037
			0	—5026	5026	0	1298	—1298
$^1/_4,\ ^1/_2,\ ^3/_4$	3,2170	2,7798	3930	3273	3930	1812	0	—1812
			4017	3113	4017	2821	0	—2821
	3,0400	2,7022	2279	0	—2279	4111	2679	4111
			2700	0	—2700	3454	1534	3454
	2,2260	2,3123	—0469	4791	—0469	—3650	0	3650
			—0935	4835	—0935	—3282	0	3282
	2,1023	2,2472	—2326	0	2326	—0631	6302	—0631
			—2490	0	2490	—1696	5521	—1696
	1,1963	1,6951	2849	—3727	2849	—3101	0	3101
			2673	—3977	2673	—2160	0	2160
	1,1627	1,6712	3630	0	—3630	—2986	2356	—2986
			3543	0	—3543	—1674	2744	—1674

ion K^+, let $s = 1$, and for Cl^-, $s = 2$.

As follows from Eq. (6) of Ref. 4, the energy of an ideal ionic crystal can be described by a quadratic function of the variables $\mathbf{p}_s^l$ and $\mathbf{P}_s^l$. The equations of free vibrations

$$m\ddot{u}_{sx}^l = -\partial U / \partial U_{sx}^l, \tag{1}$$

$$-\partial U / \partial P_{sx}^l \ (s = 1,\ 2;\ x = x, y, z) = 0,$$

upon substitution in them of a solution in the form waves

$$\mathbf{p}^l = \mathbf{p}_\mathbf{k} \exp\{i(\omega_\mathbf{k} t + \mathbf{k}\mathbf{R}_s^l)\}; \tag{2}$$

$$\mathbf{P}^l = \mathbf{P}_\mathbf{k} \exp\{i(\omega_\mathbf{k} t + \mathbf{k}\mathbf{R}_s^l)\};$$

lead to

$$\mathbf{p}_\mathbf{k} \mu_s \Omega_\mathbf{k}^2 = A_\mathbf{k}\mathbf{p}_\mathbf{k} + B_\mathbf{k}\mathbf{P}_\mathbf{k}, \quad B_\mathbf{k}^* \mathbf{p}_\mathbf{k} + C_\mathbf{k}\mathbf{P}_\mathbf{k} = 0, \tag{3}$$

where m_s is the ordinary mass and $\mu_s = m_s/\mu$ is the dimensionless mass of the ions, $\Omega_\mathbf{k} = e^{-2}\mu a^3 \omega_\mathbf{k}^2$, $\mu = m_1 m_2/(m_1 + m_2)$ is the reduced mass; $\mathbf{p}^l$ and $\mathbf{P}^l$ are the dimensionless six-component vectors with components p_{sx}^l/ae and P_{sx}^l/ae. The sixfold dimenless matrices $A_\mathbf{k}$, $B_\mathbf{k}$, and $C_\mathbf{k}$ are determined in Ref. 7 by the matrices $\Phi_\mathbf{k}$, the computed values of which have been tabulated by the author in Ref. 8. The matrices $C_\mathbf{k}^{-1}$ necessary for the solution of (3) have been listed there also. The extremely difficult calculation of the matrices $\Phi_\mathbf{k}$, for purposes of proof, was also carried out independently by Zaslavkaia and Tolpygo[9].

For the condition of solvability of the system, obtained from (3) after elimination of $\mathbf{P}_\mathbf{k}$, the six values of the frequencies $\Omega_\mathbf{k}^\alpha$ $(\alpha = 1, 2, \ldots, 6)$ were determined, and the mutually orthogonal eigenvectors $\mathbf{P}_\mathbf{k}^\alpha$ corresponding to them were also obtained. These were normalized in the Born fashion:

$$\mu_1 \mathbf{p}_{\mathbf{k}1}^\alpha \mathbf{p}_{\mathbf{k}1}^\beta + \mu_2 \mathbf{p}_{\mathbf{k}2}^\alpha \mathbf{p}_{\mathbf{k}2}^\beta = \delta_{\alpha,\beta}. \tag{4}$$

The results of the calculations are shown in the Table. The frequencies and amplitudes at the point

K{0, 0, 0} can be taken from Ref. 2. The corresponding $(\Omega_{\mathbf{k}}^{\alpha})^2$ are listed along with each frequency $\omega_{\mathbf{k}}^{\alpha}$. The amplitude vectors of the dipole moments of the ionic displacements $\mathbf{p}_{\mathbf{k}}^{\alpha}$ and the total amplitude vectors $\pi_{\mathbf{k}}^{\alpha}=\mathbf{p}_{\mathbf{k}}^{\alpha}+\mathbf{P}_{\mathbf{k}}^{\alpha}$ are listed in adjacent columns. Wherever possible, a total of 10 steps were carried out.

The frequencies for each wave vector are divided into branches: the optical (longitudinal and transverse) and acoustical (longitudinal and transverse). The longitudinal optical branch was systematically described by Iona[1], with neglect of the polarization of the ions. Inasmuch as he considered the masses of the ions to be identical, the cell of this reciprocal lattice is a cube and threre are 3 branches altogether; on the other hand, the region of variation of **k** is different. Therefore, our optical and acoustical branches, of the same K according to Iona, actually belong to different **k**. The latter circumstance helped to distribute the resultant frequencies between the branches in doubtful cases. Determination of the branches was obtained by the monotonic variation of ω and **p**, which is not always unique. The division of the vibrations into longitudinal and transverse is also not unique. The latter has meaning only for symmetric directions of the wave vector relative to the coordinate axes. Thus, for example, for $\mathbf{k}\{\pi/8; 3\pi/8; 7\pi/8\}$, the angle between **k** and $\mathbf{p}_1$ for the optical longitudinal branch amounts to more than 50°. This means that in the KCl crystal, the anisotropy is significant and therefore neglect of $\mathbf{P}_s$ in comparison with $\mathbf{p}_s$ is invalid.

The author considers it his pleasant duty to express his deep appreciation to K. B. Tolpygo for his unvarying interest in the work, and for repeated discussions.

---

[1] M. Iona, Phys. Rev. **60**, 822 (1941)

[2] K. B. Tolpygo and I. G. Zaslavskaia, Works (Trudy) Phys. Inst. Acad. Sci., Ukrainian SSR, No 4, 71 (1953).

[3] T. I. Kucher and K. B. Tolpygo, J. Exptl. Theoret. Phys. (U.S.S.R.) **31**, 1002, (1956); Soviet Phys. JETP **4**, 883 (1957).

[4] K. B. Tolpygo, J. Exptl. Theoret. Phys. (U.S.S.R.) **20**, 497 (1950)

[5] K. B. Tolpygo, Matem. sb. Kiev Univ. **5**, 99 (1951)

[6] K. B. Tolpygo, Works (Trudy) Phys. Inst. Acad. Sci., Ukrainian SSR, No. 5, 28 (1951)

[7] K. B. Tolpygo, Works (Trudy) Phys. Inst. Acad. Sci., Ukarainian SSR, No 6, 102 (1955)

[8] T. I. Liberberg-Kucher, J. Exptl. Theoret. Phys. (U.S.S.R.) **30**, 724 (1956); Soviet Phys. JETP **3**, 580 (1956).

[9] K. B. Tolpygo and I. G. Zaslavskaia, Ukrainian J. Phys. (in press).

Translated by R. T. Beyer
117

SOVIET PHYSICS JETP VOLUME 5, NUMBER 3 OCTOBER, 1957

Some Relativistic Properties of the Behavior of Spin-½ Particles

P. E. KUNIN AND I. M. TAKSAR
Latvian State University, Physical Institute
Academy of Sciences, Latvian SSR.

(Submitted to JETP editor, January 7, 1956)
J. Exptl. Theoret. Phys. U.S.S.R. **32**, 506-509 (March, 1957)

It is shown that in the case of a scalar field the Klein paradox does not arise for spin-½ particles tunneling through a potential barrier. The particle does not fall toward the center of a centrally symmetric field even when a high-order pole exists in the center. This result also holds in classical relativistic theory.

---

1. FOR a scalar interaction, the interaction potential between a particle and the field is an invariant. This is not the case for an electrostatic (vector) interaction, when the potential is the fourth component of a four-vector. Therefore, the Dirac equation for a spin-½ particle in a scalar field can be written

$$\left\{E - i\left(\alpha_1 \frac{\partial}{\partial x} + \alpha_2 \frac{\partial}{\partial y} + \alpha_3 \frac{\partial}{\partial z}\right) + \rho_3 (E_0 + U)\right\} \psi = 0. \qquad (1)$$

Here E is the total energy of the particle, E_0 is its rest energy U is the potential energy of the particles in the scalar field, and α_1, α_2, α_3, and ρ_3 are the Dirac matrices; Planck's constant and the velocity of light are set equal to unity.

We shall consider one-dimensional motion of a particle along the x axis in a field which can be represented by a square potential barrier of the form

$$U = 0\,(x < 0), \quad U = U_0\,(x > 0). \qquad (2)$$

In this case, as usual, we look for a solution of (1) in the form of plane waves:

$$\begin{aligned} \psi_i &= a_i e^{ip_1 x} + b_i e^{-ip_1 x} \quad (x < 0), \\ \psi_i &= c_i e^{ip_2 x} \quad (x > 0). \end{aligned} \qquad (3)$$

Inserting these solutions into the equation gives the dependence of the particle momentum on its energy, namely,

$$p_1^2 = E^2 - E_0^2, \quad p_2^2 = E^2 - (E_0 + U_0)^2. \qquad (4)$$

It is clear that the reflection coefficient is equal to unity when p_2 is pure imaginary, or when $E < E_0 + U_0$. In the case of a vector (electrostatic) interaction, p_2 is of the form

$$p_2^{(\text{vect})} = \sqrt{(E - U_0)^2 - E_0^2} \qquad (5)$$

and is imaginary when $E - E_0 < U_0 < E + E_0$. It is seen from this that for a scalar interaction, the particles will not tunnel through a sufficiently high barrier (the Klein paradox will not occur).

A no less "paradoxical" phenomenon, however, does take place for the scalar interaction. In this case p_2 becomes imaginary and the reflection coefficient becomes unity for a sufficiently high negative value of U_0, when $|U_0| < E + E_0$. In other words, not only is it impossible for the particle to pass through a sufficiently high barrier, but it is also impossible for it to penetrate into a sufficiently deep well.

These results remain valid not only in the case of a square barrier, but also for a "smoothed out" barrier. Let us consider, for instance, the behavior of a particle in a field whose potential for instance, the behavior of a particle in a field whose potential is of the form

$$U(x) = V / (1 + e^{-ax}), \ V = \text{const.} \qquad (6)$$

In this case it is possible to find an exact solution for the Dirac equation (1) in terms of hypergeometric functions. This solution is of the form

$$\psi_1 = \psi_2 = cy^{\mu}\left[\frac{(1-y)^{\lambda}}{\sqrt{\alpha_1\beta_1}}F(\alpha_1, \beta_1, \gamma_1; y) + \frac{(1-y)^{-\lambda}}{\sqrt{\alpha_2\beta_2}}F(\alpha_2, \beta_2, \gamma_2; y)\right],$$
$$\psi_3 = \psi_4 = -icy^{\mu}\left[\frac{(1-y)^{\lambda}}{\sqrt{\alpha_1\beta_1}}F(\alpha_1, \beta_1, \gamma_1; y) + \frac{(1-y)^{-\lambda}}{\sqrt{\alpha_2\beta_2}}F(\alpha_2, \beta_2, \gamma_2; y)\right], \quad (7)$$

where $F(\alpha, \beta, \gamma; y)$ are hypergeometric functions, c is a constant,

$$y = -e^{-ax}; \quad \mu^2 = a^{-2}[(E_0 + V)^2 - E^2];$$
$$\nu^2 = a^{-2}[E_0^2 - E^2]; \quad \lambda = -\nu / a;$$
$$\alpha_1 = \mu + \nu + \lambda; \quad \alpha_2 = \mu + \nu - \lambda; \quad (8)$$
$$\beta_1 = \mu - \nu + \lambda;$$
$$\beta_2 = \mu - \nu - \lambda; \quad \gamma_1 = \gamma_2 = 2\mu + 1.$$

Making use of the asymptotic expressions for the the hypergeometric functions, as well as several of their properties, we can calculate the reflection coefficient, which is found to be

$$R = \left|\frac{\Gamma(2\nu)\,\Gamma(\mu-\nu+\lambda)\,\Gamma(\mu-\nu-\lambda)}{\Gamma(-2\nu)\,\Gamma(\mu+\nu+\lambda)\,\Gamma(\mu+\nu-\lambda)}\right|^2 \quad (9)$$
$$\times \frac{|(\mu-\nu)^2-\lambda^2|^2}{|(\mu+\nu)^2-\lambda^2|^2}.$$

Since λ is real and ν is pure imaginary, it follows from (9) that the reflection coefficient $R = 1$ when μ is real. It follows from Eq. (8) that, independent of the magnitude of a, which determines the "steepness" of the potential energy curve, the particle can neither tunnel through a barrier of height $V < E - E_0$ nor penetrate into a well of depth $|V| < E + E_0$.

For comparison, we remark that in the case of a vector field, the Klein paradox arises for a "smoothed-out" barrier only if the potential energy increases to $2E_0$ in a distance which is smaller than the Compwavelength of the particle.

2. It is known that in the nonrelativistic quantum mechanical treatment of a spin-½ particle in a centrally symmetric field, no stable states can take place if the potential in the neighborhood of the attracting center increases as r^{-n}, where $n < 2$ (here r is the distance from the center). This result remains valid also in the relativistic treatment if the interaction is electromagnetic (of the vetor type). A different result is obtained for a scalar interaction.

Consider a particle in a scalar centrally symmetric field whose potential energy is given by

$$U = a / r^n. \quad (10)$$

Inserting (10) into the Dirac equation (1) and separating the radius and angle variables, we obtain the following radial equations:

$$(E + E_0 - U)f + (dg/dr) - lg/r = 0,$$
$$-(E - E_0 + U)g + (df/dr) + (l+2)f/r = 0, \quad (11)$$

where f and g are functions which depend only on r, and l is the azimuth quantum number. The double degeneracy of the Dirac equation lies in the fact that there exists another pair of radial equations which can be obtained from the first by replacing l by $-(l+1)$. The investigation of this second set of equations is unnecessary, since it is exactly analogous to the treatment presented below.

By eliminating one of the functions from (11), we obtain the second order equation

$$\frac{d^2f}{dr^2} + \left(\frac{2}{r} - \frac{dU/dr}{E - E_0 + U}\right)\frac{df}{dr}$$
$$+ \left[E^2 - (E_0 - U)^2 - \frac{l+2}{r}\,\frac{dU/dr}{E - E_0 + U}\right.$$
$$\left. + \frac{(l+1)(l+2)}{r^2}\right]f = 0. \quad (12)$$

The asymptotic behavior of the solutions of this equation for small r is given by the equation

$$\frac{d^2f}{dr^2} + \frac{n+2}{r}\frac{df}{dr} - \frac{a^2}{r^{2n}}f = 0. \quad (13)$$

The solution of Eq. (13) can be written in terms of Bessel functions

$$f = r^{-(n+1)/2} I_{(n+1)/2(n-1)}\left(\pm \frac{ia}{1-n} r^{1-n}\right), \quad (14)$$

and by making use of the asymptotic behavior of the Bessel functions for small r, we obtain

$$f \sim \exp\left\{\pm \frac{a}{1-n}\,\frac{1}{r^{n-1}}\right\}. \quad (15)$$

which is accurate up to a factor multiplying the exponential.

Thus when $r = 0$, one of the solutions becomes infinite and the other vanishes. The same result is easily obtained in solving the Dirac equation (in spherical coordinates) in the absence of a field. The fact that the number of finite solutions for $r=0$ does not change when a field is introduced indicates that in this field the particle does not fall into the attractive center.

3. It can be shown that the result of the previous section is not a quantum effect, but holds also in the classical (relativistic) theory.

In the quantum mechanical treatment, the energy of the scalar interaction between the particle and the field is given by a term of the form $\rho_3 U(r)$, where ρ_3 is a Dirac matrix. It is known that in the classical treatment this matrix corresponds to the factor $\sqrt{1-\beta^2}$, where β is the velocity of the particle (in the units being used).

Choosing the interaction energy between the particle and the field in the form

$$U = -ar^{-n}\sqrt{1-\beta^2}, \qquad (16)$$

when n is arbitrary, we obtain the following expression for the classical (relativistic) Lagrangian:

$$L = -E_0\sqrt{1-\beta^2} + ar^{-n}\sqrt{1-\beta^2}. \qquad (17)$$

Here E_0 is the rest energy of the particle, and a is the coupling constant between the field and the particle. Since this is a spherically symmetrical problem, it is clear that the total angular momentum is conserved. If the z axis is directed along the total angular momentum, the trajectory of the particle is in the xy plane. In cylindrical coordinates with the origin at the force center of the field, $\beta^2 = \dot{r}^2 + r^2\dot{\varphi}^2$, and since φ is a cyclic coordinate, the generalized momentum p_φ conjugate to it is conserved:

$$p_\varphi = \frac{\partial L}{\partial\dot{\varphi}} = \left(E_0 - \frac{a}{r^n}\right)\frac{r^2\dot{\varphi}}{\sqrt{1-\beta^2}} = \text{const.} \qquad (18)$$

Using the expression for p_φ and

$$p_r = \frac{\partial L}{\partial\dot{r}} = \left(E_0 - \frac{a}{r^n}\right)\dot{r}/\sqrt{1-\beta^2},$$

we find the second integral of the motion, namely the total energy of the particle in the field:

$$H = p_r\dot{r} + p_\varphi\dot{\varphi} - L \qquad (19)$$

$$= (E_0 - ar^{-n})/\sqrt{1-\beta^2} = \text{const.}$$

Further, eliminating $\dot{\varphi}$ from Eqs. (18) and 19 and making use of the expression for β^2, it is easy to obtain

$$\dot{r}^2 = 1 - H^{-2}[(E_0 - ar^{-n})^2 + p_\varphi^2/r^2]. \qquad (20)$$

It is immediatedly seen from this equation that the particle can not approach very close to the attactive center, since for sufficiently small r the right side of expression (20) becomes negative, whereas the left side is an essentially positive quantity. This result remains true for any sign of a, so that the particle can not fall into the center whether it be repulsive or attactive. From expression (20) it is also seen that in the attractive case the particle in the scalar field will move in closed trajectories when $H = E_0$. It is thus possible, in spite of a high order pole at the center, for the particle to have a stable state in the field.

Translated by E. J. Saletan
118

SOVIET PHYSICS JETP VOLUME 5, NUMBER 3 OCTOBER, 1957

On Low-Frequency Oscillations in the Plasmas of Electronegative Gases

M. V. KONIUKOV
Tula State Pedagogical Institute

(Submitted to JETP editor January 19, 1956)
J. Exptl. Theoret. Phys. (U.S.S.R.) 32, 510-514 (March, 1957)

The oscillations of ions in a plasma whose charged components are electrons, and positive and negative ions are considered. Two branches of low-frequency oscillations have been established whose frequencies depend differently on the concentration of the charged particles.

ONE of the charged components in the gas-discharge plasmas of electronegative gases (or mixtures of such gases) is composed of negative ions which arise as a result of electrons becoming attached to neutral molecules. This situation causes several peculiarities in gas discharges in these cases.* So far, however, effects due to negative ions have been taken into account only in determining steady-state distributions of charged particles[3-5], and the study of small pertubations has been restricted to plasmas containing only electrons and positive ions. It is therefore of interest to determine those changes in the behavior of small perturbations of the charged-particle densities which are due to ence of negative ions in the plasma.

We shall examine the influence of negative ions on the behavior of small density perturbations in the hydrodynamic approximation. The gas-discharge plasma in this case is considered a mixture of three ideal gases (the electron gas, the gas of positive ions, and the gas of negative ions)[6] interacting by means of a self-consistent field which leads to the appearance of additional forces on the electrons and ions. The present treatment shall differ from our previous one[6] in that it shall not take account of interactions with a neutral gas or of effects due to creation and annihilation of charged particles, so that the applicability of the results is restricted to low-frequency oscillations at pressures which are not too high. With these assumptions, the hydrodynamic equations describing the behavior of the gases can be written

$$\frac{\partial N_e}{\partial t} + \frac{\partial}{\partial x_\alpha}(N_e v_\alpha^e) = 0, \quad P_e = \Theta_e N_e,$$

$$\frac{\partial}{\partial t}(N_e v_\alpha^e) + \frac{\partial}{\partial x_\beta}(N_e v_\alpha^e v_\beta^e) = -\frac{1}{M_e}\frac{\partial P_e^\alpha}{\partial x_\alpha} + \frac{eN_e}{M_e}E_\alpha \tag{1}$$

for the electrons, with similar equations for the positive (index p) and negative (index n) ions (in the equations for N_p the opposite sign must be taken for the charge e). Here N_e, v_α^e, P_e, M_e, and Θ_e are the concentration, α-component of the velocity, partial pressure, mass of the individual particle, and temperature in ergs of the electron gas, respectively. The field is determined from Maxwell's equations for the static case, namely

$$\partial E_\alpha / \partial x_\alpha = 4\pi e (N_e + N_n - N_p),$$
$$\partial E_\alpha / \partial x_\beta - \partial E_\beta / \partial x_\alpha = 0. \tag{2}$$

Let us consider the behavior of small perturbations in the linear approximation. For the zeroth approximation we shall take the stationary case in which the gases are considered at rest and to have constant density distributions in space. The densities N_e^0, N_n^0, and N_p^0 satisfy the quasi-neutrality conditions[4]

$$N_e^0 + N_n^0 = N_p^0. \tag{3}$$

We shall look for the charged-particle densities in the first approximation in the form

$$N_e = N_e^0 + n_e, \; N_p = N_p^0 + n_p, \; N_n = N_n^0 + n_n, \tag{4}$$

where $n_e, \ldots$ are small perturbations in the electron and ion densities. Eliminating the momentum and electric field from Eqs. (1), and restricting ourselves

---

*It has been established experimentally that mixing electro-negative gasses makes stratified discharge more likely, influences the length of the stratifications, *etc.*[1,2]

to the linear terms in the deviations of the densities, velocities, and self-consistent field, we obtain a set of equations determining the behavior of small simultaneous perturbations of the charged-particle densities in the isothermal case:

$$\frac{\partial^2 n_e}{\partial t^2} - \frac{\Theta_e}{M_e}\frac{\partial^2 n_e}{\partial x^2} + \omega_e^2 n_e - \omega_e^2 n_p + \omega_e^2 n_n = 0,$$

$$\frac{\partial^2 n_p}{\partial t^2} - \frac{\Theta_p}{M_p}\frac{\partial^2 n_p}{\partial x^2} + \omega_p^2 n_p - \omega_p^2 n_e - \omega_p^2 n_n = 0',$$

$$\frac{\partial^2 n_n}{\partial t^2} - \frac{\Theta_n}{M_n}\frac{\partial^2 n_n}{\partial x^2} + \omega_n^2 n_n + \omega_n^2 n_e - \omega_n^2 n_p = 0,$$

$$\omega_e^2 = 4\pi e^2 N_e^0/M_e, \ldots \tag{5}$$

We attempt to find solutions of Eqs. (5) proportional to exp $(i\omega t - ikx)$. We then obtain a dispersion which, on the assumption of highly nonisothermal plasmas and low frequencies, breaks up into two equations; the first of these is

$$\omega^2 - (k^2\Theta_e/M_e) - \omega_e^2 = 0 \tag{6}$$

which describes high-frequency oscillations of the electrons while the ions remain at rest*, and the second is

$$\left[\omega^2 - \left(\frac{k^2\Theta_p}{M_p} + \omega_p^2\right)\right]\left[\omega^2 - \left(\frac{k_2\Theta_n}{M_n} + \omega_n^2\right)\right] = \omega_p^2\omega_n^2 \tag{7}$$

which corresponds to low-frequency oscillations of the ions about a background of uniformly distributed electrons. From Eqs. (7) we have

$$\omega_{1,2}^2 = \frac{a+b}{2} \pm \frac{a-b}{2}\sqrt{1 + \frac{4c}{(a-b)^2}}, \tag{8}$$

$$a = k^2\Theta_p/M_p + \omega_p^2,\ b = k^2\Theta_n/M_n + \omega_n^2,\ c = \omega_p^2\omega_n^2.$$

Since c is determined by the product of the positive and negative ion densities, and $(a-b)^2$ by the square of the positive ion density, for low negative ion concentrations $c \ll (a-b)^2$. Restricting ourselves to terms only of first order in $c/(a-b)^2$, we obtain from Eq. (8)

$$\omega_1^2 = \frac{k^2\Theta_p}{M_p} + \omega_p^2 + \frac{\omega_p^2\omega_n^2}{(k^2\Theta_p/M_p) + \omega_p^2 - (k^2\Theta_n/M_n) - \omega_n^2}, \tag{9}$$

$$\omega_2^2 = \frac{k^2\Theta_n}{M_n} + \omega_n^2 - \frac{\omega_p^2\omega_n^2}{(k^2\Theta_p/M_p) + \omega_p^2 - (k^2\Theta_n/M_n) - \omega_n^2}. \tag{10}$$

If we take account of the fact that[4] $\Theta_p/M_p \approx \Theta_n/M_n$, operations on (9) and (10) lead to

$$\omega_1^2 = (k^2\Theta_p/M_p) + \omega_p^4/(\omega_p^2 - \omega_n^2), \tag{11}$$

$$\omega_2^2 = (k^2\Theta_n/M_n) - \omega_n^4/(\omega_p^2 - \omega_n^2). \tag{12}$$

Thus the result when negative ions are taken into account differs from the previous ones in that there appear two branches of low-frequency oscillations whose frequencies depend in different ways on the charged-particle concentration.

Let us consider in more detail the oscillations described by Eqs. (11) and (12). When $N_p^0 \gg N_n^0$, the Langmuir frequency of free oscillations of the negative ions will be significantly lower than that of the positive ions. Then (11) reduces to

$$\omega_1^2 = (k^2\Theta_p/M_p) + \omega_p^2, \tag{13}$$

which is a dispersion equation for the positive ion

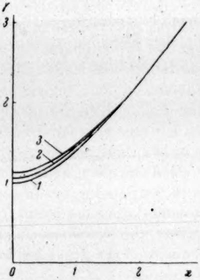

FIG. 1. The dependence of the frequency on the wave vector as given by Eq. (11) for the first branch of oscillations, in dimensionless units. The parameter taken for the negative ion concentration is N_n^0/N_p^0, and for the various curves it is equal to 1-0, 2-0.1, 3-0.2; $\gamma = \omega/\omega_p$, $\varkappa = k/k_D$ is the reciprocal of the Debye distance for positive ions.

---

*A similar result is obtained elsewhere.[6,8] The differences, however, should be noticed: in the previous works ω_e^2 was determined by the total concentration of negatively charged particles, whereas in our case it is determined only by the electron concentration.

oscillations about a background of negative charges.* The frequencies given by Equation (11) will be larger than the corresponding ones of Eq. (13). This is due to the fact that Eq. (13) describes only the oscillations of positive ions, whereas Eq. (11) determines simultaneous oscillations of positive and negative ions in opposite phase. This last situation leads to an increase of the electric field as well as of the quasielastic force and frequency determined by the field. These statements can be verified by calculating the amplitude. The relation between the amplitudes of the oscillations of the negative and positive ion concentrations corresponding to the apapproximation of Eq. (10) can be written in the form

$$n_n^0 = [(k^2\Theta_p / M_p) + \omega_p^2 - \omega^2]\, n_p^0 / \omega_p^2. \qquad (14)$$

If the value of ω^2 from Eq. (13) is inserted into (14), the oscillation amplitude of the negative ion concentration vanishes; if, on the other hand, the value of ω^2 from Eq. (11) is inserted, the relation between the amplitudes becomes

$$n_n^0 = -\left(\frac{\omega_n^2}{\omega_p^2 - \omega_p^2} - 1\right) n_p^0. \qquad (15)$$

Analysis of this expression shows that the simultaneous positive and negative ion waves have opposite phases.

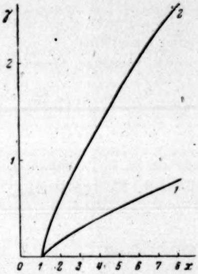

FIG. 2. The dependency of the frequency the wave vector as given by Equation (12) for the second branch of oscillations, in dimensionless units. The negative ion concentration parameter, N_n^0/N_p^0: *1* — 0,01, *2* — 0,1. For a concentration of 0.01, a temperature of 300° K and a positive ion density of 10^9 cm^{-3}, we have $k_D^2 = 4\pi e^2 N_n^0/\Theta_n = 10^2$ cm^{-2}, $\lambda_{\lim} \approx 1$ cm; for a concentration of 0.1, the other conditions remaining the same, $k_D \approx 30$ cm^{-1}, $\lambda_{\lim} \approx 0{,}1$ cm. Here $\gamma = \omega/\omega_n$, $\varkappa = k/k_D$ in units of $\sqrt{N_n^0/(N_p^0 - N_n^0)}$

Equation (12), as opposed to the case already considered, describes in-phase ion oscillations. If ω^2 as given by Eq. (12) is inserted into (14), we are led to the following relation between the amplitudes:

$$n_n^0 = \left(1 + \frac{\omega_n^4}{\omega_p^2(\omega_p^2 - \omega_n^2)}\right) n_p^0, \qquad (16)$$

which shows immediately that the positive and negative ion wave have the same phase.

We should note also another property of the oscillations described by Eq. (12). As the charged-particle density increases, the oscillation frequency decreases monotonically and finally vanishes. The wavelength at this point takes on a certain limiting value

$$\lambda_{\lim} = 2\pi\,[\Theta_n(\omega_p^2 - \omega_n^2) / M_n\omega_n^4]^{1/2}. \qquad (17)$$

Long wavelengths (for a given charged-particle density) correspond to negative frequencies which means that they cannot occur.* As the charged-particle density is increased, this limiting wavelength decreases so that the spectrum of possible wavelengths moves into the region of lower values.

So far, the oscillations and waves only of plasmas containing electrons and positive ions have been experimentally studied, and therefore it is impossible to compare the results obtained here with experiment.

In conclusion I consider it my duty to express my gratitude to Professor Ia. P. Terletskii and A. A. Zaitsev for discussions and valuable advice during the performance of this work, as well as to Professor G. V. Spivak and Professor N. A. Kaptsov for discussing the results of the work.

---

[1] R. Neubert, Phys. Z. 15, 430 (1914).

---

*In previously studied cases, an equation such as (13) described oscillations about the background of uniformly distributed electrons, whereas here the negative charge background contains both electrons and negative ions.

*This is due to the fact that the pressure gradients which cause the propagation of the wave are compensated by the action of electric forces which arise because of the displacements.

[2] K. Darrow, *Electrical Phenomena in Gases*, DNTVU, 1937, p 303 (Russian Translation)

[3] R. Seelinger and K. Kruschke, Phys. Z. **34**, 883 (1933).

[4] B. Bohm et al., *The Characteristics of Electrical Discharges in Magnetic field*, 173 (1949).

[5] V. L. Granvskii, *Electric Discharge in Gases*, GITTL, 1952, p 311.

[6] M. V. Koniukov and Ia. P. Terletskii, J. Exptl. Theoret. Phys. (U.S.S.R.) **27**, 542 (1954)

[7] J. J. Thomson and G. P. Thompson, *Conduction of Electricity Through Gases*, Cambridge **2**, 353 (1933).

[8] A. A. Vlasov, *Many-Particle Theory*, GTTI, Moscow, 1950, p 285.

Translated by E. J. Saletan
119

SOVIET PHYSICS JETP VOLUME 5, NUMBER 3 OCTOBER, 1957

Contribution to the Theory of Collective Motion of Particles in Quantum Mechanical Systems

V. M. ELEONSKII AND P. S. ZYRIANOV
Ural Polytechnic Institute

(Submitted to JETP editor January 26, 1956)
J. Exptl. Theoret. Phys. (U.S.S.R.) **32**, 515-519 (March, 1956)

A method for separating the collective motions in a system of interacting particles is presented. The connection between this method and Refs. 1-4 is established. An attempt is made to give a basis to the generalized heavy nucleus model.

1. MOST quantum mechanical systems that are dealt with in the various fields of physics consist of a large number of particles. The problems of finding the energy spectrum of such a system presents great mathematical difficulties. From among the quantum mechanical systems with large number of particles, we can separate out that class of systems in which collective motion, reminiscent of the motion of a continuous system, takes place. Among such systems are, for instance, heavy atomic nuclei, the electrons and ions of a metal, and others.

The problem of the approximate methods for describing such systems reduces to finding those terms in the Hamiltonian which correspond to collective motion. In the case of central forces, the problem of separating out the collective motions was solved by Zubarev[1], and for the case of Coulomb forces by Bohm and Pines[2] using a different method. An interesting method for describing collective motion, well set forth and of great generality, has been developed by Tomonaga[3,4]. The present article describes a method for separating out collective motions is systems, which is very simple in the sense that it does not require the complex apparatus of second quantization and unitary transformations. At the same time this method is quite general.

2. At the basis of the method lies the transformation of the Hamiltonian with the aid of auxiliary variables introduced into the wave function of the system, as has been described by Zubarev[1].

We consider the wave function $\Psi(r_1 \ldots r_N; t)$ describing a system whose Hamiltonian is

$$H = \sum_j \mathbf{p}_j^2/2M + {}^1/_2 \sum_{ij} G(\mathbf{r}_i, \mathbf{r}_j), \tag{1}$$

and introduce the auxiliary ("superfluous") variable functions $\varphi_j(r_j)$ (where $j = 1, 2, \ldots, N$), which for the time being are arbitrary, and instead of Ψ we shall consider the new wave function (a functional of the φ_j)

$$\Phi(r_1 \ldots r_N;\ \varphi_1(r_1) \ldots \varphi_N(r_N);\ t). \tag{2}$$

since Φ depends on r_j explicitly as well as through the φ_j, the operator $\mathbf{p}_j$ must be replaced by

$$-i\hbar\,[\nabla_j + (\nabla_j \varphi_j)\partial/\partial\varphi_j]. \tag{3}$$

As will be shown below, part of the potential energy can also be described in terms of the $\varphi_j(r_j)$.

Let us now make some comments about the $\varphi_j(r_j)$. We assume that $\varphi_j(r_j)$ is the wave function of the stationary state of the j-th particle in the zeroth approximation. As will be shown later, the coordinates of the collective motion can be described in terms of the φ_j. When the φ_j are given this interpretation, the description of the collective motion in the system will be most accurate if the single-particle functions φ_j are chosen accurately. We shall consider below several special choices of the φ_j. This interpretation of the φ_j makes it possible on the one hand to obtain the Hamiltonians derived in previous works[1,2,4], and on the other hand indicates the possible paths that may be taken in solving a boundary value problem. Let us now conconsider certain special choices of the $\varphi_j(r_j)$.

3. Let us make the choice

$$\varphi_j(r_j) = N^{-1/2}\exp\{-i\mathbf{k}\mathbf{r}_j\}. \tag{4}$$

This wave function describes the stationary states of a free particle with momentum $\mathbf{p}=\hbar\mathbf{k}$. The kinetic energy operator for this choice of the φ_j can be written

$$T = -(\hbar^2/2M)\sum_j[\nabla_j + (\nabla_j\rho_k)\partial/\partial\rho_k]^2, \tag{5}$$

if we bear in mind the obvious relation

$$\sum_j\varphi_j = N^{-1/2}\sum_j\exp\{-i\mathbf{k}\mathbf{r}_j\} = \rho_k\,. \tag{6}$$

In order to account for states with various $\mathbf{k}$ in Eq. (5), we must sum over all values of $\mathbf{k}$. From physical considerations $|\mathbf{k}|$ may not be infinite, and we shall therefore introduce a certain maximum wave number k_0. Thus in Eq. (5) and those that follow, whenever the index k occurs twice we are to sum over k from zero to k_0.

In the case of a central interaction the potential energy can be written

$$\frac{1}{2}\sum_{i,j}G(|\mathbf{r}_i-\mathbf{r}_j|) = \frac{N}{2}G(k)\rho_k\rho_k^* \tag{7}$$

$$+\frac{1}{2}\sum_{j,j,k>k_0}G(k)e^{i\mathbf{k}(\mathbf{r}_i-\mathbf{r}_j)} + \text{const}\,,$$

$$\text{const} = -N\sum_{k<k_0}G(k),$$

where $G(k)$ is the Fourier transform of the interaction kernel, the constant is the self-energy of the particles, and N is the number of particles per unit volume.

The sum of expressions (5) and (7) gives the Hamiltonian of the system, which agrees with the Hamiltonian as obtained by Zubarev.[1] The dynamical variables ρ_k describe the collective motion of the system and can be written in terms of the stationary state free particle wave functions of Eq. (4). Following Zubarev, the ρ_k can be treated as the Fourier transform of the particle density operator

$$\rho(\mathbf{r}) = \sum_j\delta(\mathbf{r}-\mathbf{r}_j)\,. \tag{7a}$$

If we perform the substitution

$$\begin{aligned} -i\hbar\partial/\partial\rho_k &= (4\pi e^2N^2/k^2)^{1/2}q_k, \\ \rho_k &= -i(k^2/4\pi eN^2)^{1/2}p_{-k}, \end{aligned} \tag{7b}$$

in the Hamiltonian we have obtained, we arrive at that of Bohm and Pines,[2] which is equivalent to that of Tomonaga, as has been shown[4].

The separation of the collective motion of the system is related to maintaining a term proportional to $[\nabla_j\rho_k\,\partial/\partial\rho_k]^2$ in the Hamiltonian. For the case of the electromagnetic and Coulomb interactions, this term is proportional to the square of the vector potential of the transverse and longitudinal fields, respectively.

4. As an example of a solution of a boundary value problem, let us consider a system of particles enclosed within a surface described by the equation

$$R = R_0\Big[1 + \sum_{m,l<l_0}\alpha_{lm}Y_{lm}(\vartheta,\varphi)\Big], \tag{8}$$

where Y_{lm} is a spherical function, and R_0 is the radius of the unperturbed sphere. From physical considerations, the summation in (8) is taken over all $l<l_0$. Since the surface bounding the system is defined by the set of particles on the boundary, surface oscillations of the order of the mean distance between particles have no physical meaning; this leads to the inequality $l<l_0$.

Our problem consists of choosing the $\varphi_j(r_j)$, in terms of which we can express the collective coordinates. In the approximation of a constant particle density in the system (neglecting compressibility) we may choose the $\varphi_j(r_j)$ in the form

$$\varphi_j(r_j) = \exp\{iS_j(r_j)/\hbar\}, \tag{9}$$

where the S_j give the velocity potential of the j-th particle up to a factor of $1/M$. In the constant-density approximation the stationary particle states are given by the functions of Eq. (9) with

$$S_j(r_j) = \beta_{lm} Y_{lm}(\vartheta_j, \varphi_j)\, r_j^l. \qquad (10)$$

The function S_j is a solution of the Laplace equation satisfying the boundary condition

$$(\partial S_j/\partial r_j)_{r_j=R} = \partial R/\partial t, \qquad (11)$$

which makes it possible to express the β_{lm} coefficients in terms of the normal coordinates of the surface α_{lm}. For small oscillations we have

$$\beta_{lm} = l^{-1} R_0^{2-l} \dot{\alpha}_{lm}. \qquad (12)$$

Let us consider the kinetic energy operator

$$T = -(\hbar^2/2M) \sum_j [\nabla_j + (\nabla_j S_j)\, \partial/\partial S_j]^2 \qquad (13)$$

and transform from the variables S_j to α_{lm}:

$$T = -(\hbar^2/2M) \sum_j [\nabla_j + (\nabla_j \alpha_{lm})\, \partial/\partial \alpha_{lm}]. \qquad (14)$$

Here, as in the previous problem, we sum from zero to l_0 over all indices m and l which occur twice, so as to take account of all possible stationary single-particle states.

In order to interpret the expression $(\nabla_j \alpha_{lm})$, we must write α_{lm} in terms of the particle coordinates $\mathbf{r}_j$. For this purpose, let us introduce the function $S = \Sigma_j S_j$. It is clear that

$$\nabla_j S_j \frac{\partial}{\partial S_j} = \nabla_j S \frac{\partial}{\partial S} = \beta_{lm} \nabla_j \times \Big[\sum_j r_j^l Y_{lm}(\vartheta_j \psi_j)\Big] \frac{\partial \beta_{lm}}{\partial S} \frac{\partial}{\partial \beta_{lm}}.$$

But it follows from the definition of S that

$$\frac{\partial \beta_{lm}}{\partial S} = \frac{\partial}{\partial S}(l^{-1} R^{-l+2} \dot{\alpha}_{lm}) = \Big[\sum_j r_j^l Y_{lm}(\vartheta_j \varphi_j)\Big]^{-1};$$

or

$$\nabla_j S_j \frac{\partial}{\partial S_j} = \frac{\beta_{lm} \nabla_j \big[\sum_j r_j^l Y_{lm}(\vartheta_j \varphi_j)\big]}{\sum_j r_j^l Y_{lm}(\vartheta_j \varphi_j)} \frac{\partial}{\partial \beta_{lm}}. \qquad (15)$$

Expressing the β_{lm} in Eq. (15) in terms of the α_{lm}, after multiplication and division by $4\pi/3N$ we obtain

$$\nabla_j S_j \frac{\partial}{\partial S_j} = \frac{(4\pi/3N)}{(4\pi/3N)} \frac{\alpha_{lm} \nabla_j \big[\sum_j (r_j/R_0)^l Y_{lm}(\vartheta_j \varphi_j)\big]}{\sum_j (r_j/R_0)^l Y_{lm}(\vartheta_j \varphi_j)} \frac{\partial}{\partial \alpha_{lm}}. \qquad (16)$$

Inserting (16) into (13), and comparing the result with (14), we obtain an expression for the α_{lm} which occurs in A. Bohr's phenomenological theory of the nucleus:

$$\alpha_{lm} = (4\pi/3N) \sum_j (r_j/R_0)^l Y_{lm}(\vartheta_j \varphi_j). \qquad (17)$$

Let us use the α_{lm} to write part of the potential energy. We shall assume that the potential energy is the sum of interactions between pairs of particles, so that

$$V = {}^1/_2 \sum_{ij} G(\mathbf{r}_i, \mathbf{r}_j) \qquad (18)$$

$$= {}^1/_2 \sum G_{lm}^{l'm'} r_j^l Y_{lm}(\vartheta_j \varphi_j) r_i^{l'} Y_{l'm'}(\vartheta_i \varphi_i)$$

(the summation is taken over all indices). Bearing in mind Eq. (17) and the fact that $l < l_0$, we can write (18) in the form

$$V = \left(\frac{3N}{16\pi}\right)^2 R_0^{-l-l'} G_{lm}^{l'm'} \alpha_{lm} \alpha_{l'm'} + \left(\frac{3N}{4\pi}\right) \sum_{m',\, l' > l_0;\, j} G_{lm}^{l'm'} \alpha_{lm} Y_{l'm'}(\vartheta_j \varphi_j)\, r_j^l + \frac{1}{2} \sum_{ij} G_{l_0}(\mathbf{r}_i, \mathbf{r}_j),$$

$$\frac{1}{2} \sum_{ij} G_{l_0}(\mathbf{r}_i, \mathbf{r}_j) = \frac{1}{2} \sum G_{lm}^{l'm'} r_i^l r_j^{l'} Y_{lm}(\vartheta_i \varphi_i)\, Y_{l'm'}(\vartheta_j \varphi_j), \qquad (19)$$

$$m', l', m, l > l_0.$$

When the indices m and l occur twice, we sum from zero to l_0.

The first term in Eq. (19) describes the potential energy of collective motion, the second term the interaction energy between the individual particles and the collective oscillations, and the final term the interaction between particles screened by the surface oscillations.

The final expression for the Hamiltonian describing a system undergoing small surface oscillations in the constant density approximation is given by the sum of (14) and (19). This Hamiltonian agrees with that of the phenomonological theory of the generalized nuclear model.

The introduction of auxiliary ("superfluous") variables leads to the necessity of applying subsidiary conditions to the wave function, and these can be written

$$\left(\rho_k - N^{-1/2} \sum_j \exp\{-i\,\mathbf{k}\mathbf{r}_j\}\right)\Phi = 0 \qquad (20)$$

for the first of the problems considered here (Sec. 3), and

$$\left[\alpha_{lm}' - (4\pi/3N)\sum_j (r_j/R_0)^l Y_{lm}(\vartheta_j \varphi_j)\right]\Phi = 0 \qquad (21)$$

for the case of surface oscillations.

5. The special choices of the $\varphi_j(r_j)$ considered above can be generalized for other problems. The generalization consists of indicating a method for finding the $\varphi_j(r_j)$.

In solving boundary value problems the Schrödinger equation can be written in the hydrodynamic form

$$-E_j + \frac{1}{2M}(\nabla S_j)^2 - \frac{\hbar^2}{4M}\left[\frac{\Delta p_j}{p_j} - \frac{1}{2}\left(\frac{\Delta p_j}{p_j}\right)^2\right] = 0;$$

$$\frac{1}{M}\nabla(p_j \nabla S_j) = 0, \quad \varphi_j(r_j) = \sqrt{p_j}\exp(i/\hbar S_j).$$

This representation of the Schrödinger equation is convenient in that it is simple to formulate boundary conditions for it in analogy with hydrodynamics.

In the constant density case the S_j satisfy Laplace's equation. However this is not the only generalization. The $\varphi_j(r_j)$ can, for instance, be found from self-consistent field equations.

---

[1] D. N. Zubarev, J. Exptl. Theoret. Phys. (U.S.S.R.) 25, 547 (1953).

[2] D. Bohm and D. Pines, Phys. Rev. 92, 609 (1953).

[3] S. Tomonaga, Progr. Theoret. Phys. 13, 467 (1955).

[4] S. Tomonaga, Progr. Theoret. Phys. 13, 584 (1955).

Translated by E. J. Saletan
120

SOVIET PHYSICS JETP VOLUME 5, NUMBER 3 OCTOBER, 1957

Electrical, Optical and Elastic Properties of Diamond Type Crystals. I

V. S. MASHKEVICH AND K. B. TOLPYGO
Kiev State University and Kiev Polytechnical Institute

(Submitted to JETP editor July 18, 1955)
J. Exper. Theoret. Phys. USSR 32, 520-525 (March, 1957)

The energy of a homopolar crystal is expressed as a function of the displacements and of the dipole moments of the atoms. By means of a variational method, the relation between the displacements and the deformation of the electronic shells of the atoms is established and equations of motion are presented in which the displacements and dipole moment of the atoms play the role of generalized coordinates.

As was shown in a paper by one of the authors[1], Born's atomic theory[2] can be improved by taking into consideration the deformability of the atoms. In the foundation of a theory of the lattice one must assume an expression for the energy U in the form of a quadratic function of the displacements $\mathbf{u}_s^l$ and of the dipole moments $\mathbf{P}_s^l$ of all the atoms (l is the cell number and s the number of the atom in the cell). In the calculation of delay of interaction, one can consider optical, electrical and elastic properties of crystals from a single point of view. The explicit introduction of the quantities $\mathbf{P}_s^l$ is necessary also in the microscopic theory of localized electron states in a crystal[4].

While in ionic crystals the consideration of the deformability of the ions improves the quantitative agreement of theory with experiment[1], in homopolar crystals, where the dipole moments of the displacements $\mathbf{p}_s^l = e_s \mathbf{u}_s^l$ are absent ($e_s = 0$), such considerations lead to a series of qualitatively new consequences. Owing to the dependence of the exchange integrals on the dipole moments of the atoms, the displacements of the latter will lead to their polarization and conversely. Thus, inertial polarization can exist also in homopolar crystals. This permits one to examine the interaction of a nonpolar crystal with an electromagnetic field and, in particular, the lattice absorption which was experimentally observed by Lax and Burstein[5]. The explanation given in Ref. 5 for the lattice absorption (fractional division of charges during oscillations of the atoms) pertains only to secondary combination bands. Considerations of the role of impurity in the fundamental absorption are also inconclusive in view of the weak dependence of the absorption in diamond, Si and Ge on the character and quantity of the impurity. The present investigation permits one to predict the absorption correct as to order of magnitude (approximately λ/d times smaller than in ionic crystals) without the use of any free parameters.

Finally, the presence of inertial polarization leads to an interaction of current carriers with optical oscillations of the lattice. In homopolar crystals this must lead principally to the same, only quantitatively weaker, effects, examined by Pekar[6], as they occur in ionic crystals. In the present work, a method of examining that relation between the displacements and the polarization of the atoms is given. In the following works, it is applied to the study of various properties of crystals[7].

1. THE WAVE FUNCTION AND ENERGY OF THE ELECTRONS OF A CRYSTAL.

In the examination of the dynamics of the lattice, the motion of the nuclei and the electrons of the atoms are conveniently described in an adiabatic approximation. For the first step it is necessary to find the wave function of all the electrons under arbitrary (small displacements of the nuclei. This energy will play the role of the potential energy in the problem of the motion of the nuclei. In diamond type crystals, it is sufficient to consider only the four valence electrons of each atom, introducing the screened nuclear charge $z_s(\mathbf{r})$, where $z_s \to 4$ for $r \to \infty$.

In the Fock approximation we seek a wave function of the electrons in the form of products of functions of individual σ-bonds $\Psi_{(pq)}$ (p and q are abbreviated notations of the numbers of atoms). Antisymmetrization is performed only over the strongly interacting electrons of a single bond:

$$\begin{aligned}\Psi_{(pq)} &= C_{(pq)}[\psi_{pq}(\mathbf{r}_{pq})\psi_{qp}(\mathbf{r}_{qp}) \\ &\quad + \psi_{pq}(\mathbf{r}_{qp})\psi_{qp}(\mathbf{r}_{pq})]\chi_a(\sigma_1, \sigma_2), \\ C_{(pq)} &= [2(1+|S_{pq}|^2)]^{-1/2}; \end{aligned} \tag{1}$$

S_{pq} is the nonorthogonality integral, Ψ_{pq} is the wave function of an electron $\mathbf{r}_{pq}$ in atom p which brings about its bond with atom q. The form of ψ_{pq} will be determined from a variational principle. Let $\overline{H}_{(pq)}$ denote the mean kinetic and potential energy of the electrons of the bond (pq), including their mutual interaction with the nuclei p and q, half the energy of interaction with the remaining electrons of the atoms p and q and one fourth of the energy of interaction with the nuclei of the nearest neighbors of p and q:

$$\begin{aligned}\overline{H}_{(pq)} &= 2|C_{(pq)}|^2\Big\{\int(\psi^*_{pq}(\mathbf{r}) \\ &\quad + S_{pq}\psi^*_{qp}(\mathbf{r}))\Big(-\frac{\hbar^2}{2m}\Delta_r - \frac{e^2 z_s(\mathbf{r}-\mathbf{R}_p)}{|\mathbf{r}-\mathbf{R}_p|} \\ &\quad + e^2\sum_{q'}{}'\int\frac{|\psi_{pq'}(\mathbf{r}')|^2}{|\mathbf{r}-\mathbf{r}'|}d\tau'\Big)\psi_{pq}(\mathbf{r})\,d\tau \\ &\quad + e^2\sum_{q'}{}'\Big[(|C_{(pq')}|^2-1) \\ &\quad \times\int\frac{1}{|\mathbf{r}-\mathbf{r}'|}|\psi_{pq'}(\mathbf{r}')|^2(|\psi_{pq}(\mathbf{r})|^2 \\ &\quad + S_{pq}\psi^*_{qp}(\mathbf{r})\psi_{pq}(\mathbf{r}))\,d\tau\,d\tau' + |C_{(pq')}|^2 \\ &\quad \times\int\frac{1}{|\mathbf{r}-\mathbf{r}'|}(|\psi_{pq}(\mathbf{r})|^2 + S_{pq}\psi^*_{qp}(\mathbf{r})\psi_{pq}(\mathbf{r}) \\ &\quad + |\psi_{qp}(\mathbf{r})|^2 + S_{pq}\psi^*_{pq}(\mathbf{r})\psi_{qp}(\mathbf{r}))(|\psi_{q'p}(\mathbf{r}')|^2 \\ &\quad + S'_{qp}\psi^*_{pq'}(\mathbf{r}')\psi_{q'p}(\mathbf{r}') + |\psi_{pq'}(\mathbf{r}')|^2 \\ &\quad + S_{pq'}\psi^*_{q'p}(\mathbf{r}')\psi_{pq'}(\mathbf{r}'))\,d\tau\,d\tau' + \int\frac{1}{|\mathbf{r}-\mathbf{r}'|} \\ &\quad \times|\psi_{pq'}(\mathbf{r}')|^2(|\psi_{qp}(\mathbf{r})|^2 + S_{qp}\psi^*_{pq}(\mathbf{r}) \\ &\quad \times\psi_{qp}(\mathbf{r}))\,d\tau\,d\tau' - \int\frac{e^2 z_s(\mathbf{r}-\mathbf{R}_{q'})}{4|\mathbf{r}-\mathbf{R}_{q'}|}(|\psi_{qp}(\mathbf{r})|^2 \\ &\quad + |\psi_{pq}(\mathbf{r})|^2)\,d\tau\Big] - \int\frac{e^2 z_s(\mathbf{r}-\mathbf{R}_q)}{|\mathbf{r}-\mathbf{R}_q|}(|\psi_{pq}(\mathbf{r})|^2 \\ &\quad + S_{pq}\psi^*_{qp}(\mathbf{r})\psi_{pq}(\mathbf{r}))\,d\tau\Big\} + \{p \rightleftarrows q\} \\ &\quad + e^2\int\frac{1}{|\mathbf{r}-\mathbf{r}'|}|\psi_{pq}(\mathbf{r})|^2|\psi_{qp}(\mathbf{r}')|^2\,d\tau\,d\tau' \\ &\quad + e^2\int\frac{1}{(1+|S_{pq}|^2)|\mathbf{r}-\mathbf{r}'|}(\psi^*_{pq}(\mathbf{r})\psi^*_{qp}(\mathbf{r}')\psi_{pq} \\ &\quad \times(\mathbf{r}')\psi_{qp}(\mathbf{r}) - |S_{pq}|^2|\psi_{pq}(\mathbf{r})|^2|\psi_{qp}(\mathbf{r}')|^2) \\ &\quad \times d\tau\,d\tau' + \frac{16e^2}{|\mathbf{R}_q-\mathbf{R}_p|}. \end{aligned} \tag{2}$$

The symbol $\{p \rightleftarrows q\}$ denotes the addition of the entire preceeding expression in which p and q exchange places. We denote the sum of the interaction energies of the electrons of each pair of bonds (pq) and (rs) which do not have common atoms, by

$$\overline{H}_{(pq)(rs)} = -e^2 \int \left(\frac{1}{|\mathbf{r}-\mathbf{R}_r|} + \frac{1}{|\mathbf{r}-\mathbf{R}_s|} \right) (|\psi_{pq}(\mathbf{r})|^2 + |\psi_{qp}(\mathbf{r})|^2)\, d\tau - e^2 \int \left(\frac{1}{|\mathbf{r}-\mathbf{R}_p|} + \frac{1}{|\mathbf{r}-\mathbf{R}_q|} \right) \times (|\psi_{rs}(\mathbf{r})|^2 + |\psi_{sr}(\mathbf{r})|^2)\, d\tau + \Big) \frac{e^2}{|\mathbf{R}_p - \mathbf{R}_s|} + \frac{e^2}{|\mathbf{R}_p - \mathbf{R}_r|} + \frac{e^2}{|\mathbf{R}_q - \mathbf{R}_s|} + \frac{e^2}{|\mathbf{R}_q - \mathbf{R}_r|} + \int \frac{e^2}{|\mathbf{r}-\mathbf{r}'|} (|\psi_{pq}(\mathbf{r})|^2 + |\psi_{qp}(\mathbf{r})|^2) \times (|\psi_{rs}(\mathbf{r}')|^2 + |\psi_{sr}(\mathbf{r}')|^2)\, d\tau\, d\tau'. \tag{3}$$

Then

$$\overline{H} = \sum_{(pq)} \overline{H}_{(pq)} + \sum_{(pq)(rs)}{}' \overline{H}_{(pq)(rs)}. \tag{4}$$

The overlap integrals, which are of the order of S_{pq}, are retained only in terms which contain the interaction of electrons of one atom or of one bond among themselves and with their nuclei.

Keeping in mind that the wave functions of the electrons which constitute the σ-bonds in the crystal ψ_{pq} are essentially different from the wave functions of isolated atoms, we use perturbation theory for calculation of the former, for close eigenvalues. For elements of the fourth group, the differences between the energies of s and p electrons with the same principal quantum number are of the order of the interaction energy between atoms. Therefore, on the incorporation of atoms into a crystal, there occurs a redistribution of electrons among levels and the formation of functions of σ-bonds.

Having denoted the energy levels of the valence electrons by $E_1 E_2 \ldots$, we can thus regard $\varepsilon^2 = (E_2 - E_1)/(E_5 - E_1)$ as a small expansion parameter. Obviously, S_{pq} and all the terms in $\overline{H}$ which contain products of functions with interchanged electrons must be regarded as quantities of the order of ε. We shall seek the wave function of the r-th electron of the bond (pq) in the form of a superposition of excited functions of the atom p:

$$\psi_{pq}(r) = \sum_{i=1}^{\infty} \gamma_{pqi} \psi_{pi}(\mathbf{r}), \tag{5}$$

and we expand the parameters γ_{pqi} in powers of ϵ:

$$\gamma_{pqi} = \gamma_{pqi}^{(0)} + \varepsilon^2 \gamma_{pqi}^{(2)} + \varepsilon^3 \gamma_{pqi}^{(3)} + \cdots, \tag{6}$$

(the expansion of $\overline{H}$ must be begun from terms $\sim \epsilon^2$), wherein for $i \geqslant 5$, $\gamma_{pqi}^{(0)} = 0$. In order not to complicate the problem by the introduction of an endless chain of orthogonality conditions for the functions ψ_{pq} with different q's, we restrict the class of approximating functions with the hypothesis that $\gamma_{pqi}^{(0)} + \epsilon^2 \gamma_{pqi}^{(2)}$ does not depend on the displacements of the nuclei if $i \leqslant 4$.

We subject the parameters of the approximation γ_{pqi} to the orthogonality conditions

$$\sum_{i=1}^{\infty} \gamma_{pqi}^{*} \gamma_{pq'i} = \delta_{qq'},$$

i. e.,

$$\sum_{i=1}^{4} (\gamma_{pqi}^{(0)*} + \varepsilon^2 \gamma_{pqi}^{(2)*})(\gamma_{pq'i}^{(0)} + \varepsilon^2 \gamma_{pq'i}^{(2)}) = \delta_{qq'}, \tag{7}$$

$$\varepsilon^3 \sum_{i=1}^{4} (\gamma_{pqi}^{(0)*} \gamma_{pq'i}^{(3)} + \gamma_{pq'i}^{(0)} \gamma_{pqi}^{(3)*}) = 0, \tag{8}$$

$$\varepsilon^4 \sum_{i=1}^{4} (\gamma_{pqi}^{(0)*} \gamma_{pq'i}^{(4)} + \gamma_{pq'i}^{(0)} \gamma_{pqi}^{(4)*}) + \varepsilon^4 \sum_{i=5}^{\infty} \gamma_{pqi}^{(2)*} \gamma_{pq'i}^{(2)} = 0, \tag{9}$$

and in addition, as in Ref. 1, we simultaneously use the conservation of the dipole moments $\mathbf{P}_p$ of each atom.

$$-e \int \mathbf{r} \sum_{q} |\psi_{pq}(\mathbf{r}')|^2\, d\tau = \mathbf{P}_p = \text{const},$$

i. e., with accuracy to ϵ^2:

$$-e\varepsilon^2 \sum_{q} \sum_{j=1}^{4} \sum_{i=5}^{\infty} (\gamma_{pqi}^{(2)*} \gamma_{pqj}^{(0)} (i|x|j) + \text{complex conj.}) = P_{px}$$

We assume $\gamma_{pqi}^{(0)}$ and $\gamma_{pqi}^{(2)}$ for $i \leqslant 4$ known and the conditions Eq. (7) for undisplaced nuclei fulfilled. The conditions Eqs. (8) and (9) can be satisfied through the choice of $\gamma_{pqi}^{(3)}$ and $\gamma_{pqi}^{(4)}$. Their values are not important for us since the corresponding contribution to the Hamiltonian will be of the order of ϵ^5 or ϵ^6 and at the same time we retain terms no higher than ε^4.

Since the classification of electrons into *s*, *p* and *d* states is possible only for a spherically symmetrical field, we introduce (for each atom) the Hamiltonian of the zeroth approximation $\hat{H}^{(0)}$, identical, for all the valence electrons, with interaction potential energy.

$$\frac{3e^2}{4}\sum_{i=1}^{4}\int\frac{|\psi_{pi}(r')|^2\,d\tau'}{|\mathbf{r}-\mathbf{r}'|}$$

and we shall regard the ψ_{pi} $i=1, 2 \ldots \infty$ as its characteristic functions:

$$\hat{H}_p^{(0)}\psi_{pi}=E_i^0\psi_{pi}. \tag{11}$$

2. EXPANSION OF THE ENERGY OF THE ELECTRONS IN POWERS OF THE DIPOLE MOMENTS AND DISPLACEMENTS OF THE ATOMS

Substituting the expansions Eqs. (5) and (6) in the expression for the mean energy $\overline{H}$ [Eq. (2)], we transform that part of $\overline{H}$ which contains the dipole moments $\mathbf{P}_p$, i. e., the coefficients $\gamma_{pqi}^{(2)}$, $i \geqslant 5$, taking account of the orthogonality conditions and Eq. (11). Since the exchange integrals are of the order of ϵ^2, then with accuracy to ϵ^4:

$$\overline{H}(\gamma_{pqi}^{(2)}) = \varepsilon^4\sum_{p,\,q}\sum_{i=5}^{\infty}\{(E_i^0-E_1^0)\,|\gamma_{pqi}^{(2)}|^2 + C_{pqi}\gamma_{pqi}^{*(2)}+C_{pqi}^{*}\gamma_{pqi}^{(2)}\}, \tag{12}$$

$$\begin{aligned}C_{pqi} ={}& \sum_{j,h,m=1}^{4}B_{pqihjm}\gamma_{qpj}^{(0)*}\gamma_{pqm}^{(0)}\gamma_{qph}^{(0)} + \frac{e^2}{\varepsilon^2}\sum_{j,h,m=1}^{4}\int\psi_{pi}^{*}(\mathbf{r})\,\psi_{pj}^{*}(\mathbf{r}')\\ &\times\frac{1}{|\mathbf{r}-\mathbf{r}'|}\,\psi_{pm}(\mathbf{r})\,\psi_{ph}(\mathbf{r}')\,d\tau d\tau'\\ &\times\left(\frac{1}{4}\gamma_{pqm}^{(0)}\delta_{jh}-\gamma_{pqm}^{*(0)}\gamma_{pqj}^{(0)*}\gamma_{pqh}^{(0)}\right),\end{aligned} \tag{13}$$

$$\begin{aligned}B_{pqihjm} ={}& \frac{1}{\varepsilon^2}\Big\{S_{pqih}S_{pqjm}(E_h^0+E_m^0-2E_1^0)\\ &+S_{qpjm}\int\frac{e^2z_э\psi_{qi}\psi_{qh}}{|\mathbf{r}-\mathbf{R}_p|}\,d\tau - S_{pqih}\int\frac{e^2z_э\psi_{pj}\psi_{pm}}{|\mathbf{r}-\mathbf{R}_q|}\,d\tau\\ &-e^2\int\frac{1}{|\mathbf{r}-\mathbf{r}'|}\,\psi_{pi}^{*}(\mathbf{r})\,\psi_{qh}(\mathbf{r})\,\psi_{qj}^{*}(\mathbf{r}')\,\psi_{pm}(\mathbf{r}')\,d\tau\,d\tau'\Big\}.\end{aligned}$$

$$S_{pqih}=\int\psi_{pi}^{*}\psi_{qh}\,d\tau. \tag{14}$$

Having multiplied Eqs. (10) by Lagrange multipliers μ_{px} and subtracted them from Eq. (12) we vary the obtained expression over $\gamma_{pqi}^{(2)}$. Then

$$\gamma_{pqi}^{(2)} = -\frac{C_{pqi}+\sum\limits_{x}\sum\limits_{j=1}^{4}\mu_{px}\gamma_{pqj}^{(0)}(i\,|\,x\,|\,j)\,e/\varepsilon^2}{E_i^0-E_1^0}, \tag{15}$$

$$P_{px}=\varepsilon^2\left\{\mu_{px}\alpha_{px} + e\,\frac{C_{pqi}(j\,|\,x\,|\,i)\,\gamma_{pqj}^{(0)*}+C_{pqj}^{*}(i\,|\,x\,|\,j)\,\gamma_{pqj}^{(0)}}{E_i^0-E_1^0}\right\}, \tag{16}$$

where

$$\alpha_{px}=2e^2\sum_{j=1}^{4}\sum_{i=5}^{\infty}|(i\,|\,x\,|\,j)|^2/(E_i^0-E_1^0)$$

is the polarizability of an atom along the *x* axis. Here we have supposed the functions ψ_{pj} chosen so that for any of the indices $j=1 \ldots 4$; $i \geqslant 5$, $(i\,|x|\,j)$ is different from zero only for one of the three coordinates. In addition $\gamma_{pqj}^{(0)}$ are orthogonal over the indices *j*.

Expressing μ_{px} through P_{px} from Eq. (16) and substituting them in Eq. (15), we obtain for the part of the Hamiltonian which depends on $\mathbf{P}_p$:

$$\overline{H}(\gamma_{pqi}^{(2)}) = \sum_{p}\sum_{x}\left[\frac{1}{2\alpha_{px}}P_{px}^2+\sum_{q}\frac{e\varepsilon^2}{\alpha_{px}}N_{pqx}P_{px}\right]+O(\varepsilon^4), \tag{17}$$

$$N_{pqx}=\sum_{j=1}^{4}\sum_{i=5}^{\infty}\frac{C_{pqi}^{*}\gamma_{pqj}^{(0)}(i\,|\,x\,|\,j)+C_{pqi}\gamma_{pqj}^{(0)*}(j\,|\,x\,|\,i)}{E_i^0-E_1^0}. \tag{18}$$

The quantities $O(\epsilon^4)$ do not depend on P_{px} and can be discarded in comparison with the other terms of the same form which are of the order of ϵ^2. Analogously, for the part of $\overline{H}$ which does not depend on $\gamma_{pqi}^{(2)}$, we obtain

$$\overline{H}(\gamma_{pqj}^{(0)}) = \varepsilon^2\sum_{(pq)}\sum_{j,h,l,m=1}^{4}B_{pqjhlm}\gamma_{pqj}^{(0)*}\gamma_{pqh}^{(0)}\gamma_{pql}^{(0)*}\gamma_{pqm}^{(0)}. \tag{19}$$

Finally, the sum of the integrals of Eq. (3) and of the Coulombic terms in Eq. (2) gives the dipole-dipole interaction. Thus,

$$H = \overline{H}(\gamma^{(2)}_{pqi}) + \overline{H}(\gamma^{(0)}_{pqj}) + \sum_{p,q}\left[\frac{\mathbf{P}_p\mathbf{P}_q}{R^3_{pq}} - 3\,\frac{(\mathbf{P}_p\mathbf{R}_{pq})(\mathbf{P}_q\mathbf{R}_{pq})}{|R_{pq}|^5}\right]. \tag{20}$$

The expansion of $\overline{H}$ in powers of the displacements $\mathbf{u}_p$ and of the dipole moments $\mathbf{P}_p$ of all the atoms is begun, obviously, from terms of the 2nd order, since $\overline{H}$ has a minimum for $\mathbf{u}_p = 0$, $\mathbf{P}_p = 0$.

In the expansion of the coefficients N_{pqx}, we notice that in the expression Eq. (18) quantities C_{pqi} $\gamma^{(0)}_{pqi}$ enter, which pertain only to a single bond pq in which the singled-out directions are those parallel to the vectors $\mathbf{R}_{pq}$ ($\gamma^{(0)}_{pqj}$ do not depend on the displacements). The vector $\mathbf{N}_{pq}$ will lie in the plain of the vectors $\mathbf{R}_{pq} = \mathbf{R}_p - \mathbf{R}_q$ and $\mathbf{u}_{pq} = \mathbf{u}_p - \mathbf{u}_q$ and will depend only on the components of $\mathbf{u}_{pq}$ parallel and perpendicular to $\mathbf{R}_{pq}$ which lie in the specified plane, i. e.,

$$\mathbf{N}_{pq} = \mathbf{N}_{pq}(\mathbf{r}_{pq}) + b'\,\mathbf{u}_{pq} + c'\,(\mathbf{u}_{pq}\mathbf{r}_{pq})\,\mathbf{r}_{pq}, \tag{21}$$

where b' and c' are constant coefficients.

Applying analogous considerations to the coefficients B_{pqiklm}, we can conclude that each term in the sum over all bonds (pq) in Eq. (19) will depend only on $\mathbf{u}_{pq\parallel}$ and $\mathbf{u}_{pq\perp}$. However, in the corresponding quadratic form, the cross term must be absent, since in the absence of the components $\mathbf{u}_{pq\perp}$, the force in the direction perpendicular to $\mathbf{r}_{pq}$ must also be absent. Then

$$\overline{H}(\gamma^{(0)}_{pqj}) = \sum_{(pq)}[d_p(\mathbf{u}_{pq}\mathbf{r}_{pq})^2 + g_p\mathbf{u}^2_{pq}]. \tag{22}$$

Converting to the usual notation of Born $\mathbf{r}^l_s$, $\mathbf{u}^l_s$, $\mathbf{P}^l_s$ and gathering all the terms, for a binary crystal we obtain:

$$U = \overline{H} = \sum_l\sum_{l'}\{d_p(\mathbf{u}^{ll'}_{12}\mathbf{r}^{ll'}_{12})^2 + g_p(\mathbf{u}^{ll'}_{12})^2 + b_p\mathbf{P}^{ll'}_{12}\mathbf{u}^{ll'}_{12} + c_p(\mathbf{P}^{ll'}_{12}\mathbf{r}^{ll'}_{12})(\mathbf{u}^{ll'}_{12}\mathbf{r}^{ll'}_{12})\} + \frac{1}{2\alpha}\sum_{ls}\mathbf{P}^{l2}_s - \frac{1}{2}\sum_{sl}\mathbf{P}^l_s\mathbf{E}^l_s, \tag{23}$$

where

$$\mathbf{E}^l_s = \sum_{l's'}[3(\mathbf{P}^{l'}_{s'}\mathbf{r}^{ll'}_{ss'})\,\mathbf{r}^{ll'}_{ss'}/|\mathbf{r}^{ll'}_{ss'}|^5 - \mathbf{P}^{l'}_{s'}/|\mathbf{r}^{ll'}_{ss'}|^3] \tag{24}$$

is the field established at the point $\mathbf{r}^l_s$ by all the dipoles $\mathbf{P}^{l'}_{s'}$. In the expression in Eq. (23) the first item is of the order of ϵ^2, while the remaining three are of order ϵ^4. Retention of the latter with simultaneous rejection of the terms $\sim\epsilon^4$ in $\overline{H}(\gamma^{(0)}_{pqj})$ has the justification that the dependence of the energy on $\mathbf{P}^l_s$ leads to qualitatively new consequences at the same time that retention of terms $\sim\epsilon^4$ in $\overline{H}(\gamma^{(0)}_{pqj})$ would lead merely to some other value of the parameters d_p, g_p, which will all be determined equally from experiment. Since ϵ practically is very small (the binding energy is comparable with the ionization energy), the calculation of $\mathbf{P}^l_s$ leads to consequences which are easily observable experimentally.

In comparison with the theory of ionic crystals[1], here there are four interaction parameters d_p, g_p, b_p, c_p, instead of three G, g, h. This is connected with giving up a hypothesis of central forces. These parameters must be determined from experiment since they cannot, in view of the inadequacy of our knowledge of the form of the functions ψ_{pi}, be successfully calculated.

Using Eq. (23) we write down the equations of motion:

$$m_s\ddot{u}^l_{sx} = -\partial U(u, P)/\partial u^l_{sx};\quad 0 = -\partial U(u, P)/\partial P^l_{sx}. \tag{25}$$

The second group of equations also gives the sought relation of the polarization of the atoms with their displacements. It stipulates those effects referred to in the introduction and it is examined in the following article[7].

---

[1] K. B. Tolpygo, J. Exptl. Theoret. Phys. (U.S.S.R.) **20**, 497 (1950)

[2] M. Born and Maria Cõppert-Mayer, *Theory of Solids* ONTI Leningrad, Moscow (1938) (Russian Translation)

[3] K. B. Tolpygo, *Mathematical Collection*, Kiev State U. #5, 99 (1951)

[4] I. M. Dykman, Works Physical Institute Acad. Sci., USSR No. 5, 48 (1954).

[5] M. Lax and E. Burstein, Phys. Rev. **97**, 39 (1955)

[6] S. I. Pekar, *Investigations in the Electron Theory of Crystals*. GTTI Moscow, Leningrad (1951). [German Translation, "*Untersuchungen in Elektronentheorie der Kristalle*" Berlin-Akademie Verlag (1945)]

[7] V. S. Mashkevich, J. Exptl. Theoret. Phys. (U.S.S.R) **32**, No. 4 (1957)

Translated by R. L. Eisner
121

SOVIET PHYSICS JETP VOLUME 5, NUMBER 3 OCTOBER, 1957

Calculation of the Drift Velocity of Ions in the Electric Field in Their Gas

V. I. PEREL'
Karelo-Finnish Pedagogical Institute

(Submitted to JEPT editor February 6, 1956)
J. Exptl. Theoret. Phys. (U.S.S.R) **32**, 526-533 (March, 1957)

On the basis of the "pure overcharge" model proposed by L. A. Sena, the drift velocity of ions moving in the respective gas under the influence of an electric field is calculated as a function of the ratio of the work done by the field over the length of a free path to the mean thermal energy of the atoms. The results of the calculations are in good agreement with the experimental data for inert gases.

1. STATEMENT OF THE PROBLEM. THE KINETIC EQUATION

THE problem of the motion of positive ions in a gas is divided into two main parts. The first part consists of the determination of the differential effective cross-section for collision of an ion with an atom and must be solved by the methods of quantum mechanics. The differential effective cross-section of collision being know, the second part consists in determining the velocity distribution function for the ions and mean values, of which the most important is the drift velocity of the ions in the direction of the electric field.

At the present time, it can be considered established that the chief process of interaction with neutral atoms in the motion of positive atomic ions in the respective gas is resonance overcharge[1-6].

Calculations of the drift velocity of ions moving in a gas of the same nature under the influence of a constant homogeneous electric field, based on the model of pure overcharge proposed by Sena, give values which agree well with experimental data[1,4,5]. These calculations, however, were carried out strictly only for two limiting cases: for the case of a strong electric field, when it is possible to neglect the thermal motion of atoms of the gas[4], and for the case of a weak electric field, when the energy acquired by an ion over the length of a free path under the action of the field is much smaller than the mean energy of thermal motion of a neutral atom[5]. The results obtained in Ref. 4 for intermediate cases are based on the replacement of the real velocity distribution of the atoms by two opposite fluxes. The possibility of such a consideration requires substantiation. Furthermore, the velocity of the two fluxes remains undetermined, their being know only that it must be of the order of the mean velocity of the gas atoms.

In the present work, a method of successive approximations is put forward which permits one to solve the second kinetic part of the problem on the drift velocity of ions, on the basis of the model of "pure overcharge", for any ratio of the work done by the field over the length of a free path of an ion to the mean thermal energy of the atoms of the gas.

In the calculation, the concentration of charged particles is assumed so small that their interaction with one another and also the effect of their motion on the velocity distribution function of the atoms can be disregarded.

The calculation is carried out under the assumption that the effective cross section of overcharge does not depend on velocity, however the proposed method of successive approximations is applicable also in the case where the cross section can not be considered constant.

The kinetic equation for the velocity distribution function of ions moving in the respective gas under the influence of a constant electric field E under the assumptions indicated above, has the form[4]:

$$a\lambda\frac{\partial f}{\partial v_z} = n(v)\int f(\mathbf{v}')\,|\mathbf{v}-\mathbf{v}'|\,d\mathbf{v}' - f(\mathbf{v})\int n(v')\,|\mathbf{v}-\mathbf{v}'|\,d\mathbf{v}', \qquad (1)$$

where $a = eE/m$ is the acceleration of an ion in the electric field, e and m are the charge and mass of an ion, $\lambda = 1/Nq$ its mean free path, N the concentration of gas atoms, q the effective cross section of overcharge, $f(\mathbf{v})$ the velocity distribution function of the ions, $n(v)$ the velocity distribution function of the neutral atoms and $d\mathbf{v}' = dv_x'\,dv_y'\,dv_z'$. The direction of the field is taken along the direction of the axis OZ[*]. We introduce the notation

$$u_0 = \sqrt{2kT/m}, \quad \gamma = \pi e E \lambda / 4kT,$$

u_0 is the most probable speed for atoms of the gas and the dimensionless quantity γ characterizes the ratio of the work done by the field over a free path length of an ion to the mean thermal energy of the atoms.

Taking account of the cylindrical symmetry of the problem, we introduce cylindrical coordinates in velocity space and transform to dimensionless variables:

$$z = v_z/u_0, \quad \rho = \sqrt{v_x^2 + v_y^2}/u_0; \tag{2}$$

φ is the angle which the projection of the velocity on the plane XOY makes with the axis OX. Then for the velocity distribution function of the atoms we obtain

$$n(v)\, dv_x\, dv_y\, dv_z = W_1(z)\, W_2(\rho^2)\, dz\, d\rho^2\, d\varphi/2\pi, \tag{3}$$
$$W_1(z) = \pi^{-1/2} e^{-z^2}; \qquad W_2(\rho^2) = e^{-\rho^2}. \tag{4}$$

Considering Eq. (1) as a non-homogeneous differential equation it is easy to obtain.

$$f(\rho, z) = 2W_2(\rho^2) \int_{-\infty}^{z} W_1(u)\, F(\rho, u)\, G(\rho, u, z)\, du,$$

$$f(\rho, z)\, \rho\, d\rho\, dz\, d\varphi = f(\mathbf{v})\, dv_x\, dv_y\, dv_z, \tag{5}$$

$$G(\rho, u, z) = \frac{1}{\gamma} \exp\left[-\frac{1}{\gamma} \int_{u}^{z} F_0(\rho, u')\, du'\right], \tag{6}$$

$$F(\rho, z) = \iint f(\rho', z')\, g(\rho', \rho, z - z')\, \rho'\, d\rho'\, dz', \tag{7}$$

$$F_0(\rho, z) = \iint 2W_2(\rho'^2)\, W_1(z')\, g(\rho', \rho, z - z')\, \rho'\, d\rho'\, dz', \tag{8}$$

$$g(\rho', \rho, t) = \frac{1}{4} \int_{0}^{2\pi} \sqrt{\rho^2 - 2\rho\rho' \cos\varphi + \rho'^2 + t^2}\, d\varphi. \tag{9}$$

The function $g(\rho', \rho, t)$ can be expressed through a complete elliptic integral of the second type:

$$g(\rho', \rho, t) = \sqrt{\rho\rho'}\, \frac{1}{k} E(k), \qquad k^2 = \frac{4\rho\rho'}{(\rho + \rho')^2 + t^2}. \tag{10}$$

We note that the function $g(\rho', \rho, t)$ is symmetrical with respect to interchange of the variables ρ' and ρ and is an even function of t.

2. METHOD OF SUCCESSIVE APPROXIMATIONS FOR SOLUTION OF THE KINETIC EQUATION

For an approximate solution to Eq. (5) we use the Gaussian type quadrature formulas

$$\int_{-\infty}^{\infty} W_1(z)\, \varphi_1(z)\, dz = \sum_{n=1}^{N} a_n \varphi_1(z_n), \tag{11}$$

$$\int_{0}^{\infty} W_2(t)\, \varphi_2(t)\, dt = \sum_{m=1}^{M} b_m \varphi_2(t_m), \tag{12}$$

where $W_1(z)$ and $W_2(t)$ are determined by Eqs. (4), z_n are the roots of the Hermite polynominal of degree N, t_m are the roots of the Laguerre polynominal of degree M, a_n and b_m are the corresponding Christoffel numbers. The values of a_n and z_n for $N \leqslant 9$, and of b_m and t_m for $N \leqslant 5$ were calculated by Reiz[8]. We observe that the coefficients a_n and b_m satisfy the condition

$$\sum_{m=1}^{M} \sum_{n=1}^{N} a_n b_m = 1. \tag{13}$$

Later, we shall have to evaluate approximately integrals of the form

$$\int_{-\infty}^{\infty} \frac{d\varphi_1}{dz} \left\{ \int_{-\infty}^{z} W_1(z')\, \varphi(z')\, dz' \right\} dz.$$

Integrating by parts and applying Eq. (11) we find

$$\int_{-\infty}^{\infty} \frac{d\varphi_1}{dz} \left\{ \int_{-\infty}^{z} W_1(z')\, \varphi(z')\, dz' \right\} dz =$$
$$- \int_{-\infty}^{\infty} W_1(z)\, \varphi_1(z)\, \varphi(z)\, dz = - \sum_{n=1}^{N} a_n \varphi_1(z_n)\, \varphi(z_n).$$

---

[*] V. A. Fock solved the problem of the motion of ions in a gas in an electric field under the assumption that they emerge with a Maxwellian velocity distribution and disappear as a result of overcharge. It is not difficult to obtain Equation (21) of Fock's work[7] from Eq. (1) if one regards the integral in the first term on the right as independent of velocity.

It is easy to verify the same result is obtained if we set

$$\int_{-\infty}^{z} W_1(z')\,\varphi(z')\,dz' = \sum_{n=1}^{N} a_n(z)\,\varphi(z_n), \tag{14}$$

$$\begin{aligned} a_n(z) &= 0 \quad \text{when } z < z_n, \\ a_n(z) &= a_n \quad \text{when } z > z_n. \end{aligned} \tag{15}$$

The primary argument in favor of a method based on the utilization of quadrature formulas is that to each mathematical approximation here, there corresponds a completely distinct physical model.

Actually it is not difficult to see that utilization of Eqs. (11), (12) and (14) is equivalent to the replacement of the functions $W_1(z)$ and $W_2(\rho^2)$ by the functions:

$$W_1^N(z) = \sum_{n=1}^{N} a_n\,\delta(z - z_n); \tag{16}$$

$$W_2^M(\rho^2) = \sum_{m=1}^{M} b_m\,\delta(\rho^2 - \rho_m^2); \quad \rho_m^2 = t_m. \tag{17}$$

The physical meaning of the quadrature equations (11) through (13) consists in the fact that the real motion of the atoms with a Maxwellian distribution Eq. (14) is replaced by motion with distribution corresponding to Eqs. (16) and (17).

The Gaussian method applied for a choice of points of subdivision likewise permits of a simple interpretation. Let us examine, for example, Eq. (11). For points of subdivision chosen according to the Gaussian method we obtain, using this equation, explicit values for the integrals

$$\int_{-\infty}^{\infty} W_1(z)\,z^k\,dz$$

with $k = 0, 1, 2 \ldots (2N - 1)$. These integrals represent the mean values of the various powers of z, i. e., of the projection of the velocity of an atom on the direction of the field. The more points of subdivision we take, the better will the distribution of Eqs. (16) and (17) convey the actual character of the motion of the atoms.

The method of successive approximations used by us is analogous to a method developed by Chandrasekhar[9] for the solution of a radiative transfer equation. In Chandrasekhar's method, however, use of quadature formulas is equivalent to the prior introduction of an approximate expression for an unknown function (the radiation density), while in the method set forth here, the physical model itself is approximate. Within the framework of this approximate model the problem is solved explicitly.

We note that in the case where the work done by the field over the length of the free path of the ions is much larger than the mean energy of thermal motion of the atoms, all the approximations lead to one and the same exact result. Actually, the various approximations differ one from another in the character of the motion of the atoms in the corresponding physical models, but if the field is large, the atoms can in general be regarded as immobile.

Using the quadrature equations (11) through (13), in other words, replacing W_1 and W_2 in the expressions under the integrals by the functions (16) and (17), we obtain [instead of Eqs. (5) and (8)]:

$$f(\rho, z) = 2W_2(\rho^2)\sum_n a_n(z)\,F(\rho, z_n)\,G(\rho, z_n, z), \tag{18}$$

$$F_0(\rho, z) = \sum_{n, m} g(\rho_m, \rho, z - z_n)\,a_n b_m. \tag{19}$$

Here and further on, the summation over n is carried from 1 to N, and the summation over m from 1 to M.

In Eq. (18) we replace ρ and z by ρ' and z', multiply both parts of the equation by $g(\rho', \rho, z - z')\,\rho'\,d\rho'\,dz'$ and carry out integration over ρ' and z'. Then using Eqs. (12) and (7), we obtain

$$F(\rho, z) = \sum_{m, n} F(\rho_m, z_n)\,b_m \times \int_{-\infty}^{\infty} a_n(z')\,G(\rho_m, z_n, z')\,g(\rho_m, \rho, z - z')\,dz'. \tag{20}$$

Taking account of Eq. (15), we introduce the notation

$$b_m a_n F(\rho_m, z_n) = x_{mn}, \tag{21}$$

$$a_s b_k \int_{z_n}^{\infty} G(\rho_m, z_n, z')\,g(\rho_m, \rho_k, z_s - z')\,dz' = c_{ks}^{mn}. \tag{22}$$

Assigning now the values ρ_k and z_n to ρ and z in Eq. (20) ($k = 1, 2, \ldots M$; $n = 1, 2 \ldots N$), we arrive at a system of equations for the quantities x_{mn}:

$$x_{ks} = \sum_{m, n} c_{ks}^{mn} x_{mn},$$

which in a given approximation replaces the integral equation (5).

The homogeneous system Eq. (23) can have non-zero solutions only if the determinant of its coefficients is equal to zero. Using Eqs. (19) and (22) and the properties of the function $g(\rho', \rho, t)$ we find:

$$\sum_{ks} c_{ks}^{mn} = \int_{z_n}^{\infty} G(\rho_m, z_n, z')\, F_0(\rho_m, z')\, dz',$$

whence, if Eq. (6) is considered:

$$\sum_{ks} c_{ks}^{mn} = 1. \tag{24}$$

From the relation Eq. (24) it follows at once that the determinant of the system Eqs. (23) is equal to zero and, consequently, non-zero solutions exist.

From Eqs. (23) the quantities x_m are determined, obviously, explicit up to an arbitrary common factor. This factor is found from the normalization condition:

$$\int_{-\infty}^{\infty}\int_{0}^{\infty} f(\rho, z)\, \rho\, d\rho\, dz = 1, \tag{25}$$

which, according to Eq. (18) takes the form:

$$\sum_{m,\, n} A^{mn} x_{mn} = 1; \tag{26}$$

$$A^{mn} = \int_{z_n}^{\infty} G(\rho_m, z_n, z)\, dz. \tag{27}$$

If one determines x_{mn} through Eqs. (23) and (26), then it is possible by means of Eqs. (18) and (12) to obtain the mean values of the various quantities which characterize the motion of the ions. For example, for the drift velocity we obtain:

$$\bar{z} = \int_{-\infty}^{\infty}\int_{0}^{\infty} f(\rho, z)\, z\rho\, d\rho\, dz = \sum_{m,\, n} B^{mn} x_{mn}, \tag{28}$$

$$B^{mn} = \int_{z_n}^{\infty} zG(\rho_m, z_n, z)\, dz. \tag{29}$$

In order to obtain an idea of the closeness of the various approximations, we examine the limiting cases of small and large fields. In the case of large fields ($\gamma \gg 1$), as has already been pointed out above, all the approximations give one and the same precise[4] result:

$$\bar{v}_z = \sqrt{2a\lambda/\pi}. \tag{30}$$

Equation (30) differs from the formula derived by Sena[1] by a numerical factor. This is related to the fact that in Ref. 1 the difference in duration of the free paths of various lengths was not taken into account. If this circumstance is considered, then the method used by Sena also leads to Eq. (30).

For small fields ($\gamma \ll 1$), the coefficients c_{ks}^{mn}, A^{mn}, B^{mn} can be expanded in powers of γ and restricted to terms of first degree in γ. By such means, we obtain for the drift velocity :

In the approximation $M=1$, $N=2$, $\bar{v}_z = 0.452\, a\lambda/u_0$,
In the approximation $M=1$, $N=3$, $\bar{v}_z = 0.496\, a\lambda/u_0$,
In the approximation $M=1$, $N=4$, $\bar{v}_z = 0.481\, a\lambda/u_0$,

For comparison, we quote values of $\bar{v}_z$ obtained in Ref. 5 for the case of small fields by the method of Chapman and Enskog:

In the first approximation $\bar{v}_z = 0.470\, a\lambda/u_0$,
In the second approximation $\bar{v}_Z = 0.481\, a\lambda/u_0$.

The case of small fields is the most unfavorable for the application of the method of successive approximations based on quadrature formulas inasmuch as the smaller the field the larger must be the effect of the motion of the atoms on the drift velocity of the ions. Even in the case of small fields, however, the approximation $M=1$, $N=2$ already gives a fair result for the drift velocity of the ions.

3. THE APPROXIMATION $N=2$, $M=1$. COMPARISON WITH EXPERIMENT

Let us examine in more detail the approximation $N=2$, $M=1$. The velocity distribution of the atoms corresponding to this approximation is determined by the formulas:

$$\begin{gathered} W_1^{(2)}(z) = {}^1/_2\,[\delta(z - z_1) + \delta(z + z_1)]; \\ W_2^{(1)}(\rho^2) = \delta(\rho^2 - \rho_1^2), \\ z_1 = -z_2 = 1/\sqrt{2}; \quad \rho_1 = 1; \quad a_1 = a_2 = {}^1/_2; \\ b_1 = 1. \end{gathered} \tag{31}$$

The mean energy of the atoms and the portions of it which come from motion along and transverse to the field calculated by means of Eqs. (31) coincide with the exact values of these quantities.

In the approximation $M=1$, $N=2$, the integrals which enter in Eqs. (22), (27) and (29) were evaluated for different values of γ and the drift velocity of the ions was calculated. The dependence of $\bar{z}$ on γ in this approximation is depicted in Fig. 1 on a logarithmic scale. Points for which calculations were carried out are marked with x's. For comparison there are included in Fig. 1 the lines which give the dependence of $\bar{z}$ on γ in the limiting cases of small and large fields. The values of the drift velocity calculated from the graph presented in Fig. 1 are close to the values calculated by Eq. (7) of Ref. 4. The maximum difference occurs for the case of small fields and amounts to about 10%.

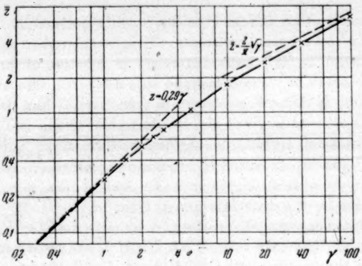

FIG. 1

The results of the calculations can be compared with data on the drift velocity of ions, obtained in the experiments of Hornbeck[10] for He^+ in He, Ne^+ in Ne and A^+ in A and in the experiments of Varney[11] for Kr^+ in Kr, and Xe^+ in Xe. Such a comparison is given in Figs. 2 and 3, where the points indicate the experimental data and the solid curves give the results of calculations according to Fig. 1. The values obtained in Ziegler's experiments[12] (energy of the ions of the order of 1 ev) were taken for the cross-sections of overcharge.

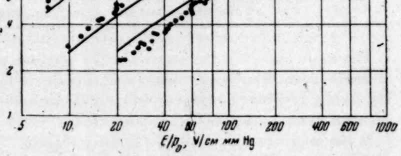

FIG. 2

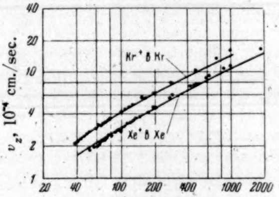

FIG. 3

From Figs. 2 and 3 it is seen that for all of the investigated gases, with the exception of He, there is good agreement of the results of the calculation with experimental data over the entire interval of values of E/p_0, attained in the experiments** (here $p_0 = p \cdot 273/T$ is the reduced pressure of the gas).

The reason for a certain discrepancy between the theoretical and experimental results for the case of He^+ and He (approximately 30%) is not clear. One should note that in this case the theoretical curve correctly conveys the course of the dependence of the drift velocity on E/p_0. In order to achieve complete agreement with experiment, it is sufficient to take 3×10^{-15} cm^2 as the value of the cross-section for overcharge instead of the 4.1×10^{-15} cm^2 value obtained by Ziegler.

On the whole, the comparison of theory with experiment shows that the model of "pure overcharge" with cross-section not depending on velocity is a good approximation for the description of the interaction of an ion with atoms of the same gas over a broad interval of values of E/p_0.

I am genuinely grateful to Dozent Iu. M. Kagan under whose guidance this work was completed, and to Professor L. E. Gurevich for a series of valuable comments.

**In comparing Figs. 2 and 3 of the present work with Figs. 1 and 2 of Ref. 4, one should keep in mind that the difference between them is related for the most part with the fact that in Ref. 4 values were taken for the cross-section of overcharge calculated according to Demkov's formulas[13], while in the present work the direct experimental data of Ziegler is used.

[1] L. A. Sena, J. Exptl. Theoret. Phys. (U.S.S.R.) **16**, 734 (1946).

[2] L. A. Sena, *Collisions of Electrons and Ions with the Atoms of a Gas* GITTL Moscow (1948)

[3] H. S. W. Massey and E. H. S. Burhop, "*Electronic and Ionic Impact Phenomena*". Oxford (1952)

[4] Iu. M. Kagan and V. I. Perel', Doklady Akad. Nauk. SSSR **98**, 575 (1954)

[5] Iu. M. Kagan and V.I. Perel', J. Exptl. Theoret. Phys. (U.S.S.R) **29**, 884 (1955)

[6] G. H. Wannier, Phys. Rev **96**, 831 (1954)

[7] V. A. Fock, J. Exptl. Theoret. Phys. (U.S.S.R) **18**, 1048 (1949)

[8] A. Reiz, Ark. f. Mathem. Astr. och. Fys., **29**, pt. IV (1943)

[9] S. Chandrasekhar, *Radiative Transfer* Oxford (1950)

[10] J. A. Hornbeck, Phys. Rev. **84**, 615 (1951)

[11] R. N. Varney, Phys. Rev. **88**, 362 (1952)

[12] B. Ziegler, Zs. f. Phys. **136**, 108 (1953)

[13] Iu. N. Demkov, Uch. Zap. Leningrad State Univ. 146 Physical Sciences Series **8**, 74 (1952)

Translated by R. L. Eisner
122

SOVIET PHYSICS JETP VOLUME 5, NUMBER 3 OCTOBER, 1957

Contribution to Field Theory Involving a Cut-off Factor

D. A. KIRZHNITS
P. N. Lebedev Physical Institute, Academy of Sciences, U.S.S.R.

(Submitted to JETP editor February 6, 1956)
J. Exptl. Theoret. Phys. (U.S.S.R.) **23**, 534-541 (March, 1957)

A study is made of the question of the uniqueness of quantum field theory involving a cut-off factor, and it is found that even finite (renormalized) expressions depend on the form of the cut-off factor. Examples are given in which the renormalized Green's function of a boson has no pole for finite momenta, but the critical momentum in the charge renormalization can be made arbitrarily large. In this connection difficulties with the vanishing of the charge and the existence of a pole in the Green's function are considered, and also the question of the domain of applicability of meson theory.

1. BECAUSE of the divergence difficulties inherent in quantum field theory, use is often made of cut-off factors, which have the effect of reducing the part played by high-frequency virtual quanta, so as to secure the convergence of the expressions occurring in the theory[1,2]. Upon completion of the intermediate calculations, the cut-off parameters (which play the part of effective limiting momenta) are let go to infinity, the cut-off factor (CF) approaches unity, and, at least formally, the original "not cut-off" theory is recovered. This procedure corresponds to regarding a point interaction as the limit of a smeared-out interaction.

In such an approach to the problems of quantum field theory there inevitably arises the question as to its uniqueness, i.e., as to the dependence of the results obtained on the form of the CF used. The most important aspect of this question is considered in the present paper: do the finite (renormalized) expressions depend on the CF?

This question has been given partial consideration in Refs. 2 and 3, where it was answered in the negative; but it will be shown that this conclusion was essentially based on the use of CF's that approached unity sufficiently rapidly with increase of the cut-off parameter. We consider below a wider class of CF's, for which the problem of lack of uniqueness takes on primary significance.

The study will be carried out in the framework of the asymptotic theory of Landau, Abrikosov, and Khalatnikov[2] (cf. also Ref. 4), with a single modification — replacement of the plateau-shaped cut-off factor by a CF of more general type (but still very close to the plateau-shaped). The basic relationships of the theory are the integral equations connecting the Green's functions G and D and the vertex part Γ, the integrands being certain combinations of G, Γ, D, and the CF. In the calculation of the asymptotic forms at large momenta it turns out that essential parts are played not only by the principal parts of G and Γ, but also by terms of the next order, which are given by increments of the corresponding integrands. For the CF's under consideration, contributions are made to these increments not only by the increments of the functions G and Γ, but also by that of the CF itself; this fact is indeed the cause of the lack of uniqueness, which turns out to be intrinsic only in the integrals that diverge quadratically, i.e., for the boson Green's function D. As for the equations for G and Γ, they give the same results as in Ref. 2.

In Secs. 3 and 4 the analysis is given for a number of cases that occur with various choices of the cut-off factors in electrodynamics and in meson theory with pseudoscalar coupling. Section 5 is devoted to a discussion of these cases from the point of view of the well-known difficulties associated with the vanishing of the charge and the existence of a pole of the D-function.

2. The introduction of the CF into the theory is accomplished by smearing out the interaction,

$$S \sim e_1 \int F\,(p,\ k,\ p-k,\ \Lambda)\,\bar{\psi}(p)\,\hat{A}\,(k)\,\psi\,(p-k)\,d^4p\,d^4k + \text{ charge conj.} \tag{1}$$

for electrodynamics, and similarly for mesodynamics. Here F is the CF, and Λ is the cut-off parameter. The CF must satisfy the conditions:

$$F \to 1 \quad \text{for} \quad \Lambda \to \infty \tag{1a}$$

$$\text{and } F\,(p,\ k,\ q) = F^{*}\,(q,\ k,\ p).$$

The second condition assures the preservation of Hermiticity under the smearing-out[5].

It is not difficult to convince oneself that when the smearing-out is introduced there must be associated with each vertex of the Feynman diagram (or with each vertex-part operator) a factor F depending on the corresponding momenta.

Concretely, the CF is taken in the factored form (but cf. footnote *):

$$F\,(p^2, k^2, (p-k)^2) = f\,(k^2)\,F\,(p^2)\,F\,((p-k)^2), \tag{2}$$

where all the functions are real. The cut-off parameters involved are in general taken to be unequal for the boson CF, $f(k^2, \Lambda_k^2)$, and the fermion CF, $F(p^2, \Lambda_p^2)$, where, following Pomeranchuk, one takes $\Lambda_p^2/\Lambda_k^2 = V > 1$. The fermion factor is chosen plateau-shaped: $F(p^2) = 0$ for $p^2 > \Lambda_p^2$ and $F(k^2) = 1$ for $p^2 < \Lambda_p^2$, and the boson function is nearly plateau-shaped: $f(k\ )\ f(k^2) = g(k^2)\,f_0(k^2)$, where $f_0(k^2) = 0$ for $k^2 > \Lambda_k^2$, $f_0(k^2) = 1$ for $k^2 < \Lambda_k^2$, and $g(k^2)$ is a function nearly equal to unity, with $g = 1$ for $\Lambda_k \to \infty$ or $k \to 0$.

3. Considering the asymptotic case in electrodynamics for $p \to \infty$ and introducing the notations used in Ref. 2, we have

$$G\,(p) = \frac{\beta\,(p)}{\hat{p}}\,,\quad \Gamma_\mu = \gamma_\mu\,\alpha, \tag{3}$$

$$D_{\mu\nu}\,(k) = \frac{1}{k^2}\left[d\,(k^2)\left(\delta_{\mu\nu} - \frac{k_\mu k_\nu}{k^2}\right) + d_l\,(k^2)\,\frac{k_\mu k_\nu}{k^2}\right].$$

Here (with the choice $d_l = 0$) we shall have $\alpha = \beta = 1$.*

The remaining equation for D (here D^0 is the unperturbed Green's function)

$$D_{\mu\nu} = D^0_{\mu\nu} - D_{\mu\sigma}\,P_{\sigma\tau}\,D^0_{\tau\nu} \tag{4}$$

already turns out to depend essentially on the CF. The polarization operator involved,

$$P_{\mu\nu}\,(k) = f^2\,(k)\,\frac{e_1^2}{\pi i}\,\mathrm{Sp}\int G\,(p)\,\Gamma_\mu \times (p,\ p-k,\ k)\,G\,(p-k)\,\gamma_\nu\,F^2\,(p)\ F^2\,(p-k)\,d^4p \tag{5}$$

diverges quadratically, which corresponds to the appearance of a photon mass. Since this last cannot be removed by any choice of a CF of the type (1)[6], it is necessary to destroy it in a formal way — either by introducing a supplementary CF of the Pauli-Villars type[1] or simply by subtracting from the expression (5) the quantity $P_{\mu\nu}(0)$, as is done in Ref. 2. Both ways give the same result, but we shall concern ourselves with the second, as the simpler. This gives $P_{\mu\nu} = 0$ for $k^2 > \Lambda_k^2$ and for $k^2 < \Lambda_k^2$

$$\begin{aligned}\tilde{P}_{\mu\nu}\,(k) &= P_{\mu\nu}\,(k) - P_{\mu\nu}\,(0) \\ &= \varphi\,(k)\,\frac{e_1^2}{\pi i}\,\mathrm{Sp}\int G\,(p)\,\Gamma_\mu\,(p,\ p,\ 0)\,G\,(p)\,\gamma_\nu\,F^4\,(p)\,d^4p \\ &+ g^2\,(k)\,\frac{e_1^2}{\pi i}\,\mathrm{Sp}\int G\,(p)\cdot\Delta\,[\Gamma_\mu\,(p,\ p-k,\ k)\,G \\ &\times (p-k)\,F^2\,(p-k)]\,F^2\,(p)\,d^4p,\quad \varphi\,(k) \\ &= g^2\,(k) - g^2\,(0) = g^2\,(k) - 1.\end{aligned} \tag{6}$$

---

* It can be shown without difficulty that in the case $d_l \neq 0$, with plateau-shaped fermion CF and arbitrary boson CF, as in Ref. 2, α and β have the form of phase factors, with $\alpha\beta = 1$.

The first term corresponds to the contribution of the increment of the CF to $\tilde{P}_{\mu\nu}$, the second to those of the increments of Γ and G (of order k^2). Equation (6) agrees with the corresponding Eq. (5) of Ref. 3, except for the first term of the right-hand member of Eq. (6), which was not taken into account in Ref. 3.

The expression (6) must be transverse,* *i.e.*,

$$\tilde{P}_{\mu\nu}(k) = P(k)(\delta_{\mu\nu} - k_\mu k_\nu / k^2);$$

then from Eq. (4) it will follow that

$$d^{-1}(k) = 1 + P(k)/k^2, \tag{7}$$

$$P(k) = (e_1^2/2\pi)\varphi(k)\Lambda_p^2 + (e_1^2/3\pi)k^2 \ln(\Lambda_p^2/k^2).$$

Here the factor $g^2(k)$ before the second integral in Eq. (6) can be dropped, with accuracy up to terms that vanish for $\Lambda \to \infty$.

For d we now obtain

$$d^{-1}(k) = 1 + \varphi(k)\frac{e_1^2}{2\pi}\frac{\Lambda_p^2}{k^2} + \frac{e_1^2}{3\pi}\ln\frac{\Lambda_p^2}{k^2}. \tag{8}$$

The cause of the lack of uniqueness of the result lies in the second term of Eq. (8); by choosing different expressions for φ, one can obtain different forms for d. On the other hand, it is more convenient in practice to prescribe d and find the corresponding CF.

A) Let us require, for example, that d agree with the usual expression in the regions

$$k^2 < Nm^2, \quad N < \exp(3\pi/e^2)$$

and $\quad \varepsilon\Lambda_k^2 < k^2 < \Lambda_k^2,$

where ϵ is a small quantity (it can go to zero for $\Lambda_k \to \infty$, but more weakly than Λ_k^{-2}). In the regions indicated one has the usual expressions[2,4]

$$d^{-1}(k) = 1 + \frac{e_1^2}{3\pi}\ln\frac{\Lambda_p^2}{k^2}, \quad \frac{e_1^2}{e^2} = 1 + \frac{e_1^2}{3\pi}\ln\frac{\Lambda_p^2}{m^2},$$

$$d_c^{-1}(k) = 1 - \frac{e^2}{3\pi}\ln\frac{k^2}{m^2}. \tag{9}$$

Here $d_c = (e_1/e)^2 d$ is the renormalized d-function. In this connection, the charge renormalization remains as before with all its inherent difficulties.[7,4]

In the intermediate region

$$Nm^2 < k^2 < \varepsilon\Lambda_k^2$$

we take d constant and equal to its value at the left-hand end:

$$d^{-1}(k) = 1 + \frac{e_1^2}{3\pi}\ln\frac{\Lambda_p^2}{Nm^2}, \tag{10}$$

$$d_c^{-1}(k) = 1 - \frac{e^2}{3\pi}\ln N.$$

The corresponding CF's are found from Eq. (8)

$$\varphi(k) = \frac{2\pi}{e_1^2}\frac{k^2}{\Lambda_p^2}\left[d^{-1}(k) - 1 - \frac{e_1^2}{3\pi}\ln\frac{\Lambda_p^2}{k^2}\right], \tag{11}$$

from which we have

---

* Strictly speaking, the first integral in Eq. (6) is a longitudinal quantity; this leads to a dependence of the function d_l on the field. But this can easily be avoided by taking a somewhat more complicated CF:

$$F(p, k, p-k) = f(p, k)F(p)F(p-k),$$

$$f^2(p, k) = 1 + 3\frac{(pk)^2}{p^2k^2}\varphi(k).$$

Then the first term of Eq. (6) becomes equal to

$$(e_1^2/2\pi)\varphi(k)\Lambda_p^2[\delta_{\mu\nu} - k_\mu k_\nu/k^2].$$

instead of the value $(e_1^2/2\pi)\Lambda_p^2\varphi(k)\delta_{\mu\nu}$ for the case of the factored CF. Therefore no attention can be given to the nontransversality of Eq. (6), if we take $\varphi(k)$ to mean not $g^2(k) - 1$, but

$$\frac{p^2k^2}{3(pk)^2}[f^2(p, k) - 1].$$

The remark about the nontransversality of Eq. (6) is due to A. A. Abrikosov.

$$\varphi(k) = \begin{cases} 0, & k^2 < Nm^2, \quad \varepsilon\Lambda_k^2 < k^2 < \Lambda_k^2 \\ (2k^2/3\Lambda_p^2)\ln(k^2/Nm^2), & Nm^2 < k^2 < \varepsilon\Lambda_k^2 . \end{cases}$$

This example gives d_c that has no pole at any finite value of k.

B) Another example relates to the change of the limiting momentum, under which, in the theory of Ref. 2, there appears the difficulty of the vanishing of the charge. We consider a d of the form

$$d^{-1}(k) = \tag{12}$$

$$\begin{cases} 1 + q\,(e_1^2/3\pi)\ln(\Lambda_p^2/k^2), & k^2 < \varepsilon\Lambda_k^2, \\ 1 + (e_1^2/3\pi)\ln(\Lambda_p^2/k^2), & \varepsilon\Lambda_k^2 < k^2 < \Lambda_k^2 . \end{cases}$$

Here

$$\frac{e_1^2}{e^2} = 1 + q\,\frac{e_1^2}{3\pi}\ln\frac{\Lambda_p^2}{m^2} = \left[1 - q\,\frac{e^2}{3\pi}\ln\frac{\Lambda_p^2}{m^2}\right]^{-1};$$

$$d_c^{-1}(k) = \begin{cases} 1 - q\,(e^2/3\pi)\ln(k^2/m^2), & k^2 < \varepsilon\Lambda_k^2, \\ 1 - (e^2/3\pi)\ln(k^2/m^2) + (e^2/3\pi)(1-q)\ln(\Lambda_p^2/m^2), & \varepsilon\Lambda_k^2 < k^2 < \Lambda_k^2 . \end{cases}$$

We find the corresponding CF from Eq. (11)

$$\varphi(k) = \tag{13}$$

$$\begin{cases} 0, & \varepsilon\Lambda_k^2 < k^2 < \Lambda_k^2 \\ -{}^2/_3\,(1-q)\,(k^2/\Lambda_p^2)\ln(\Lambda_p^2/k^2), & k^2 < \varepsilon\Lambda_k^2 . \end{cases}$$

From this it can be seen that for sufficiently small q the critical value of the momentum can be shifted as far out as one wishes.

In both examples the CF satisfy the general requirements of Sec. 2; the discontinuities appearing in them can easily be removed by taking a smoothed form of the function d.

We shall now show that in logarithmically divergent integrals there is no need to take into account the fact that the CF is not plateau-shaped. Indeed, for $\Lambda_k \to \infty$

$$\max\left(\varphi(k)\ln\frac{\Lambda_p^2}{m^2}\right) \sim \varepsilon\,\frac{\Lambda_k^2}{\Lambda_p^2}\ln\frac{\Lambda_p^2}{m^2} \to 0,$$

in virtue of

$$\varepsilon\ln(\Lambda_p^2/m^2) \to 0.$$

We can now determine for what sorts of functions $\varphi(k)$ the results of Refs. 2 and 3 remain valid. From Eq. (8) it can be seen that this is so if for finite k the quantity

$$\varphi(k)\,(\Lambda_p^2/k^2) = \varphi(k^2/\Lambda_k^2,\ k^2)\,(\Lambda_k^2/k^2)\,V$$

goes to zero as Λ_k increases. If we introduce $x = \Lambda_k^{-2}$, then for fixed k this condition will mean that $\varphi(x)/x = d\varphi/dx$ must vanish for $x \to 0$. Thus the CF will make a contribution to d if $df^2/d(\Lambda_k^{-2})$ either approaches a finite limit (as in the first example) or increases (as in the second example). The remaining details of the structure of the CF, besides the angle of inclination of the tangent at $k^2/\Lambda_k^2 = 0$, such as the curvature, *etc.*, have no residual effect on d because of the quadratic divergence of $P_{\mu\nu}$, since their contribution vanishes for $\Lambda \to \infty$.

As for the calculation of the complicated vertex-part diagrams not considered in Ref. 2, in the first example, d is equal to or smaller than the corresponding d in Ref. 3; therefore the estimates carried out in Ref. 3 can be used. The same applies to the second example.

4. Going over to mesodynamics with weak pseudoscalar coupling and using the notations of Ref. 8,

$$G(p) = \beta/\hat{p}, \quad \Gamma_\mu = \tau_\mu\gamma_5\alpha,$$

$$D_{\mu\nu}(k) = k^{-2}d(k^2)\,\delta_{\mu\nu},$$

we obtain for G and Γ the well known results:[8,4]

$$\alpha = \beta^{-2/3}, \tag{14}$$

$$d\beta/d\xi = (3g_1^2/8\pi)\,|\beta(\xi)|^{-5/3}\,d(\xi), \quad \xi = \ln(k^2/m^2).$$

The equation for d, after renormalization of the meson mass, gives:

$$d^{-1}(\xi) = 1 + \Phi(\xi) + \frac{g_1^2}{\pi}\int_{\xi}^{L_p} \beta^{4/5}(z)\,dz;$$

$$\Phi(\xi) = 2I\,\frac{g_1^2}{\pi}\,\frac{\Lambda_p^2}{k^2}\,[g^2(k) - 1],$$

$$I = \int_0^1 \beta^{4/5}(z)\,dz, \quad L = \ln\frac{\Lambda^2}{m^2}. \tag{15}$$

The CF is connected with the relationship, following from Eqs. (14) and (15),

$$\Phi(\xi) = d^{-1}(\xi) - \left[1 + \frac{g_1^2}{\pi}(L_p - L_k)\right] - \frac{g_1^2}{\pi}\int_{\xi}^{L_k} dz \Big/ \left[1 - \frac{g_1^2}{4\pi}\int_z^{L_k} d(w)\,dw\right]. \tag{16}$$

A) Let us consider a problem like the first example in electrodynamics — the destruction of a pole in the ordinary charge renormalization. We take the function *d* of the form given by $[N < \exp(4\pi/5g^2)]$:

$$d^{-1}(\xi) = \begin{cases} \left[1 + \dfrac{g_1^2}{\pi}(L_p - L_k)\right] Q^{4/5}(L_k - \xi), \\ \qquad \xi < \ln N, \quad L_k - \ln\dfrac{1}{\varepsilon} < \xi < L_k, \\ \left[1 + \dfrac{g_1^2}{\pi}(L_p - L_k)\right] Q^{4/5}(L_k - \ln N), \\ \qquad \ln N < \xi < L_k - \ln\dfrac{1}{\varepsilon}. \end{cases} \tag{17}$$

Here we have introduced the notation

$$Q(x) = \left(1 + \frac{5g_1^2}{4\pi}x\right) \Big/ \left[1 + \frac{g_1^2}{\pi}(L_p - L_k)\right].$$

The corresponding CF is given by Eq. (16)

$$g^2(k) - 1 = \begin{cases} 0, & L_k - \ln(1/\varepsilon) < \xi < L_k, \\ (k^2/\Lambda_p^2)\,A(\xi), & \ln N < \xi < L_k - \ln(1/\varepsilon), \\ (k^2/\Lambda_p^2)\,B(\xi), & \xi < \ln N, \end{cases} \tag{18}$$

where *A* and *B* are slowly varying functions of ξ, whose forms we shall not present because of their cumbersomeness.

B) We go on to the second example — the displacement of the critical momentum in the charge renormalization. We take the function

$$d^{-1}(\xi) = \begin{cases} \left[1 + \dfrac{g_1^2}{\pi}(L_p - L_k)\right] Q^{4/5}(L_k - \xi), \\ \qquad L_k - \ln\dfrac{1}{\varepsilon} < \xi < L_k, \\ d^{-1}(0)\left[1 - \dfrac{5}{4\pi}g^2\xi\right]^{4/5}, \quad \xi < L_k - \ln\dfrac{1}{\varepsilon}. \end{cases} \tag{19}$$

Here we have used the renormalized charge

$$g^2 = d(0)\,\alpha^2(0)\,\beta^2(0)\,g_1^2. \tag{20}$$

We prescribe also the charge renormalization

$$g^2 = g_1^2\left[1 + \frac{g_1^2}{4\pi}\,q\,(4L_p + L_k)\right]^{-1} \tag{21}$$

and determine by means of Eqs. (20) and (21) the quantity $d(0)$, after which we find from Eq. (16) the corresponding CF:

$$g^2(k) - 1 = \begin{cases} 0, \quad L_k - \ln\dfrac{1}{\varepsilon} < \xi < L_k, \\ -\dfrac{k^2}{2I\Lambda_p^2}\left(L_p + \dfrac{L_k}{4}\right) \\ \times (1 - q)\,Q^{-4/5}\left(\ln\dfrac{1}{\varepsilon}\right), \\ \qquad \xi < L_k - \ln\dfrac{1}{\varepsilon}. \end{cases} \tag{22}$$

In this case, just as in electrodynamics, one can find a CF that simultaneously fulfills the requirements for the CF of both of the problems considered, *i.e.*, displaces the pole in the charge renormalization and removes the pole in the *d*-function.

5. In passing on to the discussion of the examples analyzed above, it is first of all necessary to emphasize the fact of the nonuniqueness of the theory based on the limiting process. Generally speaking, the lack of uniqueness of diverging expressions with respect to the form of the limiting process has been repeatedly noted in the literature.[1,9] Examples are given above in which also the finite (renormalized) expressions depend on the type of CF used. This circumstance forces us to proceed with caution to the conclusions of a theory that makes use of a limiting process.

In all of the examples considered above, there appeared a difficulty with the vanishing of the renormalized charge [Eqs. (9), (12), (21)],[4,7] which provides evidence of the fact that the present form of quantum field theory is not a closed theory.* It is, however, also possible to take the view that the vanishing of the charge is in itself not an essential difficulty that paralyzes the development of the theory in its present form. The quantum field theory includes in itself the renormalized theory and the relation between the priming and renormalized constants. In view of the fact that only the renormalized theory is compared with experiment, it would be possible to pay no attention to the relation between the constants, leaving the difficulties connected with this to a future theory. In other words, the expressions that play the role of the renormalized quantities would in this procedure have assigned to them the values that follow from experiment, despite the fact that in the present theory they actually vanish. Such an approach does not lead to its goal when a plateau-shaped CF is used, because of the appearance of difficulties in the renormalized theory itself — besides the vanishing of the charge, a pole at a finite momentum appears in the renormalized *d*-function.

The situation is essentially altered, as is shown by the examples given above, when one uses CF's that are not plateau-shaped. On one hand, the appearance of a pole and the vanishing of the charge cease to be facts that are coupled to each other. Concrete examples have been presented of CF's for which the *d*-function does not have a pole at any finite momentum. On the other hand, the value of the critical momentum at which the renormalized charge becomes small is also essentially not uniquely determined by the theory of Landau, Abrikosov, and Khalatnikov.[2] Therefore, for example, the conclusions about the supposed inapplicability of mesodynamics already at energies $\sim Mc^2$, which are often drawn on the basis of the theory of Ref. 2 and which rest on the fact that with a plateau-shaped CF the critical momentum $\sim Mc$, cannot be regarded as entirely convincing.**

We note that in the examples considered above the well known theorem of Lehmann and Källen about the increase of the renormalized *d*-function with the momentum[10] is satisfied. In a certain sense this provides evidence of the existence in the renormalized theory of a complete orthogonal system of eigenfunctions of the energy and momentum.* One can without difficulty assume a CF such that the *d*-function has no pole and at the same time the renormalized charge is finite. For this it suffices to consider example (B), where one must take q negative (and large absolute value). Then the priming charge e_1 and the renormalized charge e will satisfy

$$\frac{e_1^2}{e^2} = 1 - \frac{e_1^2}{3\pi}\,|\,q\,|\ln\frac{\Lambda_p^2}{m^2} = \left[1 + \frac{e^2}{3\pi}\,|\,q\,|\ln\frac{\Lambda_p^2}{m^2}\right]^{-1},$$

i.e., e_1 vanishes for $\Lambda \to \infty$, and e remains finite.

The renormalized function d_c takes the form

$$d_c^{-1} = \begin{cases} 1 + |\,q\,|\,\frac{e^2}{3\pi}\ln\frac{k^2}{m^2}, & k^2 < \varepsilon\Lambda_k^2 \\ 1 + |\,q\,|\,\frac{e^2}{3\pi}\ln\frac{\Lambda_p^2}{k^2} + \frac{e^2}{3\pi}\ln\frac{\Lambda_p^2}{k^2}, & \\ \qquad \varepsilon\Lambda_p^2 < k^2 < \Lambda_k^2. & \end{cases}$$

Moreover, one can choose the CF so that in the region of small momenta d_c agrees with the perturbation theory (*cf.* example A). At the same time the correction diagrams of the vertex part are small for this case. But in this example the Lehmann-Källen theorem[10] does not hold. The question of the superiority of a plateau-shaped CF in comparison with that just considered nevertheless remains unclear, since the existence of a complete orthogonal system is only a sufficient condition for the Lehmann-Källen theorem. Therefore, even if one uses a CF that does not contradict this theorem there is no assurance of the existence of a complete orthogonal system (except for $e = 0$).

The question arises of the possibility of finding a CF such that e would be finite and at the same time the Lehmann-Källen theorem[10] would hold. Within the framework of the approximate theory[2] such a CF can easily be found. For this it suffices to let q approach zero in the example (B) just discussed, in such a way that the critical momentum will increase with Λ: $q > 0$, $q(e_1^2/3\pi)\ln(\Lambda^2/m^2) < 1$ for all Λ above a certain value. Here e_1 can be either finite or infinite. Together with this one can choose a function d_c with no pole.

---

*In this connection it is of course assumed that the approximate treatment of this question actually reflects, even if only qualitatively, the true situation.

**In electrodynamics, because of the smallness of the coupling constant, the critical momentum is very large, and there this question appears less sharply.

*Attention was called to the importance of this fact by I. Ia. Pomeranchuk.

But in the evaluation of the overlapping diagrams of a vertex part it is found that in this case the "three-gamma" approximation[2] is inadequate. This fact is of a general character. Indeed, if we begin with a theory with $e \neq 0$ and d_c increasing with the momentum, then for the diagrams in question we shall have the expression [with $\alpha = \beta = 1$ as in Eq. (3)]:

$$e_1^4 \int_{p^2}^{\Lambda^2} \frac{dk^2}{k^2} [d(k)]^2 = e^4 \int_{p^2}^{\Lambda^2} \frac{dk^2}{k^2} [d_c(k)]^2 > e^4 \ln \frac{\Lambda^2}{p^2}$$

$[d_c(0) = 1]$, which is large in comparison with the zeroth approximation. The estimates of Pomeranchuk,[3] which indicated that the part played by these chains is small, rested essentially on having $e^2 \to 0$ for $\Lambda \to \infty$. Thus the applicability of the "three-gamma" approximation is fundamentally connected with the condition $e^2 \to 0$.

Therefore the question of the possibility of choosing a CF such that the charge does not go to zero remains essentially open, because of the lack of a simple scheme of calculation in which this question could be studied.

I express my deep gratitude to Academician I. E. Tamm for his interest in this work and for valuable advice, and to Academician N. N. Bogoliubov and Prof. M. A. Markov for discussions of a number of questions that arose in the work. I also thank Prof. F. J. Dyson for undertaking the task of reporting the results of this work at the Rochester Conference in 1956.[11]

---

[1] R. Feynman, Phys. Rev. **76**, 769 (1949); collection "Newest Developments of Quantum Electrodynamics," Foreign Lit. Press, 1954. W. Pauli and F. Villars, Rev. Mod. Phys. **21**, 434 (1949); collection "Level Shifts of Atomic Electrons," Foreign Lit. Press, 1950.

[2] Landau, Abrikosov, and Khalatnikov, Dokl. Akad. Nauk SSSR **95**, 497, 773, 1177 (1954).

[3] I. Ia. Pomeranchuk, Dokl. Akad. Nauk SSSR **103**, 1005 (1955).

[4] E. S. Fradkin, J. Exptl. Theoret. Phys. (U.S.S.R.) **28**, 750; **29**, 377 (1955); Soviet Phys. JETP **1**, 604 (1955); **2**, 340 (1956).

[5] P. Kristensen and C. Møller, Kgl. Dansk. Math.-Phys. Medd. **27**, No. 7 (1952).

[6] D. A. Kirzhnits, J. Exptl. Theoret. Phys. (U.S.S.R.) **30**, 796 (1956); Soviet Phys. JETP **3**, 768 (1956).

[7] L. D. Landau and I. Ia. Pomeranchuk, Dokl. Akad. Nauk SSSR **102**, 489 (1955).

[8] Abrikosov, Galanin, and Khalatnikov, Dokl. Akad. Nauk SSSR **97**, 793 (1954).

[9] G. Wentzel, *Introduction to the Quantum Theory of Wave Fields.* A. A. Abrikosov and I. M. Khalatnikov, J. Exptl. Theoret. Phys. (U.S.S.R.) **21**, 429 (1951); D. A. Kirzhnits, J. Exptl. Theoret. Phys. (U.S.S.R.) **21**, 949 (1951).

[10] H. Lehmann, Nuovo Cim. **11**, 342 (1954). M. Gell-Mann and F. Low, Phys. Rev. **95**, 1300 (1954).

[11] Proc. Sixth Rochester Conference, III-8, 1956.

Translated by W. H. Furry
123

SOVIET PHYSICS JETP VOLUME 5, NUMBER 3 OCTOBER, 1957

Production of Proton-Antiproton Pairs by High Energy γ-Quanta

IU. A. VDOVIN

Moscow Engineering - Physics Institute

(submitted to JETP editor, December 19, 1955)

J. Exptl. Theoret. Phys. (U.S.S.R.) **32**, 542-546 (March, 1957)

The production of proton – antiproton pairs by high energy γ-quanta on nuclei is investigated by a semi-phenomenological method. A knowledge of the asymptotic expression of the function of each nucleon is sufficient for the computation of the effective cross section. On the assumption that the nucleus is "black" with respect to the nucleons, the asymptotic expression has been found as a superposition of a plane and diffracted waves. The calculations are extended to the case of an arbitrary interaction law between the nucleons and nucleus. The differential cross section is then expressed in terms of the amplitude of elastic scattering of nucleons on the nucleus.

IN view of the latest reports on the discovery of the antiproton[1], it is of interest to compute the effective cross section for formation of proton-antiproton pairs, without recourse to the weak coupling approximation. In the present paper, a semiphenomenological theory is developed which describes the formation of proton-antiproton pairs by high energy γ-quanta on nuclei; the theory is analogous to the one developed by Pomeranchuk[2] for π-mesons pair production.

We will assume that the nucleus is, with respect to the nucleon, an "absolutely black" sphere of radius R (below, we will generalize the results to an arbitrary interaction law between nucleons and nucleus). The wave function can then be determined outside the nucleus as a superposition of plane and diffracted waves. The probability of pair formation is, at small angles between the momenta of the nucleons and of the γ-quanta, totally determined by this wave function; this is so because the main role is played by distances which are large as compared to the nuclear radius. Let us note that in this ultrarelativistic region only small angles are practically important, because the cross section falls rapidly with increasing angles.

We will assume that the nucleons are described by the Dirac equation. The anomalous magnetic moment is irrelevant at such large energies of the γ-quanta.

The matrix element for pair production will be written in the form:

$$M = ie\sqrt{\frac{2\pi}{\omega}}\int\bar{\psi}_1(\gamma\mathbf{j})\psi_2 e^{i\mathbf{k}_\gamma\mathbf{r}}\,d\mathbf{r}; \qquad (1)$$

$$\gamma_k = -i\beta\alpha_k \ (k = 1, 2, 3), \ \gamma_4 = \beta, \ \bar{\psi} = \psi^*\beta.$$

Here γ_i are the Dirac matrices, $\mathbf{k}_\gamma$ is the wave vector of the γ-quantum of frequency ω and of polarization j (we put $\hbar = c = 1$ everywhere), ψ_1, ψ_2 are the proton-antiproton wave functions, respectively. Each one of them can be taken to be a superposition of plane and incoming spinor waves[3]. The expression for such a ψ-function can be obtained from the expression for a plane and outgoing spinor waves written down by Akhiezer[4]. Indeed, if we write the asymptotic expression for the solution of the Dirac equation in the form of a superposition of plane and outgoing waves:

$$\psi = ue^{i\mathbf{pr}} + f(p\theta)\frac{e^{ipr}}{r}, \quad u = \begin{pmatrix} v \\ \sigma_r v/(E+m)\end{pmatrix}, \qquad (2)$$

θ is the angle between the vectors p and r; θ is a two-dimensional angular vector. The solution of the same Dirac equation with the asymptotic expression in the form of a plane and incoming waves, is easily obtained in the form:

$$\psi' = ue^{i\mathbf{pr}} + f'(p\theta)\frac{e^{-ipr}}{r},$$

$$f'(p\theta) = i\Sigma_y f^*(-p\theta), \qquad i\Sigma_y = \begin{pmatrix} i\sigma_y & 0 \\ 0 & i\sigma_y\end{pmatrix}, \qquad (3)$$

where σ_y is the Pauli matrix. The spinor v has to be substituted by the spinor $-i\sigma_y v$.

Using expression (3) and the value of the amplitude f, we obtain:

$$\psi_1 = u_1e^{i\mathbf{p}_1\mathbf{r}} - \frac{1}{4\pi p_1}\int\left(\gamma\frac{\partial}{\partial\mathbf{r}} - \gamma_4E_1 - m\right)(\mathbf{p}_1\gamma)u_1 \times \frac{\exp\{-ip_1|\mathbf{r}-\mathbf{s}_1|\}}{|\mathbf{r}-\mathbf{s}_1|}d\mathbf{s}_1 = u_1e^{i\mathbf{p}_1\mathbf{r}} - \Phi_1,$$

$$\psi_2 = u_2 e^{-i\mathbf{p}_2\mathbf{r}} - \frac{1}{4\pi p_2}\int\left(\gamma\frac{\partial}{\partial\mathbf{r}} + \gamma_4 E_2 - m\right)(\mathbf{p}_2\gamma)\, u_2 \times \frac{\exp\{ip_2|\mathbf{r}-\mathbf{s}_2|\}}{|\mathbf{r}-\mathbf{s}_2|}\, d\mathbf{s}_2 = u_2 e^{-i\mathbf{p}_2\mathbf{r}} - \Phi_2, \quad (4)$$

where $\mathbf{p}_1$, E_1 and $\mathbf{p}_2$, E_2 are the proton and antiproton momenta and energies, respectively. The integration over $\mathbf{s}_1(\mathbf{s}_2)$ is along a circle of radius R, perpendicular to $\mathbf{p}_1(\mathbf{p}_2)$ and passing through the center of the nucleus.

Let us transform the expressions for the functions Φ_1 and Φ_2 writing them in the form of a Fourier integral

$$\Phi_1 = \frac{1}{8\pi^3 p_1}\int\left(\gamma\frac{\partial}{\partial\mathbf{r}} - \gamma_4 E_1 - m\right) \quad (5)$$

$$\times(\mathbf{p}_1\gamma)\, u_1 \frac{\exp\{-i\mathbf{q},\mathbf{r}-\mathbf{s}_1\}}{q^2 - p_1^2 + i\varepsilon}\, d\mathbf{q}\, d\mathbf{s}_1; \quad \varepsilon \to 0.$$

The fuction Φ_2 will be written in an analogous form.

Let us introduce the angular vectors $\mathbf{k}_1$, $\mathbf{k}_2$.

$$\mathbf{p}_1 = p_1\frac{\mathbf{k}_\gamma}{k_\gamma}\left(1 - \frac{k_1^2}{2p_1}\right) + \mathbf{k}_1, \quad (6)$$

$$\mathbf{p}_2 = p_2\frac{\mathbf{k}_\gamma}{k_\gamma}\left(1 - \frac{k_2^2}{2p_2}\right) + \mathbf{k}_2, \quad \mathbf{k}_\gamma\mathbf{k}_1 = \mathbf{k}_\gamma\mathbf{k}_2 = 0,$$

$$\mathbf{k}_1 + \mathbf{k}_2 = \mathbf{k}, \quad (\mathbf{k}_1 - \mathbf{k}_2)/2 = \mathbf{b}.$$

Using the condition E_1, $E_2 \gg m$, where m is the nucleon rest mass, we get

$$M = e(32\pi^3/\omega^3)^{1/2} E_1 E_2 k^{-1} R J_1(kR)\, \bar{u}_1 T u_2,$$

$$T = \frac{1}{m^2 + k_1^2}\left(\gamma\mathbf{j} - \frac{\gamma_3(\gamma\mathbf{i})(\gamma\mathbf{k})}{2p_2}\right) + \frac{1}{m^2 + k_2^2}\left(\gamma\mathbf{j} - \frac{\gamma_3(\gamma\mathbf{k})(\gamma\mathbf{i})}{2p_1}\right) + \frac{1}{m^2 + b^2}\left(-\gamma\mathbf{j} + \frac{1}{4p_1}\gamma_3(\gamma\mathbf{k})(\gamma\mathbf{j}) + \frac{1}{4p_2}\gamma_3(\gamma\mathbf{j})(\gamma\mathbf{k})\right), \quad (\gamma\mathbf{k}_\gamma) = \gamma_3\omega. \quad (7)$$

The main contribution to the integrals (1) comes from distances to the nucleus $p_1 p_2/m^2\omega \gg R$, if $k_1 \sim k_2 \leqslant m$ (see also Ref. 2). The use of the asymptotic expressions for the γ-function is therefore legitimate.

Let us make a summation of $|M|^2$ over the nucleon spins in the final state. Let us also note that, in the integration over k and b, the main role is played by the values $k \sim 1/R$ and $b \sim m$; wherever possible, we shall drop terms $\sim k$ with respect to terms $\sim b$.

The effective cross section of the process is

$$d\sigma_\mathbf{j} = 2\pi\sum|M|^2(2\pi)^{-6}\, dp_{1z}\, d\mathbf{k}_1\, d\mathbf{k}_2\, |F_{+-}|^2. \quad (8)$$

The expression for the cross section contains an auxiliary factor F_{+-}, which is a form factor determined by the indefiniteness of the nucleons and which depends on the invariant frequency of the γ-quantum in the rest system of each of the nucleons. The form factor contains as well the interaction between nucleons [2,4]:

$$F_{+-} = F_{+-}\left(\frac{m^2 + b^2}{\mu m}\frac{\omega}{2E_1};\ \frac{m^2 + b^2}{\mu m}\frac{\omega}{2E_2}\right), \quad (9)$$

where μ is the rest mass of the π-meson (the dimensions of the nucleon are assumed to be $\sim 1/\mu$). We obtain the following expression for the differential cross section of the process:

$$d\sigma_\mathbf{j} = \quad (10)$$

$$\frac{e^2R^2}{\pi^2}\frac{d\mathbf{k}\, J_1^2(kR)}{k^2}\frac{d\mathbf{b}\, dE_1}{2(m^2 + b^2)^2\omega^3}[m^2\omega^2 + b^2(E_1^2 + E_2^2) + 2E_1E_2(\mathbf{j}\times\mathbf{b})^2 - 2E_1E_2(\mathbf{j}\mathbf{b})^2]\,|F_{+-}|^2,$$

$$E_1 + E_2 = \omega, \quad d\mathbf{k} = k\, dk\, d\varphi_k, \quad d\mathbf{b} = b\, db\, d\varphi_b.$$

Averaging (10) over the γ-quantum polarizations, we obtain

$$d\sigma = \frac{e^2R^2}{2\pi^2}\frac{d\mathbf{k}\, J_1^2(kR)}{k^2}\frac{d\mathbf{b}\, dE_1}{(m^2 + b^2)^2\omega^3}[m^2\omega^2 + b^2E_1^2 + b^2(\omega - E_1)^2]\,|F_{+-}|^2. \quad (11)$$

Integrating over $\mathbf{k}$ and over the directions of the vector $\mathbf{b}$, we get

$$d\sigma = e^2R^2\frac{b\,db\,dE_1}{(m^2 + b^2)^2\omega^3}[m^2\omega^2 + b^2E_1^2 + b^2(\omega - E_1)^2]\,|F_{+-}|^2. \quad (12)$$

Let us note that the differential cross section reaches large nuclear values for small angles between the momenta of the formed particles and the γ-quantum momenta $b \lesssim m$. The integration over E_1 and b can be performed only by letting $F_{+-} = 1$.

$$d\sigma(E_1) = \frac{e^2R^2}{2}\left\{\frac{b_{\max}^2}{m^2 + b_{\max}^2}\frac{1}{\omega} + \frac{E_1^2 + (\omega - E_1)^2}{\omega^3} \times\left(\ln\frac{m^2 + b_{\max}^2}{m^2} - \frac{b_{\max}^2}{m^2 + b_{\max}^2}\right)\right\}dE_1 \quad (13)$$

where $b_{\max} \sim m$ and is limited by the condition that all the derivation is valid only for small angles. The total cross section of the process has the form:

$$\sigma = \frac{e^2R^2}{3}\left(\frac{1}{2}\frac{b_{\max}^2}{m^2+b_{\max}^2} + \ln\frac{m^2+b_{\max}^2}{m^2}\right). \quad (14)$$

This integration can give erroneous results because, for large values of its arguments (as in our case), the form factor can decrease the cross section appreciably. Some properties of the form factor, important for the theory, can be obtained by comparing the differential cross section with the experimental data. If we let $F_+ = 1$, then it can be seen from (11) that the effective angles are $\theta \sim m/E$.

Formula (13) gives the energy distribution of the formed protons. It has a minimum for $E_1 = E_2 = \omega/2$. Let us note that the total cross section for pair formation turns out to depend neither on the energy of the inpinging quantum, nor on the rest mass of the formed particles.

The results obtained for a concrete model of the nucleus – the "absolutely black" nucleus – can be generalized to an arbitrary interaction law between nucleon and nucleus – in analogy to what has been done for the π-meson[5]. In this case the cross section is expressed through the spinor amplitudes for elastic scattering of nucleons on a nucleus.

The wave function will be written in the form

$$\begin{aligned} \psi_1 &= u_1 e^{i\mathbf{p}_1\mathbf{r}} + f_1(p_1\theta_1)\, e^{-ip_1r}/r, \\ \psi_2 &= u_2 e^{-i\mathbf{p}_2\mathbf{r}} + f_2(p_2\theta_2)\, e^{ip_2r}/r, \end{aligned} \quad (15)$$

where θ^i is the angle between the vector $\mathbf{r}$ and $-\mathbf{p}_i = 1,2$. The amplitude f_1 is obtained from the usual spinor amplitude f for elastic scattering, in the transition to a converging asymptote[3].

Let us transform to the Fourier representation:

$$\bar{f}_1(p_1\theta_1)\frac{e^{ip_1r}}{r} = \int \bar{\chi}_1(\mathbf{q})\, e^{i\mathbf{q}\mathbf{r}}\, d\mathbf{q}; \quad (16)$$

$$\bar{\chi}_1(\mathbf{q}) = (2\pi)^{-3}\int \bar{f}_1(p_1\theta_1)\frac{e^{ip_1r}}{r}\, e^{-i\mathbf{q}\mathbf{r}}\, d\mathbf{r} \quad (17)$$

and analogously for f_2. The polar axis is chosen in the direction of the vector $-\mathbf{p}_1$. Making use of the smallness of all the angles, we get

$$\bar{\chi}_1(\mathbf{q}) = (2\pi)^{-3}\int \bar{f}_1(p_1\theta)\exp\left\{i(p_1-q)r + \frac{iqr}{2}(\theta-\theta_{1q})^2\right\} r\,dr\,d\theta$$

$$= (2\pi)^{-2}\bar{f}_1(p_1\theta_{1q})/(q^2-p_1^2-i\varepsilon); \quad \varepsilon \to 0. \quad (18)$$

Analogously, we have;

$$\chi_2(\mathbf{q}) = (2\pi)^{-2} f_2(p_2\theta_{2q})/(q^2-p_2^2-i\varepsilon); \quad \varepsilon \to 0. \quad (19)$$

Here θ_{iq} is the angle between the vectors $-\mathbf{p}_i$ and $\mathbf{q}$, $i = 1,2$.

Let us investigate the integrals involved in the matrix element (1). The integrals containing either f_1 or f_2 are:

$$\begin{aligned} &\int\left(\bar{f}_1(p_1\theta_1)\frac{e^{ip_1r}}{r}(\gamma\mathbf{j})\, u_2 e^{-i\mathbf{p}_2\mathbf{r}} + \bar{u}_1 e^{-i\mathbf{p}_1\mathbf{r}}(\gamma\mathbf{j})\, f_2(p_2\theta_2)\frac{e^{ip_2r}}{r}\right) e^{i\mathbf{k}_\gamma\mathbf{r}}\, d\mathbf{r} \\ &= \int\left(\bar{\chi}_1(\mathbf{q})(\gamma\mathbf{j})\, u_2 e^{i(\mathbf{q}+\mathbf{k}_\gamma-\mathbf{p}_2)\mathbf{r}} + \bar{u}_1(\gamma\mathbf{j})\,\chi_2(\mathbf{q})\, e^{i(\mathbf{q}+\mathbf{k}_\gamma-\mathbf{p}_1)\mathbf{r}}\right) d\mathbf{q}\, d\mathbf{r} \\ &= \frac{4\pi}{\omega(m^2+b^2)}\left(p_2\bar{f}_1(\mathbf{k})(\gamma\mathbf{j})\, u_2 + p_1\bar{u}_1(\gamma\mathbf{j})\, f_2(\mathbf{k})\right). \end{aligned} \quad (20)$$

The integral containing both f_1 and f_2 has the form

$$\begin{aligned} &\int \bar{f}_1(p_1\theta_1)\frac{e^{ip_1r}}{r}(\gamma\mathbf{j})\, f_2(p_2\theta_2)\frac{e^{ip_2r}}{r}\, e^{i\mathbf{k}_\gamma\mathbf{r}}\, d\mathbf{r} \\ &= \int \bar{\chi}_1(\mathbf{q})(\gamma\mathbf{j})\,\chi_2(\mathbf{q}')\, e^{i(\mathbf{q}+\mathbf{q}'+\mathbf{k}_\gamma)\mathbf{r}}\, d\mathbf{q}\, d\mathbf{q}'\, d\mathbf{r} \\ &= (2\pi)^3\int \bar{\chi}_1(\mathbf{q})(\gamma\mathbf{j})\,\chi_2(-\mathbf{k}_\gamma-\mathbf{q})\, d\mathbf{q}. \end{aligned} \quad (21)$$

We let $\mathbf{q} = \mathbf{q}_z + \mathbf{g}\,(\mathbf{k}_\gamma \cdot \mathbf{g}) = 0$. (21) is then rewritten in the following form:

$$\frac{2}{\pi}\int d\mathbf{g}\,\bar{f}_1(\mathbf{k}_1+\mathbf{g})(\gamma\mathbf{j})\, f_2(\mathbf{k}_2-\mathbf{g}) \int_{-\infty}^{\infty} dq_z/(q_z^2+g^2-p_1^2-i\varepsilon)(|\omega+q_z|^2+g^2-p_2^2-i\varepsilon). \quad (22)$$

Let us evaluate the integral over q_z. Introducing the new variable $\boldsymbol{\eta} = \mathbf{k}_1 + \mathbf{g}$, we get

$$\frac{2i}{\omega(m^2+b^2)}\int \bar{f}_1(\boldsymbol{\eta})(\gamma\mathbf{j})\, f_2(\mathbf{k}-\boldsymbol{\eta})\, d\boldsymbol{\eta}. \quad (23)$$

We have made use of the fact that the effective $k \sim 1/R \ll b \sim m$. The integration over $\boldsymbol{\eta}$ in (23) is performed over the whole surface orthogonal to the vector $\mathbf{k}_\gamma$. In the evaluation of the integrals (20) and (23), the main role is played by distances $p_1p_2/\mu^2\omega \gg R$, therefore the use of the asymptotic expressions for the ψ-function is legitimate.

The differential cross section for the process is

$$d\sigma_{\mathbf{j}} = \frac{e^2}{\pi^2}\frac{E_1^2E_2^2}{\omega^3(m^2+b^2)^2}|F_{+-}|^2\sum\Big|\frac{1}{p_2}\bar{u}_1(\gamma\mathbf{j})f_2(\mathbf{k})$$

$$+\frac{1}{p_1}\bar{f}_1(\mathbf{k})(\gamma\mathbf{j})u_2 \tag{24}$$

$$+\frac{i}{2\pi p_1p_2}\int\bar{f}_1(\boldsymbol{\eta})(\gamma\mathbf{j})f_2(\mathbf{k}-\boldsymbol{\eta})\,d\boldsymbol{\eta}\Big|^2 dE_1\,d\mathbf{k}\,d\mathbf{b}$$

($E_1+E_2=\omega$). The summation over spins can be performed in a general form if the functions f_1 and f_2 have the form (we change the notation $u_1f_1(\mathbf{k})$, where f_1 and f_2 are scalar quantities. Then, averaging (24) over j, we get:

$$d\sigma' = \frac{e^2}{2\pi^2}\frac{m^2\omega^2+b^2(E_1^2+E_2^2)}{(m^2+b^2)^2\omega^3}\Big|\frac{1}{p_1}f_1^*(\mathbf{k})+\frac{1}{p_2}f_2(\mathbf{k})$$

$$+\frac{i}{2\pi p_1p_2}\int f_1^*(\boldsymbol{\eta})f_2(\mathbf{k}-\boldsymbol{\eta})\,d\boldsymbol{\eta}\Big|^2|F_{+-}|^2\,d\mathbf{k}\,d\mathbf{b}\,dE_1. \tag{25}$$

The distribution in k, i. e., in momenta transferred to the nucleus, is therefor model-dependent.

In the semi-transparent model of the nucleus[6], using $k\sim 1/R \ll k_1$, $k_2\sim m$:

$$f_1(k) = -ip_1u_1\int_0^R\left(1-\exp\{-\alpha_1^*\sqrt{R^2-s_1^2}\}\right)$$

$$\times J_0(ks_1)\,s_1ds_1;$$

$$f_2(k) = ip_2u_2\int_0^R\left(1-\exp\{-\alpha_2\sqrt{R^2-s_2^2}\}\right) \tag{26}$$

$$\times J_0(ks_2)\,s_2\,ds_2;$$

$$\alpha_1 = \varkappa_1 - 2ip_1(n_1-1),\quad \alpha_2 = \varkappa_2 - 2ip_2(n_2-1).$$

where $\varkappa$ and n are the absorption coefficient and the index of refraction of the nucleonic wave in the nucleus. Using these amplitudes, and integrating over k and φ_b, we get

$$d\sigma(b_1E_1) = \tag{27}$$

$$\frac{e^2}{\pi}\frac{m^2\omega^2+b^2E_1^2+b^2(\omega-E_1)^2}{(m^2+b^2)^2\omega^3}\sigma_s|F_{+-}|^2\,bdbdE_1.$$

Here σ_s is the total elastic diffraction scattering cross section for a nucleon on a semi-transparent nucleus, with a total absorption coefficient $\varkappa=\varkappa_1+\varkappa_2$ and, correspondingly, with a total phase shift $2p_1(n_1-1)+2p_2(n_2-1)$, where the coefficients 1 and 2 refer the proton and antiproton.

As a conclusion, I wish to express my thankfulness to I. Ia. Pomeranchuk for the position of the problem and helpful advices.

Note added in proof. In the case of the "black" nucleus, the cross section is obtained in the assumption that the nucleus has the same radius with respect to protons as well as antiprotons. If one rejects this assumption and assumes that the radius is R_1 with respect to protons and R_2 with respect to antiprotons, the expressions(10) to (14) obtained above will be made valid by replacing R by R_1 (if $R_1>R_2$), or by R_2 (if $R_2>R_1$). In the case of a semi transparent nucleus, we obtain cumbersome results which we do not report here.

---

[1] Chamberlain, Sogre, Wiegand and Ypsilantis, Phys. Rev. **100**, 947 (1955)

[2] I. Ia. Pomeranchuk, Dokl. Akad. Nauk SSSR **96**, 265, 481 (1954)

[3] L. Landau and E. Lifshitz, *Quantum Mechanics*, GITTL Moscow, 1948. p. 481 G. Breit and H. Bethe, Phys. Rev **93**, 888 (1954)

[4] A. I. Akhiezer, Dokl. Akad. Nauk SSSR **94**, 281 (1954)

[5] Iu. A. Vdovin, Dokl. Akad. Nauk SSSR **105**, 947 (1955)

[6] Fernbach, Serber and Taylor, Phys. Rev. **75**, 1352 (1949)

Translated by E. S. Troubetzkoy
124

SOVIET PHYSICS JETP VOLUME 5, NUMBER 3 OCTOBER, 1957

On the Absorption of High Energy Nuclear-Active Particles

S. Z. BELEN'KII AND N. M. GERASIMOVA
P. N. Lebedev Physical Institute, Academy of Science, USSR

(Submitted to JETP editor December 29, 1955)
J. Exptl. Theoret. Phys. (U.S.S.R.) 32, 547-551 (March, 1957)

The propagation of nuclear-active particles in matter is computed from the cross sections for the elementary collision act, obtained on the basis of the hydrodynamic theory of multiple particle production.

THE experimental data[1] show that the process of multiple particle production occurs in nuclear collisions in the high energy region ($\sim 10^{12}$ ev and higher). The secondary particles of high enough energy can, in their collision with the nuclei of the matter, lead to additional multiple production (we will call such particles nuclear-active). In this fashion not only absorption, but also multiplication, of the nuclear-active particles occurs as they propagate through matter. For the solution of the problem of propagation of nuclear-active particles, we will start from the expression for the energy distribution in the elementary act, obtained on the basis of the hydrodynamic theory of multiple particle production[2,3]. We use the following formulas[3] for the collision of a pion or a nucleon with a nucleus:

$$dN = C_1 (2\pi L)^{-1/2} \exp\{-L/2 + \sqrt{L^2 - \lambda^2}\}\, d\lambda; \quad (1)$$

$$E = C_2 \exp\left\{\frac{5}{6} L + \lambda + \frac{1}{3}\sqrt{L^2 - \lambda^2}\right\}. \quad (2)$$

where dN is the number of particles produced in the interval $d\lambda$; λ is a parameter related to the energy E of the particle by the relationship (2). Formulas (1) and (2) give the particle distribution in a parametric form. The parameter λ varies in the range $-\sqrt{3}L/2 < \lambda < \sqrt{3}L/2$. The magnitude L is related to the energy of the primary particle.

As shown in Refs. 1 and 3, the collision of the particle with the nucleus can be considered as the collision of the particle with a "tube" cut out from the nucleus, of cross section equal to that of the nucleon; the length of this tube varies between the nuclear diameter and a length of the order of the nucleon's size. In the center-of-mass system, the dimensions of the impinging particle and of the tube are subject to a Lorentz contraction in the direction of motion. The quantity e^{-L} represents the ratio of the transverse dimensions of the system at the first instant after the collision, to the longitudinal dimensions:

$$e^{-L} = [2Mc^2 \chi(\bar{l}) / E_0]^{1/2}, \quad \chi(\bar{l}) = \bar{l}\,(1/\bar{l} + \bar{l})^2. \quad (3)$$

where M is the nucleon mass; E_0 is the energy of the impinging particle in the laboratory system; l is the average length of the tube in units of the nucleonic radius;

$$\bar{l} = 2[A - (2A^{1/3} - 1)^{3/2}] / 3(A^{1/3} - 1)^2, \quad (4)$$

where A is the atomic number. For air, for instance, $A = 14.8$, $l = 2.25$. In what follows we will use this value of l.

The coefficients C_1 and C_2 in Eqs. (1) and (2) are determined by the energy conservation law and by the normalization of the number of particles. The total number of particles, in the case of the collision of a nucleon (or a π-meson) with a nucleus, is taken to be[3]:

$$N = kA^{0,19} (E_0 / 2Mc^2)^{1/4}, \quad (5)$$

where $k \approx 2$. The coefficients C_1 and C_2 are equal to:

$$C_1 = kA^{0,19} [\chi(\bar{l})]^{1/4};$$

$$C_2 = 5\sqrt{5}\, Mc^2 [\chi(\bar{l})]^{3/4} / 2\sqrt{3}\, kA^{0,19}. \quad (6)$$

Making use of Eqs. (1) and (2), we assume that the energy distribution in the collision with the tube does not differ much from the energy distribution in the collision with a nucleon. Equations (1) and (2) also do not take into account the fact that not only π-mesons, but also particles of different kinds, occur in the stars. Furthermore, the nuclons present in the tube which collide with the primary particle acquire a substantial energy, and are active in the further nuclear-cascade process. A production of a certain number of antinucleons is also not impossible. In the present paper we shall not account for the nucleons, which do not play a very substantial role at the very high energies ($>10^{14}$); we also shall not consider the influence of the heavy mesons and hyperons – this will be the object of another report.

Let us consider now the kinetic equation which determines the distribution of the nuclear-active particles. If we assume that only π-mesons are produced in the elementary process, we have the following equation:

$$\frac{\partial P(y,t)}{\partial t} = -P(y,t) + \frac{2}{3}\int\limits_y^\infty P(y_0,t)\,\frac{\partial N}{\partial y}\,dy_0. \quad (7)$$

where $P(y,t)$ is the number of particles in the interval dy, $y=\ln E$; t is the quantity of matter traversed by the particles. The quantity of matter is measured in units of t, where t is the "nuclear mean free path" of the particles in the considered matter; $y_0=\ln E_0$, where E_0 is the energy of the primary particle. The factor 2/3 is present because not all the π-mesons are nuclear-active. A number of π^0-mesons, equal on the average to 1/3 of the total number of mesons, decay before any interaction with nuclei. The decay of charged π-mesons is already negligible at energies of $\sim 10^{12}$ ev, and is therefore not accounted for by our equations.

We choose the following for the boundary condition for Eq. (7):

$$P(y,0) = Be^{-\gamma y}, \quad (8)$$

where $\gamma=1.5-1.75$. This corresponds to the fact that the nucleons falling on the atmospheric boundary have a spectrum of power form[4]. In addition, the atmospheric boundary is subject to a cascade of nuclei of different elements, with a predominant part of α-particles.

The solution of equations of the form (7) have been obtained numerically by Zatsepin and Guzhavin[5] by a modified method of successive approximations[6]. Analogous numerical calculations, starting from the expression for the elementary act obtained by Fermi, have been performed later[7]. In the present paper we propose to obtain an analytic expression for the dependence of the number of nuclear-active particles on the energy and depth.

In the first place, we make the substitution

$$P(y,t) = e^{-t}\varphi(y,t). \quad (9)$$

Equation (7) then reduces to

$$\frac{\partial\varphi(y,t)}{\partial t} = \int\limits_y^\infty \varphi(y_0,t)\,\frac{\partial N}{\partial y}\,dy_0, \quad (10)$$

which can be written in the form

$$\partial\varphi(y,t)/\partial t = \mathscr{L}[\varphi(y,t)], \quad (10)$$

where $\mathfrak{L}$ is a linear integral operator. Let us examine some of the properties of the operator $\mathfrak{L}$. Let us assume that the operator $\mathfrak{L}$ operates on a function which has a power dependence on E and an exponential dependence on y, i.e., a function $\varphi(y,t)=Be^{\gamma y}$. Substituting the expression for dN/dy under the integral sign [see Eqs. (1) and (2)], we get

$$\mathscr{L}[Be^{-\gamma y}] =$$

$$B_1\int\limits_{L_{\min}}^{L_{\max}} \frac{\sqrt{L^2-\lambda^2}\exp\{-(2\gamma+{}^1/_2)L+\sqrt{L^2-\lambda^2}\}}{\sqrt{2\pi L}\,(\sqrt{L^2-\lambda^2})-\lambda/3)}\,dL,$$

$$B_1 = {}^4/_3 B[2MC^2\chi(\bar{l})]^{-\gamma}C_1; \quad (11)$$

$$L_{\min} = 0{,}536\,(y-\ln C_2), \quad L_{\max} = 7{,}4\,(y-\ln C_2).$$

Equation (11) obviously, has to be completed by Eq. (2), which we write in the following form

$$y = \ln C_2 + 5L/6 + \lambda + \sqrt{L^2-\lambda^2}/3.$$

It is not difficult to see that the function in the exponent under the integral sign of (11) has a sharp maximum. Let us recall that the formulas giving the energy distribution in the elementary act are themselves derived with exponential accuracy, and the factors of the exponentials are determined by the normalization conditions. It is natural, therefore, to limit the evaluation of the integral (11) to the exponential accuracy. Let us expand the function in the exponent of formula (11) in a series, around the maximum, including terms up to the second derivative; the factor of the exponential will be put equal to its value at the maximum. We obtain:

$$\mathscr{L}[Be^{-\gamma y}] = Be^{-\gamma y} S(\gamma)\, e^{-\delta(\gamma)\, y}; \tag{12}$$

$$S(\gamma) = \frac{{}^4/_3\, kA^{0.19} [\chi(\bar{l})]^{1/4} \sqrt{1-\nu^2(\gamma)}\, [\sqrt{1-\nu^2(\gamma)} - \nu(\gamma)/3]}{{}^5/_6 + \nu(\gamma) + \sqrt{1-\nu^2(\gamma)}/3}\, C_2^{\gamma+\delta(\gamma)} [2Mc^2\chi(\bar{l})]^{-\gamma}, \tag{13}$$

$$\nu(\gamma) = \frac{-(2\gamma/3+1) + (2\gamma + {}^1/_2)\sqrt{(2\gamma/3+1)^2 + (2\gamma+{}^1/_2)^2 - 1}}{(2\gamma+{}^1/_2)^2 + (2\gamma/3+1)^2}, \tag{14}$$

$$\delta(\gamma) = \frac{(2\gamma+{}^1/_2) - \sqrt{1-\nu^2(\gamma)}}{{}^5/_6 + \nu(\gamma) + \sqrt{1-\nu^2(\gamma)}/3} - \gamma. \tag{15}$$

In the evaluation of the integral in (10), $L_{\min}$ and $L_{\max}$ have been replaced by $-\infty$ and $+\infty$. The calculation shows that the quantity $\delta(\gamma)$ for $\gamma = 1.5 - 2$ is small, and therefore the factor $e^{\delta(\gamma)y}$ leads to a y dependence, small compared to $e^{-\gamma y}$ (see Table 1)

TABLE I

γ=	1,5	1,6	1,7	1,8	1,9	2
$\delta(\gamma)$=	0,07	0,08	0,09	0,1	0,11	0,12

It follows from (12) that the operator $\mathfrak{L}$ operating on a function having a power dependence on the energy again gives a power spectrum, only slightly smoothed with respect to the primary one. Bearing this result in mind, we seek a solution of Eq. (10) in the form

$$\varphi(y, t) = Be^{-\gamma y} f(y, t), \tag{16}$$

we will consider $f(y, t)$ as depending weakly on y. Let us substitute the expression (16) in Eq. (10).

For the evaluation of the integral, let us make use of the assumption on $f(y, t)$, and take the value of this function at the point where the function in the exponent has a maximum. We obtain the following equation for $f(y, t)$:

$$\partial f(y, t)/\partial t = \Delta(y, \gamma) f(y_1, t), \tag{17}$$

$$\Delta(y, \gamma) = S(\gamma) e^{-\delta(\gamma)\, y}, \tag{18}$$

y_1 is the point at which the function in the exponent has a maximum.

y_1 is related to y by the relationship

$$y_1 = 2d(\gamma)(y - \ln C_2) + \ln 2Mc^2\chi(\bar{l}), \tag{19}$$

$$d(\gamma) = [{}^5/_6 + \nu(\gamma) + \sqrt{1-\nu^2(\gamma)}/3]^{-1}. \tag{20}$$

Table 2 gives the values of y_1 and $\Delta(y, \gamma)$ for γ=1.75 and 1.5 and for different y's

TABLE II

y	32,2		34,5		36,8		39,2		41,4	
γ	1,5	1,75	1,5	1,75	1,5	1,75	1,5	1,75	1,5	1,75
y_1	34,8	34,8	37,4	37,4	39,9	39,9	42,5	42,5	45	45
$\Delta(y, \gamma)$	0,131	0,06	0,111	0,048	0,095	0,038	0,08	0,03	0,07	0,024

For the solution of (17), let us make a Laplace transformation with respect to the variable t:

$$f(y, t) = \frac{1}{2\pi i}\int_{\varepsilon - i\infty}^{\varepsilon + i\infty} e^{pt} f(y, p)\, dp; \quad f(y, p) = \int_0^\infty e^{-pt} f(y, t)\, dt. \tag{21}$$

Taking the boundary condition into account we obtain, instead of (17),

$$pf(y, p) - \Delta(y, \gamma) f(y_1, p) = 1. \qquad (22)$$

It is easy to see that the solutions of this equation can be written in the form of the following series

$$f(y, p) = \frac{1}{p - \Delta(y, \gamma)} \qquad (23)$$

$$+ \frac{\Delta(y, \gamma)}{p} \frac{[\Delta(y_1, \gamma) - \Delta(y, \gamma)]}{[p - \Delta(y, \gamma)][p - \Delta(y_1, \gamma)]}$$

$$+ \frac{\Delta(y, \gamma)\Delta(y_1, \gamma)}{p^2} \frac{[\Delta(y_2, \gamma) - \Delta(y_1, \gamma)]}{[p - \Delta(y_1, \gamma)][p - \Delta(y_2, \gamma)]} + \ldots +$$

$$\frac{\Delta(y, \gamma)\Delta(y_1, \gamma)\ldots\Delta(y_n, \gamma)[\Delta(y_{n+1}, \gamma) - \Delta(y_n, \gamma)]}{p^{n+1}[p - \Delta(y_n, \gamma)][p - \Delta(y_{n+1}, \gamma)]} + \ldots$$

Here y_2 is related to y_1 the same way as y_1 is related to y. In this fashion, if $y_1 = \psi(y)$ according to (19)

$$y_2 = \psi(y_1), \quad y_3 = \psi(y_2), \ldots y_n = \psi(y_{n-1}).$$

Using the relationship (21) one can compute

$$f(y, t) = f_0(y, t) + f_1(y, t) + f_2(y, t) + \ldots \qquad (24)$$

$$f_0(y, t) = e^{\Delta(y, \gamma) t}; \; f_1(y, t) =$$

$$\Delta(y, \gamma)\left[\frac{e^{\Delta(y_1, \gamma) t} - 1}{\Delta(y_1, \gamma)} - \frac{e^{\Delta(y, \gamma) t} - 1}{\Delta(y, \gamma)}\right]$$

$$f_2(y, t) = \Delta(y, \gamma)\Delta(y_1, \gamma) \qquad (25)$$

$$\times\left[\frac{e^{\Delta(y_2, \gamma) t} - 1}{\Delta^2(y_2, \gamma)} - \frac{e^{\Delta(y_1, \gamma) t} - 1}{\Delta^2(y_1, \gamma)}\right]$$

$$- t\Delta(y, \gamma)\left[\frac{\Delta(y_1, \gamma)}{\Delta(y_2, \gamma)} - 1\right].$$

It is easy to see that the series (2) converges. It can also be shown that $f(y, t)$ does indeed change slowly with y; this justifies the transition from Eq. (10) to Eq. (17) for which the function $f(y, t)$ was evaluated at the point where the function in the exponent has a maximum.

Let $y = 32.2$ and 36.8 ($E = 10^{14}$ ev and 10^{16} ev and $t = 10$. In the first case ($y = \ln 10^{14}$)

$$f_1(y,t) / f_0(y, t) = -0{,}09;$$

$$f_2(y, t) / f_0(y, t) = -0{,}02.$$

In the second case ($y = \ln 10^{16}$):

$$f_1(y, t) / f_0(y, t) = -0{,}065;$$

$$f_2(y,t) / f_0(y, t) = -0{,}005.$$

The function $P(y, t)$ can be written in the following form [see (9)]:

$$P(y, t) = Be^{-\gamma y}\exp\{-[1 - D(\gamma, y, t)]t\};$$

$$D(\gamma, y, t) = t^{-1}\ln f(y, t). \quad (26) \qquad (26)$$

TABLE III

t	$y = 32{,}2$	$y = 36{,}8$
2	0,13	0,09
10	0,12	0,08
15	0,11	0,07

Table 3 gives values of $D(\gamma, y, t)$ for different t, y and $\gamma = 1.5$. For $\gamma = 1.75$ and different y and t: $D(\gamma, y, t) \simeq 0.05$. For energies smaller than 10^{14} ev the results obtained are already erroneous. The investigation of the absoprtion of nuclear-active particles for these energies will be given in a further report.

---

[1] I. L. Rozental′ and D. C. Chernavskii, Usp. Fiz. Nauk 52, 185 (1954)

[2] L. D. Landau, Izv. Akad. Nauk SSR ser fiz. 17, 51 (1953)

[3] S. Z. Belenkii and L. D. Landau, Usp. Fiz. Nauk 56, 309 (1955)

[4] Bartlett, Bollinger, Cocconi, Eisenberg and Greisen, Rev. Mod. Phys. 24, 133 (1952)

[5] Guzhavina, V. V. Guzhavin and G. T. Zatsepin, J. Exptl. Theoret. Phys. (U.S.S.R.) 31, 819 (1956); Soviet Phys. JETP 4, 690 (1957)

[6] I. L. Rosental′, J. Exptl. Theoret. Phys. (U.S.S.R.) 23, 440 (1952) G. T. Zatsepin and I. L. Rozental′ Dokl. Akad. Nauk SSSR 99, 369 (1954)

[7] V. Haber-Schaim, Nuovo Cimento 11, 172 (1954); Amaldi, L. Mezzetti and Soppini, Nuovo Cimento 10, 803 (1953)

Translated by E. S. Troubetzkoy
125

SOVIET PHYSICS JETP VOLUME 5, NUMBER 3 OCTOBER, 1957

On the Possibility of Formulating a Meson Theory with Several Fields

A. D. GALANIN

(Submitted to JETP editor February 7, 1956)
J. Exptl. Theoret. Phys. (U.S.S.R.) **32**, 552-8 (March, 1957)

The following cases of interaction of several fields are considered: 1) N fermion and n boson fields with the same coupling constant, 2) two fermion and two boson fields, interacting with different constants, 3) fermion and boson fields with different isotopic properties. In all cases considered the physical charge tends to zero as the extended interaction approaches a point one.

IN articles by Pomeranchuk[1] it has been shown that in pseudoscalar meson theory the interaction constant tends to zero as the transition from an extended interaction to the limit of a point one is carried out. It was assumed that the result does not depend upon the particular way of carrying out the limiting procedure, and therefore a special form proposed by Abrikosov and Khalatnikov[2] was employed.

In the several examples, we consider this conclusion is not changed by the introduction of several interacting fields.

1. As a first example we consider N fermion fields (all with isotopic spin ½) and n boson fields (all scalar or pseudoscalar with isotopic spin 1) interacting with each other with the same coupling constant g. We do not introduce any selection rules, so that all types of fermions can transform into each other, as can all types of bosons (the problem presents itself as a purely methodological one and the relation of the fields introduced to real particles is not considered).

It is necessary to take into account the fact that virtual bosons (or fermions) can be transformed from one type into another. Therefore the Green's function of the bosons D_{ab} is a matrix, in which the indices a and b can take on n values. The diagonal elements D_{aa} correspond to the propagation of a boson of type a without transformation, and the non-diagonal elements D_{ab} to the preparation of a boson of type a with transformation into one of type b.

Neglecting the mass of the bosons, we express

$$D_{ab} = d_{ab} / k^2.$$

In view of the fact that all bosons are equivalent (have the same charge, differences in mass being unimportant in the study of the asymptotic Green's function), all diagonal elements d_{ab} are equal ($d_{aa} \equiv d_1$), as well as all non-diagonal elements ($d_{ab} \equiv d_2$, $a \neq b$). The matrix d_{ab} is connected with the polarization operator in the following way (P is the polarization operator, divided by k^2):

$$d_{ab} + d_{ac} P_{cb} = \delta_{ab}. \tag{1}$$

From the equivalence of all bosons it follows that all elements of P_{ab} are equal ($P_{ab} \equiv P$). Then Eq. (1) gives

$$d_1 + d_1 P + (n-1) d_2 P = 1,$$

$$d_2 + d_1 P + (n-1) d_2 P = 0,$$

from which

$$d_1 = \frac{1 + (n-1) P}{1 + nP}, \quad d_2 = -\frac{P}{1 + nP}. \tag{2}$$

We consider now a given boson line of a given diagram. To each such line there will correspond a factor

$$n d_1 + n(n-1) d_2 \equiv n\Delta$$

(n cases of propagation of a boson without transformation, $n(n-1)$ with transformation). From Eq. (2) follows

$$\Delta = 1/(1 + nP). \tag{3}$$

Analogously, for each fermion line it is necessary to write

$$N\beta_1 + N(N-1)\beta_2 \equiv NB,$$

where β_1 corresponds to propagation of a fermion without transformation, and β_2, with transformation (the fermion Green's function G is, for large momenta, equal to $G = \beta/\mathbf{p}$). Analogous to Eq. (3) we have

$$B = 1/(1+NM), \tag{4}$$

where M is the mass operator (divided by $\mathbf{p}$).

We note that Δ and B satisfy the same initial conditions as d and β in the theory with one boson and fermion, that is $\Delta(L) = B(L) = 1$, where L is the momentum at which the interaction is cut off. In fact, when their interaction is excluded, the particles cannot undergo mutual transformations and therefore $d_2(L) = \beta_2(L) = 0$.

Now if we turn our attention to the fact that the polarization operator arises from two fermion lines, the mass operator from one fermion and one boson line, and the vertex part from two fermion lines and one boson line, and take into account that all possible transitions of one fermion and boson into another are allowed, then it is immediately obvious that the equations for the Green's function and vertex parts in our case can be obtained from the corresponding equations of the theory with one boson and fermion, using the simple substitutions

$$d \to \Delta,\ \beta \to B,\ \Gamma \to \Gamma,\ g \to N^2 ng.$$

From this it follows that all conclusions which are valid for the theory with one boson and one nucleon can be automatically carried over to the case of many interacting fields considered.

2. Now we consider the case of different (in magnitude or in sign) charges. The general form of the interaction Lagrangian is as follows:

$$\mathscr{L} = \sum_{i,k,l} a_{ik,l}\bar{\psi}_i\psi_k\varphi_l.$$

By using a linear transformation of the fields ψ_1 it is possible to bring the quadratic form $\sum_{ik} a_{ik,l}\,\bar{\psi}_i\psi_k$ into diagonal form, leaving the Lagrangian of the free fermion field unchanged.

Then

$$\mathscr{L} = \sum_{il} a_{i,l}\,\bar{\psi}_i\psi_i\varphi_l.$$

The further transformation of the Lagrangian using the substitution $\Phi_i = \sum_i a_{i,l}\varphi_l$ leads — in so far as this transformation is not, in general, orthogonal — to complicated free equations for the boson fields and does not simplify the problem.

We consider the following Lagrangian

$$\mathscr{L} = g_{11}\bar{\psi}_1\psi_1\varphi_1 + g_{22}\bar{\psi}_2\psi_2\varphi_2 + g_{12}\bar{\psi}_1\psi_1\varphi_2 + g_{21}\bar{\psi}_2\psi_2\varphi_1. \tag{5}$$

Looking at the equations for the vertex parts we see that it is sufficient to introduce two vertex parts

$$\Gamma_{\psi_1\psi_1\varphi_1} = \Gamma_{\psi_1\psi_1\varphi_2} \equiv \Gamma_1;\ \Gamma_{\psi_2\psi_2\varphi_1} = \Gamma_{\psi_2\psi_2\varphi_2} \equiv \Gamma_2.$$

From these equalities it follows that the polarization operator (and also the boson Green's function) are symmetrical: $P_{ik} = P_{ki}$. From the equality

$$d_{ij} + d_{ik}P_{kj} = \delta_{ij} \tag{6}$$

we obtain

$$d_{11} = (1+P_{22})\,\Delta_1^{-1};\ d_{22} = (1+P_{11})\,\Delta_1^{-1}; \qquad d_{12} = -P_{12}\Delta_1^{-1}, \tag{7}$$

$$P_{11} = -1 + d_{22}\Delta^{-1};\ P_{22} = -1 + d_{11}\Delta^{-1}; \qquad P_{12} = -d_{12}\Delta^{-1}, \tag{8}$$

where

$$\Delta = d_{11}d_{22} - d_{12}^2; \qquad \Delta_1 = (1+P_{22})(1+P_{11}) - P_{12}^2,\ \Delta\Delta_1 = 1. \tag{9}$$

Symbolically, the equation for Γ_1 has the following form (we always consider the problem in the same approximation as in Ref. 3):

$$\Gamma_1 = 1 + \Gamma_1G_1\Gamma_1G_1\Gamma_1\,(g_{11}^2D_{11} + g_{22}^2D_{22} + 2g_{11}g_{22}D_{12}), \tag{10}$$

where G_1 is the Green's function for the field ψ_1. Just as in the theory with a single field, we obtain for high momenta: [The case where the boson field has isotopic spin 1 is considered; the arguments of all functions are $\xi = \ln(-p^2/m^2)$. The prime indicates differentiation with respect to ξ.]

$$\alpha_1'/\alpha_1 = -\lambda_1;\ \alpha_2'/\alpha_2 = -\lambda_2; \tag{11}$$

$$\begin{aligned}\lambda_1 &= (\alpha_1^2\beta_1^2/4\pi)\,(g_{11}^2d_{11} + g_{12}^2d_{22} + 2g_{11}g_{12}d_{12}),\\ \lambda_2 &= (\alpha_2^2\beta_2^2/4\pi)\,(g_{21}^2d_{11} + g_{22}^2d_{22} + 2g_{22}g_{21}d_{12}).\end{aligned} \tag{12}$$

For the fermion Green's function we have (the calculation is completely analogous to the theory with a single field[4]):

$$\beta_1'/\beta_1 = 3\lambda_1/2;\ \beta_2'/\beta_2 = 3\lambda_2/2. \tag{13}$$

The polarization operator P_{ij} satisfies equations which can be written symbolically

$$k^2 P_{ij} = \sum_{l=1}^{2} g_{lj} g_{ij} G_l \Gamma_l G_l. \tag{14}$$

From this we obtain*

$$P'_{11} = -\frac{1}{\pi}\left(g_{11}^2 \beta_1^2 \alpha_1^2 + g_{21}^2 \alpha_2^2 \beta_2^2\right), \tag{15}$$

$$P'_{22} = -\frac{1}{\pi}\left(g_{12}^2 \alpha_1^2 \beta_1^2 + g_{22}^2 \alpha_2^2 \beta_2^2\right),$$

$$P'_{12} = -\frac{1}{\pi}\left(g_{11} g_{12} \alpha_1^2 \beta_1^2 + g_{22} g_{21} \alpha_2^2 \beta_2^2\right).$$

Using Eqs. (7) – (9), it is easy to show that

$$\Delta' / \Delta = 4(\lambda_1 + \lambda_2). \tag{16}$$

From (12) we obtain

$$\frac{\lambda'_1}{\lambda_1} = 2\frac{\alpha'_1}{\alpha_1} + 2\frac{\beta'_1}{\beta_1} + \frac{g_{11}^2 d'_{11} + g_{12}^2 d'_{22} + 2 g_{11} g_{12} d'_{12}}{g_{11}^2 d_{11} + g_{12}^2 d_{22} + 2 g_{11} g_{12} d_{12}},$$

or, using Eqs. (11), (13), (7) – (9), we have

$$\lambda'_1 / \lambda_1 = 5\lambda_1 + 4\lambda_2 \tag{17}$$
$$- 4\alpha_1^2 \alpha_2^2 \beta_1^2 \beta_2^2 (g_{11} g_{22} - g_{21} g_{12})^2 \Delta / (4\pi)^2 \lambda_1.$$

The quantities λ_1 and λ_2 characterize the effective interaction of two fermions ψ_1, ψ_1 or ψ_2, ψ_2. In addition, the interaction of ψ_1 and ψ_2 can be considered. We denote by λ_3 the corresponding effective charge

$$\lambda_3 = (\alpha_1 \alpha_2 \beta_1 \beta_2 / 4\pi)\,[g_{11} g_{21} d_{11} + g_{12} g_{22} d_{22} \tag{18}$$
$$+ (g_{11} g_{22} + g_{12} g_{21})\, d_{12}].$$

It is easy to verify that

$$\lambda_3^2 = \lambda_1 \lambda_2 - \alpha_1^2 \alpha_2^2 \beta_1^2 \beta_2^2 (g_{11} g_{22} - g_{21} g_{12})^2 \Delta / (4\pi)^2,$$

and therefore Eq. (17) can be written as

$$\lambda'_1 / \lambda_1 = 5\lambda_1 + 4\lambda_3^2 / \lambda_1 \tag{19}$$

and analogously

$$\lambda'_2 / \lambda_2 = 5\lambda_2 + 4\lambda_3^2 / \lambda_2, \quad \lambda'_3 / \lambda_3 = 9(\lambda_1 + \lambda_2) / 2. \tag{19'}$$

We note that although four constants occur in the Lagrangian (5), only three combinations of these constants have physical meaning, as one can show by making the substitutions

$$\sqrt{g_{11}^2 + g_{12}^2}\,\Phi_1 = g_{11}\varphi_1 + g_{12}\varphi_2,$$

$$\sqrt{g_{22}^2 + g_{21}^2}\,\Phi_2 = g_{21}\varphi_1 + g_{22}\varphi_2.$$

Also, effective charges λ_i correspond to these three combinations of constants.

From Eq. (19) it is seen that all derivatives of λ_i are positive, *i.e.*, λ_i decreases with decreasing momentum.

Following Abrikosov and Khalatnikov,[2] we introduce two limiting momenta: Λ_k for the integration over virtual bosons, and Λ_p for the integration over virtual fermions, with $L_p - L_k = \ln \Lambda_p / \Lambda_k \gg 1$. The Eqs. (19) are valid for $\xi < L_k$ and the values of $\lambda_i(L_k)$ are initial conditions for them. Just as in the theory with a single field, for sufficiently large $L_p - L_k$ the values of $\lambda_i(L_k)$ must be small.

In fact, following Ref. 2, we obtain from the equations for the polarization operator the following boundary conditions for P_{ij} at $\xi = L_k$:

$$P_{11} = \frac{1}{\pi}(g_{11}^2 + g_{21}^2)(L_p - L_k),$$

$$P_{22} = \frac{1}{\pi}(g_{12}^2 + g_{22}^2)(L_p - L_k),$$

$$P_{12} = \frac{1}{\pi}(g_{11} g_{12} + g_{22} g_{21})(L_p - L_k).$$

From this we have, for example, for $\lambda_i(L_k)$:

$$\lambda_1(L_k) = \frac{1}{4\pi}\,\frac{g_{11}^2 + g_{12}^2 + \frac{1}{\pi}(L_p - L_k)(g_{11} g_{22} - g_{12} g_{21})^2}{1 + \frac{1}{\pi}(L_p - L_k)(g_{11}^2 + g_{22}^2 + g_{12}^2 + g_{21}^2) + \frac{1}{\pi^2}(L_p - L_k)^2 (g_{11} g_{22} - g_{21} g_{12})^2},$$

from which it is clear, for sufficiently large $L_p - L_k$, that indeed $\lambda_1(L_k) \ll 1$.

If $\lambda_i(L_k) \ll 1$, then Eqs. (19) are exact in so far as the more complicated vertex parts play no role.[1] In order that the physical charge (*i.e.*, the solution of Eqs. (19) for small momenta) tends to zero as $L_k \to \infty$, it is sufficient in these conditions that the right-hand sides of Eqs. (19) are positive. We see that this condition is fulfilled.

---

* We do not give the calculation in so far as it coincides completely with that in Ref. 4. The only question arising concerns "small additions" to the vertex part. One can verify directly that, just as in the theory with a single field, their contribution is two powers of α higher in the expressions for β' and P'_{ij}.

Thus, the conclusion about the physical charge being zero still holds in the case considered.

3. We consider now a mixture of fields with different isotopic spins. The most characteristic peculiarities of this mixture of fields will be made clear by an example of four interacting fields: the ψ field, which is a spinor in ordinary space and a spinor in isotopic space; the Y_i field, which is a spinor in ordinary space and a vector in isotopic space; the φ_i field, pseudoscalar in ordinary space and vector in isotopic space; the θ field, scalar in ordinary space (it can also be taken as pseudoscalar) and spinor in isotopic space.

The interaction Lagrangian has the form ($\overline{\psi} = \beta\psi^*$; $\overline{Y} = \beta Y^*$, ϵ_{ijk} is the completely antisymmetrical tensor):

$$\mathscr{L} = ig_1\overline{\psi}\gamma_5\tau_j\psi\varphi_j + ig_2\overline{Y}_i\gamma_5 Y_k\varphi_j i\varepsilon_{ikj} + g_3\overline{\psi}\tau_i Y_j\theta. \tag{20}$$

We denote the Green's functions of the fields ψ, Y, φ and θ as follows:

$$G_\psi = \beta_1/\mathbf{p};\ G_Y = \beta_2/\mathbf{p};\ D_\varphi = d_1/k^2,\ D_0 = d_2/k^2. \tag{21}$$

It is necessary to consider three vertex parts

$$\Gamma_{\psi\psi\varphi_j} = \tau_j\gamma_5\alpha_1;\ \Gamma_{Y_i Y_k\varphi_l} = i\varepsilon_{ikl}\gamma_5\alpha_2;\ \Gamma_{\psi Y_j\theta} = \tau_j\alpha_3. \tag{22}$$

The equations for the mass and polarization operators and the vertex parts are shown schematically on the figure.

The structure of the equations for α, β and d do not differ at all from the theory with one pseudoscalar. If we introduce the following three effective charges

$$\lambda_1 = (g_1^2/4\pi)\,\alpha_1^2\beta_1^2 d_1; \tag{23}$$

$$\lambda_2 = (g_2^2/4\pi)\,\alpha_2^2\beta_2^2 d_1; \qquad \lambda_3 = (g_3^2/4\pi)\,\alpha_3^2\beta_1\beta_2 d_2,$$

then the equations for the functions α_i, β_i, d_i have the form

$$\beta_1'/\beta_1 = 3\lambda_1/2 + 3\lambda_3/2;\ \beta_2'/\beta_2 = \lambda_2 + \lambda_3;$$

$$d_1'/d_1 = 4(\lambda_1 + \lambda_2);\ d_2'/d_2 = 6\lambda_3,$$

$$\alpha_1'/\alpha_1 = -\lambda_1 - 2\lambda_3\sqrt{\lambda_2/\lambda_1};$$
$$\alpha_2'/\alpha_2 = \lambda_2 - 2\lambda_3\sqrt{\lambda_1/\lambda_2};$$
$$\alpha_3'/\alpha_3 = 3\lambda_3 - 2\sqrt{\lambda_1\lambda_2}. \tag{24}$$

The negative sign of the second terms in the equations for α comes from the choice of sign for the charges g_1 and g_2 (if θ is the pseudoscalar field, then the equations have the same form under a different choice of the relative sign of g_1 and g_2).

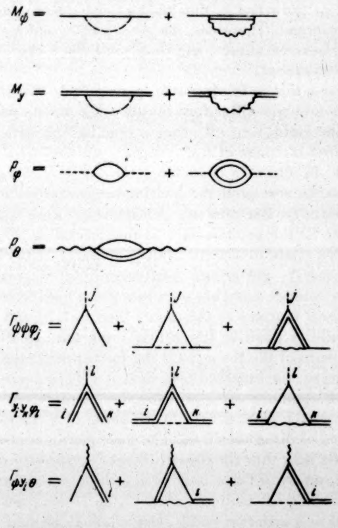

M_ψ =
+
M_y =
+
P_φ =
+
P_θ =
$\Gamma_{\psi\psi\varphi_j}$ =
j
+
+
$\Gamma_{Y_iY_k\varphi_l}$ =
l
i
k
$\Gamma_{\psi Y_i\theta}$ =
i

Schematical description of the equations for mass and charge operators and vertex parts. Conventions: —— ψ field, - - - - φ field, ～～ θ field, ═══ Y field.

Employing Eqs. (23) and (24), we obtain the following equations for the effective charges

$$\lambda_1'/\lambda_1 = 5\lambda_1 + 4\lambda_2 + 3\lambda_3 - 4\lambda_3\sqrt{\lambda_2/\lambda_1},$$
$$\lambda_2'/\lambda_2 = 4\lambda_1 + 8\lambda_2 + 2\lambda_3 - 4\lambda_3\sqrt{\lambda_1/\lambda_2}, \tag{25}$$
$$\lambda_3'/\lambda_3 = 3\lambda_1/2 + \lambda_2 + 29\lambda_3/2 - 4\sqrt{\lambda_1\lambda_2}.$$

Again using two limiting momenta, it is possible to show that the initial conditions for the system of equations (25) are $\lambda_i(L_k) \ll 1$. To guarantee the validity of this conclusion, it is only necessary that the d_i'/d_i in Eqs. (24) are positive.

From Eqs. (25) it can be seen that if λ_1, λ_2 and λ_3 are of the same order, then all derivatives λ_1', λ_2', and λ_3' are positive and all charges λ_i decrease with diminishing momentum. If initial values of λ_i of different order are given at the limiting momenta Λ_k, for example, $\lambda_1(L_k) \gg \lambda_2(L_k)$; $\lambda_3(L_k) \sim \lambda_1(L_k)$, then as the momentum decreases, λ_2 will grow and λ_1 will diminish. Therefore, the point will come where the derivative of λ_2 changes sign and λ_2 also starts to decrease. Finally, if $\lambda_1(L_k)$ and $\lambda_2(L_k)$ are of the same order and $\lambda_3(L_k)$ is large, then λ_1 and λ_2 grow and λ_3 diminishes (with decreasing momentum). Therefore, the growth of λ_1 and λ_2 will become slower, and finally all three charges will decrease.

From this it is clear that qualitatively the situation does not differ from the theory with one pseudoscalar field, *i.e.*, all charges tend to zero with unlimited increase of L_k.

4. In all cases considered, the physical charge was equal to zero after the limiting momentum tended to infinity. For this two characteristics are important: (1) the positive sign of the derivative d'/d, which leads to a small effective charge at the momentum Λ_k and allows restriction to the approximation considered. This sign is a consequence of general features of the theory (see Ref. 5) and should be positive (the d-function grows) in all variants of the theory; (2) the further decrease of charges, for momenta less than Λ_k. This decrease of charges occurs in all examples considered, although the derivative λ'/λ, in general, contains terms of different signs. The case more complicated than that considered in Sec. 3, namely, the interaction of three fermion and three boson fields with different isotopic spins (0, ½, 1) does not lead to a different result. One might think that also the second characteristic is connected with general features of all variants of contemporary field theory.

We note that we required $L_p - L_k = \ln(\Lambda_p/\Lambda_k)$ to be large compared to unity, but finite. If we require the stronger condition, namely, $\ln(\Lambda_p/\Lambda_k) \to \infty$ as $\Lambda_p \to \infty$ and $\Lambda_k \to \infty$, then the physical charge will go to zero also for $\lambda' = 0(\xi < L_k)$ and even for $\lambda' < 0(\xi < L_k)$, provided only that $\ln(\Lambda_p/\Lambda_k)$ increases sufficiently rapidly as $\Lambda_p \to \infty$ and $\Lambda_k \to \infty$. If, however, this case actually occurs in some variant of the theory, then this signifies that there is ambiguity in the limiting transition from an extended interaction to a point one. In fact, setting $\Lambda_k = \Lambda_p$ in this case, we come to the conclusion that the physical charge can differ from zero.

The analysis of the different variants of the theory given above shows that the case $\lambda' \leq 0$ does not occur.

Thus, the construction of a meson theory with several nucleon and meson fields is apparently just as impossible as the construction, in the framework of modern quantum field theory, of a non-contradictory theory with one meson field.

The author would like to use this opportunity to express his gratitude to I. Ia. Pomeranchuk, who suggested the necessity of studying the theory with several fields, and also to V. B. Berestetskii, B. L. Ioffe, K. A. Ter-Martirosian and L. B. Okun' for discussion of a number of problems touched upon here.

---

[1] I. Ia. Pomeranchuk, Dokl. Akad. Nauk SSSR **103**, 1005; **104**, 51; **105**, 461 (1955); J. Exptl. Theoret. Phys. (U.S.S.R.) **29**, 869 (1955); Soviet Phys. JETP **2**, 739 (1956).

[2] A. A. Abrikosov and I. M. Khalatnikov, Dokl. Akad. Nauk SSSR **103**, 933 (1955).

[3] Landau, Abrikosov and Khalatnikov, Dokl. Akad. Nauk SSSR **95**, 497, 773, 1177 (1954)

[4] Abrikosov, Galinin and Khalatnikov, Dokl. Akad. Nauk SSSR **97**, 793 (1954); Galinin, Ioffe and Pomeranchuk, J. Exptl. Theoret. Phys. (U.S.S.R.) **29**, 51 (1955); Soviet Phys. JETP **2**, 37 (1956)

[5] H. Lehmann, Nuovo Cimento **11**, 342 (1954)

Translated by G. E. Brown
126

SOVIET PHYSICS JETP VOLUME 5, NUMBER 3 OCTOBER, 1957

Skin Effect in Thin Films and Wires

B. M. BOLOTOVSKII

P. N. Lebedev Physical Institute, Academy of Sciences, USSR

(Submitted to JETP editor February 9, 1956)

J. Exptl. Theoret. Phys. (U.S.S.R.) 32, 559-565 (March, 1957)

Equations are obtained for the skin effect in thin films and wires by using kinetic theory. A method is developed for the approximate solution of these equations which gives expressions for the impedance of thin films and wires.

1. A KINETIC theory of skin effect for bulk conductors was developed by Reuter and Sondheimer[1]. If $l \ll \delta_0$, where l is the electron free path in a metal and δ_0 is the classic skin layer depth, then the usual or normal skin effect occurs. If $l \gtrsim \delta_0$ or $l \gg \delta_0$, the skin effect is anomalous. In the case of samples of small size (wires of radius $R \lesssim l$ or films of thickness $h \lesssim l$), just as in the $\delta_0 \lesssim l$ case, it is impossible to the use the normal skin effect theory. Hence, the kinetic approach for thin films and wires is necessary for direct current[2-6]. Also the question arises of the behavior of small-size samples in an alternating field. Dingle[7] considered the question for the optical frequency case, taking only diffusion reflection of the electrons from the metal surface into account. The work of Azbel' and Kaganov[8] is also devoted to this question, where, as in Ref. 7, the passage of a plane electromagnetic wave through a film is analyzed. Hence, the impedance for this plane wave passage is calculated in these works. It is also interesting to determine the impedance of thin films and wires with respect to the high-frequency current flowing therein.

Below, we consider the conclusions to which kinetic theory leads for the case of skin-effect in thin conductors, *i.e.*, in such conductors as are much less thick than the free path length of the electrons in an unlimited metal. To be specific, let us visualize cylindrical wires of radius R and plane films of thickness h.

2. Let us direct the z axis parallel to the wire axis (or parallel to the film surface). Let us impose an electric field $E = E_z e^{i\omega t}$, directed along the z axis, on the sample. The quantity E_z is a function of the points in the wire cross section. If this function is known, then the energy losses in the conductor are characterized by the impedance*

$$Z = R + iX = (4\pi i\omega / c\alpha)\, E(P) / E'(P), \qquad (1)$$

where P is a point on the conductor surface, $E'(P)$ is the normal derivative relative to the conductor surface, and

$$\alpha = \begin{cases} 1 & \text{for a conducting half-space} \\ 2 & \text{for films} \\ 2\pi R & \text{for wires.} \end{cases} \qquad (2)$$

The real part of the impedance R gives the ohmic resistance of the conductor and the imaginary part X gives the inductance.

The classical skin effect theory, valid for $l \ll h$, $l \ll \delta_0$, leads to the following expression for films of thickness h:

$$Z = -\frac{2\pi i\omega}{c^2 k_0} \operatorname{ctg} k_0 \frac{h}{2} = -\frac{4\pi i\omega}{c^2 k_0^2 h}\left[1 - \frac{1}{12}(k_0 h)^2 - \cdots\right], \qquad (3)$$

$$k_0^2 = -2i / \delta_0^2 = -4\pi i\omega\sigma_0 / c^2, \qquad (4)$$

where σ_0 is the conductivity of the unlimited sample.

3. As shown in Refs. 2-6, if the lateral dimensions of the conductor become comparable to the free path length l, the direct current sample conductivity ($\omega = 0$) starts to depend on the lateral dimensions. For thin films with $h \ll l$, we have[2]:

$$\sigma = \sigma_0 \frac{3}{4} \frac{1+\varepsilon}{1-\varepsilon} \frac{h}{l} \ln \frac{l}{h} \quad (\text{if } \varepsilon \leqslant 1); \qquad (5)$$

$$\sigma = \sigma_0 \quad (\text{if } \varepsilon = 1),$$

where ε is the portion of the electrons reflected specularly from the sample surface. For thin wires with $R \ll l$, we have[4]:

$$\sigma \doteq \sigma_0 \frac{1+\varepsilon}{1-\varepsilon} \frac{2R}{l} \quad (\text{if } \varepsilon \leqslant 1); \quad \sigma = \sigma_0 \quad (\text{if } \varepsilon = 1). \qquad (6)$$

4. In deriving the skin effect equations, we used the Chambers method[5] which, being equivalent to the kinetic equations method, permits a whole set of intermediate calculations to be avoided. The generalization of the Chambers method to the case of a field dependent on the coordinates is made without difficulty. This method yields for the average velocity increment (in the z direction) taken by electrons arriving at a point M from P in the volume of the conductor (Fig. 1):

---

*We use the impedance definition $Z = E(P)/I$, which leads to (1) and (2) under the assumption of field symmetry over the wire cross-section. Consequently, we will always select the solutions corresponding to field symmetry subsequently.

$$\Delta v_z = \frac{e}{mv}\left[\int_a E(s)\,e^{-s/l}\,ds + \frac{\varepsilon e^{-a/l}}{1-\varepsilon e^{-b/l}}\int_b E(s)\,e^{-s/l}\,ds\right], \tag{7}$$

where $a = PM$ and the same notation is used as in Ref. 5. If E is independent of s, the result of Ref. 5 is obtained from (7).

The expression (7) permits the current at the point M to be expressed through E_z:

$$j_z(M) = \int v^2 dv d\,\Omega\, e v_z \frac{\partial f_0}{\partial v_z}\Delta v_z, \tag{8}$$

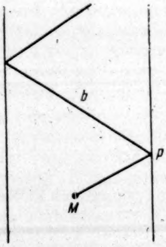

FIG. 1

where f_0 is the equilibrium distribution of the electrons in the metal. Substituting (8) in the equation for E_z

$$\Delta E_z + (\omega/c)^2 E_z = (4\pi i\omega/c^2)\,j_z,$$

we obtain an integro-differential equation for E_z. Let us give the final form of the equation. For films of thickness h:

$$\frac{d^2E}{\partial x^2} + \frac{\omega^2}{c^2}E = \frac{3i}{2\,\delta_0^2 l}\int_0^h E(x')\,[\varphi_1(x-x') + \varepsilon\varphi_2(x-x')]\,dx', \tag{9}$$

where $\varphi_1(x) = \int_1^\infty e^{-t|x|/l}\left(\frac{1}{t}-\frac{1}{t^3}\right)dt,$

$$\varphi_2^{(x)} = 2\int_1^\infty \frac{e^{-ht/l}}{1-\varepsilon e^{-ht/l}}\,\mathrm{ch}\,\frac{xt}{l}\left(\frac{1}{t}-\frac{1}{t^3}\right)dt. \tag{10}$$

For wires of radius R

$$\frac{d^2E}{dr^2} + \frac{1}{r}\frac{dE}{dr} + \frac{\omega^2}{c^2}E = \frac{3i}{2\pi\delta_0^2 l}\int_0^{2\pi} d\varphi\int_0^R E(r') \times [\varphi_1(|\mathbf{r}-\mathbf{r}'|) + \varepsilon\varphi_2(|\mathbf{r}-\mathbf{r}'|)]\,r'\,dr', \tag{11}$$

$$\varphi_1(|\mathbf{r}|) = \frac{2}{r}\int_1^\infty e^{-rt/l}\sqrt{t^2-1}\,\frac{dt}{t^3} = \frac{2}{r}S_3\left(\frac{r}{l}\right);$$

$$\varphi_2(|\mathbf{r}|) = \frac{2}{r}\int_1^\infty \frac{e^{-at/l}+e^{-bt/l}}{1-\varepsilon e^{-bt/l}}\,e^{-rt/l}\sqrt{t^2-1}\,\frac{dt}{t^3}. \tag{12}$$

In the expressions (12), S_3 is a function introduced in Ref. 4, **r** and **r′** are points in the wire cross section, b is the length of the chord drawn through **r** and **r′**, $b-a$ and a are segments into which the point **r** divides the chord (Fig. 2). We neglected the relaxation time in deriving these equations. The relaxation time can be taken into account if $l/(1-i\omega\tau)$ is written instead of l in (10) and (12) for φ_1 and φ_2. We will neglect the quantity $\omega\tau$ in comparison with unity below.

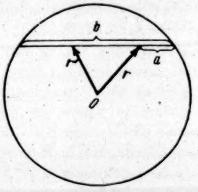

FIG. 2

5. Let us turn to the solution of the equations obtained. Let us first analyze Eq. (9) for the thin films. This equation is easily reduced to the integral equation

$$E(x) = \cos\frac{\omega}{c}\left(x-\frac{h}{2}\right) + \frac{3i}{2\,\delta_0^2 l}\int_0^h K(x,x')\,E(x')\,dx'; \tag{13}$$

$$K(x,x') = \frac{c}{\omega}\int_{h/2}^{x}\sin\frac{\omega}{c}(x-t)\,[\varphi_1(t-x') + \varepsilon\varphi_2(t-x')]\,dt. \tag{14}$$

It is easy to be convinced of the equivalence of (9) and (13) by calculating the quantity $E'' + (\omega/c)^2 E$ using (13). This quantity gives the right side of (9).

While the kernel of the original equation (9) would have a logarithmic singularity at $x = x'$, the kernel of Eq. (13) is bounded. If

$$\left| \frac{3ih}{2\delta_0^2 l} \max K(x, x') \right| < 1, \tag{15}$$

Eq. (13) can be solved by an iteration method. Putting $\cos \frac{\omega}{c}(x - \frac{h}{2}) = 1$ in the $h \ll c/\omega$ case, and taking $E_0 = 1$ for the zero approximation, we obtain

$$E(x) = 1 + \frac{3i}{2\delta_0^2 l} \int_0^h K(x, x') dx' \tag{16}$$

$$+ \left(\frac{3i}{2\delta_0^2 l} \right)^2 \int_0^h \int_0^h K(x, x') K(x', x'') dx' dx'' + \ldots$$

Substituting (16) in (1) for the impedance, we find the latter as the ratio of two power series in the parameter (15). In its turn, this ratio can be expanded in a power series in the same parameter. The first term of the expansion is independent of the field frequency ω and gives the ohmic resistance of the film to direct current:

$$Z_0 = \frac{1}{\sigma_0 l} \left[\frac{h}{l} \right. \tag{17}$$

$$\left. - \frac{3}{2}(1 - \varepsilon) \int_1^\infty \left(\frac{1}{t^3} - \frac{1}{t^5} \right) \frac{1 - e^{-ht/l}}{1 - \varepsilon e^{-ht/l}} dt \right]^{-1} = \frac{1}{\sigma h}.$$

This expression is equivalent to that obtained earlier by Sondheimer[6]. It can be used as a definition of the film conductivity σ in a direct current. The expression (5) for σ is obtained from (17) for $h \ll l$.

The evaluation of the next terms of the expansion of Z in powers of the parameter (15) appears to be somewhat complex. Let us give the results for the case of purely diffuse ($\varepsilon = 0$) and purely specular ($\varepsilon = 1$) reflection for $h \ll l$. In both cases,

$$Z = Z_0 [1 - (kh)^2 / 12 + \cdots], \tag{18}$$

where Z is defined by (17) and k by (4) if σ_0 is replaced by $\sigma(\varepsilon)$ according to (5). It is easy to see that the parameter (15) is the square of the ratio of the film thickness to the depth of field penetration into an unlimited sample with conductivity equal to the film conductivity.

As is seen from (3) and (18), the first terms of the impedance expansion in the normal skin effect case (h, $\sigma_0 \gg l$) agree with the terms of the impedance expansion for thin films ($h \ll l$, $\sigma \gg l$) with k replaced by k_0. The region of such "quasi-normal" skin effect in thin films appears to be broader than the region of normal skin effect in bulk conductors. Higher terms of the impedance expansion in powers of kh were not calculated. It should not be expected that the coefficients of the expansions (3) and (18) will agree exactly. As will be clear from the sequel, it can be imagined that they will be close in order of magnitude.

6. In order to determine the impedance at higher frequencies, it is convenient to use a less exact approximate method of solution which we will illustrate first by an example of a metallic half-space (a problem analyzed in Ref. 1). In this case, the skin effect equation is (for simplicity, we consider the reflection to be diffuse):

$$E'' + \frac{\omega^2}{c^2} E = \frac{3i}{2\delta_0^2 l} \int_0^\infty \varphi_1(x - y) E(y) dy. \tag{19}$$

As is seen from (19), the current intensity at the given point x is determined by the whole region near this point. The effective distance characterizing the size of this region equals (in order of magnitude):

$$\lambda = \int_0^\infty \varphi_1(x) x dx \Big/ \int_0^\infty \varphi_1(x) dx = \frac{3}{8} l \tag{20}$$

[see Eq. (10)]. In order to determine the impedance, we must know how the field itself behaves in the depth of the metal, even if values of the field and its derivative on the metal surface are essential. In the region close to the metal surface ($x = 0$), E satisfies the equation

$$E'' + \frac{\omega^2}{c^2} E = \frac{3i}{2\delta_0^2 l} \int_0^\infty \varphi_1(y) E(y) dy. \tag{21}$$

Let us replace the kernel $\varphi_1(y)$ by a function which equals a certain constant β in the limits from 0 to λ [Eq. (20)] and which becomes zero outside this range. Then (21) becomes:

$$E'' + \frac{\omega^2}{c^2} E = \frac{3i\beta}{2\delta_0^2 l} \int_0^\lambda E(y) dy. \tag{22}$$

This equation admits of a solution $E(x) = e^{-kx}$. Substitution in (22) gives an equation for k

$$k^2 + \omega^2/c^2 = (3i\beta/2\delta_0^2 lk)(1 - e^{-3kl/8}). \tag{23}$$

If $|kl| \ll 1$, *i.e.*, if the field attenuates at distances much larger than the free path length l, then (23) becomes

$$k^2 + (\omega/c)^2 = 9\,i\beta/16\delta_0^2. \tag{24}$$

Inasmuch as the classical skin-effect theory is valid in this case[1], the right side must be equal to $2i/\delta_0^2$. Hence, we find:

$$\beta = 32/9. \tag{25}$$

In the other extreme case, we obtain for $|kl| \gg 1$, neglecting displacement currents:

$$k = (16i/3\delta_0^2 l)^{1/3} = (\sqrt{3} + i)\,(2/3\delta_0^2 l)^{1/3}, \tag{26}$$

from which the impedance is

$$Z = 4\pi i\omega/c^2 k = (1 + i\sqrt{3})\,(3\pi^2 l\omega^2/4\sigma_0 c^4)^{1/3}. \tag{27}$$

According to exact theory[1],

$$Z = (1 + i\sqrt{3})\,(\sqrt{3}\,\pi l\omega^2/\sigma_0 c^4)^{1/3}. \tag{27a}$$

These values are very close. If both λ and β are considered as adjustable parameters, then exact agreement is obtained with the Reuter-Sondheimer theory for

$$\lambda = \sqrt{3}\,l/2\pi, \quad \beta = 8\pi/3\sqrt{3}.$$

It is understood that the agreement with exact theory can hold in the two extreme cases: $|kl| \gg 1$ and $|kl| \ll 1$ since the exact solution is slightly different from the exponential e^{-kx} only in these cases (see Ref. 1, Appendix III).

7. Let us use this rough theory in the thin film case ($h \ll l$). In this case, we can again write (22), where the film thickness h should be substituted as the upper limit of integration instead of λ [Eq. (20)]:

$$E''(h) + \frac{\omega^2}{c^2}E(h) = \frac{3i\beta}{2\delta_0^2 l}\int_0^h E(y)\,dy. \tag{28}$$

Let us look for the solution as $E = \cos k(x - h/2)$. Substituting this function into (28), again neglecting the term ω^2/c^2 in comparison with k^2, we obtain

$$k^3 \cos(kh/2) = (3i\beta/\delta_0^2 l)\sin(kh/2). \tag{29}$$

Hence, for $|kh| \ll 1$, we find

$$k^2 = 3i\beta h/2\delta_0^2 l. \tag{30}$$

As in Sec. 6, the constant β can be determined by requiring that the impedance agree with (17), obtained in Sec. 5 by the iteration method, $\omega \to 0$. This yields

$$\beta = \frac{4l\sigma}{3h\sigma_0} = \frac{4}{3}\frac{l}{h} \tag{31}$$

$$- 2\frac{l^2}{h^2}(1 - \varepsilon)\int_1^\infty \left(\frac{1}{t^3} - \frac{1}{t^5}\right)\frac{1 - e^{-ht/l}}{1 - \varepsilon e^{-ht/l}}\,dt.$$

In the $|kh| \gg 1$ case, we find

$$k = {}^1\!/_2(\sqrt{3} + i)\,(3\beta/\delta_0^2 l)^{1/3}. \tag{32}$$

In this case, we find for the impedance

$$Z = (1 + i\sqrt{3})\,(\pi^2\omega^2 h/4\sigma c^4)^{1/3}, \tag{33}$$

where σ is the static conductivity of the film of thickness h.

An approximate expression can be obtained from (27a) by replacing l by h and σ_0 by σ therein.

8. Simplifying (11) for thin wires ($R \ll l$) by the same method, we obtain:

$$\frac{d^2E}{dr^2} + \frac{1}{r}\frac{dE}{dr} + \frac{\omega^2}{c^2}E = \frac{3i\beta}{2\pi\delta_0^2 l}\int_0^R E(r')\,dr'. \tag{34}$$

We look for the solution of this equation as $E(r) = J_0(kr)$. Substituting $J_0(kr)$ in (34), we find:

$$\left(\frac{\omega^2}{c^2} - k^2\right)J_0(kr) = \frac{3i\beta}{2\pi\delta_0^2 l}\int_0^R J_0(kr')\,dr'. \tag{35}$$

Hence, again neglecting the quantity ω^2/c^2, we obtain for $|kR| \ll 1$:

$$k^2 = -3i\beta R/2\pi\delta_0^2 l. \tag{36}$$

Just as in the thin film case, we determine the constant β from the condition that the impedance at zero frequency should give the known expression[4] for the resistance of a thin wire. This yields

$$\beta = \frac{4\pi l\sigma}{3R\sigma_0} = \frac{8\pi}{3}\frac{1 + \varepsilon}{1 - \varepsilon}\ (\varepsilon \leqslant 1). \tag{37}$$

Hence, we obtain for $|kR| \gg 1$

$$Z \doteq \frac{1 + i\sqrt{3}}{2\pi R}\left(\frac{2\pi^2\omega^2 R}{c^4\sigma}\right)^{1/3}. \tag{38}$$

9. Let us discuss the results obtained. The parameter characterizing the skin effect in the conducting half-space case is the ratio l/δ_0, where δ_0 is the classical skin layer depth. As follows from our computations, the critical parameter in the thin conductors case is the ratio of the size of the conductor cross-section (film thickness h or wire radius R) to the depth of field penetration in a bulk conductor with the same static conductivity as in the thin conductor. Namely, if the depth of field penetration is large in comparison with the film thickness or with the wire radius [see inequality (15)], the analog of the classic skin effect holds with the difference, however, that the conductivity is determined by (5) and (6) in the thin conductor case. In this case, the field and the impedance can be found by a power series expansion in the parameter (15). As is easy to see, the real part of the impedance (the ohmic resistance) is expanded in even powers of the frequency ω in this case, just as in the classic skin effect case, and the imaginary part of the impedance, in odd powers of ω. The expansions for thick and thin films agree to the accuracy of terms of order $(kh)^2$ (with the difference that k_0 replaces k in the thick films case). The order of magnitude of the next terms of the expansion can be determined by using an approximate method explained in Secs. 6, 7 and 8. According to this method, the impedance of a thin sample can be obtained from the expansion (3) if we speak of a thin film and from a similar expansion for a wire, by replacing the conductivity of the unlimited sample σ_0 by the conductivity of a thin conductor σ. Hence, the normal skin effect theory can actually be used to estimate the impedance of thin samples in the frequency band under consideration. Let us note that the frequency band where such a quasi-classical skin effect occurs appears to be much broader than the region of classical skin effect in bulk conductors. Actually, condition (15) for a thin conductor or the corresponding condition $|kh| \ll 1$ ($|kR| \ll 1$) in the approximate method, is satisfied, as is easy to see, for a much larger frequency band than in the bulk conductor. A case is even possible when anamalous skin effect conditions are not generally realized in thin conductors. This occurs when condition (15) is violated at such high frequencies for which it is impossible to neglect the relaxation time and to take the relaxation time τ into account yields a condition analogous to the inequality (9) of Ref. 1, *i.e.*, again the classical skin effect condition.

When there is an anomalous skin effect region (as always occurs if the conductor is not too thin), the impedance of the thin conductors is expressed by the approximate formulas (33) and (38). In this case, the impedance depends on the thickness of the film wire. The impedances of thin wires and thin films are, respectively, proportional to

$$\frac{1}{R}\left[\frac{1-\varepsilon}{1+\varepsilon}\right]^{1/3} \text{and} \left[\frac{1-\varepsilon}{1+\varepsilon}\left(\ln\frac{l}{h}\right)^{-1}\right]^{1/3}.$$

The impedance of a thin film depends on h as $h^{1/3}$ and the impedance of a thin wire is proportional to $R^{-2/3}$ for $\omega=1$, $\sigma=\sigma_0$. The skin effect in a thin film was analyzed earlier by Ginzburg[9], where $\sigma_{\text{eff}}=\sigma_0\gamma h/l$ with $\gamma\approx 1$ was assumed for the thin film. As is clear from the above, $\gamma=\ln(l/h)$.

It is impossible to compare the conclusions obtained with the results of Dingle[7] and Azbel' and Kaganov[8] since they determined the impedance for the passage of a plane wave and not for a current as in the present work.

The author thanks V. L. Ginzburg for formulating the problem and for many discussions, V. P. Silin for discussions and also M. I. Kaganov for a number of interesting remarks.

---

[1] G. E. H. Reuter and E. H. Sondheimer, Proc. Roy Soc. (London) **195A**, 366 (1948)

[2] K. Fuchs: Proc. Camb. Phil. Soc. **34**, 100 (1938)

[3] D. K. C. MacDonald and K. Sarginson, Proc. Roy. Soc. (London) **203A**, 223 (1950)

[4] R. B. Dingle, Proc. Roy. Soc. (London) A, 201, 545 (1950)

[5] R. G. Chambers, Proc. Roy. Soc. (London) A, 202, 378 (1950)

[6] E. H. Sondheimer, Adv. in Phys. 1, 1 (1952)

[7] R. B. Dingle: Physica 19, 1187 (1953)

[8] M. Ia. Azbel' and M. I. Kaganov, Uchen. zap. Kharkov Univ., Works (Trudy), Physics section of Physics-Mathematica faculty, 6, 59 (1955)

[9] V. L. Ginzburg, J. Exptl. Theoret. Phys. (U.S.S.R.) 21, 979, 1951; Usp. Fiz. Nauk. 42, 169, 333 (1950); 48, 25 (1952)

[10] V. L. Ginzburg, G. P. Motulevich, Usp. Fiz. Nauk **55**, 469 (1955)

Translated by M. D. Friedman

SOVIET PHYSICS JETP VOLUME 5, NUMBER 3 OCTOBER, 1957

Concerning Some Possibilities of Formulation of a Relativistically Invariant Theory of Extended Particles

V. S. BARASHENKOV
Academy of Sciences, USSR

(Submitted to JETP editor, February 12, 1956)
J. Exptl. Theoret. Phys. (U.S.S.R.) **32**, 566-569 (March, 1957)

Various problems pertaining to the theory of extended particles are examined in the case of the classical (non-quantum) theory of interacting dynamically indeformable extended particles. Although the structure of the theory is not of the Hamiltonian type, a formulation in Lagrangian variables $\mathbf{x}_k$; $\dot{\mathbf{x}}_k$; A_μ; $\dot{A}_\mu$, as well as Hamiltonian variables $\mathbf{x}_k$; $\mathbf{p}_k$; A_μ; π_μ can be given. The possibility of a many time formalism is examined and the latter is found to be non-unique. However, in none of the cases was a transition to a single-time theory found and the system of equations of motion was found to be inconsistent.

---

1. LAGRANGIAN AND HAMILTONIAN VARIABLES.

NUMEROUS attempts to formulate a theory of extended particles are described in literature[1-8]. The search of possible ways leading in this direction is carried on up to the present time[2,8]. In the published works, however, the conditions of relativistic invariance are not sufficiently well formulated. The present work has for its aim the investigation of possible covariant formulations.

It is easy to obtain the equations of motion of the particles and of the field from the action principle[3,4]:

$$m_i du_{i\alpha}/ds_i - u_{i\beta}\int\limits_{-\infty}^{+\infty} F^{\alpha\beta}(x)\, G(x-x_i)\, d^4x = 0; \tag{1}$$

$$\partial^2 A_\alpha(x)/\partial x_\mu \partial x^\mu + \sum_i e_i \int\limits_{-\infty}^{+\infty} G(x-x_i)\, u_{i\alpha} ds_i = 0. \tag{2}$$

In contrast with the local interaction theory, where the equations of motion of the particles and of the field can be obtained from tha action principle

$$\delta S = \int \delta L(t)\, dt = 0, \tag{3}$$

with the function $L(t)$ defined in a unique way (with the exception of an irrelevant divergence), in a nonlocal theory the expression under the sign of integral in Eq. (3), that is, $L(t)$, can be represented in two basically different forms

$$S = \int L_i(t)\, dt = \int (\mathscr{L}_0(t) + \mathscr{L}'_i(t))\, dt; \tag{4}$$

$$\mathscr{L}'_1(t) = \sum_i \dot{e}_i v^\mu(t) \int A_\mu(x)\, G(x-x_i)\, d^4x; \tag{5}$$

$$\mathscr{L}'_2(t) = \sum_i e_i \int A_\mu(x)\, d^3x \int v_i^\mu(\tau)\, G(x-x_i(\tau))\, d\tau, \tag{6}$$

where $\mathfrak{L}_0(t)$ is the Lagrangian of the non-interacting particles and the field.

Making use of $L_1(t)$ we can obtain the equations of motion of the particles, but it is impossible to obtain the equations of motion of the field, since $\delta\mathfrak{L}'_1(t)/\delta A_\nu(x) = 0$. Using $L_2(t)$, on the other hand, we can obtain the equations of motions of the field but, since $\partial\mathfrak{L}'_2(t)/\partial \mathbf{v}_i = 0$, it is impossible to obtain the equations of motion of the particles. If we formally assume that the terms $\delta\mathfrak{L}'_1(t)/\delta A_\nu$ and $\partial\mathfrak{L}'_2(t)/\partial\mathbf{v}_i$ in the equations of motion vanish, then these equations can be written by means of one function $\mathfrak{L}(t) = \mathfrak{L}_0(t) + \mathfrak{L}'_1(t) + \mathfrak{L}'_2(t)$. In this case, however, $\mathfrak{L}$ does not approach the Lagrange function of the local theory $\mathscr{H}(t)$:

$$\mathscr{H}(t) = \sum_i e_i \int A_0(x)\, G(x-x_i)\, d^4x + \sum_i \sqrt{\mathbf{P}_i^2 + m_i^2} - \sum_i e_i \int A_\mu(x)\, v_i^\mu(\tau)\, G(x-x_i)\, d^3x\, d\tau + \mathscr{H}_0(t); \tag{7}$$

$$\mathbf{v}_i(\tau) = \mathbf{P}_i(\tau) / \sqrt{\mathbf{P}_i^2 + m_i^2}; \quad v_i^0 = 1; \qquad \mathbf{P}_i = \mathbf{p}_i - e_i \int \mathbf{A}(x)\, G(x-x_i)\, d^4x, \tag{8}$$

where $\mathscr{H}_0(t)$ is the Hamiltonian of the free electromagnetic field.

We shall further determine the Hamilton system of equations by means of a well-known procedure. In these equations, the dynamical variables $\mathbf{x}_i$; $\mathbf{P}_i$; A_μ; π_μ tend to the corresponding Hamiltonian variables of the local theory as $\lambda \to 0$; they can therefore be regarded as their generalization. Both in the "Lagrange" and in the "Hamilton" equations, however, the dynamical variables are taken for different moments of time, and the state of a physical system at the time t does not determine, in a unique way, the state of the system at the time $t+\delta t$.[10] The functions $\mathfrak{L}(t)$ and $\mathscr{H}(t)$ are only auxiliary functions and are useful for the study of the relativistically invariant generalizations of the theory.

2. MANY-TIME FORMULATION OF THE EQUATIONS OF MOTION.

A relativistically invariant generalization of the theory can be obtained within the framework of the many-time formalism of Dirac, Fock and Podolsk[4]. For this purpose, we shall generalize the Hamilton system of equations known from the local theory, making use of Eq. (7) in the following way:

$$\partial \mathbf{p}_i/\partial t_j = -\partial \mathscr{H}'_j(t_j)/\partial \mathbf{x}_i; \quad \partial \mathbf{x}_i/\partial t_j = \partial \mathscr{H}'_j(t_j)/\partial \mathbf{p}_i; \tag{9}$$

$$\partial P^\mu_k/\partial t_j = -\partial \mathscr{H}''_j(t_j)/\partial Q^\mu_k; \quad \partial Q^\mu_k/\partial t_j = \partial \mathscr{H}''_j(t_j)/\partial P^\mu_k; \tag{10}$$

$$\mathscr{H}'_j = e_j \int A_0(x)\, G(x-x_j)\, d^4x + \sqrt{\mathbf{P}_i^2 + m_j^2}; \tag{11}$$

$$\mathscr{H}''_j = -e_j \int A_\mu(x)\, d^3x \int v^\mu_j(\tau_j)\, G(x - x_j(\tau_j))\, d\tau_j; \tag{12}$$

$$A^\mu(x) = \sum_k \left\{ \frac{1}{k} P^\mu_k \cos(\mathbf{kx} - kt) + Q^\mu_k \sin(\mathbf{kx} - kt) \right\}, \tag{13}$$

v^μ_j being determined by Eq. (8).

Clearly, we have

$$\partial^2 A^\mu(X)/\partial X_\nu \partial X^\nu = 0, \tag{14}$$

where $\mathrm{X} = \{X, T, Z, T\}$ are the space-time coordinates of the field.

Equations (9) and (10) can be written in the form

$$m_i du^\mu_i/\partial s_j = e_i \delta_{ij} u_{i\nu} \int F^{\mu\nu}(x)\, G(x-x_i)\, d^4x - e_i e_j \int u^\mu_j(s_j)\, G(x-x_j)\, D \times (x-x_i)\, d^3x\, ds_j/\sqrt{1-v_j^2}, \text{ where } x_0 \equiv t_j; \tag{15}$$

$$dA^\mu(x)/dt_j = e_i \int u^\mu_j(s_j)\, D(x'-x) \times G(x'-x_j)\, d^3x'\, ds_j, \text{ where } x'_0 \equiv t_j. \tag{16}$$

Since for any relativistically invariant function we have $G(x) = \int g(k^2) e^{i\mathbf{kx}} d^4k$ and for any function $B(x)$ fulfilling Eq. (14) the following identity is true

$$\int B(x')\, G(x-x')\, d^4x' = B(x),$$

then the expression (11) does not differ from the Hamiltonian of the local theory, and the first term of the right-hand side of Eq. (15) can be written in the form*

$$e_i \delta_{ij} u_{i\nu} F^{\mu\nu}(X_i; t_1; t_2; \ldots).$$

It is important to note that the system of equations (9) and (10) [or (15) and (16)] is not the only possible many-time generalization of the single-time equations. For example, the equation

$$dA^\mu(x)/dt_j = e_i \int u^\mu_j(s_j)\, D(x_i - x') \times G(x'-x)\, d^3x'\, ds_j \quad \text{etc.}$$

may be chosen instead of Eq. (16). In all cases, however, the conclusions of Sec. 3 and 4 remain in remain in force.

3. IMPOSSIBILITY OF TRANSITION TO SINGLE-TIME EQUATIONS.

In transition to a single-time theory, it is necessary to take into account the fact that, for an arbitrary function $R(x; t_1; t_2; \ldots)$, we have

$$dR(x)/dt = \left\{ \left(d/dT + \sum_i d/dt_i \right) R(x; t_1; t_2; \ldots) \right\}_{t=T=t_i}.$$

Putting $R(x; t_1; \ldots) = dA^\mu(x; t_1; \ldots)/dT$ we obtain making use of Eqs. (14) and (16),

$$\partial^2 A^\mu(x)/\partial x_\nu \partial x^\nu + \sum_i e_i \int u^\mu_i(t_i; t)\, G(x - x_i(t_i))\, ds_i = 0, \tag{17}$$

where $u^\mu_i(t_i; t) = u^\mu_i(t_1; t_2; \ldots)|_{t=t_1=\ldots=t_{i-1}=t_{i+1}=\ldots;\, t_i \neq t}$.

The resulting equation does not coincide with Eq.

---

*This cannot be done if the form function depends on any four-dimensional vectors characterizing the system of interacting particles or their internal structure.

(2), since it is not permissible to equate t_i with t under the sign of integral. In an analogous way, for the Eq. (15), we obtain

$$m_i du_i^{\mu}/dt = e_i u_{i\nu} \int F^{\mu\nu}(x_i;\, t)\, G(x' - x_i)\, d^4x' \qquad (18)$$

$$= e_i u_{i\nu} F^{\mu\nu}(x_i),$$

which is different from Eq. (1). If we determine the first term on the right-hand side of Eq. (15) as follows:

$$e_i \delta_{ij} \int u_{i\nu}(s_i)\, G(x - x_i(s_i))\, F^{\mu\nu}(x')\, ds_i\, d^3x';\; x_0' = t_i,$$

then, in transition to the single time theory, Eq. (15) will be different from Eq. (18) as well as from Eq. (1).

4. CONDITIONS OF CONSISTENCY OF THE MANY-TIME EQUATIONS.

Similarly to the case of the theory dealing with point particles, the system of equations of motion can be integrated only if the Bloch conditions are fulfilled. From Eq. (10) and (15), we obtain, for $i \neq j$,

$$m_j \partial^2 P_k^{\mu}/\partial t_i \partial t_j = \qquad (19)$$

$$- e_j^2 e_i \int \sin(\mathbf{kx} - kt_j)\, v_i^{\mu}(\tau')\, \sqrt{(1 - \mathbf{v}_j^2(\tau))^3}$$

$$\times G(x - x_j(\tau))\, D(x' - x_j(\tau))\, G(x' - x_i(\tau'))$$

$$\times d^3(xx')\, d(\tau\tau'),$$

where

$$x_0 = t_j \neq \tau; \quad x_0' = t_i \neq \tau'.$$

The expression for $\partial^2 P_k^{\mu}/\partial t_j \partial t_i$ we can obtain from Eq. (19) by exchanging the indices i and j. It can be easily seen that, for $G(x) \neq \delta(x)$, the Bloch condition is not satisfied:

$$\partial^2 P_k^{\mu}/\partial t_i dt_j - \partial^2 P_k^{\mu}/\partial t_j \partial t_i \neq 0.$$

The actual choice of the generalization of Eqs. (1) and (2) in the form (9) and (10) does not impair the generality of discussion. Repeating the procedure analogous to that which leads to relation (19), it can easily be seen that the presence of a form-function, even if only in one of the equations of motion, which does not vanish in accordance with Eq. (17), always leads to an inconsistent system of equations.*

In conclusion I wish to express my gratitude to Prof. D. I. Blokhintsev for his interest and valuable advice, and to Prof. M. A. Markov for interesting comments concerning the various problems of the theory with the form-factor.

---

[1] G. Wataghin, Z. Physik **88**, 92 (1934)

[2] G. F. Chew, Phys. Rev. **95**, 1669 (1954)

[3] D. I. Blokhintsev, Vestn. Moscow State Univ. (phys) 77, 3 (1945); J. Phys. (U.S.S.R.) **10**, 162 (1946); J. Exptl. Theoret. Phys (U.S.S.R.) **16**, 480 (1946); **18**, 566 (1948)

[4] R. E. Peierls, 8th Conseil de Physique, Inst. Solvay p. 291 (1948); R. E. Peierls and H. McManus, Proc. Roy. Soc. (London) **195A**, 323 (1948); I. Irving, Proc. Phys. Soc. (London) **62**, 780 (1949)

[5] Iu. M. Shirokov, J. Exptl. Theor. Phys. (U.S.S.R.) **24**, 47 (1953)

[6] M. A. Markov, J. Exptl. Theor. Phys. (U.S.S.R.) **10**, 1311 (1940); **16**, 790 (1946); **21**, 11 (1951)

[7] M. A. Markov, J. Exptl. Theor. Phys. (U.S.S.R.) **25**, 527 (1953)

[8] M. A. Markov, Dokl. Akad. Nauk. SSSR **101**, 51, 449 (1955)

[9] M. A. Markov, J. Phys. **7**, 42 (1944)

[10] V. S. Barashenkov, J. Exptl. Theor. Phys. (U.S.S.R.) **31**, 694 (1956); Soviet Phys. JETP **4**, 599 (1957)

[11] W. Pauli, Nuovo Cimento **10**, 648 (1953)

[12] Y. Takahashi and H. Umezawa, Progr. Theor. Phys. **9**, 14, 501 (1953); C. Hayashi, Progr. Theor. Phys. **10**, 533 (1953); Y. Katayama, Progr. Theor. Phys. **10**, 31 (1953)

Translated by H. Kasha

128

---

*The attempts to obtain a covariant Lagrange or Hamilton system of equations by the method of Pauli[11] or by the generalized Young-Feldman method[12] have also been futile[10].

SOVIET PHYSICS JETP VOLUME 5, NUMBER 3 OCTOBER, 1957

Electron-Loss Probabilities for Multiply-Charged Ions

I. S. DMITRIEV
Moscow State University

(Submitted to JETP editor February 12, 1956)
J. Exptl. Theoret. Phys. (U.S.S.R) **32**, 570-575 (March, 1957)

The electron-loss probability for fast multiply-charged ions moving in a medium is considered. It is assumed that the loss probability depends only on the ratio of ion velocity to electron orbital velocity. Using this assumption, it is possible to compute the effects of electronic interactions between fast ions and matter by summing over individual electrons of the ion. Results of calculations of the mean charge, equilibrium charge distribution, specific ionization and range in air are presented for helium, lithium, beryllium, and nitrogen ions. The computed values are found to be in good agreement with the available experimental data.

IN analyzing the effects which arise in the passage of multiply-charged ions through matter, it is usually assumed that those electrons, the velocity of which is below a certain given value, are completely stripped while the remaining electrons remain with the ion, that is, the probability for electrons loss changes sharply at a given electron velocity. In the original theory, as given by Bohr[1], it was assumed that $v/v_e = 1$. Here v is the ion velocity for which the probabilities for electron capture and electron loss are equal and v_e is the orbital electron velocity, calculated on the basis of the Fermi-Thomas model. As more experimental data became available, the original Bohr criteria were refined. Thus, Branning, Knipp and Teller[2,3] have taken $v/v_e = \gamma$. However, γ is determined experimentally, and the values of this quantity in different ions and in a given ion are a function of velocity.

It is of great interest to find more general criteria for determining the electron-loss probabilities for fast multiply-charged ions. Starting from the fact that the interaction energy between individual electrons within the atom is small compared with the electronic binding energy, and neglecting the screening of inner electrons (this last assumption is somewhat debatable, especially for *K*-electrons, but is justifiable for strong ionization), we propose the following.

1. The probability for the loss of a given electron P, depends only on the ion velocity v and is independent of the loss of other electrons:

$$P = P(v)$$

2. The function $P(v/v_I)$ is the same for inner and outer electrons of all atoms. Here, v_I is the electron orbital velocity. Although the velocity of the electron depends on the degree of ionization, in what follows we will use the constant value $v_I = \sqrt{2I/\mu}$ derived from the ionization potential for a given electron I.

The form of the function $P(v/v_I)$ can be obtained from measurements of the mean charge of ions of atomic hydrogen as a function of velocity, that is, the case of ions with a single electron. The function $P(v/v_I)$ for hydrogen ions is somewhat different in different media. In the following analysis use will be made of the function $P(v/v_I)$ measured in air[4-6]. For the hydrogen ion $v_I = v_0 = e^2/h = 2.19 \times 10^8$ cm/sec.

The ratio of the electron-loss cross section for a given level to the capture cross section for the same level may be written in the form

$$\sigma_{\text{loss}}/\sigma_{\text{cap}} = P/(1-P), \tag{1}$$

that is, this quantity also depends only on the velocity of the ion. Gluckstern[7] has determined the electron-capture and loss cross-sections for multiply-charged ions experimentally and has also calculated these quantities on the basis of the Fermi-Thomas model; however, in the work of this author these quantities appear as cross-sections summed over all electrons in the loss case and over all unfilled levels in the capture case and the present analysis does not apply directly.

In a multiply-charged ion the loss probability for each electron, P, can be obtained as a function of velocity by multiplying the abscissa $P(v/v_0)$ by the corresponding orbital velocity for the electron v_I. In this case, the density of the medium must be such that the time between charge-exchange collisions does not allow reforming of the electron shells[8].

Using these assumptions it is possible to calculate the mean charge $\bar{z}$, the equilibrium charge distribution Φ, the specific ionization dE/dx and the range R of multiply-charged ions as a function of velocity. Below, we present the results of these calculations for helium, lithium, beryllium and nitrogen ions and certain values for oxygen and fluorine ions.

For a given velocity the mean ion charge is found by summing the loss-probabilities over all electrons, that is,

$$\bar{z} = \sum_{i=1}^{z} P_i . \qquad (2)$$

In Fig. 1 is shown the dependence of $\bar{z}$ on velocity for the ions He, Li, Be, and N. In this same figure, we plotted the experimental values of $\bar{z}$ for helium in hydrogen, air, and mica and for nitrogen in nickel, in the thin organic film, in Formvar and in nitrogen.

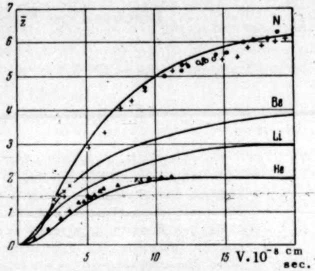

FIG. 1. Dependence of $\bar{z}$ on velocity for He, Li, Be and N ions. ▲ measured values of $\bar{z}$ for helium ions in hydrogen, air and mica[9,10]. Measurements of $\bar{z}$ for nitrogen ions: + in nickel[11], ○ in thin organic films[12], ● in Formvar[13], × in nitrogen[14].

TABLE I

Ion	N^{14}			O^{16}		F^{19}
V.10^{8} cm/sec.	14,3	13,7	13,2	14,3	8,6	14,3
$\bar{z}$ experimental.	5,49	5,40	5,35	6,22	4,86	6,63
$\bar{z}$ calculated from Eq.(2)	5,73	5,65	5,58	6,38	4,86	6,94
$\bar{z}$ calculated in Ref. 12 using assumption "a".	5,88	5,86	5,84	6,78	5,68	7,63
The same using assuption "b".	5,26	5,18	5,12	5,83	4,52	6,36

Table 1 shows values of $\bar{z}$ as measured in a thin organic film for N^{14}, O^{16} and F^{19} ions[12] and as calculated from Eq. (2). For comparison purposes, in this same table are given values of $\bar{z}$ calculated in Ref. 12 on the basis of the Fermi-Thomas statistical model under the assumptions that a) the electrons with smallest binding are stripped and b) the outermost electrons are stripped.

The equilibrium charge distribution Φ_i, that is, the fraction of ions with a charge i, is found by summing the quantities φ_{ij} – the fractions of ions with charge i for different fixed configurations of the remaining electrons j.

$$\Phi_i = \sum_{j=1}^{C_z^i} \varphi_{ij} = \sum_{j=1}^{C_z^i} \left[\prod^{i} P_k \prod_{k+q}^{z-i} (1-P_q)\right]. \qquad (3)$$

For example, we obtain the following expressions for the equilibrium charge distribution for lithium ions

$$\Phi_0 = (1-P_1)(1-P_2)(1-P_3),$$

$$\Phi_1 = P_1(1-P_2)(1-P_3) + P_2(1-P_1)(1-P_3) + P_3(1-P_1)(1-P_2),$$

$$\Phi_2 = P_1P_2(1-P_3) + P_1P_3(1-P_2) + P_2P_3(1-P_1),$$

$$\Phi_3 = P_1P_2P_3.$$

The number of terms in the sum for Φ_i is equal to the number of components C_z^i; however, some of the P_i are unity and the corresponding φ_{ij} become zero.

In Table 2 are shown the values of the equilibrium distributions obtained with thin films using nitrogen, oxygen and fluorine ions[12]. The experimental values of Φ (expressed in percent) are listed in the columns marked "a" and those calculated from Eq. (3) are in the columns marked "b".

The equilibrium charge distribution as a function of velocity is shown in Fig. 2 a–b for helium, lithium, beryllium and nitrogen ions. (The absence of

TABLE II

Ion	N^{14}						O^{16}				F^{19}	
$V.10^{-8}$ cm/sec.	14.3		13.7		13.2		14.3		8.6		14.3	
i	a	b	a	b	a	b	a	b	a	b	a	b
1		0		0		0		0		0,06		0
2		0		0		0		0		2,1		0
3	0,4	0,2	0,2	0,2	0,5	0,3		0,04	4,5	8,6		0,02
4	6,0	4,1	7,5	5,6	8,6	6,6	0,5	0,1	26,4	24,8		0,5
5	45,6	35,8	50,1	38,0	51,7	39,9	14,0	13,6	47,5	36,4	8,8	5,9
6	40,5	44,6	36,6	42,7	34,3	41,1	51,8	41,9	21,6	22,7	32,6	24,2
7	7,5	15,3	5,6	13,5	4,9	12,4	30,3	35,6	0	4,9	46,5	41,7
8							3,4	8,8	0	0,3	10,8	23,6
9											1,3	4,1

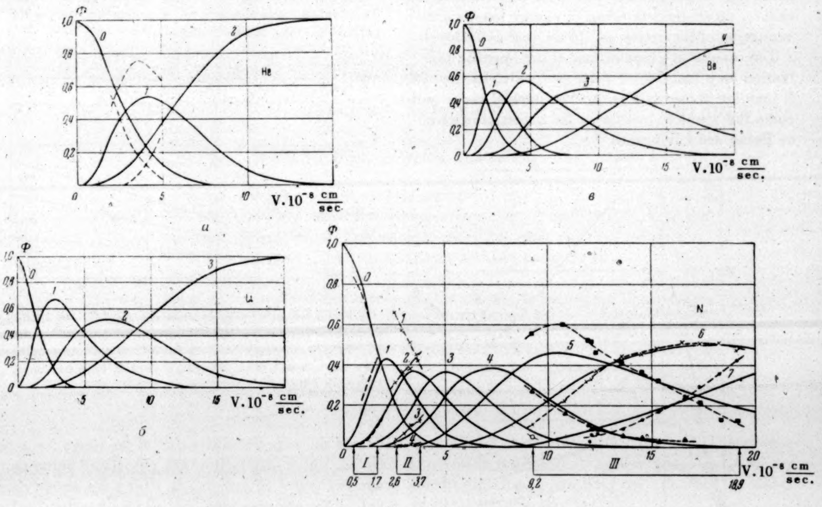

FIG. 2. Equilibrium charge distribution as a function of velocity: a) helium ions; the dashed curves pertain to the experimental values of Φ measured in air[15]; b) lithium ions; c) beryllium ions; d) nitrogen ions; the dashed curves denote the experimental values of Φ: I) $0.5 \leqslant v \leqslant 1.7 \times 10^8$ cm/sec. Measurements in nitrogen[6]. In calculating the equilibrium distribution it has been assumed that $\Phi_3/\Phi_2=0$; II) $2.6 \leqslant v \leqslant 3.7 \times 10^8$ cm/sec. Measurements in nitrogen; it is assumed that at these velocities $\Phi_0=0$[14]; III) $9.2 \leqslant v \leqslant 18.9 \times 10^8$ cm/sec. Measurements in Formvar[13].

data on the magnitude of the neutral component of the nitrogen ion beam[14] obviously leads to a high value for the singly and doubly-charged components.)

The experimental curves for the equilibrium distribution start systematically at ion velocities higher than the calculated values. This may be explained by the fact that the inner electrons are shielded by the outer electrons; for equal values of the ratio v/v_I it should be more difficult to remove inner electrons.

Inasmuch as a beam of multiply-charged ions, moving in a medium, consists of component beams with charge $i = 0, 1, 2 \ldots z$, between which dynamic equilibrium obtains, the specific ionization is found by summing over all component beams, that is

$$\frac{dE}{dx} = N\left(\sum_{i=1}^{z} \Phi_i i^2\right)\sigma_e, \qquad (4)$$

where the sum of squares of the charges, taken with appropiate weighting factors Φ_i is multiplied by the quantity σ_e the specific electron stopping cross-section calculated by Knipp and Teller[2], and by N – the number of atoms per cm^3 of the medium (in this procedure, no account is taken of energy losses due to excitation of the atoms and to nuclear collisions).

The results of calculations of the specific ionization as a function of velocity for He, Li, Be and N ions are shown in Fig. 3. The dashed curve indicates the specific ionization for α-particles given by Bethe and Livingston[16].

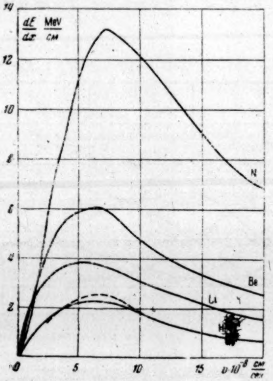

FIG. 3. Specific ionization due to ions as a function of ion velocity. The dashed curve pertains to the specific ionization of α-particles given in Ref. 16.

Numerical integration of the specific ionization gives the range of the ion in the medium

$$R = \int_0^E \frac{1}{dE/dx}\,dE. \qquad (5)$$

In Figs. 4 and 5 are shown the range-energy relations for He^4, Li^8, Be^9 and N^{14} ions in air. The points denote the experimental value of the range for α-particles, which differs from the calculated value by approximately 10 percent. In Fig. 4 are shown range values for nitrogen ions obtained by Blackett and Lees in a Wilson cloud chamber[17]. In Fig. 5 are also shown range values calculated for Li^8 ions in air[18] and N^{14} ions in a photo-emulsion[19]. The range-energy curve for Li^8 given by Kuznetsov, Lukirskii, and Perfilov[20] lies considerably below the calculated curve.

In conclusion it should be noted that the calculated results, in general, are in satisfactory agreement with the available experimental data; the discrepancies which are observed in a number of cases can be attributed to limitations imposed by the assumptions which have been used and to experimental errors.

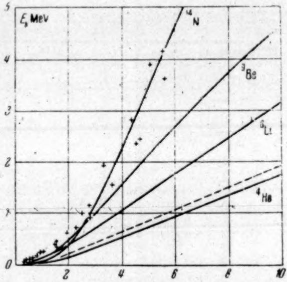

FIG. 4. Range-energy relation for ions (in *mm* of air). The dashed curve denotes the experimental values for helium[16], + the same for nitrogen[17].

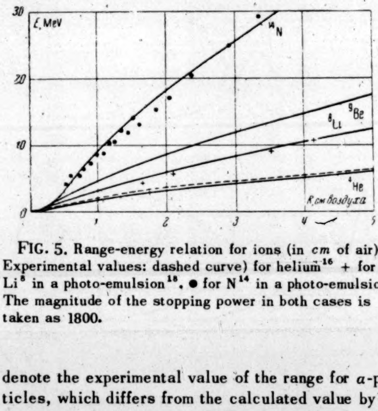

FIG. 5. Range-energy relation for ions (in *cm* of air). Experimental values: dashed curve) for helium[16] + for Li^8 in a photo-emulsion[18]. ● for N^{14} in a photo-emulsion[19]. The magnitude of the stopping power in both cases is taken as 1800.

[1] N. Bohr, Phys. Rev. **58**, 654 (1940); **59**, 270 (1941)

[2] D. Knipp and E. Teller, Phys. Rev. **59**, 659 (1941)

[3] Brannings, Knipp and Teller, Phys. Rev. **60**, 657 (1941)

[4] H. Bartels, Ann. Physik **13**, 373 (1932)

[5] H. Kanner, Phys. Rev. **84**, 1211 (1951)

[6] Stier, Barnett and Evans, Phys. Rev. **96**, 973 (1954)

[7] R. L. Gluckstern, Phys. Rev. **98**, 1817 (1955)

[8] N. Bohr and J. Lindhard, Kgl. Danske Videnskab. Selskab., Mat.-fys. Medd **28**, 7 (1954)

[9] P. L. Kapitza, Proc. Roy. Soc. (London) **106**, 602 (1924)

[10] E. Rutherford, Phil. Mag. **47**, 277 (1924)

[11] Reynolds, Scott and Zucker, Phys. Rev. **95**, 671 (1954)

[12] K. G. Stephens and D. Walker, Proc. Roy. Soc. (London) **229A**, 376 (1955)

[13] Reynolds, Wyly and Zucker, Phys. Rev. **98**, 474 (1955)

[14] Korsunskii, Pivovar, Markus and Leviant, Dokl. Akad. Nauk SSSR **103**, 399 (1955)

[15] E. Snitzer, Phys. Rev. **89**, 1237 (1953)

[16] H. A. Bethe and M. S. Livingston, Rev. Mod. Phys. **9**, 245 (1937)

[17] P. M. S. Blackett and D. S. Lees, Proc. Roy. Soc. (London) **134A**, 658 (1932)

[18] W. H. Barkas, Phys. Rev. **89**, 1019 (1953)

[19] H. L. Reynolds and A. Zucker, Phys. Rev. **96**, 393 (1954)

[20] Kuznetsov, Lukirskii and Perfilov, Dokl. Akad. Nauk SSSR **100**, 665 (1955)

Translated by H. Lashinsky
129

SOVIET PHYSICS JETP VOLUME 5, NUMBER 3 OCTOBER, 1957

Inelastic Proton-Proton Scattering

IU. I. KULAKOV
Moscow State University

(Submitted to JETP editor February 12, 1956)
J. Exptl. Theoret. Phys. (U.S.S.R.) **32**, 576-83 (March, 1957)

The problem of inelastic proton-proton scattering at 690 Mev is considered. It is assumed that in the intermediate state an isobar is formed which decays into a nucleon and π-meson. Limiting the consideration to isobars in S-states, using the laws of conservation of angular momentum and parity, and taking into account the Pauli principle, it was found possible to obtain the angular distribution of scattered nucleons, with the introduction of only one arbitrary constant.

INTRODUCTION

WE base our consideration of proton-proton scattering on the experimental fact[1] of the existence of an excited state of the nucleon (isobar) with ordinary and isotopic spins equal to 3/2. We consider further that in the collision process an isobar with a definite mass $M = 1.31$* is formed in an S-state. Neglect of P- and D-state isobars is possible for energies of the incident nucleon not greatly exceeding the 650 Mev threshold energy for formation on an isobar with mass $M = 1.31$. In connection with this, all calculations were carried out for an incident proton energy of 690 Mev, which is the energy obtained on the accelerator of the Institute for Nuclear Problems, Academy of Sciences. The assumptions made proved to be sufficient to obtain an angular distribution, containing one arbitrary constant, for the scattered protons.

It must be noted, however, that because of the finite lifetime of the isobar ($\sim 10^{-23}$sec) the energy spectrum and angular distribution of the scattered protons at 690 Mev should be rather strongly smeared out, and only upon increasing the energy of the incident protons to 800 Mev and above does the picture become more clear cut.

1. KINEMATICAL CALCULATION

We consider collisions of two particles of mass m_1 and m_2 such that two new particles of mass M_1 and M_2 are formed in place of the initial ones. Let one of the particles (say, m_2) be at rest, and the other in motion, having energy E. Then, making use of the laws of energy and momentum conservation, it is possible to show that the energy of the new particle of mass M_1 emerging at angle φ_1 is equal to

---

*An absolute mass unit corresponding to 931 m_e is taken as mass and energy unit.

$$E_1 = \frac{Em_2 + A_1 \pm M_1 \frac{E^2 - m_1^2}{E + m_2} \cos^2\varphi_1 \left[1 - \frac{M_1^2 (E + m_2)^2 - (Em_2 + A_1)^2}{M_1^2 (E^2 - m_1^2) \cos^2 \varphi_1} \right]^{1/2}}{E + m - \cos^2 \varphi_1 (E^2 - m_1^2) / (E + m_2)}, \tag{1.1}$$

$$A_1 = (M_1^2 - M_2^2 + m_1^2 + m_2^2) / 2.$$

a) *Formation of isobars.* The production of an isobar in the collision of two nucleons takes place as a result of one of the six following processes

$$\begin{tikzcd}[row sep=small] & I^{++} + n \\ p + p \arrow[ur] \arrow[dr] & \\ & I^{+} + p \end{tikzcd} , \quad \begin{tikzcd}[row sep=small] & I^{+} + n \\ p + n \arrow[ur] \arrow[dr] & \\ & I^{0} + p \end{tikzcd} ,$$

$$\begin{tikzcd}[row sep=small] & I^{0} + n \\ n + n \arrow[ur] \arrow[dr] & \\ & I^{-} + p \end{tikzcd}$$

All of these processes occur with different probabilities, but are kinematically equivalent, if the neutron-proton mass difference is neglected. It can be shown that in proton-proton scattering the ratio of probabilities of production of the isobars I^{++} and I^+ is 3 : 1. In fact, we have

$$\Psi_{1,1} = C_{1,1}^{3/2,\, 1/2;\, 1/2,\, 1/2} \Phi_{3/2,\, 1/2} \chi_{1/2,\, 1/2} \tag{1.2}$$

$$+ C_{1,1}^{3/2,\, 3/2;\, 1/2,\, -1/2} \Phi_{3/2,\, 3/2} \chi_{1/2,\, -1/2},$$

where $\Psi_{1,1}$ is the wave function of the system in the intermediate state, $\Phi_{3/2,\, I_z}$ and $\chi_{1/2,\, I_z}$ are the wave functions of the isobar and nucleon, respectively, with isotopic spin projection I_z. Using the expressions for the Clebsch-Gordan coefficients[2] we obtain

$$\Psi_{1,1} = -\frac{1}{2} \Phi_{3/2,\, 1/2} \chi_{1/2,\, 1/2} + \frac{\sqrt{3}}{2} \Phi_{3/2,\, 3/2} \chi_{1/2,\, -1/2}, \tag{1.3}$$

from which

$$\sigma(I^+, p) = {}^1\!/_3\, \sigma(I^{++}, n). \tag{1.4}$$

The expression for the energies of the nucleons scattered through angle θ_1 is obtained from the general formula (1.1) by substituting

$$\varphi_1 = \theta_1, \quad m_1 = m_2 = M_1 = 1, \quad A_1 = (3 - M^2) / 2.$$

With the 60 Mev half-width[1] of the isobar level taken into account, the energy E_1 of the scattered nucleons depends on the incident energy E as shown on Fig. 1 for $\theta_1 = 15°$ and $M = 1.26$, 1.31, 1.37. From this figure it can be seen that the presence of the isobar changes the spectrum of the scattered nucleons substantially. Thus, in the case of elastic scattering, the energy of the nucleons scattered through $\theta = 15°$ will be simply 712 Mev for $E = 800$ Mev. If an isobar of mass M lying in the interval $1.26 < M < 1.37$ is produced in the collision of nucleons, then a maximum, which splits into two with increasing incident energy, should appear in the energy spectrum of the scattered nucleons (see Fig. 2).

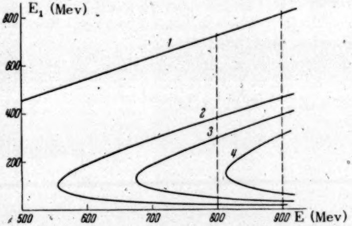

FIG. 1. Dependence of the energies of the scattered nucleons on the energies of incident nucleons for M equal to: *1* – 0; *2* – 1.26; *3* – 1.31; *4* – 1.37.

b) *Decay of isobars.* The isobar decay into nucleon and π-meson proceeds in the following way:

$$I^{++} \to p + \pi^+, \quad \begin{tikzcd}[row sep=small] & p + \pi^0 \\ I^{+} \arrow[ur] \arrow[dr] & \\ & n + \pi^+ \end{tikzcd} , \quad \begin{tikzcd}[row sep=small] & n + \pi^0 \\ I^{0} \arrow[ur] \arrow[dr] & \\ & p + \pi^- \end{tikzcd} ,$$

$$I^- \to n + \pi^-.$$

If only proton-proton scattering is considered, then only the first three processes take place.

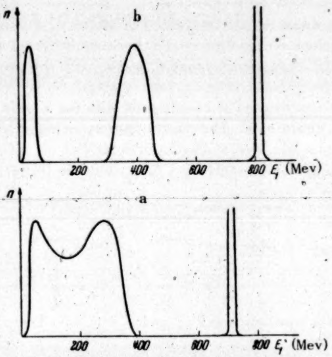

FIG. 2. Setting in of the splitting of the maximum in the energy spectrum of the scattered nucleons for energies E of the incident nucleons equal to: a – 800 Mev and b – 900 Mev.

Using, as in the case of formation of the isobar, the isotopic spin formalism, it is possible to show that the probabilities of the second and third processes are in the ratio 2 : 1, i.e.,

$$^1/_2\, \sigma(p, \pi^0) = \sigma(n, \pi^+). \tag{1.5}$$

Thus, if proton-proton scattering proceeds by way of isobar formation, then from (1.4) and (1.5) it follows that the probabilities of the processes

$$p + p \rightarrow p + n + \pi^+ \quad \text{and}$$
$$p + p \rightarrow p + p + \pi^0$$

are in the ratio of 5 : 1.

In order to obtain an expression for the energies of nucleons and mesons, coming from the decay of isobars, it is necessary to substitute in the formula (1.1): for nucleons

$$\varphi_1 = \theta, \quad m_1 = M; \quad m_2 = 0, \quad M_1 = 1,$$
$$M_2 = \mu = 0{,}142,$$
$$A = {}^1/_2 (M^2 + 1 - \mu^2);$$

for mesons

$$\varphi_1 = \theta_2, \quad m_1 = M, \quad m_2 = 0, \quad M_2 = 1,$$
$$M_1 = \mu = 0{,}142,$$
$$A = {}^1/_2 (M^2 - 1 + \mu^2).$$

2. FORMATION OF ISOBARS

We determine the probability of formation of isobars with a given spin projection on the direction of motion taking into account only S-scattering in the final state. We designate the scattering matrix which transforms the incident wave into the scattered one by

$$(\mathbf{n}, S_{n_0} \mid R \mid \mathbf{n}_0, S^0_{n_0}),$$

were $\mathbf{n}_0$ and $\mathbf{n}$ are the unit vectors in the direction of motion of the particle before and after collision in the center of mass system; $S^0_{n_0}$ and S_{n_0} are the projections of total spin of the system on direction $\mathbf{n}_0$ before and after collision.

In order to characterize all possible spin states, we introduce the index r, denoting: $r = 1$ – singlet ($S = 0$) state of the two nucleons, $r = 2$ – triplet ($S = 1$) state of the two nucleons, $r = 3$ – triplet ($S = 1$) state of the isobar and nucleon, $r = 4$ – quintet ($S = 2$) state of the isobar and nucleon.

In order to use the conservation of total angular momentum j and its projection m, we expand the scattering matrix in terms of the orthonormal system of eigenfunctions $J^r_{jm}(\mathbf{n}, S_n)$:

$$(\mathbf{n}, S_{n_0} | R | \mathbf{n}_0, S^0_{n_0}) = \sum_{j,\, m,\, r} \sum_{j_0,\, m_0,\, r_0} (j, m, r \mid R \mid j_0, m_0, r_0) \times J^r_{jm}(\mathbf{n}, S_{n_0}) \overset{+}{J}{}^{r_0}_{j_0 m_0}(\mathbf{n}_0, S^0_{n_0}). \tag{2.1}$$

Using the fact that, because of the conservation of j and m and the lack of a preferred direction, $(j, m, r \,|R|\, j_0, m_0, r_0)$ has the form

$$(j, m, r \mid R \mid j_0, m_0, r_0) = (r \mid R_j \mid r_0)\, \delta_{jj_0} \delta_{mm_0}, \tag{2.2}$$

we obtain

$$(\mathbf{n}, S_{n_0} \mid R \mid \mathbf{n}_0, S^0_{n_0}) = \sum_{j,\, r,\, r_0} (r \mid R_j \mid r_0)\, W^{r, r_0}_j (\mathbf{n}, S_{n_0}; \mathbf{n}_0, S^0_{n_0}),$$
$$W^{r, r_0}_j (\mathbf{n}, S_{n_0}; \mathbf{n}_0, S^0_{n_0}) = \sum_{m=-j}^{j} J^r_{jm}(\mathbf{n}, S_{n_0}) \overset{+}{J}{}^{r_0}_{j_0 m_0}(\mathbf{n}_0, S^0_{n_0}). \tag{2.3}$$

For $j = 0$ a single state with $l = S$ corresponds to each r. For $j = 1$ the state $r = 1 (S = 0)$ can be obtained in only one way ($l = 1$). The states $r = 2, 3$ ($S = 1$) are possible for the three values $l = 0$, 1, 2. The values

$l=1, 2, 3$ correspond to the state $r=4\,(S=2)$. For $j=2$, one value $l=2$ corresponds to the state $r=1$ $r=1\,(S=0)$. The states $r=2,3\,(S=1)$ are possible for three values $l=1, 2, 3$ and, finally, the state $r=4$ is possible for five values $l=0, 1, 2, 3, 4$[*].

Together with the authors of Refs. 3 and 4 we will consider that a pseudoscalar isobar is formed in the nucleon collision process. Then, because of conservation of parity, all matrix elements corresponding to transitions with changes of l of ± 1, $\pm 3 \ldots$ should be zero.

Thus, 4 complex or 8 real constants enter into the description of the transition: nucleon + nucleon → isobar + nucleon (in S-states). However, the situation alters materially if one considers the collision of two identical nucleons. In this case it is necessary to take into account the Pauli principle, according to which all matrix elements corresponding to initial states with even S and odd l and with odd S and even l are zero.

Considering that the contribution of terms with $l>0$ is small in the final states, we find that one[**] real parameter C is sufficient to describe the collision of two identical nucleons.

Thus, in the collision of two identical nucleons, the scattering matrix has the form

$$(\mathbf{n}, S_{n_0} \mid R \mid \mathbf{n}_0, S^0_{n_0}) = C W_2^{4,1}(\mathbf{n}, S_{n_0}; \mathbf{n}_0, S^0_{n_0}). \quad (2.4)$$

Using the well known expression for spherical vectors[5], we obtain

$$J^4_{2m}(\mathbf{n}, S_{n_0}) = Y_{0,0}(\mathbf{n})\,\Phi^{(2)}_m(S_{n_0}),$$

$$J^1_{2m}(\mathbf{n}, S_{n_0}) = Y_{2m}(\mathbf{n}), \quad (2.5)$$

where $\Phi^{(2)}_m(S_{n_0})$ are spin functions corresponding to total spin $S=2$ and projection $S_{n_0}=m$.

Thus, the operator $W_2^{4,1}(\mathbf{n}, S_{n_0}; \mathbf{n}_0, S^0_{n_0})$ can be written as

$$W_2^{4,1}(\mathbf{n}, S_{n_0}; \mathbf{n}_0, S^0_{n_0}) = (4\pi)^{-1/2} \sum_m \Phi^{(2)}_m(S_{n_0})\, Y^*_{2m}(\mathbf{n}_0). \quad (2.6)$$

If the Z-axis is directed along $\mathbf{n}_0$, then

$$W_2^{4,1}(\mathbf{n}, S_{n_0}; \mathbf{n}_0, S^0_{n_0}) = (\sqrt{5}/4\pi)\,\Phi^{(2)}_0(S_{n_0}). \quad (2.7)$$

But since we are interested in states with spin projections on the direction $\mathbf{n}$, because different angular distributions correspond to states with different spin projections, it is necessary to transform $\Phi^{(2)}_0(S_{n_0})$ to the new system of coordinates with the Z-axis along the direction $\mathbf{n}$. The matrix corresponding to the irreducible representation of order l of the rotation through Euler angles φ_1, θ, φ_2, has the following form[6]

$$T^l = e^{-im\varphi_1} P^l_{mn}(\cos\theta)\, e^{-in\varphi_2},$$

$$P^l_{mn}(x) = A(1-x)^{-(n-m)/2}(1+x)^{-(n+m)/2} \frac{d^{l-n}}{dx^{l-n}} \times [(1-x)^{l-m}(1+x)^{l+m}]. \quad (2.8)$$

In our special case $l=2$ and $\varphi_1 = \varphi_2 = 0$. Therefore, we have

$$\Phi'(S_n) = T^2\Phi^{(2)}_0(S_{n_0}) = -\frac{1}{2}\sqrt{\frac{3}{2}}\sin^2\theta\,(\Phi^{(2)}_{-2}(S_n) + \Phi^{(2)}_2(S_n)) + i\sqrt{\frac{3}{2}}\sin\theta\cos\theta\,(\Phi^{(2)}_{-1}(S_n) + \Phi^{(2)}_1 \times (S_n)) + \frac{1}{2}(3\cos^2\theta - 1)\,\Phi^{(2)}_0(S_n).$$

Now (see Ref. 2)

$$\Phi^{(2)}_{\mp 2}(S_n) = \Phi_{\mp 3/2}(\Sigma_n)\,\chi_{\mp 1/2}(\sigma_n),$$

$$\Phi^{(2)}_{\mp 1}(S_n) = \frac{1}{2}\Phi_{\mp 3/2}(\Sigma_n)\,\chi_{\mp 1/2}(\sigma_n) + \frac{\sqrt{3}}{2}\Phi_{\mp 1/2}(\Sigma_n)\,\chi_{\mp 1/2}(\sigma_n),$$

$$\Phi^{(2)}_0(S_n) = \frac{1}{\sqrt{2}}\Phi_{-1/2}(\Sigma_n)\,\chi_{1/2}(\sigma_n) + \frac{1}{\sqrt{2}}\Phi_{1/2}(\Sigma_n)\,\chi_{-1/2}(\sigma_n).$$

Thus, the probabilities of different states corresponding to different projections of the spin of the isobar Σ_n and spin of the nucleon σ_n on the direction $\mathbf{n}$ are equal to

$$\begin{array}{lll} {}^3/_8\sin^4\theta & \text{for } \Sigma_n = \mp {}^3/_2, & \sigma_n = \mp {}^1/_2; \\ {}^3/_8\sin^2\theta\cos^2\theta & \text{for } \Sigma_n = \mp {}^3/_2, & \sigma_n = \mp {}^1/_2; \\ {}^9/_8\sin^2\theta\cos^2\theta & \text{for } \Sigma_n = \mp {}^1/_2, & \sigma_n = \mp {}^1/_2; \\ {}^1/_8(3\cos^2\theta - 1)^2 & \text{for } \Sigma_n = \mp {}^1/_2, & \sigma_n = \mp {}^1/_2 \end{array} \quad (2.9)$$

and, summing over the two possible projections of the nucleon spin, we obtain

$$\begin{array}{ll} {}^3/_8\sin^2\theta & \text{for } \Sigma_n = \pm {}^3/_2, \\ {}^3/_8\cos^2\theta + {}^1/_2 & \text{for } \Sigma_n = \mp {}^1/_2. \end{array} \quad (2.10)$$

Integrating the expression obtained over all solid angle, we find that the total probabilities of states with spin projections of the isobar ± 3/2 and ± 1/2 are the same.

---

[*] The coefficients $(r|R_j|r_0)$ for $j \geqslant 3$ are not considered because after collision the state with $l=0$ (S-scattering) is not possible for $j \geqslant 3$.

[**] In general, C is a complex number, but in so far as the absolute value of the phase is not important, only the modulus of C need be considered.

3. DECAY OF THE ISOBAR

The determination of the differential cross section for decay of an isobar into a nucleon and π-meson is most simple in the center-of-mass system of the isobar. According to Ref. 7, the components of the wave function of the isobar in the center of mass system are

$$S_z = \frac{3}{2}: \quad B_1 = \frac{1}{\sqrt{2}}\begin{pmatrix}1\\0\\0\\0\end{pmatrix}; \quad B_2 = \frac{1}{\sqrt{2}}\begin{pmatrix}i\\0\\0\\0\end{pmatrix}; \; B_3 = B_4 = 0;$$

$$S_z = \frac{1}{2}: \quad B_1 = \frac{1}{\sqrt{6}}\begin{pmatrix}0\\1\\0\\0\end{pmatrix}; \quad B_2 = \frac{1}{\sqrt{6}}\begin{pmatrix}0\\i\\0\\0\end{pmatrix}; \quad B_3 = \frac{1}{\sqrt{6}}\begin{pmatrix}-2\\0\\0\\0\end{pmatrix}; \; B_4 = 0; \tag{3.1}$$

$$S_z = -\frac{1}{2}: \quad B_1 = \frac{1}{\sqrt{6}}\begin{pmatrix}1\\0\\0\\0\end{pmatrix}; \quad B_2 = \frac{1}{\sqrt{6}}\begin{pmatrix}-i\\0\\0\\0\end{pmatrix}; \quad B_3 = \frac{1}{\sqrt{6}}\begin{pmatrix}0\\2\\0\\0\end{pmatrix}; \; B_4 = 0;$$

$$S_z = -\frac{3}{2}: \quad B_1 = \frac{1}{\sqrt{2}}\begin{pmatrix}0\\1\\0\\0\end{pmatrix}; \quad B_2 = \frac{1}{\sqrt{2}}\begin{pmatrix}1\\-i\\0\\0\end{pmatrix}; \; B_3 = B_4 = 0. \tag{3.1'}$$

If the 4-momentum of the π-meson in the center of mass system of the isobar is designated by q_μ, then the matrix element of the transition can be written

$$U = g\psi^+ q_\mu B_\mu. \tag{3.2}$$

Using the above expressions for B_μ, we have

$$S_z = \frac{3}{2}: \quad q_\mu B_\mu = -\frac{1}{\sqrt{2}} q \sin\theta\, e^{i\varphi}\begin{pmatrix}1\\0\\0\\0\end{pmatrix};$$

$$S_z = \frac{1}{2}: \quad q_\mu B_\mu = \frac{1}{\sqrt{6}} q \begin{pmatrix}2\cos\theta\\-\sin\theta e^{i\varphi}\\0\\0\end{pmatrix}; \tag{3.3}$$

$$S_z = -\frac{1}{2}: \quad q_\mu B_\mu = -\frac{1}{\sqrt{6}}\begin{pmatrix}\sin\theta e^{-i\varphi}\\2\cos\theta\\0\\0\end{pmatrix};$$

$$S_z = -\frac{3}{2}: \quad q_\mu B_\mu = -\frac{1}{\sqrt{2}} q \sin\theta e^{-i\varphi}\begin{pmatrix}0\\1\\0\\0\end{pmatrix},$$

where $q = |\mathbf{q}|$ and θ, φ are the angles defining the direction of motion of the nucleon in the center of mass system of the isobar.

Substituting in (3.2) definite values of ψ and $q_\mu B_\mu$, corresponding to particular orientations of the spins of nucleon and isobar, we obtain the matrix elements and, consequently, the probabilities of various transitions. Thus, we have

$$\begin{aligned} &W_{3/2,\,1/2} = {}^1/_2 \sin^2\theta, && W_{3/2,\,-1/2} = 0,\\ &W_{1/2,\,1/2} = {}^2/_3 \cos^2\theta, && W_{1/2,\,-1/2} = {}^1/_6 \sin^2\theta\\ &W_{-1/2,\,1/2} = {}^1/_6 \sin^2\theta, && W_{-1/2,\,-1/2} = {}^2/_3 \cos^2\theta,\\ &W_{-1/2,\,1/2} = 0, && W_{-3/2,\,-1/2} = {}^1/_2 \sin^2\theta, \end{aligned} \tag{3.4}$$

where $W_{S_z,\,\sigma_z}$ is the probability of decay of an isobar with spin projection S_z into a π-meson and nucleon with spin projection σ_z.

Summing over different orientations of nucleon spins, we obtain

$$W_{3/2} = \sin^2\theta, \quad W_{1/2} = {}^4/_3 \cos^2\theta + {}^1/_3 \sin^2\theta, \tag{3.5}$$

where $W_{3/2}$, $W_{1/2}$ are the probabilities of decay of an isobar with $|S_z| = 3/2,\ 1/2$.

4. TRANSITION TO THE LABORATORY SYSTEM

The probability $w^1_{S_z}(\psi)$ of formation of an isobar in the laboratory coordinate system is connected with the probability of formation $W^1_{S_z}(\psi')$ in the system of the center of mass of the colliding nucleons by the following relation

$$W^1_{S_z}(\psi')\sin\psi'\,d\psi' = w^1_{S_z}(\psi)\sin\psi\,d\psi, \tag{4.1}$$

whereas there is the following relation between the angles of emergence of the isobars ψ' and ψ in the different systems:

$$\cos\psi' = (P(\psi)\cos\psi - p/2)/(P^2(\psi) - pP(\psi)\cos\psi + p^2/4)^{1/2}, \quad (4.2)$$

where $P(\psi)$ is the momentum of the isobar, p the momentum of the incident nucleon. But in the laboratory system, to each ψ correspond two values of $P(\psi)$ (P^+ and P^-) and consequently, also two values of ψ'. In this connection, we definite $w^1_{S_z,\lambda}$ to be the probability, in the laboratory system, of formation of an isobar with spin projection S_z and momentum P^+, if $\lambda=1$, and P^-, if $\lambda=2$.

If the total probability of formation of an isobar is normalized to unity, then

$$w^1_{\frac{3}{2},\lambda} = \frac{3}{16\pi}\sin^2\psi\,\frac{1-\frac{K_\lambda}{2}\left(\cos\psi+\frac{1}{P_\lambda}\frac{dP_\lambda}{d\psi}\sin\psi\right)}{(1-K_\lambda\cos\psi+K_\lambda^2/4)^{5/2}},$$
$$w^1_{\frac{1}{2},\lambda} = \frac{\left(\frac{1+3\cos^2\psi}{4}-K_\lambda\cos\psi+\frac{K_\lambda^2}{4}\right)\left(1-\frac{K_\lambda}{2}\left(\cos\psi+\frac{1}{P_\lambda}\frac{dP_\lambda}{d\psi}\sin\psi\right)\right)}{4\pi(1-K_\lambda\cos\psi+K_\lambda^2/4)^{5/2}}, \quad (4.3)$$
$$K_\lambda(\psi) = p/P_\lambda(\psi).$$

The transition from the center-of-mass system of the isobar to the system where the Z-axis coincides with the direction of flight of the isobar in the laboratory system is accomplished in an analogous fashion.

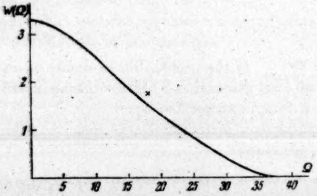

FIG. 3. Angular distribution of the scattered protons in the laboratory system.

Thus, we let $w^1_{S_z,\lambda}(\psi)$ be the probability of formation of an isobar with momentum P_λ in the laboratory system, and $w^2_{S_z,\lambda,\mu}(\theta)$ be the probability of formation of a nucleon with momentum $p_\mu(\theta)$ ($\mu=1$ for p_+ and $\mu=2$ for p_-) as a result of decay of an isobar of type S_z, λ in the system of coordinates connected with the direction of motion of the isobar. Then the probability of emergence of the nucleon at angle Ω in the laboratory system relative to the direction of the incident nucleon is equal to

$$W(\Omega) = \sum_{S_z,\lambda,\mu}\int w^1_{S_z,\mu}(\psi)\, w^2_{S_z,\lambda,\mu}(\theta)\, d\psi\, d\theta, \quad (4.4)$$
$$\cos\theta = \cos\Omega\cos\psi + \sin\Omega\sin\psi\sin\varphi.$$

In order to simplify the calculation of the double integral Eq. (4.4) we replace the probabilities $w^1_{S_z,\lambda}(\psi)$ by δ-functions, corresponding to the most probable angles, taking the exact expressions for $w^2_{S_z,\lambda,\mu}(\theta)$. The results of such calculations are given on Fig. 3. In order to evaluate such an approximation, a numerical integration of the expression Eq. (4.4) was carried out for a single value $\Omega = 18°$. It turned out that the error coming from the replacement mentioned above was 16%.

In conclusion, I should like to use this opportunity to express my deep gratitude to Iu. A. Gol'fand and Acad. I. E. Tamm for valuable advice and critical remarks and constant interest in this work.

---

[1] Anderson, Martin and Nagle, Phys. Rev. 91, 155 (1953)

[2] L. D. Landau and E. M. Lifshitz, *Quantum Mechanics*, GITTL, 1948

[3] Minami, Nakano, Nishijima, Okonogi and Yamada, Prog. Theor. Phys. 8, 531 (1952)

[4] Tamm, Gol'fand and Fainberg, J. Exptl. Theoret. Phys. (U.S.S.R.) 26, 649 (1954)

[5] A. I. Akhiezer and V. B. Berestetskii, *Quantum Electrodynamics*, GITTL, Moscow, (1953)

[6] I. M. Gel'fond and Z. Ia. Shapiro, Usp. Matem. Nauk. 7, (1952)

[7] V. L. Ginzburg, J. Exptl. Theoret. Phys. (U.S.S.R.) 13, 33 (1943)

Translated by G. E. Brown
130

SOVIET PHYSICS JETP VOLUME 5, NUMBER 3 OCTOBER, 1957

The Application of the Microcanonical Distribution to the Statistical Theory of Multiple Production of Particles

V. B. MAGALINSKII AND IA. P. TERLETSKII
Moscow State University
Institute for Nuclear Problems, Academy of Sciences, USSR

(Submitted to JETP editor February 12, 1956)
J. Exptl. Theoret. Phys. (U.S.S.R.) **32**, 584-591 (March, 1957)

The general statistical method of the microcanonical distribution is applied to the problem of the computation of statistical weights for the reactions of production of π-mesons in collisions of nucleons with nucleons. A general formula is derived for computation of the statistical weight of a state with an arbitray set of particles, considering not only the laws of conservation of energy and momentum, but also the different type of statistics for fermions and bosons. In allowing all particles to obey Boltzmann statistics, this general formula reduces to the formula proposed in Ref. 2. In particular, corrections are found which are due to consideration of the type of statistics for all possible collision processes of nucleons with nucleons, in which not more than three mesons are created.

THE statistical theory of multiple production of mesons proposed by Fermi[1], was made more exact by a series of authors[2-4]. The most general formula for computation of the statistical weights of processes of different multiplicity was put forth by Lepore and Stuart[2].

In contrast to Ref. 1, the authors of Ref. 2 took into account exactly not only the law of conservation of energy, but also the law of conservation of momentum for particles of arbitrary mass; however, both in Ref. 1 and in Ref. 2, the different type of statistics for fermions and bosons was not considered. For calculation of the statistical weights in Refs. 1 and 2, a method was used which is suitable only for a set of particles obeying Boltzmann statistics.

For calculating the probabilities of the states of a system with different numbers of particles, taking into account both the conservation laws and the type of statistics, it is simpler to use the general statistical method of Gibbs. In the given case, for a system with exactly given total energy and total momentum, it is obviously necessary to use the formula for the microcanonical distribution. We shall use this distribution to derive a more general formula than that of Lepore and Stuart. We shall consider the general case of a system in which there may exist and be created particles of several kinds, both bosons and fermions, having arbitrary masses. Finally, after an analysis of the general properties of the expressions for the probabilities of different states with given numbers or particles, several applications of the derived formulas to the processes of multiple production of π-mesons will be considered.

1. THE MICROCANONICAL DISTRIBUTION

Let us consider a system consisting of ν kinds of noninteracting particles having masses $m_1, m_2, \ldots$ The total energy E of the system and the total momentum $\mathbf{P}$ is given, but the total number of particles of arbitrary kind is in no way limited. Let the discrete set of vectors $\mathbf{p}_s$ (*i.e.*, $\mathbf{p}_s', \mathbf{p}_s'', \ldots$) represent all possible momenta of one particle of type s. Inasmuch as the particles do not interact with each other, the set of vectors $\mathbf{p}_s$ also represents the possible states of the whole system, while the set of occupation numbers $n_s(\mathbf{p}_s)$ completely determines the state of the system under consideration.[*] The probability of a given set of occupation numbers can be represented in the form

$$w\{n_1(\mathbf{p}_1), n_2(\mathbf{p}_2), \ldots, n_\nu(\mathbf{p}_\nu)\}$$
$$= A\delta\left\{E - \sum_{s=1}^{\nu}\sum_{\mathbf{p}_s}\varepsilon_s(\mathbf{p}_s)\, n_s(\mathbf{p}_s)\right\}\delta\left\{\mathbf{P} - \sum_{s=1}^{\nu}\sum_{\mathbf{p}_s}\mathbf{p}_s n_s(\mathbf{p}_s)\right\}$$
$$\times\prod_{s=1}^{\nu}\Omega_s\{n_s(\mathbf{p}_s)\}, \quad (1)$$

where δ is the Dirac δ-function; A a normalization factor; $\Omega_s\ \{n_s(\mathbf{p}_s)\}$ is the multiplicity of a state with given $\mathbf{p}_s$; $\varepsilon_s(\mathbf{p}_s) = (\mathbf{p}_s^2 + m_s^2)^{1/2}$ is the energy of this state*; the summation over $\mathbf{p}_s$ is taken over all permitted values of this vector and over all states of polarization.

---

[*] Particles having the same momentum $\mathbf{p}_s$ can be found in different states of polarization; therefore it is necessary to keep in mind that to each vector $\mathbf{p}_s$ correspond g_s independent states.

Obviously, both in the case of Bose statistics and in the case of Fermi statistics $\Omega_s = 1$ on account of the indistinguishability of the particles. But in the case of Boltzmann statistics,

$$\Omega_s\{n_s(\mathbf{p}_s)\} = \Big[\sum_{\mathbf{p}_s} n_s(\mathbf{p}_s)\Big]!\prod_{\mathbf{p}_s}[n_s(\mathbf{p}_s)!]^{-1}, \tag{2}$$

where the product is taken over all $\mathbf{p}_s$.

The probability of a state in which there are N_1 particles of the first kind, N_2 particles of the second kind, *etc.*, is clearly equal to

$$W_{N_1N_2\ldots N_\nu} = \sum_{n_1,\, n_2,\, \ldots} w\{n_1(\mathbf{p}_1), \ldots, n_\nu(\mathbf{p}_\nu)\}\prod_{s=1}^{\nu}\delta\Big\{N_s - \sum_{\mathbf{p}_s} n_s(\mathbf{p}_s)\Big\}, \tag{3}$$

where $\delta\{N\} = \delta_{N0}$ is the Kronecker symbol; the summation is carried out over all occupation numbers, *i.e.*,

$$\sum_{n(\mathbf{p})} f\{n(\mathbf{p})\} = \sum_{n'}\sum_{n''}\ldots f(n', n'', \ldots),$$

whereby in the cases of Boltzmann and Bose statistics all $n^{(k)}$ run through the values 0, 1, 2, 3, ...; in the case of Fermi statistics, however, only the two values $n^{(k)} = 0, 1$ are allowed. Obviously from the normalization conditions

$$\sum_{N_1,\, N_2,\, \ldots = 0}^{\infty} W_{N_1N_2\ldots N_\nu} = \sum_{n_1,\, n_2,\, \ldots} w\{n_1(\mathbf{p}_1), \ldots, n_\nu(\mathbf{p}_\nu)\} = 1, \tag{4}$$

and, consequently, according to Eqs. (1) and (4),

$$W_{N_1N_2\ldots N_\nu} = \sigma(E, \mathbf{P}; N_1, \ldots, N_\nu) \Big/ \sum_{N_1,\, N_2,\, \ldots = 0}^{\infty} \sigma(E, \mathbf{P}; N_1, \ldots, N_\nu), \tag{5}$$

where σ is the statistical weight determined by

$$\sigma(E, \mathbf{P}; N_1, \ldots, N_\nu) = \sum_{n_1,\, n_2,\, \ldots} \delta\Big\{E - \sum_{s=1}^{\nu}\sum_{\mathbf{p}_s}\varepsilon_s n_s(\mathbf{p}_s)\Big\} \times \delta\Big\{\mathbf{P} - \sum_{s=1}^{\nu}\sum_{\mathbf{p}_s} p_s n_s(\mathbf{p}_s)\Big\}\prod_{s=1}^{\nu}\delta\Big\{N_s - \sum_{\mathbf{p}_s} n_s(\mathbf{p}_s)\Big\} \times \Omega_s\{n_s(\mathbf{p}_s)\}. \tag{6}$$

Noting that the δ-function and the δ-symbol can be represented in the form

$$\delta(x) = \frac{1}{2\pi}\int_{-\infty - i\beta}^{+\infty - i\beta} e^{i\alpha x}\, d\alpha, \quad \delta\{N\} = \frac{1}{2\pi}\int_0^{2\pi} e^{i\varphi N}\, d\varphi,$$

where β is a small, positive quantity, set equal to zero in the final equation,* we get

$$\sigma(E, \mathbf{P}; N_1, \ldots, N_\nu) = \frac{1}{(2\pi)^{4+\nu}}\int_{-\infty - i\beta}^{+\infty - i\beta}\iiint_{-\infty}^{+\infty} \times \underbrace{\overbrace{\int\ldots\int}^{2\pi}}_{0} \exp\Big\{i\Big(\alpha E + \mathbf{b}\mathbf{P} + \sum_{s=1}^{\nu}\varphi_s N_s\Big) + \sum_{s=1}^{\nu}\Phi_s(\alpha, \mathbf{b}, \varphi_s)\Big\}\, d\alpha\, d\mathbf{b}\, d\varphi_1 \ldots d\varphi_\nu, \tag{7}$$

$$e^{\Phi_s(\alpha,\, \mathbf{b},\, \varphi_s)} = \sum_{n_s}\prod_{\mathbf{p}_s}\exp\{-in_s(\mathbf{p}_s)[\alpha\varepsilon_s(\mathbf{p}_s) + \mathbf{b}\mathbf{p}_s + \varphi_s]\}\,\Omega_s\{n_s(\mathbf{p}_s)\}. \tag{8}$$

The last sums can be easily calculated both in the case of Fermi and Bose statistics and in the case of Boltzmann statistics. For Fermi and Bose statistics, $\Omega_s = 1$, but it is necessary to sum over all $n_s^{(k)} = 0, 1$ in the former case and over all $n_s^{(k)} = 0, 1, 2, 3, \ldots$ in the latter. Carrying out these summations we get

$$\Phi_s(\alpha, \mathbf{b}, \varphi_s) = \pm\sum_{\mathbf{p}_s}\ln\{1 \pm \exp(-i[\alpha\varepsilon_s(\mathbf{p}_s) + \mathbf{b}\mathbf{p}_s + \varphi_s)]\}. \tag{9}$$

Here as in what follows, the upper sign refers to the case of Fermi statistics and the lower sign to the case of Bose statistics. But in the case of Boltzmann statistics, according to Eqs. (2) and (8), we get

---

*Here a system of units has been chosen in which the velocity of light $c = 1$.

* The introduction of a small parameter β enables one, in integrations to come, to avoid a pole, analogously to the way this was done in Ref. 4.

$$\Phi_s(\alpha, \mathbf{b}, \varphi_s) = \sum_{\mathbf{p}_s} \exp\{-i[\alpha\varepsilon_s(\mathbf{p}_s) + \mathbf{b}\mathbf{p}_s + \varphi_s]\} + \ln N_s! \,. \tag{10}$$

Expanding the logarithm after the summation sign in Eq. (9) into a series and interchanging the order of summation, we obtain for the Fermi and Bose cases*

$$\Phi_s(\alpha, \mathbf{b}, \varphi_s) = \sum_{k=1}^{\infty} k^{-1} (\mp 1)_s^{k+1} \sum_{\mathbf{p}_s} \exp\{-i[\alpha\varepsilon_s(\mathbf{p}_s) + \mathbf{b}\mathbf{p}_s + \varphi_s]k\}, \tag{11}$$

from which it is seen that the case of Boltzmann statistics corresponds to a limitation of the series (11) to only the first term, with addition of a term $\ln N_s!$.

If the linear dimensions L of the volume of space $V = L^3$ occupied by the gas are sufficiently large, or if, in a finite volume, the energy is sufficiently large that the de Broglie wavelengths of the different particles are small compared with L, then the summation over p in Eq. (11) can be replaced by integration and instead of (11) one can take the approximate expression

$$\Phi_s(\alpha, \mathbf{b}, \varphi_s) = \sum_{k=1}^{\infty} k^{-1} (\mp 1)_s^{k+1} \frac{g_s}{\omega} \int \exp\{-i[\alpha\varepsilon_s(\mathbf{p}) + \mathbf{b}\mathbf{p}_s + \varphi_s]k\}\, d\mathbf{p}_s, \tag{12}$$

where $\omega = (2\pi\hbar/L)^3$ is the volume of the elementary cell in momentum space. Introducing the notation

$$B_s(km_s, \alpha, \mathbf{b}) = \frac{g_s k^3}{\omega} \int \exp\{-i[\alpha(\mathbf{p}_s^2 + m_s^2)^{1/2} + \mathbf{b}\mathbf{p}_s]k\}\, d\mathbf{p}_s, \tag{13}$$

we have in place of Eq. (12)

$$\Phi_s(\alpha, \mathbf{b}, \varphi_s) = \sum_{k=1}^{\infty} k^{-4} (\pm 1)_s^{k+1} e^{-ik\varphi_s} B_s(km_s, \alpha, \mathbf{b}). \tag{14}$$

It is possible to carry out the integration over the angular variables in the space of the vector $\mathbf{p}_s$, as a result of which we obtain

$$B_s = \frac{g_s k^3}{\omega} \frac{2\pi}{ikb} \int_{-\infty}^{+\infty} \exp\{ik[bp - \alpha\sqrt{p^2 + m_s^2}]\}\, p\,dp = \frac{2\pi^2 g_s (km_s)^2 \alpha}{\alpha^2 - b^2} H_2^{(2)}[km_s(\alpha^2 - b^2)^{1/2}], \tag{15}$$

where $H_2^{(2)}[x]$ is Hankel function. (For an analogous transformation, see Ref. 4).

To compute σ, according to Eq. (7) it is necessary to calculate the intermediate integrals

$$I_s(\alpha, \mathbf{b}) = \frac{1}{2\pi} \int_0^{2\pi} \exp\{iN_s\varphi_s + \Phi_s(\alpha, \mathbf{b}, \varphi_s)\}\, d\varphi_s, \tag{16}$$

where Φ_s is determined by means of Eqs. (14) and (15).

Carrying out the change of variables $z = e^{-i\varphi}$, we get, according to the calculus of residues,

$$I_s = -\frac{i}{2\pi} \int_{C^+} z^{-N_s-1} e^{\Phi_s(z)}\, dz = \frac{1}{N_s!} \left[\frac{d^{N_s}}{dz^{N_s}} e^{\Phi_s(z)}\right]_{z=0}, \tag{17}$$

where the cymbol C^+ denotes that the integration is taken counterclockwise along the contour $|z| = 1$.

Putting Eq. (17) into Eq. (7), and integrating over all directions of the vector b, in analogy with Eq. (15), we get

$$\sigma(E, \mathbf{P}; N_1, \ldots, N_\nu) = \frac{2}{(2\pi)^3} \int_0^{\infty} \int_{-\infty-i\beta}^{+\infty-i\beta} \frac{\sin bP}{bP} e^{i\alpha E} \times \prod_{s=1}^{\nu} \left[\frac{1}{N_s!} \frac{d^{N_s}}{dz^{N_s}} e^{\Phi_s(z)}\right]_{z=0} b^2\,db\,d\alpha. \tag{18}$$

On account of Eqs. (14) and (15), the last formula can be written in the following final form:

$$\sigma(E, \mathbf{P}; N_1, \ldots, N_\nu) = \frac{2}{(2\pi)^3} \int_0^{\infty} \int_{-\infty-i\beta}^{+\infty-i\beta} \frac{\sin bP}{bP} e^{i\alpha E} \times \prod_{s=1}^{\nu} \left[\frac{1}{N_s!} \frac{d^{N_s}}{dz^{N_s}} \times \exp\left\{\frac{2\pi^2 g_s \alpha}{\omega(\alpha^2 - b^2)} \sum_{k=1}^{\infty} k^{-4} (\mp 1)_s^{k+1} \times (km_s)^2 H_2^{(2)}[km_s(\alpha^2 - b^2)^{1/2}]\, z^k\right\}\right]_{z=0} b^2\,db\,d\alpha. \tag{19}$$

Inasmuch as it is necessary in the case of Boltzmann statistics to limit oneself, according to Eq. (10), to only the first term in the sum over k in the exponent of the integrand, and to add $\ln N_s!$ to it in this case

---

*Here $(\pm 1)_s = -1$ for all s designating particles obeying Fermi statistics, and $(\pm 1)_s = +1$ correspondingly for the case of Bose statistics.

$$\sigma_0(E, \mathbf{P}; N_1, \ldots, N_\nu) = \frac{2}{(2\pi)^3}\frac{(2\pi^2)^N}{\omega^N} \times \int_0^\infty \int_{-\infty-i\beta}^{+\infty-i\beta} \frac{\sin bP}{bP} \frac{\alpha^N e^{i\alpha E}}{(\alpha^2-b^2)^N} \times \prod_{s=1}^{\nu} \{g_s m_s^2 H_2^{(2)}[m_s(\alpha^2-b^2)^{1/2}]\}^{N_s} b^2 db\, d\alpha, \tag{20}$$

where $N = \sum_{s=1}^{\nu} N_s$ is the total number of all particles in the system. For $P=0$ this formula agrees with the corresponding formula in Ref. 4.

In this way Eq. (19) is a more exact formula, correctly taking into account the type of statistics for computation of the statistical weights. But the formula of Lepore and Stuart is correct only for the case when all particles obey Boltzmann statistics.

2. STATISTICAL WEIGHTS FOR REACTIONS PRODUCING MESONS IN NUCLEON-NUCLEON COLLISIONS

We shall apply the general formula (18) to the determination of the statistical weight of the reactions of meson production in collisions of a nucleon with a nucleon. Since the greatest interest in connection with experiments on the cosmotron is provided by the cases in which 1, 2, or 3 mesons are created, we shall limit outselves to particular expressions obtained from Eq. (18) when at the end of the reaction there are formed not more than three identical particles of each kind.

The factors entering into the integrand of Eq. (18) in the cases $N_s = 0$, 1, 2, and 3 are, according to Eq. (14), respectively equal to

$$\left[\frac{d^0}{dz^0} e^{\Phi_s(z)}\right]_{z=0} = 1; \quad \left[\frac{d^1}{dz^1} e^{\Phi_s(z)}\right]_{z=0} = B_s(m_s),$$

$$\left[\frac{d^2}{dz^2} e^{\Phi_s(z)}\right]_{z=0} = [B_s(m_s)]^2 \mp \frac{1}{2^3} B_s(2m_s), \tag{21}$$

$$\left[\frac{d^3}{dz^3} e^{\Phi_s(z)}\right]_{z=0} = [B_s(m_s)]^3 \mp \frac{3}{2^3} B_s(2m_s) B_s(m_s) + \frac{2}{3^3} B_s(3m_s),$$

where as before the upper sign refers to particles obeying Fermi statistics and the lower sign to particles obeying Bose statistics.

From Eqs. (18) and (21), it is seen that in the case in which all $N_s \leqslant 1$, Eq. (18) does not differ from Eq. (20), obtained for Boltzmann statistics, which in the notations of Eqs. (18) and (14) takes the form

$$\sigma_0(E, \mathbf{P}; N_1, m_1; \ldots; N_\nu, m_\nu) = \frac{2}{(2\pi)^3} \int_0^\infty \int_{-\infty-i\beta}^{+\infty-i\beta} \frac{\sin bP}{bP} e^{i\alpha E} \prod_{s=1}^{\nu} [B_s(m_s)]^{N_s} b^2 db\, d\alpha. \tag{22}$$

But in the case when any of the N_s are equal to 2 or 3, it is necessary to add to the statistical weight, calculated according to Eq. (22) and multiplied by $(\prod_{s=1} N_s!)^{-1}$, additional terms which also can be calculated according to Eq. (22), but for particles of double or triple mass.

We shall compute σ for all possible cases in which at the end of the reaction there are 2 Fermi particles of mass M (*i.e.* nucleons) and 1, 2, or 3 Bose particles of mass μ (*i.e.* π-mesons). We concisely designate the statistical weights (18) and (22) by means of bracket expressions, in which the figures in the upper line denote the numbers of particles of each kind, while in the lower line below each figure is correspondingly indicated the mass of the particle, *i.e.*,

$$\sigma \equiv \begin{pmatrix} N_1, & N_2, & \ldots, & N_\nu \\ m_1, & m_2, & \ldots, & m_\nu \end{pmatrix}, \quad \sigma_0 \equiv \begin{pmatrix} N_1, & N_2, & \ldots, & N_\nu \\ m_1, & m_2, & \ldots, & m_\nu \end{pmatrix}_0.$$

According to Eqs. (18), (21), and (22), we obtain for the statistical weights σ, computed by the strict formula (18) their expressions in terms of the statistical weights computed according to the formula [Eq. (22)] of Lepore and Stuart. In the table presented below, expressions are given for σ in terms of σ_0, and the corresponding concrete reactions are written down.

From the table it is seen that corrections for the type of statistics have a twofold character. Firstly, there are the corrections which do not depend on the difference between Fermi and Bose statistics and are caused only by the indistinguishability of the particles. These corrections lead to a decrease in the statistical weight by a factor of $N_1! \ldots N_\nu!$ Secondly three occur specific corrections, the sign of which depends on the difference between Fermi and Bose statistics. We shall call these corrections "corrections of the second kind" in distinction to the corrections caused only by indistinguishability, which we call "corrections of the first kind". From the expressions presented in the table it is seen that the corrections of the second kind decrease the statistical weights in the case of the presence of identical particles obeying Fermi statistics, and they increase them in the case of the presence of identical particles obeying Bose statistics.

Therefore, the calculation of exact statistical weights, with consideration of the type of statistics, for all reactions at the end of which no more than three mesons are formed and two nucleons are left, reduces to calculation of statistical weights of the same reactions by Boltzmann statistics and of statistical weights of states with fewer numbers of particles, but with double or triple masses, also by Boltzmann statistics, *i.e.*, by Eq. (22).

Statistical weight	Type of reaction		
	np	*pp*	*nn*
$\begin{pmatrix}1&1&1\\M&M&\mu\end{pmatrix}=\begin{pmatrix}1&1&1\\M&M&\mu\end{pmatrix}_0$	$np\,0$	$np+$	$np-$
$\begin{pmatrix}2&1\\M&\mu\end{pmatrix}=\frac{1}{2}\begin{pmatrix}2&1\\M&\mu\end{pmatrix}_0-\frac{1}{2^4}\begin{pmatrix}1&1\\2M&\mu\end{pmatrix}_0$	$nn+$ $pp-$	$pp\,0$	$nn\,0$
$\begin{pmatrix}1&1&1&1\\M&M&\mu&\mu\end{pmatrix}=\begin{pmatrix}1&1&1&1\\M&M&\mu&\mu\end{pmatrix}_0$	$np+-$	$np+0$	$np-0$
$\begin{pmatrix}1&1&2\\M&M&\mu\end{pmatrix}=\frac{1}{2}\begin{pmatrix}1&1&2\\M&M&\mu\end{pmatrix}_0+\frac{1}{2^4}\begin{pmatrix}1&1&1\\M&M&2\mu\end{pmatrix}_0$	$np\,00$		
$\begin{pmatrix}2&1&1\\M&\mu&\mu\end{pmatrix}=\frac{1}{2}\begin{pmatrix}2&1&1\\M&\mu&\mu\end{pmatrix}_0-\frac{1}{2^4}\begin{pmatrix}1&1&1\\2M&\mu&\mu\end{pmatrix}_0$	$nn+0$ $pp-0$	$pp+-$	$nn+-$
$\begin{pmatrix}2&2\\M&\mu\end{pmatrix}=\frac{1}{4}\begin{pmatrix}2&2\\M&\mu\end{pmatrix}_0-\frac{1}{2^5}\begin{pmatrix}1&2\\2M&\mu\end{pmatrix}_0+\frac{1}{2^5}\begin{pmatrix}2&1\\M&2\mu\end{pmatrix}_0-\frac{1}{2^8}\begin{pmatrix}1&1\\2M&2\mu\end{pmatrix}_0$		$pp\,00$ $nn++$	$pp--$ $nn\,00$
$\begin{pmatrix}1&1&1&1&1\\M&M&\mu&\mu&\mu\end{pmatrix}=\begin{pmatrix}1&1&1&1&1\\M&M&\mu&\mu&\mu\end{pmatrix}_0$	$np+-0$		
$\begin{pmatrix}1&1&2&1\\M&M&\mu&\mu\end{pmatrix}=\frac{1}{2}\begin{pmatrix}1&1&2&1\\M&M&\mu&\mu\end{pmatrix}_0+\frac{1}{2^4}\begin{pmatrix}1&1&1&1\\M&M&2\mu&\mu\end{pmatrix}_0$		$np+00$ $np++-$	
$\begin{pmatrix}1&1&3\\M&M&\mu\end{pmatrix}=\frac{1}{6}\begin{pmatrix}1&1&3\\M&M&\mu\end{pmatrix}_0+\frac{1}{2^4}\begin{pmatrix}1&1&1&1\\M&M&2\mu&\mu\end{pmatrix}_0+\frac{1}{3^4}\begin{pmatrix}1&1&1\\M&M&3\mu\end{pmatrix}_0$	$np\,000$		
$\begin{pmatrix}2&1&1&1\\M&\mu&\mu&\mu\end{pmatrix}=\frac{1}{2}\begin{pmatrix}2&1&1&1\\M&\mu&\mu&\mu\end{pmatrix}_0-\frac{1}{2^4}\begin{pmatrix}1&1&1&1\\2M&\mu&\mu&\mu\end{pmatrix}_0$		$pp+-0$	$nn+-0$
$\begin{pmatrix}2&2&1\\M&\mu&\mu\end{pmatrix}=\frac{1}{4}\begin{pmatrix}2&2&1\\M&\mu&\mu\end{pmatrix}_0-\frac{1}{2^5}\begin{pmatrix}1&2&1\\2M&\mu&\mu\end{pmatrix}_0+\frac{1}{2^5}\begin{pmatrix}2&1&1\\M&2\mu&\mu\end{pmatrix}_0-\frac{1}{2^8}\begin{pmatrix}1&1&1\\2M&2\mu&\mu\end{pmatrix}_0$	$pp-00$ $pp--+$ $nn+00$ $nn++-$	$nn++0$	$pp--0$
$\begin{pmatrix}2&3\\M&\mu\end{pmatrix}=\frac{1}{12}\begin{pmatrix}2&3\\M&\mu\end{pmatrix}_0+\frac{1}{2^5}\begin{pmatrix}2&1&1\\M&2\mu&\mu\end{pmatrix}+\frac{1}{2\cdot3^4}\begin{pmatrix}2&1\\M&3\mu\end{pmatrix}_0-\frac{1}{3\cdot2^5}\begin{pmatrix}1&3\\2M&\mu\end{pmatrix}_0-\frac{1}{2^8}\begin{pmatrix}1&1&1\\2M&2\mu&\mu\end{pmatrix}_0-\frac{1}{6^4}\begin{pmatrix}1&1\\2M&3\mu\end{pmatrix}_0$		$pp\,000$	$nn\,000$

3. STATISTICAL WEIGHTS FOR CREATION OF SINGLE MESONS.

As the simplest example of the application of the relations derived, we shall consider the statistical weights of the reactions

$$p+p\rightarrow n+p+\pi^{+}\quad\text{and}\quad p+p\rightarrow p+p+\pi^{0}.$$

Inasmuch as direct calculations by Eq. (22) are tedious, we limit ourselves to only the simplified particular cases when the π-mesons can be considered ultrarelativistic, while the nucleons are nonrelativistic. In this case, according to Ref. 4, one can approximately compute

$$\sigma_0=\frac{2^s}{\omega^N}\left[\frac{M^{3s/2}(2\pi)^{3(s-1)/2}}{(sM)^{3/2}}\right]\frac{2^{3n}\pi^n T^{3s/2+3n-5/2}}{\Gamma\,[^3/_2\,(s-1)+3n]},\quad(23)$$

where s is the number of nucleons, n the number of π-mesons, $T=E-\sum_{s=1}^{\nu}m_s N_s$ the kinetic energy. According to the table and Eq. (23) we obtain

$$\frac{\sigma(pp \rightarrow pp\,0)}{\sigma(pp \rightarrow pn\,+)} = \frac{1}{2}\left[1 - \frac{35\,\omega}{208\sqrt{2}\,\pi\,(MT)^{3/2}}\right]. \quad (24)$$

The last equation is valid for $\mu < T < M$. In this region, the change from summation to integration in Eqs. (11) and (12) can be considered justified.

Assuming, as in Ref. 1, $L^3 = (4\pi/3)(\hbar/\mu)^3$ and, consequently, $\omega = (2\pi\hbar/L)^3 = 6\pi^2\mu^3$, we get

$$\frac{\sigma(pp \rightarrow pp\,0)}{\sigma(pp \rightarrow np\,+)} = \frac{1}{2}\left[1 - 2{,}24\left(\frac{\mu}{M}\right)^{3/2}\left(\frac{\mu}{T}\right)^{3/2}\right]. \quad (25)$$

From the last formula it is seen that the correction caused by the difference between Fermi and Bose statistics, in the region of its applicability, amounts approximately to from 1 to 10%.

4. SOME REMARKS ABOUT THE METHOD

The method of the microcanonical distribution applied in this article is most exact for computation of statistical weights for a system of noninteracting particles with precisely given energy and momentum, but with arbitrary, unspecified total angular momentum. In a system of colliding nucleons, the angular momentum is not fixed in advance, but certain values of the total angular momentum of the final system may be forbidden, which must lead to a change in the statistical weights, as was remarked by Fermi[1,5]. For evaluation of this circumstance it is obviously necessary to change at the very beginning the assumptions about the allowed states of the system of noninteracting particles and to consider not the states with given momenta, but states of a system of particles with given angular momenta. However, this requires special investigations.

Consideration of the conservation of charge and of the relations between the cross-sections resulting from conservation of isotopic spin can be introduced into the present method even in the final expressions (as was done in making up the table, where the laws of conservation of charge were taken into account).

In case of sufficiently large energy, one can use the mathematically simpler canonical distribution instead of the microcanonical distribution. Obviously the "statistical" weight, calculated according to the formulas of the canonical distribution (σ_θ) is expressed in terms of the statistical weight by the equations of the microcanonical distribution, as

$$\sigma_\Theta(N_1, \ldots, N_\nu) = \int\limits_{E_0}^{\infty} \iiint\limits_{-\infty}^{+\infty} e^{-E/\Theta}\sigma(E, \mathbf{P}; N_1, \ldots, N_\nu) \times dE\, d\mathbf{P}. \quad (26)$$

The general relations for the statistics with conserved charge, found in Ref. 6, are a particular case of formulas which can be derived from Eq. (26). The so-called thermodynamical method, applied by Fermi[1,5] for computing the average number of particles formed in collisions of nucleons with extremely high energies, is also a special case of the method of the canonical distribution.

It is well known that in the limit of sufficiently large energies, and correspondingly for large average numbers of particles, the results given by the microcanonical and the canonical distributions practically coincide. Thus the method of the canonical distribution and, in particular, the thermodynamical method, applied in the region of small average numbers of particles, are approximate methods of computation of statistical weights, which are more exactly computed by the method of the microcanonical distribution.

---

[1] E. Fermi, Prog. Theoret. Phys. **5**, 570 (1950)

[2] J. V. Lepore and R. N. Stuart, Phys. Rev. **94**, 1724 (1954)

[3] I. L. Rozental', J. Exptl. Theoret. Phys. (U.S.S.R.) **28**, 118 (1955); Soviet Phys. JETP **1**, 166 (1955)

[4] R. H. Milburn, Rev. Mod, Phys. **27**, 1 (1955)

[5] E. Fermi, *Elementary Particles*, (Yale Univ. Press) 1951

[6] V. B. Magalinskii and Ia. P. Terletskii, J. Exptl. Theoret. Phys. (U.S.S.R.) **29**, 151 (1955); Soviet Phys. JETP **2**, 143 (1956)

Translated by C. W. Helstrom
131

SOVIET PHYSICS JETP VOLUME 5, NUMBER 3 OCTOBER, 1957

Reconstruction of the Scattering Matrix of a Two-Nucleon System*

L. PUZIKOV, R. RYNDIN AND Ia. SMORODINSKII

United Institute for Nuclear Studies

(Submitted to JETP editor November 1, 1956)

J. Exptl. Theoret. Phys. (U.S.S.R.) **32**,592-600 (March, 1957)

The types of experiments needed for determination of all elements of the scattering matrix are investigated. It is shown that because of the unitarity condition the required number of experiments equals the number of complex functions entering into the scattering matrix. For nucleon-nucleon scattering, the inelastic scattering matrix can be determined on the basis of five experiments measuring the cross section, polarization, normal components of the polarization correlation tensor and of the triple scattering tensors (for the scattered and recoil particles). It is shown that experiments involving spin rotation by a magnetic field are not necessary for a phase shift analysis.

1. INTRODUCTION

THE LITERATURE contains a large amount of experimental information concerning nucleon-nucleon scattering in a very wide range of energies.*

A phase shift analysis of the experimental findings has also appeared in many articles. But it is seen in all of these articles that the phase shift analysis is not unique and the authors usually present a few sets of phases which provide equally good descriptions of the result. The phase-shift analysis begins with a preliminary limitation of the number of states which participate in the scattering. Then the algebraic equations for a finite number of phases are written out. But for particles with spin, it is not clear which experiments provide the data for these equations.

The clearest example is proton-proton scattering at low energies. The two principal states involved in this case are $^1S_0$ and $^3P_0$. These states cannot be distinguished by either cross section or polarization measurements. Yet they can easily be separated by polarization correlation. Thus more complicated experiments are obviously needed. In other instances, where the scattering is anisotropic and the determination of a finite number of phases may appear to be formally possible, it is not clear to what extent these phases can also describe more complex scattering such as multiple scattering.

It therefore seemed important to attempt an analysis of all possible experiments in order to show which of these are independent in the sense that a complete reconstruction of the scattering matrix is possible when their results are known. For the purpose of clarity, we shall begin with two very simple examples: the scattering of spin-zero particles in a central force field and of particles with spin ½ by spin-zero nuclei. Subsequently we shall consider nucleon-nucleon scattering.

The case of arbitrary spin, which thus far possesses only theoretical significance and the case of photon scattering will be examined in future communications. In the present article we shall also limit ourselves to the study of the scattering matrix for a given energy. The energy dependence of the matrix elements requires further study.

2. SCATTERING OF SPIN-ZERO PARTICLES

Measurement of the differential cross section of a spin-zero particle determines a function $\sigma(\vartheta)$ which is the square of the absolute value of the scattering amplitude:

$$\sigma(\vartheta) = |f(\vartheta)|^2. \tag{2.1}$$

It is clear that when this quantity is measured for only one value of the energy and of the angle ϑ the phase of the complex function $f(\vartheta)$ is not completely determined.

However, when the scattering is measured at all angles and is known to be elastic, the phase of $f(\vartheta)$ is also determined. Indeed, the unitarity condition for the amplitude $f(\vartheta)$ can be written as[2]

$$4\pi \operatorname{Im} f(\vartheta) = k\int d\omega f^*(\vartheta'') f(\vartheta'). \tag{2.2}$$

Here ϑ' is the angle between **k** (the initial wave vector) and the variable vector **k**″ over whose directions $d\omega$ the integration is carried out. ϑ'' is the angle between the final wave vector **k**′ and **k**″. If we denote

---

*Wolfenstein[1] has given us a good review of recent data. We take this opportunity to thank Professor Wolfenstein for sending us his manuscript before publication.

$$f(\vartheta) = \sqrt{\sigma(\vartheta)}\,\exp[i\alpha(\vartheta)], \tag{2.3}$$

we obtain from (2.2) an integral equation for $\alpha(\vartheta)$ when $\sigma(\vartheta)$ is known:

$$4\pi\sin\alpha(\vartheta) = k\int\left[\frac{\sigma(\vartheta')\,\sigma(\vartheta'')}{\sigma(\vartheta)}\right]^{1/2}\cos[\alpha(\vartheta') - \alpha(\vartheta'')]\,d\omega. \tag{2.4}$$

The solution of Eqs. (2.1) and (2.2) or of (2.4) is equivalent to a phase-shift analysis. The representation of $f(\vartheta)$ as a finite sum of Legendre polynomials is clearly only one method of solution, which is useful when it is known that only a few phases are involved in the solution. For the general case the direct solution of (2.4) may be more convenient.

Equation (2.4) is seen to be invariant with respect to the substitution $f(\vartheta) \to -f^*(\vartheta)$ or, equivalently,

$$\alpha(\vartheta) \to \pi - \alpha(\vartheta). \tag{2.5}$$

This transformation represents a change of sign of all scattering phases. It indicates the ambiguity in the reconstruction of the scattering amplitude from its absolute value. We know that this ambiguity is eliminated by consideration of the interference with Coulomb scattering (for charged particles) or by study of the energy dependence of scattering at low energies. Therefore, the measurement of the scattering cross section at a given energy and at all angles is a complete experiment in the sense that it provides a possibility of completely reconstructing the scattering amplitude (except possibly for the indicated ambiguity).

3. SCATTERING OF A PARTICLE WITH SPIN ½

The scattering amplitude for a particle with spin ½ is described in the usual manner as

$$M = a(\vartheta) + b(\vartheta)(\boldsymbol{\sigma}\mathbf{n}), \tag{3.1}$$

where $\boldsymbol{\sigma}$ is the Pauli matrix and $\mathbf{n} = \mathbf{kk}'/|\mathbf{kk}'|$ is the unit normal to the scattering plane.

The cross section and polarization (double scattering) are measured experimentally, thus enabling us to determine two functions:

$$\begin{aligned} \sigma(\vartheta) &= |a|^2 + |b|^2 = {}^1/_2\,(|f_+|^2 + |f_-|^2), \\ \sigma(\vartheta)\,P(\vartheta) &= 2\,\mathrm{Re}\,ab^* = {}^1/_2\,(|f_+|^2 - |f_-|^2). \end{aligned} \tag{3.2}$$

Equation (3.2) clearly determines two moduli*:

$$|f_+|^2 = |a+b|^2, \quad |f_-|^2 = |a-b|^2. \tag{3.3}$$

If the measurements are carried out over all angles and the scattering is elastic the phases of the complex functions $f_+(\vartheta)$ and $f_-(\vartheta)$ are determined again by the unitarity conditions:

$$\begin{aligned} 4\pi\,\mathrm{Im}\,a(\vartheta) &= k\int d\omega\left[a^*(\vartheta'')\,a(\vartheta') + b^*(\vartheta'')\,b(\vartheta')\,\frac{\cos\vartheta - \cos\vartheta'\cos\vartheta''}{\sin\vartheta'\sin\vartheta''}\right], \\ 4\pi\,\mathrm{Re}\,b(\vartheta) &= k\int d\omega\left[2\,\mathrm{Im}\,a^*(\vartheta'')\,b(\vartheta')\,\frac{\cos\vartheta\cos\vartheta' - \cos\vartheta''}{\sin\vartheta\sin\vartheta'} + \right. \\ &\left. + b^*(\vartheta'')\,b(\vartheta')\,\frac{1 + 2\cos\vartheta\cos\vartheta'\cos\vartheta'' - \cos^2\vartheta - \cos^2\vartheta' - \cos^2\vartheta''}{\sin\vartheta\sin\vartheta'\sin\vartheta''}\right]. \end{aligned} \tag{3.4}$$

Equations (3.2) and (3.4) also permit a certain invariant transformation. In order to determine this we note that the transformation (reversal of the signs of all scattering phases)

$$a(\vartheta) \to -a^*(\vartheta), \quad b(\vartheta) \to b^*(\vartheta) \tag{3.5}$$

does not affect the cross section and unitarity conditions but that it does reverse the polarization. This This is also true for the Minami[3,4] transformation

$$\begin{aligned} a(\vartheta) &\to a(\vartheta)\cos\vartheta + ib(\vartheta)\sin\vartheta, \\ b(\vartheta) &\to -ia(\vartheta)\sin\vartheta - b(\vartheta)\cos\vartheta. \end{aligned} \tag{3.6}$$

Therefore the product of the two transformations:

---

*We note that (3.3) represents the scattering cross sections of a polarized particle whose spin is directed "up" or "down" with respect to **n**.

$$a(\vartheta) \to -a^*(\vartheta)\cos\vartheta + ib^*(\vartheta)\sin\vartheta, \quad b(\vartheta) \to + ia^*(\vartheta)\sin\vartheta - b^*(\vartheta)\cos\vartheta \qquad (3.7)$$

leaves all quantities invariant.*

Thus for a particle with spin ½, the measurement of the cross section and of the polarization is a complete experiment. Non-uniqueness of the phases resulting from the existence of the transformation (3.7) can be eliminated by investigating the energy dependence of the cross section at low energies. We also add that, as was shown by Wolfenstein[5], this non-uniqueness can be eliminated by the study of triple scattering (in which the scattering planes of interest are mutually perpendicular).

4. NUCLEON-NUCLEON SCATTERING

Nucleon-nucleon scattering can be described by the matrix

$$M = \alpha(\vartheta) + \beta(\vartheta)(\boldsymbol{\sigma}_1\mathbf{n})(\boldsymbol{\sigma}_2\mathbf{n}) + \gamma(\vartheta)(\boldsymbol{\sigma}_1 + \boldsymbol{\sigma}_2)\mathbf{n} + \delta(\vartheta)(\boldsymbol{\sigma}_1\mathbf{m})(\boldsymbol{\sigma}_2\mathbf{m}) + \varepsilon(\vartheta)(\boldsymbol{\sigma}_1\mathbf{l})(\boldsymbol{\sigma}_2\mathbf{l}). \qquad (4.1)$$

Here $\boldsymbol{\sigma}_1$ and $\boldsymbol{\sigma}_2$ are the Pauli matrices of the two particles and **m**, **l** and **n** are the unit orthogonal vectors of the Cartesian coordinates, which are parallel to $\mathbf{k}-\mathbf{k}'$, $\mathbf{k}+\mathbf{k}'$ and $[\mathbf{k}\mathbf{k}']$, respectively (in the center-of-mass system)[6]. This system is obviously suitable when we note that in the laboratory system the unit vectors are parallel to the wave vectors of the two particles after scattering and to the normal to the scattering plane.

Equation (4.1) differs from the general scattering matrix for two particles with spin ½ by the absence of a term proportional to $\boldsymbol{\sigma}_1 - \boldsymbol{\sigma}_2$. This results from identity of the particles for a *p–p* system and charge invariance for a *n–p* system.

For identical particles the matrix coefficients in (4.1) are symmetrical with respect to the substitution $\vartheta \to \pi - \vartheta$. These can be formulated conveniently by introducing new functions which will also be useful subsequently[7]:

$$a = \alpha + \beta, \; b = \alpha - \beta, \; c = \delta + \varepsilon, \; d = \delta - \varepsilon, \; e = 2\gamma. \qquad (4.2)$$

It can then be shown that for identical particles

$$a(\pi - \vartheta) = -a(\vartheta), \quad b = (\pi - \vartheta) = -c(\vartheta), \quad c(\pi - \vartheta) = -b(\vartheta), \; d(\pi - \vartheta) = d(\vartheta), \quad e(\pi - \vartheta) = e(\vartheta). \qquad (4.3)$$

Therefore for identical particles the measurement is performed only for the angles $0 \leftrightarrow \pi/2$. For the scattering of neutrons by protons the interval of measurement is doubled to $0 \leftrightarrow \pi$, which corresponds to doubling of the number of states in this system.

Before making use of the unitarity condition, we shall briefly describe the experiments needed in a two-nucleon system.

If we have an unpolarized beam of nucleons the first scattering determines the differential cross section, which is associated with the elements of the scattering matrix by the formula

$$\sigma(\vartheta) = {}^1\!/_2(|a|^2 + |b|^2 + |c|^2 + |d|^2 + |e|^2). \qquad (4.4)$$

The first scattering gave rise to a beam polarized along the **n** direction. In the second scattering the polarization in hydrogen is measured:

$$\sigma(\vartheta)P(\vartheta) = \mathrm{Re}\, ae^*. \qquad (4.5)$$

It is clear that in order to obtain polarization the first scattering can be produced by any target with certain properties (the polarizer). The polarization of the recoil particle agrees with $P(\vartheta)$ ($\boldsymbol{\sigma}_1 - \boldsymbol{\sigma}_2$ is absent in *M*) and need not be measured.

A third target can be added in two ways. Measurment of the P_{nn} component of the correlation tensor gives

$$\sigma(\vartheta)P_{nn}(\vartheta) = {}^1\!/_2(|a|^2 - |b|^2 - |c|^2 + |d|^2 + |e|^2). \qquad (4.6)$$

In these measurements all three scatterings take place in a single plane. It is possible in addition to measure the polarization of the particle after the second scattering. When it is measured by the third target (which can be any analyzer) we obtain two quantities which correspond to the two particles participating in the second scattering[5]. If all three scatterings occur in the same plane we shall have for these quantities

$$\sigma(\vartheta)D_{nn}(\vartheta) = {}^1\!/_2\{|a|^2 + |b|^2 - |c|^2 - |d|^2 + |e|^2\} \qquad (4.7)$$

(for the scattered particle) and

$$\sigma(\vartheta)K_{nn}(\vartheta) = {}^1\!/_2\{|a|^2 - |b|^2 + |c|^2 - |d|^2 + |e|^2\} \qquad (4.8)$$

(for the recoil particle). For neutron scattering by protons, the difference between these two quantities is evident; for identical particles, the first quantity corresponds to measurement in the angular interval

---

*In terms of the phase shifts $\delta(j, l)$ this transformation represents $\delta(j, j - {}^1\!/_2) \rightleftarrows -\delta(j, j + {}^1\!/_2)$.

0 to $\pi/2$ and the second to the angular interval $\pi/2$ to π.

The methods which have been described give us five equations from which we easily determine the absolute values of the five functions $a+e$, $a-e$, b, c, d. Further consideration follows the path indicated earlier. In order to determine the phases of these complex functions measured over all angles we must make use of the unitarity condition. It can be shown (see Ref. 8) that five such conditions exist. [These conditions (see Appendix 2) are invariant with respect to

$$\alpha(\vartheta) \to -\alpha^*(\vartheta), \quad \beta(\vartheta) \to -\beta^*(\vartheta), \quad \gamma(\vartheta) \to \gamma^*(\vartheta),$$
$$\delta(\vartheta) \to -\delta^*(\vartheta), \; \varepsilon(\vartheta) \to -\varepsilon^*(\vartheta),$$

which is equivalent to simultaneous reversal of the signs of all phases (as in the preceding case this substitution reverses the polarization); a substitution which corresponds to the Minami transformation does not exist for nucleon-nucleon scattering[9].] Hence it follows that the indicated set of experiments is a complete set.

The preceding considerations are characterized by the important conclusion that determination of the scattering matrix does not require measurement of quadruple scattering or the introduction of a magnetic field but can be confined to experiments with three targets and parallel scattering planes. Up to the present time, however, such a complete set of experiments has not been performed for any single energy; this is the cause of the ambiguities in the analysis of these experiments.

In connection with the determination of the scattering matrix there arises the question of its relation to the potential. It is noteworthy that the number of independent functions in the scattering amplitude coincides with the number of scalar functions that appear in the interaction Hamiltonian. Indeed, it is easily shown that the general form of the interaction of two protons, for example, will be

$$V = V_1(r) + V_2(r)(\sigma_1\sigma_2) + V_3(r)(\sigma_1\mathbf{r})(\sigma_2\mathbf{r})$$
$$+ V_4(r)(\sigma_1+\sigma_2)\mathbf{L} + V_5(r)(\sigma_1\mathbf{L})(\sigma_2\mathbf{L})$$

where $\mathbf{L}$ is the orbital angular momentum. It would be very interesting to determine how the scattering matrix is affected when one or more V_i vanishes. In other words, can anything be known qualitatively regarding the form of V from the characteristics of the scattering matrix?

In conclusion we wish to thank Professors E. Segre and O. Chamberlain for interesting discussions which we had with them during the summer of 1956 concerning nucleon scattering experiments.

APPENDIX 1. FORMULAS FOR POSSIBLE NUCLEON-NUCLEON SCATTERING EXPERIMENTS

Since the set of five experiments indicated above for the determination of the nucleon-nucleon scattering matrix is not the only one possible, we shall now briefly review all conceivable experiments. These experiments can differ first in the polarization of the primary beam and secondly in the nature of the quantities to be measured (cross section, polarization of the scattered particle, polarization of the recoil particle, polarization correlation). They can be summarized in the following table:

Measured quantity	Initial spin state			
	A	B	C	D
	Unpolarized beam—unpolarized target	Polarized beam—unpolarized target	Unpolarized beam—polarized target	Polarized beam—polarized target
1. Cross section	σ^*	$\sigma_i^{(1)}$	$\sigma_k^{(2)}$	σ_{ik}
2. Polarization of scattered particle	$P_p^{(1)*}$	$D_{ip}^{(1)*}$	K'_{hp}	$T_{ikp}^{(1)}$
3. Polarization of recoil particle	$P_q^{(2)}$	K_{iq}^*	$D_{kq}^{(2)}$	$T_{ikq}^{(2)}$
4. Polarization correlation	P_{qp}^*	$P_{ipq}^{(1)*}$	$P_{kpq}^{(2)}$	T_{ikpq}^*

Here each column represents a definite initial spin state of the two-nucleon system and each line gives a characteristic of the scattering process which can be measured. The subscript *i* denotes the direction of initial polarization of the incident particle; *k* denotes the initial polarization of the target; *p* denotes the measured polarization component of the scattered particle; *q* denotes the measured polarization component of the recoil particle. Each experiment will hereinafter be denoted by a letter (for the column) and numeral (for the line) indicating the initial spin state of the system and the characteristic of the scattering process which is to be measured. For example, B2 means measurement of the set of quantities $D_{ip}^{(1)}$ which determine the influence of the *i*-component of incident particle polarization on the *p*-component of scattered particle polarization, *etc.*

Not all of the experiments in this table are different. Some of them are actually identical because of symmetry. Thus in the absence of singlet-triplet transitions (the absence of the $\sigma_1 - \sigma_2$ component) there is essential identity of experiments A2 and A3, B1 and C1, B4 and C4, D2 and D3, B2 and C3. For identical particles (see the symmetry properties in (4.3)) experiments B2 and B3 determine the quantities of B2 for supplementary angles (ϑ and $\pi - \vartheta$). Experiments C3 and C2 are related in the same way.

Because of the time-reversal symmetry of the matrix *M* the experiments which are situated symmetrically with respect to the main diagonal of the table are equivalent (A2 and B1, A4 and D1 etc.). Thus the only distinct experiments are denoted by asterisks in the table. It appears immediately that a polarized target is needed in principle only for the most complicated experiments. But, as we have seen, for the actual determination of the scattering matrix even these experiments are unnecessary.

We now proceed to review the characterstics which are determined in the different experiments.

A1. The cross section is measured:

$$\sigma(\vartheta) = {}^1/_4 \, \mathrm{Sp}\, MM^+$$

$$= {}^1/_2 (|a|^2 + |b|^2 + |c|^2 + |d|^2 + |e|^2).$$

A2. The polarization is measured:

$$\sigma(\vartheta) P(\vartheta) = {}^1/_4 \, \mathrm{Sp}\, (\sigma_1 \mathbf{n}) MM^+ = \mathrm{Re}\, ae^*.$$

B2. The tensor is determined:

$$\sigma(\vartheta) D_{ip}(\vartheta) = {}^1/_4 \, \mathrm{Sp}\, M\sigma_{1i} M^+ \sigma_{1p}$$
$$= {}^1/_2 (|a|^2 + |b|^2 - |c|^2 - |d|^2 + |e|^2)\, n_i n_p$$
$$+ \mathrm{Re}\,(a^* b + c^* d)\, m_i m_p$$
$$+ \mathrm{Re}\,(a^* b - c^* d)\, l_i l_p - \mathrm{Im}\, b^* e\, (m_i l_p - l_i m_p).$$

From triple-scattering experiments with parallel and perpendicular planes these components are determined:

$$\sigma(\vartheta) D_{nn}(\vartheta) = {}^1/_2 (|a|^2 + |b|^2 - |c|^2 - |d|^2 + |e|^2),$$

$$\sigma(\vartheta) D_{xm}(\vartheta) = -\cos\frac{\vartheta}{2}\, \mathrm{Re}\,(a^* b + c^* d)$$
$$+ \mathrm{Im}\, b^* e \sin\frac{\vartheta}{2}.$$

The determination of the components

$$\sigma(\vartheta) D_{zm}(\vartheta) = \sin\frac{\vartheta}{2}\, \mathrm{Re}\,(a^* b + c^* d) + \cos\frac{\vartheta}{2}\, \mathrm{Im}\, b^* e,$$

$$\sigma(\vartheta) D_{xl}(\vartheta) = \sin\frac{\vartheta}{2}\, \mathrm{Re}\,(a^* b - c^* d) + \cos\frac{\vartheta}{2}\, \mathrm{Im}\, b^* e$$

requires either quadruple scattering or triple scattering with a magnetic field between the targets. The unit vectors **z** and **x** are along the directions **k** and [**nk**], respectively.

B3. The tensor is measured:

$$\sigma(\vartheta) K_{iq}(\vartheta) = {}^1/_4 \, \mathrm{Sp}\, M\sigma_{1i} M^+ \sigma_{2q} = {}^1/_2 (|a|^2 - |b|^2$$
$$+ |c|^2 - |d|^2 + |e|^2)\, n_1 n_q + \mathrm{Re}\,(a^* c + b^* d)\, m_i m_q$$
$$+ \mathrm{Re}\,(a^* c - b^* d)\, l_i l_q - \mathrm{Im}\, c^* e\, (m_i l_q - l_i m_q).$$

The components K_{nn} and $K_{x,l}$ are determined from triple scattering and K_{xm} and $K_{z,l}$ from quadruple scattering.

For identical particles this is equivalent to the measurement of corresponding components of D_{ip} for supplementary angles ($\vartheta \to \pi - \vartheta$) giving $D_{nn}(\pi - \vartheta) = K_{nn}(\vartheta)$, $D_{xm}(\pi - \vartheta) = K_{x,-l}(\vartheta)$, $D_{zm}(\pi - \vartheta) = -K_{z,-l}(\vartheta)$, $D_{xl}(\pi - \vartheta) = -K_{x,m}(\vartheta)$.

A4. The polarization correlation tensor is measured:

$$\sigma(\vartheta) P_{pq}(\vartheta) = {}^1/_4 \, \mathrm{Sp}\, \sigma_{1p}\sigma_{2q} MM^+$$
$$= \frac{1}{2} (|a|^2 - |b|^2 - |c|^2 + |d|^2 + |e|^2)\, n_p n_q$$
$$+ \mathrm{Re}\,(a^* d + b^* c)\, m_p m_q + \mathrm{Re}\,(b^* c - a^* d)\, l_p l_q$$
$$+ \mathrm{Im}\, de^*\, (m_p l_q + m_q l_p).$$

The component

$$\sigma(\vartheta) P_{\ n}(\vartheta) = {}^1/_2 (|a|^2 - |b|^2 - |c|^2 + |d|^2 + |e|^2)$$

is determined by an experiment in which the planes of the analyzing scatterings coincide with the basic scattering plane.

The determination of the component

$$\sigma(\vartheta) P_{ml}(\vartheta) = \operatorname{Im} de^{*} = -\sigma(\vartheta) P_{m-l}(\vartheta)$$

requires an experiment in which the planes of the analyzing scatterings are perpendicular to the basic scattering plane.

Experiments in which the planes of the analyzing scatterings are perpendicular to the basic plane, with a magnetic field perpendicular to the primary scattering plane placed in front of one of the analyzers, determine the components

$$\sigma(\vartheta) P_{mm}(\vartheta) = \operatorname{Re}(a^{*}d + b^{*}c),$$

$$\sigma(\vartheta) P_{ll}(\vartheta) = \operatorname{Re}(b^{*}c - a^{*}d).$$

B4. The tensor is measured:

$$\begin{aligned}
\sigma(\vartheta) P_{ipq}(\vartheta) &= {}^{1}/_{4} \operatorname{Sp} M\sigma_{1i} M^{+}\sigma_{1p}\sigma_{2q} = \\
&= \operatorname{Re} ae^{*} n_i n_p n_q + \operatorname{Re} be^{*} [m_i m_p n_q + l_i l_p n_q] - \\
&- \operatorname{Im}(a^{*}b + c^{*}d) l_i m_p n_q + \operatorname{Im}(a^{*}b - c^{*}d) m_i l_p n_q - \\
&- \operatorname{Im}(a^{*}c + b^{*}d) l_i n_p m_q + \operatorname{Im}(a^{*}c - b^{*}d) m_i n_p l_q + \\
&+ \operatorname{Im}(a^{*}d + b^{*}c) n_i l_p m_q + \operatorname{Im}(a^{*}d - b^{*}c) n_i m_p l_q + \\
&+ \operatorname{Re} e^{*}c [m_i n_p m_q + l_i n_p l_q] + \operatorname{Re} e^{*}d [n_i m_p m_q - n_i l_p l_q].
\end{aligned}$$

C4. For this experiment a polarized target is required. The tensor components are measured:

$$\begin{aligned}
\sigma(\vartheta) T_{ikpq}(\vartheta) &= {}^{1}/_{4} \operatorname{Sp} M\sigma_{1i}\sigma_{2k} M^{+}\sigma_{1p}\sigma_{2q} = \\
&= {}^{1}/_{2}(|a|^2 + |b|^2 + |c|^2 + |d|^2 + |e|^2) n_i n_k n_p n_q + \\
&+ {}^{1}/_{2}(|a|^2 + |b|^2 + |c|^2 + |d|^2 - |e|^2)(m_i m_k m_p m_q + l_i l_k l_p l_q) + \\
&+ \operatorname{Re}(a^{*}b + c^{*}d)(n_i l_k n_p l_q + l_i n_k l_p n_q) + \\
&+ \operatorname{Re}(a^{*}b - c^{*}d)(n_i m_k n_p m_q + m_i n_k m_p n_q) + \\
&+ {}^{1}/_{2}(|a|^2 + |b|^2 - |c|^2 - |d|^2 - |e|^2)(m_i l_k m_p l_q + l_i m_k l_p m_q) + \\
&+ {}^{1}/_{2}(|a|^2 - |b|^2 + |c|^2 - |d|^2 - |e|^2)(m_i l_k l_p m_q + l_i m_k m_p l_q) + \\
&+ {}^{1}/_{2}(-|a|^2 + |b|^2 + |c|^2 - |d|^2 + |e|^2)(m_i m_k l_p l_q + l_i l_k m_p m_q) + \\
&+ \operatorname{Re}(a^{*}c + b^{*}d)(l_i n_k n_p l_q + n_i l_k l_p n_q) + \\
&+ \operatorname{Re}(a^{*}c - b^{*}d)(n_i m_k m_p n_q + m_i n_k n_p m_q) - \\
&- \operatorname{Re}(a^{*}d + b^{*}c)(l_i l_k n_p n_q + n_i n_k l_p l_q) + \\
&+ \operatorname{Re}(a^{*}d - b^{*}c)(n_i n_k m_p m_q + m_i m_k n_p n_q) + \\
&+ \operatorname{Im} e^{*}c (m_i n_k n_p l_q + n_i m_k l_p n_q - n_i l_k m_p n_q - l_i n_k n_p m_q) + \\
&+ \operatorname{Im} e^{*}d (n_i n_k m_p l_q + n_i n_k l_p m_q - m_i l_k n_p n_q - l_i m_k n_p n_q) + \\
&+ \operatorname{Im} a^{*}e (l_i m_k m_p m_q + m_i l_k m_p m_q + l_i l_k m_p l_q + l_i l_k l_p m_q - \\
&- m_i l_k l_p l_q - l_i m_k l_p l_q - m_i m_k m_p l_q - m_i m_k l_p m_q) + \\
&+ \operatorname{Im} b^{*}e (l_i n_k m_p n_q + n_i l_k n_p m_q - n_i m_k n_p l_q - m_i n_k l_p n_q).
\end{aligned}$$

APPENDIX 2 UNITARITY CONDITIONS

These are the unitarity conditions for nucleon-nucleon scattering:

$$4\pi \operatorname{Im} \alpha(\vartheta) = \frac{k}{4} \int \operatorname{Sp} [M^{+}(\mathbf{k}', \mathbf{k}'') M(\mathbf{k}, \mathbf{k}'')] \, d\omega_{\mathbf{k}''},$$

$$4\pi \operatorname{Im} \beta(\vartheta) = \frac{k}{4} \int \operatorname{Sp} [M^{+}(\mathbf{k}', \mathbf{k}'') M(\mathbf{k}, \mathbf{k}'') (\boldsymbol{\sigma}_1 \mathbf{n})(\boldsymbol{\sigma}_2 \mathbf{n})] \, d\omega_{\mathbf{k}''},$$

$$4\pi \operatorname{Re} \gamma(\vartheta) = \frac{ik}{8} \int \operatorname{Sp} [M^{+}(\mathbf{k}', \mathbf{k}'') M(\mathbf{k}, \mathbf{k}'') (\boldsymbol{\sigma}_1 + \boldsymbol{\sigma}_2) \mathbf{n}] \, d\omega_{\mathbf{k}''},$$

$$4\pi \operatorname{Im} \delta(\vartheta) = \frac{k}{4} \int \operatorname{Sp} [M^{+}(\mathbf{k}', \mathbf{k}'') M(\mathbf{k}, \mathbf{k}'') (\boldsymbol{\sigma}_1 \mathbf{m})(\boldsymbol{\sigma}_2 \mathbf{m})] \, d\omega_{\mathbf{k}''},$$

$$4\pi \operatorname{Im} \varepsilon(\vartheta) = \frac{k}{4} \int \operatorname{Sp} [M^{+}(\mathbf{k}', \mathbf{k}'') M(\mathbf{k}, \mathbf{k}'') (\boldsymbol{\sigma}_1 \mathbf{l})(\boldsymbol{\sigma}_2 \mathbf{l})] \, d\omega_{\mathbf{k}''}.$$

The calculation of the traces in the unitarity conditions is elementary but results in complicated expressions which we shall not reproduce here. It should be noted that when Wolfenstein's[5] form of M is used the unitarity condition for $B(\vartheta)$ (singlet scattering) is of the same form as the unitarity condition for the scattering of spin-zero particles.

---

[1] L. Wolfenstein, Ann Rev. Nucl. Sci 6,(1956)

[2] R. Glauber and V. Schomaker, Phys. Rev. 89, 667 (1953)

[3] S. Minami, Progr. Theor. Phys. 11, 213 (1954)

[4] R. Ryndin and Ia. Smorodinskii, Dokl. Akad. Nauk SSSR 103, 69 (1955)

[5] L. Wolfenstein, Phys. Rev. 96, 1654 (1954)

[6] R. Oehme, Phys. Rev. 98, 147 (1955)

[7] R. Oehme, Phys. Rev. 98, 216 (1955)

[8] R. Ryndin and Ia. Smorodinskii, J. Exptl. Theoret. Phys. (U.S.S.R.) (in press)

[9] R. Ryndin and Ia. Smorodinskii, CERN Symposium 2, 141 (1956)

Translated by I. Emin
132

Letters to the Editor

Energy Dependence of the Effective Cross Section of Inelastic Scattering of Particles near the Threshold

G. F. DRUKAREV
Leningrad State University

(Submitted to JETP editor May 13, 1956;
resubmitted December 1, 1956)
J. Exptl. Theoret. Phys. (U.S.S.R.) **32**, 601-603 (March, 1957)

A METHOD is presented in the present paper for the investigation of the energy dependence of inelastic scattering near the threshold. As an illustration, let us consider a system A consisting of a fixed force center and a particle a bound to it. Let particle b fall on this system. We shall consider that a and b are different, in order to avoid difficulties connected with the Pauli principle (in the case of identical particles a and b, the results are not changed in principle, but the calculations are more complicated).

We are interested in the inelastic scattering of b, in which a undergoes a transition from a state with energy E_0 to another state with energy E_1. Expanding the wave function of the system $A + b\,\Psi(r_1r_2)$ in the eigenfunctions ψ_α of system A

$$\Psi(\mathbf{r}_1\mathbf{r}_2) = \sum_\alpha \psi_\alpha(\mathbf{r}_1)\,F_\alpha(\mathbf{r}_2), \tag{1}$$

we get for F_α the system of equations[1]

$$\Delta F_\alpha + k_\alpha^2 F_\alpha = \sum_\beta V_{\alpha\beta}F_\beta \tag{2}$$

with asymptotic behavior

$$F_\alpha \sim \exp(i\mathbf{k}_\alpha\mathbf{r}_\alpha)\,\delta_{\alpha 0} + q_\alpha r^{-1}\exp(ik_\alpha r). \tag{3}$$

We introduce the notation $\hbar^2k_0^2/2m_b$ for the energy of the particle before collision:

$$\hbar^2k_\alpha^2/2m_b = \hbar^2k_0^2/2m_b + (E_0 - E_\alpha), \tag{4}$$

$$k_0^2 = k_\alpha^2 + k_{\alpha 0}^2,\ \varkappa_\alpha = k_0 - k_{\alpha 0} = (k_\alpha^2 + k_{\alpha 0}^2)^{1/2} - k_{\alpha 0}. \tag{5}$$

The effective cross section of the transition 0 → a is related to the amplitude q_α by the equation:

$$\sigma_{0\alpha} = (k_\alpha/k_0)\int |q_\alpha|^2 d\Omega. \tag{6}$$

We shall consider the system (2) in an approximation in which we can separate the two equations for F_0 and F_1 and neglect the coupling of these equations with the other equations (regarding this approximation, see Refs. 1, 2).

We shall then have

$$(\Delta + k_0^2)F_0 = V_{00}F_0 + V_{01}F_1,\ (\Delta + k_1^2)F_1 = V_{11}F_1 + V_{10}F_0. \tag{7}$$

We limit ourselves to the simplest case of a transition between s states; moreover, we shall take into account only the s state of particle b which undergoes scattering. Then F_1 and F_2 will be spherically symmetric. Setting $F_\alpha = f_\alpha/r$, we get

$$d^2f_\alpha/dr^2 + k_\alpha^2 f_\alpha = \sum_{\beta=0}^{1} V_{\alpha\beta}f_\beta\ (\alpha = 0;\ 1). \tag{8}$$

For large r,

$$f_\alpha \sim k_\alpha^{-1}\sin k_\alpha r\,\delta_{\alpha 0} + q_\alpha \exp ik_\alpha r. \tag{9}$$

We can convert the system (8) with asymptotic conditions (9) to the integral equations

$$f_\alpha = c_\alpha\varphi_\alpha + \sum_{\beta=0}^{1}\int_0^r G_{\alpha\beta}(r,s)\,f_\beta(s)\,ds\quad (\alpha = 0;\ 1), \tag{10}$$

$$G_{\alpha\beta}(r,s) = \frac{1}{k_\alpha}\sin k_\alpha(r-s)\,V_{\alpha\beta}(s);\ \varphi_\alpha = \frac{\sin k_\alpha r}{k_\alpha},$$

$$c_\alpha = \delta_{\alpha 0} - \sum_{\beta=0}^{1}\int_0^\infty e^{ik_\alpha s}\,V_{\alpha\beta}(s)\,f_\beta(s)\,ds.$$

For q_α we have

$$q_\alpha = -\frac{1}{k_\alpha}\sum_{\beta=0}^{1}\int_0^\infty \varphi_\alpha(s)\,V_{\alpha\beta}(s)\,f_\beta(s)\,ds. \tag{11}$$

We set

$$f_\alpha = \sum_{\beta=0}^{1} c_\beta x_{\alpha\beta}\quad (\alpha = 0;\ 1) \tag{12}$$

and introduce the notation

$$M_{\alpha\gamma} = \sum_{\beta=0}^{1}\int_0^\infty e^{ik_\alpha s}\,V_{\alpha\beta}x_{\beta\gamma}(s)\,ds. \tag{13}$$

We then obtain

$$x_{\alpha\beta} = \varphi_\alpha\delta_{\alpha\beta} + \sum_{\gamma=0}^{1}\int_0^r G_{\alpha\gamma}(r,s)\,x_{\gamma\beta}(s)\,ds, \tag{14}$$

$$c_\alpha = \delta_{\alpha 0} - \sum_{\gamma=0}^{1} M_{\alpha\gamma}c_\gamma. \tag{15}$$

Solving the system (15), and taking Eqs. (11)-(13) into account, we get for the amplitude of the excitation

$$q_1 = \frac{M_{10}k_1^{-1}\,\mathrm{Im}\,M_{11} - (1+M_{11})\,k_1^{-1}\,\mathrm{Im}\,M_{10}}{(1+M_{00})\,(1+M_{11}) - M_{01}M_{10}}\,. \quad (16)$$

Taking it into consideration that $\sin k_\alpha r/k_\alpha$ is an analytic function of k_α^2, we can represent $x_{\alpha\beta}$ in the form of a series in k_1^2. Substituting this series in $M_{1\gamma}$, and expanding $\exp ik_1 s$ in the radicand in powers of k_1, we get

$$M_{1\gamma} = M_{1\gamma}^{(0)} + ik_1 M_{1\gamma}^{(1)} + k_1^2 M_{1\gamma}^{(2)} + ik_1^3 M_{1\gamma}^{(3)} + \ldots \quad (\gamma = 0; 1). \quad (17)$$

The series (17) converges, generally speaking, only over some region of variation of k_1. The radius of convergence is determined by the form of $V_{\alpha\beta}(r)$. So far as $M_{0\gamma}$ is concerned, we can, by making use of (5), transform Eq. (13) to the form

$$M_{0\gamma} = \sum_\beta \int_0^\infty e^{i\varkappa_1 s + ik_{01}s}\, V_{0\beta}(s)\, x_{\beta\gamma}(s)\, ds. \quad (18)$$

Expanding $\exp i\kappa_1 s$ in powers of κ_1, we get

$$M_{0\gamma} = M_{0\gamma}^{(0)} + i\varkappa_1 M_{0\gamma}^{(1)} + \varkappa_1^2 M_{0\gamma}^{(2)} + k_1^2 M_{0\gamma}^{(3)} + \cdots \quad (19)$$

Substituting (17) and (19) in Eq. (16), and then in Eq. (6), and limiting ourselves to terms of no higher order in k_1 and κ_1 than the second, we obtain

$$\sigma = 4\pi \frac{k_1}{k_0}\, a_1 \frac{1 + a_2 k_1^2}{1 + a_3 k_1 + a_4 \varkappa_1 + a_5 \varkappa_1^2 + a_6 \varkappa_1 k_1 + a_7 k_1^2}\,. \quad (20)$$

The coefficients $a_1 \ldots a_7$ are expressed in terms of $M_{\alpha\gamma}^{(i)}$. In the case in which the threshold of excitation is sufficiently high, we can expand κ_1 near the threshold in powers of k_1^2. We then have, with accuracy up to terms in k_1^2,

$$\sigma = 4\pi\,(k_1/k_0) a_1\,(1 + a_2 k_1^2)\,/\,(1 + a_3 k_1 + a_4 k_1^2). \quad (21)$$

In a number of cases, we can neglect the term $V_{10}F_0$ in (7). This is the so-called method of distorted waves.[1,2] In such an approximation, $M_{01} = 0$, whence, as is easy to show, $a_3 = 0$. Thus, in the approximate method of distorted waves, the linear term of Eqs. (20) and (21) is absent.

---

[1] N. Mott and G. Massey, *Theory of atomic collisions*, IIL, Ch. VIII (Russian translation).

[2] H. S. W. Massey, Rev. Mod. Phys. **28**, 3 (1956).

Translated by R. T. Beyer
133

Statistical Retardation in Dielectric Breakdown of Solid Dielectrics

E. A. KONOROVA
P. N. Lebedev Physical Institute,
Academy of Sciences, USSR

(Submitted to JETP editor June 28, 1956)
J. Exptl. Theoret. Phys. (U.S.S.R.) **32**, 603-604 (March, 1957)

SEITZ[1] made the assumption that, in computing the dielectric strength of crystals on the basis of Hippel's criterion, it is necessary to account for the fluctuations in the behaviour of the electrons in the energy exchange with the lattice. The possibility of such fluctuations is described by a certain probability that the electron will be accelerated to the ionization potential without collisions with the lattice. This assumption leads to the possibility of statistical retardation in the breakdown of thin layers of solid dielectrics, and also to the dependence of the dielectric strength of crystals on thickness (for the thickness range 10^{-3} to 10^{-4} cm).[2,3] In 1952-1954, Japanese investigators[2,5] obtained data on the dependence of dielectric strength on the time of application of the voltage and on the thickness for samples of mica 3 to 5×10^{-4} cm thick (dotted lines in Figs. 1, 2). These authors concluded that Seitz' assumptions were confirmed experimentally. The size of electron avalanches and also the number of initial electrons formed per second were computed. The quantities computed in this manner were in accordance with the approximate computations of Seitz.

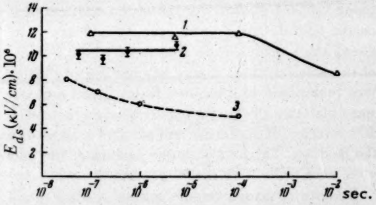

FIG. 1. Dependence of the dielectric strength of glass and mica on the duration of voltage application. 1 – glass, 2 – mica, 3 – mica according to the data, Ref. 5

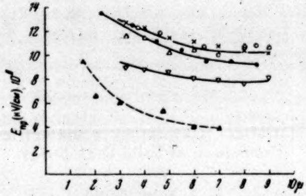

FIG. 2. Dependence of electric strength of glass and mica on the thickness. ● – mica; ▲ – mica, Ref. 2; △ – glass, 5 μ sec pulse; ○ – glass, 0.2 μ sec pulse; × – glass, 100 μ sec pulse; ▽ – glass 10^{-2} sec pulse.

We have also measured the dielectric strength and its dependence on the time of application of the voltage and on the thickness of mica-muscovite and glass of the following composition: $SiO_2 - 68\%$, $B_2O_3 - 20\%$, $Al_2O_3 - 3\%$, $Na_2O - 4\%$, $K_2O - 5\%$, $As_2O_3 - 0.25\%$. A linearly increasing voltage was applied to the samples. The time from the beginning of the voltage rise to the puncture of the sample could be varied between 10^{-2} sec and 5×10^{-8} sec. The dependence of the puncture voltage (E_p) on the sample thickness was obtained for pulse duration of 5×10^{-6} sec. Measurements of the puncture voltage for short pulses were made with the CRT oscillograph type KO-20 (experimental factory VEI), and for pulses of 10^{-2} sec duration with an electrostatic voltmeter across the kenotron. Errors in voltage measurements did not exceed 10% and, judging by the calibration oscillograms, were generally smaller.

Mica plates 2 to 10μ thick and glass films 3 to 10μ thick were used in the experiments. Silver electrodes were formed on the mica surfaces, after carefully cleaning of the latter with benzol, by evaporation in a vacuum in form of two discs 1.5 mm diameter on one side and 5 mm diameter on the other. The samples were placed between two electrodes, sphere and plane (sphere diameter 4mm) with a mixture of glycerine and alcohol poured over them. Since in most cases the samples were punctured at the center of of the smaller disc, it may be considered that puncture took place in a uniform field. Glass samples were punctured between sphere-plane electrodes; a 50% mixture of glycerine and alcohol was used as the medium. Thickness measurements of the samples were made with a ±3% accuracy.

Results of measurements are shown in Figs. 1 and 2. Each point on the graph represents the mean value of dielectric strength measurements on 10 to 16 samples. The mean square error does not exceed 6%. As seen from Fig. 2, the puncture strength of mica and glass increases noticeably with the decrease in thickness from 5 to 2.5μ. This is in agreement with the data obtained earlier (Joffe and Aleksandrov, 1932) for mica at constant voltage, although at constant voltage secondary phenomena could have taken place, such as heating of the sample and formation of space charges. The general form of this dependence agrees also with results of measurements obtained by Ryu and Kawamura[2] for mica-biotite (dotted curve, Fig. 2). However, no dependence of the puncture strength on the duration of voltage application was observed even in sufficiently thin samples, which is contrary to the results of the Japanese investigators (dotted curve, Fig. 1).

The dependence of dielectric strength on the duration of voltage application is very frequently determined by the non-uniformity of the field in the sample. Since the absolute values of dielectric strength for mica-muscovite obtained in our experiments are higher than those published in Ref. 3, the question arises whether the dependence obtained in Refs. 3 and 5 is not in fact related to a non-uniform field.

For glass, with sufficiently short pulses (from 10^{-4} and shorter), the dielectric strength also does not depend on time, and is noticeably lower for pulses of 10^{-2} sec duration. As shown in Refs. 6 to 8, this dependence can be satisfactorily explained as due to the heating of the sample by the prepuncture currents, increased in the ionic conductivity and, as a result of this, formation of ionic space charges which distort the field at the electrodes.

Thus, it may be considered that in the puncture of glass or mica, statistical retardation is generally either absent or less than 10^{-8} sec.

As far as the dependence of the dielectric strength on thickness, in this range of thicknesses, it can be explained not only on the basis of Seitz' assumptions but also on the basis of other theories of electric puncture, for example the theory of Chuchenkov[9].

It appears to us, on the basis of these investigations, that there are not sufficient grounds so far for the conclusions made in Refs. 2 and 5.

The author takes this opportunity to thank Prof. G. I. Skanavi for his interest and attention to this work.

---

[1] F. Seitz, Phys. Rev. 76, 1376 (1949)

[2] G. Ryu and H. Kawamura, J. Phys. Soc. Japan 9, 438 (1954)

[3] Kawamura, Onuki and Ohkura, J. Phys. Soc. Japan 7, 528 (1952)

[4] H. Kawamura, J. Phys. Soc. Japan 8, 731 (1953)

[5] Kawamura, Ohkura and Kikuchi, J. Phys. Soc. Japan 9, 541 (1954)

[6] K. G. Keller, Physica, 14, 475 (1948)

[7] K. G. Keller, Physica, 17, 511 (1951)

[8] I. Wermeer, Physica 20, 313 (1954)

[9] V. A. Chuchenkov, Usp. Fiz. Nauk 54, 185 (1954)

Translated by J. L. Herson
134

The Applicability of the Relation of Detailed Balance for a Cluster of Ions of Stationary Composition

IA. M. FOGEL'
Physical-Technical Institute,
Academy of Sciences, U.S.S.R.

(Submitted to JETP editor July 15, 1956)
J. Exptl. Theoret. Phys. (U.S.S.R.) 32, 604-605
(March, 1957)

IN a recently published work of Korsunskii, Leviant, and Pivovar[1] on the basis for the treatment of the experimental data presented in another work of these authors[2], a confirmation is made of the fact that to processes of charge exchange between ions of a cluster and molecules of a substance, occurring upon passage of the ionic cluster through the substance, one can apply the relation

$$\sigma_{ik} / \sigma_{ki} = N_k / N_i, \tag{1}$$

where σ_{ik} and σ_{ki} are effective cross sections for an ionic transition from the charge-state i to the charge-state k and vice versa; N_k/N_i is the ratio of the number of ions with charge k to the number of ions with charge i in a cluster of stationary composition. The composition of a cluster passing through a layer of material is determined by the differential equations

$$dN_k / dn = \sum_{i=1}^{m} \sigma_{ik} N_i - N_k \sum_{i=1}^{m} \sigma_{kl}, \tag{2}$$

where n is the thickness of the layer of material in atoms per cm^2, and 1, 2, ... m are the charge-states of the ions of the cluster. The cluster attains a stationary state for the condition $dN_k/dn = 0$. The relation (1) is obtained from this condition for the charge-states fulfilling the condition $|i-k| = 1$, if for $|i-k| > 1$ all $\sigma_{ik} = \sigma_{ki} = 0$ (processes of exchange of more than one electron do not occur). Since the conditions indicated in Ref. 2 are not satisfied, its fulfillment in this work proves to be purely by chance, inasmuch as the relation (1) is not derived from any sort of general considerations.

The applicability of Eq. (1) can be subjected to a direct check in processes of capture and loss of two electrons in single collisions of protons and negatively charged hydrogen ions with molecules of hydrogen. For these processes, according to Eq. (1), the equality

$$\sigma_{1-1} / \sigma_{-11} = N^- / N^+. \tag{3}$$

must hold. The effective cross-sections σ_{1-1} for capture of two electrons by protons upon collision with hydrogen molecules, and the ratios N^-/N^+ in a hydrogen cluster of stationary composition, formed in the passage of protons through hydrogen, were determined in the work of Fogel' and Mitin[3]. On the other hand, we determined the effective cross sections of σ_{-11} for the loss of two electrons in collisions of negative hydrogen ions with molecules of hydrogen[4]. In the Table, values of the quantities $\sigma_{1-1}/\sigma_{-11}$ and N^-/N^+ are presented for various energies of the ions of the cluster. The

Energy of Ions, kev.	$\sigma_{1-1}\cdot 10^{18}$ cm^2	$\sigma_{-11}\cdot 10^{17}$ cm^2	$\frac{\sigma_{1-1}}{\sigma_{-11}}\cdot 10^2$	$\frac{N^-}{N^+}\cdot 10^2$	$\frac{\sigma_{1-1}/\sigma_{-11}}{N^-/N^+}$
10,3	7,2	3,8	18,7	17,5	1,1
15,2	11,4	4,1	28,1	13,1	2,1
20,7	12,3	3,8	32,3	9,1	3,6
24,9	8,9	3,9	25,7	6,3	4,1
29,6	7,2	3,7	19,5	4,3	4,5
31,8	4,2	3,1	13,1	3,5	3,7

errors in measurement of the quantities in the table are as follows: for $\sigma_{1\text{-}1}$, ±30%; for N^{-}/N^{+}, +18%; and for $\sigma_{\text{-}11}$, ±15%. As is seen from this Table, the equality (3) is not satisfied in a significant part of the energy interval investigated.

Thus the relation (1) cannot be of universal applicability to processes of energy exchange between an ionic cluster and a material.

---

[1] Korsunskii, Leviant, and Pivovar, Dokl. Akad. Nauk SSSR **107**, 664 (1956).

[2] Korsunskii, Leviant, Markus, and Pivovar, Dokl. Akad. Nauk SSSR **103**, 399 (1955).

[3] Ia. M. Fogel' and R. V. Mitin, J. Exptl. Theoret. Phys. **30**, 450 (1956); Soviet Phys. JETP **3**, 334 (1956).

[4] Fogel', Ankudinov and Slabospitskii, J. Exptl. Theoret. Phys. **32**, 453 (1957).

Translated by C. W. Helstrom
135

On the Possibility of Observing the Variation of the Chemical Potential of Electrons of a Metal in a Magnetic Field

M. I. KAGANOV, I. M. LIFSHITZ and K. D. SINEL'NIKOV
Physico-technical Institute, Academy of Sciences, Ukrainian SSR

(Submitted to JETP editor September 27, 1956)
J.Exptl.Theoret.Phys.(U.S.S.R.) **32**, 605-607 (March, 1957)

1. AS is known, the quantization of the energy levels of electrons in a magnetic field leads to a number of phenomena (diamagnetism of the electron gas, De Haas-van Alfen effect, Shubnikov-de Hass effect, *et el.*) As a rule, the variation of the chemical potential of the electron gas in the magnetic field is insignificant in all these phenomena.

The dependence of the chemical potential ζ on the magnetic field can be detected directly by measuring the contact potential difference $\delta\varphi$ between two samples of the same metal, if one of these samples is placed in a strong magnetic field.

The contact potential difference which arises is determined by the difference of the chemical potentials

$$e\,\delta\varphi = \zeta(H) - \zeta_0; \qquad \zeta_0 = \zeta(0).$$

to the accuracy of a constant component related to the different states of the sample surfaces.

According to Ref. 1, this difference is:

$$e\,\delta\varphi = \frac{2\sqrt{2\pi}}{dU/d\zeta}\left(\frac{e\hbar H}{c}\right)^{3/2}\frac{G(\zeta_0, H)}{\left|\partial^2 S(\zeta_0, p_z)/\partial p_z^2\right|^{1/2}}, \qquad (1)$$

where

$$G(\zeta_0,H) = \sum_{k=1}^{\infty}\frac{1}{k^{3/2}}\Psi(k\lambda)\sin\left[\frac{kc}{ehH}S_m(\zeta_0) \mp \frac{\pi}{4} - 2\pi k\gamma\right]$$

$$\times\cos\left[\frac{k}{2m_0}\frac{dS_m}{d\zeta}\right];$$

$$\Psi(z) = z/\sinh z; \quad \lambda = (\pi c\theta/e\hbar H)\,dS_m/d\zeta$$

(the notation is the same as in Ref. 1). If the expression for the oscillating part of the magnetic moment $\mathbf{M}_{\text{osc}}$ [Ref. 1, Eq. (3.2)] is used, then there can be obtained:

$$e\,\delta\varphi = -\frac{\alpha\,\mathbf{MH}_{\text{osc}}}{N}, \quad \alpha = U\frac{dS_m}{d\zeta}\Big/ S_m\frac{dU}{d\zeta}; \qquad (2)$$

α is a nondimensional function of the angles between the field and the crystallographic directions; $\alpha = \frac{2}{3}$ in case of an isotropic quadratic dependence; N is the number of electrons.

We took into account only that variation of the chemical potential in (1), which is related to the oscillating component of the thermodynamic potential since that variation of the chemical potential which is caused by the presence of monotonic components (diamagnetic and paramagnetic) is proportional to

$$\delta\zeta \sim \mu H(\mu H/\zeta),$$

and, as we will see below, is considerably less than the oscillatory part (certainly, for low temperatures).

In order to estimate the order of magnitude of the effect expected, it can be considered that

$$\left|\partial^2 S(\zeta_0, p_z)/\partial p_z^2\right|_m^{-1/2} G(\zeta_0, H) \sim 1,$$
$$e\,\delta\varphi \sim (\mu H/\zeta_0)^{1/2}; \quad \mu = e\hbar/m^{*}c.$$

For

$$H \sim 10^4\,\text{G}, \qquad \zeta_0 \sim 10^{-12}\ \text{эрг}, \quad \mu \sim 10^{-20}; \qquad \delta\varphi \sim 10^{-6}\ \text{V}.$$

This estimate is lowered considerably since it is not taken into account that the effective mass of the majority of metals for which the De Haas-van

Alfen effect is observed is considerably less than the mass of the free electron (for which $\mu \sim 10^{-20}$). If $m^* = 10^{-2} m_0$ is taken, then it is shown that $\delta\varphi \sim 10^{-3}$ V. Moreover, it should be taken into account that $\zeta_0 \sim 10^{-12}$ erg corresponds to one electron per atom ($n \sim 1$) which, as a rule, also does not hold ($n < 1$).

If there are several electron groups then the potential difference arising is determined as

$$e\,\delta\varphi = 2\sqrt{2\pi}\left(\frac{e\hbar H}{c}\right)^{3/2} \sum \left|\frac{\partial^2 S}{\partial p_z^2}\right|_m^{-1/2} G \Big/ \sum dU_0/d\zeta\,. \quad (3)$$

Here, the summation in the numerator and denominator is made over all the electron groups. However, it should be taken into account that even the weak domain structure, which always exists in single crystals, leads to the diffusion or the total smoothing of the oscillations in components corresponding to the bands with a large number of electrons for small fields. Actually, it is easy to show[1] that it is simply necessary to average the right side of (3) over the various domains to take the domain structure into account. Here, naturally, the components containing the significant random variations of the sine argument drop out,* *i.e.*, precisely those components which correspond to bands with a large number of electrons.

2. The variation of the chemical potential of an electron gas in a magnetic field leads to a dependence of the emission current (both the cold and the thermionic emission) on the magnetic field[2]. Hence, the oscillations in the magnetic field must be observed only in the cold electron emission case**. Portions of the electrons located on the "tail" of the Fermi distribution where they behave substantially as classical particles participate in the thermionic emission. Consequently, a periodic dependence on the magnetic field naturally does not arise.

Direct calculation of the thermionic current under the assumption that the magnetic field is perpendicular to the metal surface and that the dispersion law is quadratic and isotropic, yields

$$I(H) = \frac{\beta H}{kT}\frac{\cosh(\beta_0 H / kT)}{\sinh(\beta H / kT)} I_0,$$

where I_0 is the thermionic current in the absence of the magnetic field, $\beta = e\hbar/2m^*c$ is the electron diamagnetic moment, m is its effective mass, $\beta_0 = e\hbar/2mc$ is the electron spin magnetic moment.

It is interesting to note that the thermionic current can either increase or decrease in strong magnetic fields depending on the relation between the effective mass m^* and the mass of the free electron m. If $m^* = m$, then

$$I(H) = \frac{\beta H}{kT \tanh(\beta H / kT)} I_0,$$

that is, the thermal current increases linearly with the magnetic field $\tanh x \sim 1$, $x \gg 1$ for $\beta H \gg kT$.

It should be noted that the experimental observation of thermionic current variation in a magnetic field is extremely difficult because of the low current intensity at low temperatures.

---

* We note that $S_m(\zeta)$ is a function of the angles between the magnetic field and the crystallographic axes.

** The variation of the total cold emission current in a magnetic field is extremely slight. In particular, a periodic dependence on the magnetic field is apparently not observable in practice. Consequently, we do not dwell on these questions here.

[1] I. M. Lifshitz and A. M. Kosevich, J. Exptl. Theoret. Phys. (U.S.S.R.) **29**, 730 (1955); Soviet Phys. JETP **2**, 636 (1956).

[2] L. N. Rozentsveig, J. Exptl. Theoret. Phys. (U.S.S.R.) **31**, 520 (1956); Soviet Phys. JETP **4**, 455 (1957).

Translated by M. D. Friedman
136

Natural Line Widths of Microwaves

V. M. FAIN
Gorkii State University

(Submitted to JETP editor November 24, 1956)
J. Exptl. Theoret. Phys. (U.S.S.R.) 32, 607-608
(March, 1957)

WHEN molecules are contained in a space whose linear dimensions are much smaller than the emitted wavelength, as often occurs in the microwave range, the molecules radiate as a single quantum-mechanical system and the line width of the spontaneous emission depends on the number of molecules. Dicke and Romer[1,2] showed that the line width is proportional to the number of molecules for "bound" states. The present note will show that this result is also valid for "unbound" states of a molecular system.

We shall consider the practical case of a Boltzmann distribution of molecular energies. For simplicity we shall assume that the molecules are in only two nondegenerate energy states E_+ and E_- ($E_+ > E_-$). The molecular radiation will be regarded as approximately dipolar. It will be assumed that direct molecular interactions can be neglected. Let $n_\pm$ be the numbers of molecules in states of energy $E_\pm$. Then when the gas is in thermal equilibrium with a thermostat at temperature T:

$$n_- - n_+ \approx nE/2kT;\; n = n_- + n_+;\; E = E_+ - E_- = \hbar\omega_0. \tag{1}$$

Here we have taken account of the smallness of E compared with kT, as is usually the case for microwaves.

According to Dicke[1], the states of the gas are characterized by the quantum number $m = (n_+ - n_-)/2$ and the "cooperation number" r. The following condition is satisfied:

$$|m| \leqslant r \leqslant n/2. \tag{2}$$

The radiation intensity from a gas in state (r, m) is[1]

$$I = I_0\,(r + m)\,(r - m + 1), \tag{3}$$

where I_0 is the intensity of spontaneous emission from a single isolated molecule.

When the molecular system is in state (1), $\bar{m} = -nE/4kT$. The bar denotes averaging over the Boltzmann energy distribution. By Eq. (2), r cannot be smaller than $|m|$. It also cannot be much larger than $|m|$ because states with large r are of small statistical weight[1]. When $r = -m$ there is no spontaneous emission because $|m|$ then increases by unity and violates condition (2). Thus it is physically significant to consider the radiation from a gas in the state $m = \bar{m} + 1$; $r = -\bar{m}$. The radiation intensity from such a gas is*

$$I = -I_0 2\bar{m} = I_0 nE/2kT, \tag{4}$$

and thus proportional to n. We shall determine the natural line width when the initial state is $m = \bar{m} + 1$, $r = -\bar{m}$. For the probability amplitudes $b(r, m, \nu)$. where ν denotes the number of photons of frequency ω_λ) in the radiation field, the method of Weisskopf and Wigner[3,4] gives the equations

$$-i\hbar\dot{b}(-\bar{m}, \bar{m} + 1{,}0) = \sum_\lambda (-\bar{m}, \bar{m} + 1{,}0\,|H'|-\bar{m}, \bar{m}, 1)$$

$$\times\, b(-\bar{m}, \bar{m}, 1)\, e^{i(\omega_\lambda - \omega_0)t}, \quad -i\hbar\dot{b}(-\bar{m}, \bar{m}, 1)$$

$$= (-\bar{m}, \bar{m}, 1\,|H'|-\bar{m}, \bar{m} + 1{,}0)$$

$$\times\, b(-\bar{m}, \bar{m} + 1{,}0)\, e^{i(\omega_0 - \omega_\lambda)t},$$

where H' is the interaction energy operator. These equations are solved as in Refs. 3, 4 (for more details see Ref. 5). We use Dicke's relation[1]

$$(r, m\,|H'|\,r, m - 1) = (E_+\,|H'|\,E_-)\,[(r + m)\,(r - m + 1)]^{1/2},$$

where $(E_+|H'|E_-)$ is the transition matrix element for a single independent molecule. The resulting spectral intensity distribution is

$$J(\omega)\,d\omega = \frac{-2\bar{m}\,\gamma_0}{2\pi}\;\frac{\hbar\,\omega\,d\omega}{[(\omega - \omega_0)^2 + \bar{m}^2\gamma_0^2]}.$$

Thus in this case the natural line width is

$$\gamma = -2\bar{m}\,\gamma_0 = (\hbar\,\omega/2kT)n\,\gamma_0, \tag{5}$$

where γ_0 is the natural line width for a single molecule. We shall now estimate γ. Let $\omega_0 = 2 \times 10^{11}$ $\sec^{-1}$ ($\lambda \approx 1$ cm):

$$\gamma_0 \approx \mu_{ab}^2\,\omega_0^3/\hbar\, c^3 \text{(cf. Ref. 4)},\; \mu_{ab} = 10^{-18}\,\text{CGSE};$$

then $\gamma_0 = 3 \times 10^{-7}$ $\sec^{-1}$. This would be the natural line width of a gas where the molecules are assumed to radiate independently. If in a distance of the order of 1 mm, $n = 10^{15}$ molecules are to be found (on levels E_- and E_+) and $T = 300°K$, then $nh\,\omega_0/2kT = 25 \times 10^{13}$ and $\gamma = 10^5$ $\sec^{-1}$. Thus the natural line width of microwaves is not negligibly small, as is usually assumed.

It is easily shown that absorption lines also have the width given by (5)[5]. This follows from general considerations.

We note in conclusion that there is a classical analogue of the effect which has been described. In a system of oscillators whose separation is small compared with the emitted wavelength there is always an indirect interaction through the total radiation field. In the dipole approximation, the radiation damping force which acts on each oscillator is[6]

$$K_{\text{rad}} = (2e^2/3c^3)\sum_{h=1}^{n} \dddot{r}_h. \tag{6}$$

By using (6), it is easily found that the width of the emitted line is $\gamma = n\,\gamma_0$, where n is the number of oscillators. This will be discussed in greater detail in another article.

---

*We note that for spontaneous emission by a system of molecules separated by distances much greater than the emitted wavelength, we would have $I = n_+ I_0$, which disagrees with (4).

The author is indebted to Professor V. L. Ginzburg for comprehensive discussions.

---

[1] R. H. Dicke, Phys. Rev. **93**, 99 (1954)

[2] R. H. Dicke and R. H. Romer, Rev. Sci. Instr. **26**, 915 (1955)

[3] V. Weisskopf and E. Wigner, Z. Physik **63**, 54 (1930); **65**, 18 (1930)

[4] W. Heitler, *Quantum Theory of Radiation*.

[5] V. M. Fain, Dissertation, Gorkii State University, 1956

[6] L. D. Landau and E. M. Lifshitz, *Classical Theory of Fields*, 2nd Ed., Moscow, 1948

Translated by I. Emin
137

Double Absorption Peaks in Electron Resonance at Saturation

N. S. GARIF'IANOV
Physico-Technical Institute, Kazan Branch,
Academy of Sciences, USSR

(Submitted to JETP editor November 24, 1956)
J. Exptl. Theoret. Phys. (U.S.S.R.) **32**, 609
(March, 1957)

SMALLER[1] observed the splitting of nuclear resonance lines when the modulation frequency of the magnitude field was of the order of the line width. We have observed the same type of double peaks of electron resonance absorption in strong fields, when the angle α between the magnetic component H_ν of the radiofrequency field and the static magnetic field H_0 differs from 90°.

Measurements were performed by Zavoiskii's[2] grid current method from 3 to 300 Mc at room temperature. The method is described in detail in Ref. 3. The oscilloscope screen showed twin resonance peaks. The splitting was produced by a 50Mc magnetic field.

For the free radical of $\alpha\alpha$-diphenyl-β-trinitrophenyl-hydrazyl in weak radiofrequency fields when α is changed from 90° to 0° only the ordinary resonance absorption peak is observed with $g_{\mathrm{eff}} = h\nu/\beta H_0 = 2$ (Fig. 1 *a*). This peak has maximum intensity when $\alpha = 90°$ and vanishes when $\alpha = 0$. In strong fields, the free radical with $\alpha \neq 90°$ (Fig. 2) reveals additional absorption peaks (Fig. 1b) which result from modulation of the static magnetic field H_0 by the parallel component $H_{\nu\parallel}$. The number and position of these peaks depend both on the field strength and the angle α; they are given by $\nu_0 = \nu + n\nu$, where $n = 1, 2, 3 \ldots$ This is a special case of Smaller's condition[1].

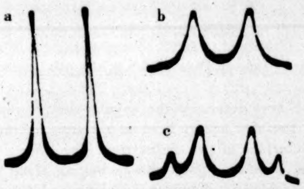

FIG. 1. Twin resonance absorption in the free radical of $\alpha\alpha$-diphenyl-β-trinitrophenyl-hydrazl at $\nu = 30$ Mc and $T = 300°K$. *a)* $\alpha = 90°$ with field ($H_\nu \approx 0.1$ oersted) *b)* $\alpha = 90°$ and *c)* $\alpha = 45$ with strong field ($H_\nu = 2$ oersteds)

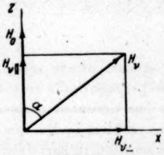

FIG. 2.

Additional peaks were also observed in anthracite from the Kuznets basin and in metallic lithium.

---

[1] B. Smaller, Phys. Rev. **83**, 812 (1951)

[2] E. K. Zavoiskii, Dissertation, Physics Institute, Academy of Sciences, USSR, Moscow, 1944

[3] N. S. Garif'ianov and B. M. Kozyrev, J. Exptl. Theoret. Phys. (U.S.S.R.) **30**, 272 (1956); Soviet Phys. JETP **3**, 255 (1956)

Translated by I. Emin
138

Radiation of a Point Charge Moving Along the Boundary between Two Media

V. E. PAFOMOV
P. N. Lebedev Physical Institute
Academy of Sciences, USSR

(Submitted to JETP editor October 25, 1956)
J. Exptl. Theoret. Phys. (U.S.S.R.) **32**, 610 (March, 1957)

WE here determine the angular distribution of radiated energy from an electron moving above the interface of two dielectrics. The special case of radiation by a point charge moving along the plane separation between a vacuum and dielectric has been considered by Danos[1] and Linhart[2], but Ref. 2 contains incorrect results and Ref. 1 contains misprints.

We assume that the electron is in uniform rectilinear motion with velocity v at distance d from the interface of two media with dielectric constants ϵ_1 and ϵ_2 which are assumed to be real. Let ϵ_1 be the dielectric constant of the medium in which the electron is moving. When the condition for Cerenkov radiation is satisfied only in the second medium ($\epsilon_1\beta^2 < 1$; $\epsilon_2\beta^2 > 1$), all of the energy is radiated into the second medium, and the intensity distribution along the generating lines of the Cerenkov cone is

$$\frac{dW}{dz} = \frac{2e^2}{\pi v^2} \int\limits_{\varepsilon_2\beta^2>1} \omega d\omega \int\limits_0^\pi d\varphi \, \frac{[(\varepsilon_2\beta^2-1)(\varepsilon_1+\varepsilon_2)\cos^2\varphi + \varepsilon_2(1-\varepsilon_1\beta^2)](\varepsilon_2\beta^2-1)\sin^2\varphi}{(\varepsilon_2-\varepsilon_1)[(\varepsilon_1+\varepsilon_2)\sin^2\varphi + \varepsilon_2\beta^2(\varepsilon_2\cos^2\varphi - \varepsilon_1\sin^2\varphi)]} \times \exp\left\{-2d\frac{\omega}{v}[(\varepsilon_2-\varepsilon_1)\beta^2 - (\varepsilon_2\beta^2-1)\sin^2\varphi]^{1/2}\right\}, \tag{1}$$

where φ is the azimuth whose zero is such that the plane $\varphi = \pi/2$ is perpendicular to the interface of the two media*. The Cerenkov cone is defined as in the homogeneous problem by the condition $n\beta\cos\vartheta = 1$, and since this condition is satisfied only below the interface the cone will be semicircular.

Ginzburg and Frank[3] (see also Ref. 4) have considered the radiation from an electron moving along the axis of a channel cut through a dielectric. For wavelengths shorter than the channel radius, the radiation energy decreases exponentially as the radius increases. This is also true qualitatively for the present case.

When $\epsilon_1\beta^2 > 1$ and $\epsilon_2\beta^2 > 1$, the result depends on the ratio of ϵ_1 and ϵ_2. When $\epsilon_1 > \epsilon_2$, the distribution of energy radiated into the second medium is

$$\frac{dW}{dz} = \frac{2e^2c^2}{\pi v^4} \int\limits_{\varepsilon_2\beta^2>1} \omega d\omega \int\limits_0^\pi \frac{A}{B^2} d\varphi;$$

$$A = \{(\varepsilon_1\beta^2-1) + [\sqrt{(\varepsilon_1\beta^2-1)-(\varepsilon_2\beta^2-1)\cos^2\varphi}\cdot\sin\varphi + \sqrt{\varepsilon_2\beta^2-1}\cdot\cos^2\varphi]^2(\varepsilon_2\beta^2-1)\}(\varepsilon_2\beta^2-1)\sin^2\varphi,$$

$$B = \varepsilon_1\sqrt{\varepsilon_2\beta^2-1}\sin\varphi + \varepsilon_2\sqrt{(\varepsilon_1\beta^2-1)-(\varepsilon_2\beta^2-1)\cos^2\varphi} \tag{2}$$

When for $\epsilon_1\beta^2 > 1$ and $\epsilon_2\beta^2 > 1$ we have $\epsilon_1 < \epsilon_2$, then in the region where $\cos^2\varphi < (\epsilon_1\beta^2-1)/(\epsilon_2\beta^2-1)$, the integrand in (2) must be replaced by the integrand in (1).

The flux into the first medium which results from interference is expressed by a more complicated formula that we shall not present here. We shall only mention that for $d = 0$, which means motion in the plane of the boundary, this flux is obtained from (1) and (2) when ϵ_1 and ϵ_2 are everywhere interchanged.

Since our case is not symmetrical with respect to the electron trajectory, a force arises which deflects the electron from its rectilinear motion; this is of interest in some cases. This effect will be the object of a separate investigation.

The author wishes to thank B. M. Bolotovski for discussions.

---

* For $\epsilon_1 = 1$, Eq. (2) is not transformed into the corresponding formulas of Refs. 1 and 2, because of inaccuracies in these articles.

[1] M. Danos, J. Appl. Phys. **26**, 2 (1955)
[2] J. G. Linhart, J. Appl. Phys. **26**, 527 (1955)
[3] V. L. Ginzburg and I. M. Frank, Dokl. Akad. Nauk SSSR **56**, 699 (1947)
[4] B. M. Bolotovskii, Dissertation, Physics Institute, Academy of Sciences, USSR, 1955

Translated by I. Emin
139

Temperature Dependence of the Overhauser Effect in Metallic Lithium

N. A. BEKESHKO AND E. I. KONDORSKII
Moscow State University

(Submitted to JETP editor November 5, 1956)
J. Exptl. Theoret. Phys. (U.S.S.R.) **32**, 611-612
(March, 1957)

OVERHAUSER has shown[1,2] that in metals the saturation of resonance associated with conduction electrons must result in a high degree of nuclear polarization.

Brovetto and Cini[3] have considered the case of high temperature and weak constant magnetic fields and have obtained the following formula for the quantity P which characterizes the degree of nuclear polarization:

$$P = (1 + I)(\gamma_n + s\,|\gamma_e|)\,\hbar H_0 / 3kT. \qquad (1)$$

Here γ_e and γ_n are the gyromagnetic ratios of the electrons and nuclei of the metal, I is the nuclear spin, H_0 is the magnetic field strength, T is the absolute temperature and s is the saturation parameter of electron resonance.

Brovetto and Ferroni[4] found that the equilibrium value of the nuclear polarization is independent of the relaxation time and depends only on the magnetic field strength, temperature and degree of saturation of electron resonance. Bloch[5] and Korringa[6] showed that nuclear polarization must also be observed in nonmetals.

The nuclear polarization predicted by Overhauser and others was first observed by Carver and Slichter[7] in experiments with metallic lithium and later by Beljers, Van der Kint and Wieringen[8] in experiments with the free radical of diphenylpicrylhydrozyl. We present here the results of an investigation of nuclear polarization in metallic lithium at various temperatures from 77.2 to 373° K.

This experiment was performed in a constant magnetic field of 30.1 oersteds generated by Helmholtz coils. The sample consisting of 6 cm^3 of metallic lithium dispersed in oil was placed in a glass test tube within the two coils. The first coil was connected to an oscillator with an output of about 70 watts. The frequency of this oscillator was set equal to 83.6 Mc, the Larmor precession frequency of electrons in the magnetic field. The second coil was included in a double T bridge supplied by an oscillator of frequency 49.89 kc, which was the Larmor precession frequency for nuclei in the same field. The specimen was prepared by cooling during continous stirring of the lithium powder in oil heated above the melting point of lithium (in an argon atmosphere) followed by cavitation crushing in a sound field. The lithium particles were smaller than the depth of the skin layer at 83.6 Mc.

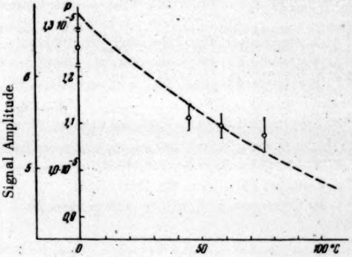

The increase of nuclear polarization was observed through the strengthening of the nuclear magnetic resonance signal. The 49.89 kc signal was transformed into a 465 kc signal which was detected, amplified and observed on an oscilloscope screen. The signal was modulated with 200 cycles. The constant magnetic field, the hf magnetic field and the 49.89 kc magnetic field were mutually perpendicular. The coils and samples were placed in a special housing and the hf oscillator was in a brass container. When the hf was not switched on the nuclear magnetic resonance signal could not be observed because it was weaker than the amplifier noise. In all of the measurements, the same amplifier gain and degree of bridge balance were maintained.

The results are shown in the Figure. For comparison of experiment and theory, the figure includes the curve which represents the temperature dependence of nuclear polarization of lithium in a field of 30.1 oersted as calculated from Eq. (1) with $s = 0.9$ (broken curve). The separate circles represent the experimental values. The ordinates of the circles represent the nuclear magnetic resonance signal amplitude in arbitrary units of a corresponding scale; the strength of the nuclear resonance signal is known to be proportional to the degree of nuclear polarization. We note also that Ref. 7 contains a quantitative comparison between the theoretical and the experimentally observed degree of polarization at room temperature.

The figure shows that with increasing temperature, the signal strength is reduced. The experimental signal strength ratio at 0 and 57° is 1.15, and the corresponding ratio of the values of P calculated from Eq. (1) is 1.21.

Our data are a basis for concluding that the resonance line width increases as the temperature drops.

---

[1] A. W. Overhauser, Phys. Rev. **89**, 689 (1953).

[2] A. W. Overhauser, Phys. Rev. **92**, 411 (1953).

[3] P. Brovetto and G. Cini, Nuovo Cimento **11**, 618 (1954).

[4] P. Brovetto and S. Ferroni, Nuovo Cimento **12**, 90 (1954).

[5] F. Bloch, Phys. Rev. **93**, 944 (1954).

[6] J. Korringa, Phys. Rev. **94**, 1388 (1954).

[7] T. R. Carver and C. P. Slichter, Phys. Rev. **92**, 212 (1953).

[8] Beljers, Van der Kint and Wieringen, Phys. Rev. **95**, 1683 (1954).

Translated by I. Emin
140

The Character of Nucleonic Forces

A. Z. DOLGINOV
Leningrad Physico-Technical Institute,
Academy of Sciences, USSR

(Submitted to JETP editor November 6, 1956)
J. Exptl. Theoret. Phys (U.S.S.R.) 32, 612-614
(March, 1957)

ANALYSIS of experimental data on proton-proton scattering apparently allows us to draw the conclusion that the principal role is played by $^1S_0$ and $^3P_0$ states in the energy region up to 400 Mev[1-3]. There is no basis for thinking that the concept of a potential is generally inapplicable in this region of energy; however, numerous attempts to explain the observed character of the scattering and polarization for *pp* and *np* collisions, using central, tensor and (lS)-forces[4], have been unsuccessful. In order to describe the large contribution of $^3P_0$ and the small contribution of $^3P_1$ and $^3P_2$ states, we introduce the interaction operator in the form

$$\hat{U} = {}^1/_4(1-\sigma_1\sigma_2)V_1 + {}^1/_3 V_2[(lS)^2-\beta], \qquad (1)$$

where $\frac{1}{2}\sigma$ and l are the spin and orbital momentum operators of the nucleon, $S=(\sigma_1+\sigma_2)/2$; V_1, V_2 and β are functions of the invariants r, $\partial/\partial r$, S^2 and l^2, while β is such a function that $\beta\psi_{3P} = \psi_{3P_0}$; ψ_{3P} is the wave function of the system in ^3P states. It is not difficult so to choose β that the second term in (1) plays a role only in the triplet states, for example, $\beta = l^2S^2/4$. It is obvious that

$$\hat{U}\psi_{3P_0} = V_2\psi_{^3P_0}, \quad \hat{U}\psi_{^3P_1} = \hat{U}\psi_{3P_2} = 0,$$

i.e., $\hat{U}$ does not act on the $^3P_1$ and $^3P_2$ states.

We shall not consider here a possible explicit form for V_1 and V_2, since the existing phase analysis is not unique and does not give reliable information on the phases. Nevertheless, data on the character of the interaction in ^3P states make reasonable the separation of the forces in the form (1) and the consideration of the remaining part of the potential (which leads to scattering into the states $^3P_1$ and $^3P_2$) as a small correction. It is possible to choose the values of V_1 and V_2 to account for δ_{1S_0} and δ_{3P_0}, and to guarantee the smallness of all the remaining phases[5,6].

A more accurate description of $^1D_2$, ^3F and the other states, and also an account of the small contribution of $^3P_1$ and $^3P_2$ can be achieved by the introduction into $\hat{U}$ of additional terms [tensor forces, (lS) forces] of corresponding magnitude. We note that a small phase shift δ_{3P_1} and δ_{3P_2}, which does not appreciably disturb the isotropy of the angular distribution, can have a strong effect on the character of the polarization of the nucleons.

Data on *np* scattering at $T=0$ could be explained on the basis of the assumption of a central static potential[1]. If a detailed analysis shows that forces of the form $V_2[(lS)^2-\beta]$ do not give an appreciable contribution at $T=0$, then V_2 can be multiplied by $(1+\tau_1\tau_2)$, where τ is the isobaric spin operator of the nucleons.

A number of authors[7,8] have pointed out that in the nuclear shell model, along with $(l\sigma)$ forces, one must introduce other, velocity-dependent forces. For example, Nilsson[8] has observed that the expression for the average potential of a nucleus ought to contain terms proportional to l^2. We note that $l^2 \equiv (l\sigma)^2$, *i.e.*, it has the same character as the operator $(lS)^2$ in Eq. (1). It is well known that velocity-potentials are equivalent to nonlocal potentials (the potential operator is an integral operator). It is possible that the appearance of terms of the form $V_2[(\mathbf{l}\mathbf{S})^2-\beta]$ in the interaction potential of two nucleons (for $T=1$) reflects the nonlocal character of of this interaction.

Let us consider the general case of velocity-dependent forces. The potential between two nucleons can depend on four vector operators $\mathbf{n}=\mathbf{r}/r$, $\boldsymbol{\sigma}_1$, $\boldsymbol{\sigma}_2$ and $\mathbf{l}$, and on the scalar operators r, $\partial/\partial r$, l^2.

Examples are given in the papers of Simon[9] and Racah[10] of irreducible tensor operators acting on spin space. In similar fashion we can introduce operator functions $Y_{N\nu}(\mathbf{l})$, whose components are transformed in a rotation of coordinates according to a $(2N+1)$ dimensional irreducible respresentation. For example,

$$Y_{00}(\mathbf{l})=1;\quad Y_{10}(\mathbf{l})=l_z;\quad Y_{1\pm1}(\mathbf{l})=\pm\sqrt{\frac{1}{2}}\,(l_x\pm il_y);$$

$$Y_{20}(\mathbf{l})=\sqrt{\frac{1}{6}}\,(3l_z^2-l^2);$$

$$Y_{2\pm1}(l)=\pm\frac{1}{2}[(l_x\pm il_y)\,l_z+l_z\,(l_x\pm il_y)];$$

$$Y_{2\pm2}(\mathbf{l})=\frac{1}{2}\,(l_x\pm il_y)^2.$$

$Y_{N\nu}(\mathbf{l})$ must be so constructed that its form does not change upon permutation of l_z and $l_x \pm il_y$. Only in this case will the representation be irreducible.

An explicit form for $Y_{N\nu}(\mathbf{l})$ can be found by means of the relation

$$Y_{N\nu}(\mathbf{l})=\frac{1}{2}\sum_{\nu_1,\nu_2}C^{N\nu}_{N-1\nu_1,\,1\nu_2}\{Y_{N-1\nu_1}(\mathbf{l}),\ Y_{1\nu_2}(\mathbf{l})\},\qquad(2)$$

where { } represents and anti-commutator, while $C_{\dots}$ are the Clebsh-Gordan coefficients:

$$Y_{N\nu}(\mathbf{l})\,Y_{lm}(\vartheta\varphi)=A_{Nl}C^{l\mu}_{N\nu lm}Y_{l\mu}(\vartheta\varphi).\qquad(3)$$

In order to compute the A_{Nl}, it is necessary to make use of the explicit form of $Y_{N\nu}(\mathbf{l})$, where we can take any convenient values for ν and m, since the A_{Nl} do not depend on them.

Let S be the operator of the total spin of the system of particles of spin ½. We can then construct [in a fashion similar to (2)] operator functions $Y_{N\nu}(S)$. By virtue of the commutation properties of the σ_k, they can be shown to differ from zero only for $N\leqslant 2S$. For example, $Y_{N\nu}(\sigma)\neq 0$ only for $N=0$ or 1.

Since T is a sufficiently good quantum number, transitions between singlet and triplet states are improbable; this means that $\boldsymbol{\sigma}_1$ and $\boldsymbol{\sigma}_2$ ought to enter symmetrically into the potential. Therefore, we have only $\mathbf{n}$ and $\mathbf{l}$ left at our disposal. The invariant function of these operators, which can be regarded as the interaction potential, has the form

$$\hat{U}=\sum B^{N_g}_{N_1N_2}\left(r,\frac{\partial}{\partial r},S^2,l^2\right)\gamma_g C^{N\nu}_{N_1\nu_1N_2\nu_2}Y^{\bullet}_{N\nu}(\vartheta\varphi)\,Y_{N_1\nu_1}$$
$$\times(\mathbf{l})\,Y_{N_2\nu_2}(S),\qquad(4)$$

where $\gamma_0=1$, $\gamma_1=\tau_1\,\tau_2$; $B^{Ng}_{N_1N_2}$ are functions of invariant operators. The summation is taken over all possible values of N_i, ν_i and g. Only those N_i are possible which leave (4) invariant relative to inversion of the coordinate system ($\mathbf{r}\to-\mathbf{r}$) and to time reversal ($\mathbf{l}\to-\mathbf{l}$, $\sigma\to-\sigma$). It is easy to see that $\hat{U}$ contains all forms of potentials which are usually considered.

If account is taken of the possibility of transitions between states with different S, then we make the following substitution in Eq. (4):

$$Y_{N_2\nu_2}(S)\to\sum b^{N_2}_{N_3N_4}C^{N_2\nu_2}_{N_3\nu_3N_4\nu_4}Y_{N_3\nu_3}(\sigma)\,Y_{N_4\nu_4}(\sigma).$$

where $b^{N_2}_{N_3N_4}$ is a function of the invariant operators, symmetrized for N_3, ν_3 and N_4, ν_4. The operator $(\mathbf{l}\mathbf{S})^2-\beta$ selects one state of all the possible states with $S=1$ and $l=1$, the state with the definite value of total angular momentum $J=0$. We give a general method for the construction of such projection operators for arbitrary l, S and J. We shall seek the projection operator in the form

$$\Pi^J_{lS}\psi^{j\mu}_{lS}=\sum_{N\nu}a^N_{lS}(-1)^\nu Y_{N-\nu}(S)\,Y_{N\nu}(\mathbf{l})\,\psi^{j\mu}_{lS}=\delta_{Jj}\psi^{j\mu}_{lS},$$

where $\psi^{j\mu}_{ls}$ is the wave function with definite values of the total angular momentum j and momenta l and S:

$$\psi^{j\mu}_{lS}=\sum_{m,\sigma}C^{j\mu}_{lmS\sigma}\psi_{S\sigma}(\xi)\,Y_{lm}(\vartheta\varphi).\qquad(5)$$

Making use of Eq. (3) and the orthogonality relations for the Racah functions[10] $W(abcd;ef)$, we obtain

$$a^N_{lS}=(2N+1)(2J+1)(-1)^{S+l-J}A^{-1}_{NS}A^{-1}_{Nl}[(2l+1)$$
$$\times(2S+1)]^{-1/2}W(llSS;\ NJ).\qquad(6)$$

Since

$$(\mathbf{l}\mathbf{S})=\sum_\nu(-1)^\nu Y_{1-\nu}(\mathbf{S})\,Y_{1\nu}(\mathbf{l}),$$

then, for $S=½$, we obtain the well-known relation

$$\Pi^J_{l\frac{1}{2}} = [2J + 1 + 8(J - l)(lS)][2(2l + 1)]^{-1}.$$

The projection operator on the state with given L, S and J of the form

$$P^J_{LS}\psi^{j\mu}_{ls} = \delta_{Jj}\delta_{Ll}\delta_{Ss}\psi^{J\mu}_{LS}$$

is an integral operator with kernel

$$\sum_M \psi^{JM}_{LS}(\xi, \vartheta, \varphi)\, \psi^{JM}_{LS}(\xi', \vartheta', \varphi').$$

---

[1] Ia. A. Smorodinskii, Probl. sovrem. fiz IIL, No. 7, 1954.

[2] A. Zimin, Dokl. Akad. Nauk SSSR **105**, 73 (1955).

[3] H. Feshbach and E. Lomon, Phys. Rev. **102**, 891 (1956).

[4] K. Case and A. Pais, Phys. Rev. **80**, 203 (1950).

[5] R. Jost and W. Kahn, Dan Mat. Fys. Medd. **29**, No. 9 (1953).

[6] V. Marchenko, Dokl. Akad. Nauk SSSR **104**, 695 (1955).

[7] W. E. Frahn, Nuovo Cimento **4**, 313 (1956).

[8] S. G. Nilsson, Dan. Mat Fys. Medd. **29**, No. 16 (1955).

[9] A. Simon, Phys. Rev. **92**, 1050 (1953).

[10] Racah, Phys. Rev. **62**, 442 (1942).

Translated by R. T. Beyer
141

Photodisintegration of Neon Nuclei

A. P. KOMAR AND I. P. IAVOR
Leningrad Institute of Technical Physics
of the Academy of Sciences, USSR

(Submitted to the JETP editor November 24, 1956)
J. Exptl. Theoret. Phys. (U.S.S.R.) **32**, 614-615
(March, 1957)

A NATURAL mixture of neon isotopes contained in a fast acting Wilson cloud chamber under a pressure of 1.4 atm, was irradiated by γ-rays from the synchrotron up a to maximum energy of 80 Mev. The Wilson chamber was in a magnetic field of 5750 Oersted.

The following reactions were observed (a total of 719 cases): (γp), (γpn), ($\gamma 2p$), ($\gamma 2a$), (γap) and ($\gamma 5a$). Reactions (γp) and (γpn) were distinguished by the pulse size and direction of the recoil nucleons, reactions (γp) and (γa) were distinguished by the ionization density and the tracks of the recoil nuclei.

The orientation and length of tracks were determined by the reprojection method. The angular distribution (in the laboratory system of coordinates) of photoprotons from 1 to 15 Mev was studied. The dependence of the relative number of protons per unit solid angle on the angle θ between the direction of proton flight and the axis of the γ-ray beam is shown in the Figure in diagram form in 20° intervals. The angular distribution is well described by a formula of the form $a + b\sin^2\theta$, where $b/a \approx 2.5$.

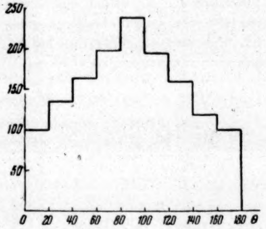

The number of observed cases for the separate types of reactions is as follows:

Type of disintegration:	(γp)	(γpn)	($\gamma 2p$)	($\gamma 2a$)	(γap)	($\gamma 5a$)
Number of cases:	352	137	64	21	143	2

It should be noted that there is a substantial difference in the angular distributions of photoprotons for argon[1] and neon. Since the neon and argon nuclei are even-even, this difference cannot be due to the difference in nuclear spins but is apparently associated with the difference in the shell structures of the nuclei. The integral (γp) reaction cross section for neon determined relative to the (γp) reaction cross section for helium[2] turned out to be 0.16 ± 0.08 Mev-bn.

---

[1] A. P. Komar and I. P. Iavor, J. Exptl. Theoret. Phys. (U.S.S.R.) **31**, 531 (1956); Soviet Phys. JETP **4**, 432 (1957).

[2] E. R. Gaerttner and M. L. Yeater, Phys. Rev. **83**, 146 (1951).

Translated by J. L. Herson
142

Concerning the Lifetime of the Two Forms of the π^0 Meson

A. V. ROMANKEVICH
Moscow State University

(Submitted to JETP editor February 12, 1956)
J. Exptl. Theoret. Phys. (U.S.S.R.) 32, 615 (March, 1957)

ACCORDING to the theory of Fermi and Jang[1], it is assumed that π mesons are formed by nucleons in contact interaction (potential well of width $\hbar/Mc \sim 10^{-14}$ and depth 25×10^9 ev. According to this theory there exist two forms of π^0 mesons; π^0 $(P+\overline{P})$ and $\pi^0\,(N+\overline{N})$; where P denotes proton, N neutron, $\overline{P}$ antiproton, $\overline{N}$ antineutron. In this note are presented results of calculations of the lifetime for the two form of the π^0 meson.

Computations were made by the general method of the invariant perturbation theory for a pseudoscalar meson with pseudoscalar coupling in the approximation $(\mu/M)^2 \ll 1$, where μ denotes the mass of the meson and M the mass of the nucleon, under the assumption that the expansion in the power of $g^2/\hbar c$ is valid. It was considered that the disintegration of the two forms of π^0 mesons occurs according to two mutually exclusive Feynman diagrams (Figs. 1a and b),

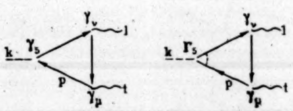

where k is the 4-momentum of the meson, t, l are 4-momentum quanta, p is the 4-momentum of the virtual nucleon, $\gamma_i = -i\beta a_i$ $(i = 1, 2, 3)$, $\gamma_4 = \beta$, $\gamma_5 = \gamma_1, \gamma_2, \gamma_3, \gamma_4$, $\gamma_5^2 = 1$, $\hbar = c = 1$, the upper portion which includes the charged meson, computed in Refs. 2 and 3.

The life time obtained was:

$$\frac{1}{\tau} \approx \left[1;\ \frac{3}{\pi^2}\left(\frac{g^2}{\hbar c}\right)^2\right] \frac{1}{16\pi^2}\left(\frac{g^2}{\hbar c}\right)\left(\frac{e^2}{\hbar c}\right)^2\left(\frac{\mu}{M}\right)^2\frac{\mu c^2}{\hbar},$$

where the first term in the square parenthesis corresponds to the $\pi^0\,(P+\overline{P})$ meson, the second term to the $\pi^0\,(N+\overline{N})$ meson. Within the limits of the method used, the life times of the two π^0 mesons, are generally speaking, different.

By the same method and using the same approximations the conversion probability of one π^0 meson into the other was evaluated by the simpler diagram (Fig. 2)

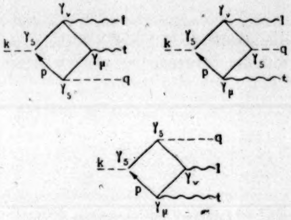

where q denotes the 4-momentum of the end meson. The logarithmic deviation was removed by subtraction. For the life time in this process we obtained the value:

$$1/\tau \approx (N^4/192\pi)\,(g^2/\hbar c)^2\,(e^2/\hbar c)^2\,(\mu/M)^4\,(m/\mu)^3\,mc^2/\hbar,$$

where m denotes the mass of the electron, $N = (\mu_1 - \mu_2)/m$ the mass difference of the mesons.

---

[1] E. Fermi and C. Jang, Phys. Rev. 76, 1739 (1949).

[2] A. D. Galanin, J. Exptl. Theoret Phys. (U.S.S.R.) 26, 417 (1954).

[3] A. D. Galanin and V. G. Solovev, J. Exptl. Theoret Phys. (U.S.S.R.) 27, 112 (1954).

Translated by J. L. Herson
143

On the Derivation of the Low Equation in the Theory of Meson Scattering

A. M. BRODSKII
Moscow State University

(Submitted to JETP editor November 27, 1956)
J. Exptl. Theoret. Phys. (U.S.S.R.) 32, 616-617
(March, 1957)

THERE is shown in this note a new method of deriving Low's equations, the analysis of which is very important in discussions pertaining to the theory of scattering of mesons by nucleons. It is shown that they may be written in a form, where the concrete type of interaction enters in a simple way through a nonhomogeneous term.* In the analysis of the scattering of π-mesons by nucleons, let us introduce the amplitude (T-matrix) of scattering connected with the corresponding matrix element of the S-matrix in the following manner.

---

*It should be noted that a series of causality conditions and renormalization, assumed in the derivation of the dispersion relations, are thereby imposed on the interaction and also the condition of sufficiently rapid decay of certain expressions under the integral in Refs. 3, 4.

$$(p'\sigma', k'j \mid S \mid p\sigma, ki) = \delta_{\sigma\sigma'}\,\delta_{ij}\,\delta(\mathbf{p}' - \mathbf{p})\,\delta(\mathbf{k} - \mathbf{k}') - (2\pi i)\,[(2\pi)^3\, 2k_0'\, 2k_0]^{-1/2}\,\delta(p' + k' - p - k) \times (p'\sigma', k'j \mid T \mid p\sigma, ki). \tag{1}$$

Here $p, k (p', k^1)$ denote the momenta at $-\infty\ (+\infty)$ of the incident (scattered) nucleon and meson, satisfying the relations

$$p + k = p' + k', \quad \gamma p = \gamma p' = -m^2, \quad k^2 = k'^2 = -\mu^2, \tag{2}$$

where m and μ are experimental masses; all other magnitudes are considered also renormalized.

From the definition of the scattering amplitude and the unitarity condition of the S-matrix it follows directly that

$$\{T - T^+\} \equiv [(p'\sigma', k'j \mid T \mid p\sigma, ki) - (p'\sigma', k'j \mid T^+ \mid p\sigma, ki)] = -2\pi i \sum_n \int dp_n\,(n \mid T \mid p'\sigma', k'j)^*\,(n \mid T \mid p\sigma, ki) \times \delta(p_n - p - k), \tag{3}$$

where it is necessary to take $p + k = p^1 + k^1$ on the right side of the equation; (n) is the complete specification of the state as an example of which we choose the system of eigenfunctions of the energy vector—the momentum P at infinity with eigenvalues $p^2 = p_n^2$. Note that for coherent forward scattering the left side of equation (3) is the imaginary part of the scattering amplitude, and on the right side represents the complete scattering cross section with an accuracy up to a coefficient proportional to the flow of the incident particles. Thus, in this case, (3) is equivalent to the well-known "optical" theorem.[5]

Let us further make use of the scatter amplitude written in a general form which follows[6-8] from the investigation of the property of invariance and symmetry of the given amplitude*

$$(p'\sigma', k'j \mid T \mid p\sigma, ki) = -\bar{u}(p'\sigma')\left\{(1 + \mathrm{Int}) \sum_{\lambda_i = 1,0} (\gamma k)^{\lambda_1} (\tau_j \tau_i)^{\lambda_2}\, \rho_{\lambda_1\lambda_2}((p+k)^2, (p - p')^2)\right\} u(p, \sigma),$$
$$\mathrm{Int} \equiv k \leftrightarrow -k', \quad i \leftrightarrow j; \quad p' + k' = p + k. \tag{4}$$

Here $\rho\lambda_1\lambda_2(p + k)^2, (p - p^1)^2)$ denote certain functions which can be represented, as analysis of the Feynman diagrams[6] and consideration of the causality condition will show, in the form:

$$\rho_{\lambda_1\lambda_2}((p+k)^2, (p - p')^2) = \frac{\delta(\lambda_1\lambda_2)}{(p+k)^2 + m^2 - i\varepsilon} + \int\limits_{(m+\mu)^2}^{\infty} dM_1^2 \int\limits_{(2\mu)^2}^{\infty} dM_2^2\, \frac{\omega_{\lambda_1\lambda_2}(M_1^2, M_2^2)}{[(p+k)^2 + M_1^2 - i\varepsilon]\,[(p - p')^2 + M^2 - i\varepsilon]}, \tag{5}$$

where $\delta(\lambda_1\lambda_2)$ is a constant depending on the method of renormalization of the charge; dependence of $\delta(\lambda_1\lambda_2)$ on λ_{21} is determined by the form of interaction and can be readily established by comparing $P\lambda_1\lambda_2$ with the first term of the perturbation theory expansion. Further analysis will be conducted in the laboratory system of coordinates $[p = (m,0)]$.

The following inequalities which follow from (2) are valid for the subsequent portion of the analysis;

$$(p - k')^2 + M_1^2 = -(m + \mu)^2 + 2m(k_0' + \mu) + M_1^2 > 0,$$
$$(p + k)^2 + m^2 = -2mk_0 - \mu^2 < 0,$$
$$(p - p')^2 + M_2^2 = -2m(m - p_0') + M_2^2 > 0. \tag{6}$$

Considering (4-6) and making use of (2), the difference ($T - T$ +) [Eq. (3)] can be written in form**

$$\{T - T^+\} \equiv -2i\bar{u}(p'\sigma')\left\{(1 + \mathrm{Int}) \sum_{\lambda_i = 1,0} (\tau_j\tau_i)^{\lambda_2} (\gamma_k)^{\lambda_1}\, \mathrm{Im}\,[\rho_{\lambda_1\lambda_2}((p+k)^2, (p - p')^2)]\right\} u(p\sigma)$$
$$= -2\pi i\bar{u}(p'\sigma')\left[\sum_{\lambda_i = 1,0} (\tau_j\tau_i)^{\lambda_2} (\gamma_{k'})^{\lambda_1}\, P \int\limits_{(2\mu)^2}^{\infty} \frac{\omega_{\lambda_1\lambda_2}(-(p+k)^2, M_2^2)}{(p - p')^2 + M_2^2}\, dM_2^2\right] u(p, \sigma) \tag{7}$$

$(p + k) = p^1 + k^1$. It follows from the comparison of (3) and (7) that in the laboratory system of computation,

---

* The symbols of Ref. 6 are generally used herein.

** For the derivation of (6) it is necessary to remember that, according to the accepted symbols, $u = u^*\gamma_0$, $(\gamma_0\gamma_u)^+ = \gamma_0\gamma_\mu$

$$P \int\limits_{(m+\mu^2)}^{\infty} dM_1^2 \int\limits_{(2\mu)^2}^{\infty} dM_2^2 \frac{\omega_{\lambda_1\lambda_2}(M_1^2, M_2^2)}{[-(\mu^2+m^2+2mk_0)+M_1^2]\,[(p-p')^2+M_2^2]}$$

$$= \frac{1}{\pi i}\int\limits_{\mu}^{\infty} d\widetilde{k}_0 \frac{\operatorname{Im}\rho_{\lambda_1\lambda_2}((\mu^2+m^2+2m\widetilde{k}_0),(p-p')^2)}{\widetilde{k}_0-k_0}\Bigg|_{p+k=p'+k'} \qquad (8)$$

Now, separating in (3) the obvious dependence on p_0+k_0, and examining separately the terms of the expression of (7) within the square parentheses, Eq. (4) can from the present viewpoint, be finally rewritten in a form equivalent to the first of Low's infinite system of equations:

$$(p'\sigma', k'j\,|\,T\,|\,p\sigma, ki)$$

$$= -\bar{u}(p'\sigma')\left\{(1+\mathrm{Int})\sum_{\lambda_i=1,0}(\gamma_k)^{\lambda_1}(\tau_j\tau_i)^{\lambda_2}\frac{\delta(\lambda_1\lambda_2)}{(p+k)^2-m^2-i\varepsilon}\right\}u(p,\sigma) \qquad (9)$$

$$+(1+\mathrm{Int})\sum_n{}'\int dp_n\left\{\frac{(n\,|\,T\,|\,p'\sigma', k'j)^*(n\,|\,T\,|\,p\sigma, ki)}{p_{0n}-p_0-k_0-i\varepsilon}\,\delta(\mathbf{p}_n-\mathbf{p}-\mathbf{k})\right\},$$

where prime at the summation symbol indicates that the summation is carried out over all n, except the case $p^2 n=-m^2$ and the momenta satisfy conditions (2). Thereby also, the physical state of the nucleon is considered as the lowest stable state and the difference between the proton and neuteron masses is neglected. We note that this reasoning could have been simplified by the introduction of Gilbert's concept of the transformation operator, since the hermitian and the skew hermitian operators $T+T^+$ and $T-T^+$ are, in view of the causality principle, mutual forms in the sense of Hilbert's transformation, with an accuracy up to the addition of terms which differ by a permutation of the integrations.

In conclusion the author expresses his deep gratitude to Prof. D. D. Ivanenko, whose remark with reference to Low's equation and dispersion relations, made at the Moscow Conference on High Energy in May 1956, served as the starting point for this work.

---

[1] F. E. Low. Phys. Rev. 97, 1392 (1955).

[2] G. F. Chew and F. E. Low, Phys, Rev. 101, 1570 (1956).

[3] M. L. Goldberger, Phys. Rev. 99, 979,(1955).

[4] M. Oeheme, Phys. Rev. 101, 1503 (1956).

[5] M. Lax, Phys. Rev. 78, 306 (1950).

[6] A. M. Brodskii, Dokl. Akad, Nauk. SSSR 111, 787 (1956).

[7] Y. Nambu, Phys. Rev. 100, 394 (1955).

[8] G. Feldman and Matthews, Phys. Rev. 102, 1421 (1956).

**For the derivation of (6) it is necessary to remember that, according to the accepted symbols, $u=u^*\gamma_0$, $(\gamma_0\gamma_\mu)^+=\gamma_0\gamma_\mu$.

Translated by J. L. Herson
144

The Hall Effect in Bismuth Under Pressures up to 30,000 Kg/cm^2

A. I. LIKHTER AND L. F. VERESHCHAGIN
Laboratory for the Physics of Ultra-High Pressures, Academy of Sciences, USSR

(Submitted to JETP editor November 27, 1956)
J. Exptl. Theoret. Phys. (U.S.S.R.) 32, 618
(March, 1957)

IN the course of our work on the investigation of the Hall effect in bismuth[1], we built an apparatus for measurements at pressures up to 30,000 kg/cm^2. A pressure up to 30,000 kg/cm^2 is created inside a microlite matrix, which is surrounded on all sides by a lead casing and receives support on almost all sides in a steel conical mounting. The microlite matrix was prepared for us in the Glass Laboratory the Mendeleev Moscow Chemico-Technical Institute.* The means for transmitting the pressure is silver chloride, which transmits hydrostatic pressure sufficiently well for a pressure chamber of diameter 11-12 mm and height 4 mm. A thin plate of bismuth is embedded in the silver chloride, with five contacts which make it possible to measure the resistance, the dependence of resistance on magnetic field, and the Hall effect, as functions of pressure. The magnetic field is introduced into the matrix through the plungers exerting the pressure. In one of the plungers are found four miniature electrical conductors. The measurements were made on bismuth of 99.99% purity.

---

*We consider it our pleasant duty to express our thanks to Prof. I. I. Kitaigorodskii and scientific technician Ts. M. Gurevich for the great labor furnished by them in working out the technology and preparing these matrices.

The occurrence of the I-II and II-III transitions in bismuth was clearly seen by jumps in the resistance. With increasing pressure the Hall effect in bismuth progressivley decreases, and in modification III, it becomes at least three orders of magnitude smaller than for bismuth under normal pressure. The dependence of resistance on magnetic field in modification III also falls below the limits of sensitivity of the measuring system. Noting that in modification III, according to the measurements of Bridgman[2] and also of Butuzov and Gonikberg[3], the melting point increases with pressure; and that, according to the measurements of Chester and Jones[4], superconductivity occurs in bismuth III, it is obviously possible to assume that bismuth III is a true metal, in contrast to bismuth I, which is characterized as a "semi-metal". Since details of the change of Hall effect with pressure in modification I obviously depend on the orientation of the plate, the necessity arose of carrying out the experiments with monocrystalline plates, after which we shall publish a detailed article.

---

[1] A. I. Likhter and L. F. Vereshchagin, Dokl. Akad. Nauk SSSR **103**, 791 (1955).

[2] P. W. Bridgman, Phys. Rev. **48**, 893 (1935).

[3] V. P. Butuzov and M. G. Gonikberg, J. Inorg. Chem **1**, 1543 (1956).

[4] P. F. Chester and G. O. Jones, Phil. Mag. **44**, 1281 (1953).

Translated by C. W. Helstrom
145

Hydrodynamic Fluctuations

L. D. LANDAU AND E. M. LIFSHITZ
Intitute for Physical Problems,
Academy of Sciences, USSR

(Submitted to JETP editor November 29, 1956)
J. Exptl. Theoret. Phys. (U.S.S.R.) 32, 618-619
(March, 1957)

A GENERAL theory of hydrodynamic fluctuations can be constructed by introducing "outside" terms into the equation of motion of the liquid, as was done by Rytov[1] for the fluctuations of an electromagnetic field in continuous media; he introduced corresponding "outside" fields in Maxwell's equations.

The introduction of such additional terms can be accomplished in different equivalent ways. The most advantageous is the form in which the fluctuations of the "outside quantities" at the various points of the liquid are not correlated with one another. This is accomplished by the introduction of "outside stress tensor" s_{ik} in the Navier-Stokes equation and the "outside heat flow" vector **g** in the heat conduction equation (the equation of continuity remains unchanged). The system of hydrodynamic equations then takes the form

$$\frac{\partial\rho}{\partial t} + \operatorname{div}(\rho\mathbf{v}) = 0, \tag{1}$$

$$\rho\frac{\partial v_i}{\partial t} + \rho(\mathbf{v}\nabla)v_i = -\frac{\partial\rho}{\partial x_i} + \frac{\partial\sigma'_{ik}}{\partial x_k}, \tag{2}$$

$$\rho T\left(\frac{\partial s}{\partial t} + \mathbf{v}\nabla s\right) = \frac{1}{2}\sigma'_{ik}\left(\frac{\partial v_i}{\partial x_k} + \frac{\partial v_k}{\partial x_i}\right) - \operatorname{div}\mathbf{q}, \tag{3}$$

$$\sigma'_{ik} = \eta\left(\frac{\partial v_i}{\partial x_k} + \frac{\partial v_k}{\partial x_i} - \frac{2}{3}\delta_{ik}\frac{\partial v_l}{\partial x_l}\right) + \zeta\frac{\partial v_l}{\partial x_l}\delta_{ik} + s_{ik}, \tag{4}$$

$$\mathbf{q} = -\varkappa\Delta T + \mathbf{g} \tag{5}$$

(all the notation agrees with that used in our book[2]). To these equations should be added the relations which define the mean values of the products of components s_{ik} and g_i. We do this by first assuming the fluctuations to be classical (*i.e.*, their frequencies $\omega \ll kT/\hbar$), while the viscosity and the thermal conductivity of the liquid are non-dispersive.

The rate of change of the total entropy of the liquid S is given by the expression [see Ref. 2, Sec. 49]

$$\dot{S} = \int\left\{\frac{\sigma'_{ik}}{2T}\left(\frac{\partial v_i}{\partial x_k} + \frac{\partial v_k}{\partial x_i}\right) - \frac{\mathbf{q}\nabla T}{T^2}\right\}dV. \tag{6}$$

Following the general rules of fluctuation theory laid down in Ref. 3, Secs, 117, 120, we select as the values $\dot{x}_a$ figuring in this theory the components of the tensor σ'_{ik} and the vector q[*]. It is then evident from Eq. (6) that the role of the corresponding quantities X_a will be played by

$$-\frac{1}{2T}\left(\frac{\partial v_i}{\partial x_k}+\frac{\partial v_k}{\partial x_i}\right)\Delta V \quad \text{и} \quad \frac{1}{T^2}\frac{\partial T}{\partial x_i}\Delta V,$$

while Eqs. (4) and (5) play the role of the relations $\dot{x}_a = -\gamma_{ab}X_b + y_a$ (see Ref. 3, Sec. 120), where the s_{ik} and g_i correspond to the quantities y_a. The coefficients γ_{ab} in these relations determine directly the mean values

$$\overline{y_a(t_1)\,y_b(t_2)} = k(\gamma_{ab}+\gamma_{ba})\,\delta(t_1-t_2).$$

The final formulas have the form:

$$\begin{aligned}\overline{s_{ik}(\mathbf{r}_1,t_1)s_{lm}(\mathbf{r}_2,t_2)} &= 2kT\,[\eta\,(\delta_{il}\delta_{km}+\delta_{im}\delta_{kl}) \\ &\quad + (\zeta-2\eta/3)\,\delta_{ik}\delta_{lm}]\,\delta(\mathbf{r}_2-\mathbf{r}_1)\,\delta(t_2-t_1), \qquad (7)\\ \overline{g_i(\mathbf{r}_1,t_1)\,g_k(\mathbf{r}_2,t_2)} &= 2kT^2\varkappa\delta_{ik}\delta(\mathbf{r}_2-\mathbf{r}_1)\,\delta(t_2-t_1),\\ \overline{g_i(\mathbf{r}_1,t_1)\,s_{lm}(\mathbf{r}_2,t_2)} &= 0.\end{aligned}$$

If use is made of the spectral components of the fluctuating quantities, which are defined by

$$x_\omega = \frac{1}{2\pi}\int_{-\infty}^{\infty} x(t)\,e^{i\omega t}\,dt, \qquad \overline{x^2} = \iint_{-\infty}^{\infty}\overline{x_\omega x_{\omega'}}\,d\omega\,d\omega',$$

then the factor $\delta(t_2-t_1)$ in eqs. (7) is replaced by $\delta(\omega+\omega')/2\pi$.

These results are generalized without difficulty to the case of the presence of dispersion in the coefficients of viscosity or thermal conductivity and the quantum nature of the fluctuations with the aid of the general theory of Callen and others, in the form set forth in Ref. 4. There appears only the factor $(\hbar\omega/2kT)\coth\hbar\omega/2kT$ in the expressions for the average values of the products of the spectral components s_{ik} and g_i, while the quantities η, ζ, $\varkappa$ are to be replaced by their real parts.

---

[1] S. M. Rytov, *Theory of electrical fluctuations and heat radiation*, Academy of Sciences Press, 1953.

[2] L. D. Landau and E. M. Lifshitz, *Mechanics of continuous media*, 2nd edition, Gostekhizdat, 1954.

[3] L. D. Landau and E. M. Lifshitz, *Statistical physics*, 3rd edition, Gostekhizdat, 1951.

[4] L. D. Landau and E. M. Lifshitz, *Electrodynamics of continuous media*, Gostekhizdat, in press.

---

[*] An inessential difference, connected with the fact that we are dealing here with a continuous (values at each point of the liquid) as against a discrete set of fluctuating quantities (for which the formulas in Ref. 3 were developed), can easily be removed formally by dividing the volume of the liquid into small but finite regions ΔV and carrying out the transition $\Delta V \to 0$ in the final equations.

Translated by R. T. Beyer
146

Dipole Moment of the HDSe Molecule

V. G. VESELAGO
P. N. Lebedev Physical Institute,
Academy of Sciences, USSR

(Submitted to JETP editor December 6, 1956)
J. Exptl. Theoret. Phys. (U.S.S.R.) **32**, 620 (March, 1957)

THE dipole moment of the D_2Se, molecule has been determined[1] from the Stark splitting of its rotational spectrum. For the dipole moment, the relatively small value of 0.24 Debye units was obtainned. It would be interesting to confirm this result with another isotopic form of hydrogen selenide, HDSe. In the investigation[2] of the microwave spectrum of this molecule, the transitions $2_{20}-2_{21}$, $4_{31}-4_{32}$ and $9_{54}-9_{55}$ were identified. For the purpose of determining the dipole moment of HDSe, the Stark splitting of four lines was investigated: $2_{20}-2_{21}$, $4_{31}-4_{32}$, $9_{54}-9_{55}$ and $7_{43}-7_{44}$. The $7_{43}-7_{44}$ transition was observed by us at 22,229.8 Mc. Although a natural selenium mixture contains five isotopes we used only the most abundant isotope Se^{80}.

The splitting $\Delta\nu$ in Mc for a Stark component corresponding to a given quantum number M_j is given by

$$\Delta\nu = 2\cdot 0{,}5535\,[M_J^2\,/\,J(J+1)(2J+1)]\,(S/\nu)\,\mu_a^2E^2.$$

Here μ_a is the component of the dipole moment along the a axis (in Debye units), E is the applied electric field strength in volts/cm, S is the dipole matrix element for the given transition and ν is the transition frequency in Mc. Terms proportional to μ_b^2 in the expression for $\Delta\nu$ are very small and have therefore been neglected.

In order to avoid the error associated with inaccurate determination of the field strength in the wave guide, we measured the Stark effect for semiheavy water HDO. For this purpose we used the 8577.7 and 22307.67 Mc lines[3]. The field strength

Transition	$\alpha = \mu_a\,(\text{HDSe})/\mu_a\,(\text{HDO})$
$2_{20}-2_{21}$	$0{,}68 \pm 0{,}02$
$4_{31}-4_{32}$	$0{,}67 \pm 0{,}02$
$7_{43}-7_{44}$	$0{,}70 \pm 0{,}02$
$9_{54}-9_{55}$	$0{,}67 \pm 0{,}02$
	$\alpha_{av} = 0{,}68 \pm 0{,}02$

for these measurements was 2kv/cm. The resulting value of a is the ratio of the dipole components along the a axis for the molecules HDSe and HDO; values are given in the table. The total dipole moment of HDSe is associated with a by the simple expression

$$\mu\,(\text{HDSe}) = \alpha\,\mu\,(\text{HDO}) \sin \delta_2 / \sin \delta_1,$$

where μ(HDO) is the dipole moment of HDO and δ_1 and δ_2 are the angles between the a axis and the direction of the dipole moment for HDSe and HDO respectively. δ_1 is approximately 45°, and if we take $\delta_2 = 20°30'$ and $\mu(\text{HDO}) = 1.84$ Debye units[4] we obtain 0.62 Debye units for the dipole moment of HDSe, which differs extremely from the value of 0.24 Debye units obtained in Ref 1.

---

[1] Jache, Moser and Gordy, J. Chem Phys. **25**, 209 (1956).

[2] V. G. Veselago and A. M. Prokhorov, J. Exptl. Theoret. Phys. (U.S.S.R.) **31**, 731 (1956); Soviet Phys. JETP **4**, 750 (1957).

[3] Weisbaum, Beers and Herrmann, J. Chem. Phys. **23**, 1601 (1955).

[4] M. W. P. Strandberg, J. Chem. Phys. **17**, 901 (1949).

Translated by I. Emin
147

Second Relaxation in a Spin System at Room Temperature

P. G. TISHKOV
Physico-Technical Institute, Kazan Branch,
Academy of Sciences, USSR

(Submitted to JETP editor December 11, 1956)
J. Exptl. Theoret. Phys. (U.S.S.R.) 32, 620-621
(March, 1957)

THE investigation of paramagnetic absorption in $Cr(NO_3)_3 \cdot 9H_2O$ in parallel fields at 300° K, employing Zavoiskii's grid current method[1], revealed an effect which is unusual at room temperature. The absorption $\chi''(H_{\parallel})$ plotted in the figure for a 160 Mc oscillating field has quite a narrow peak. The right-hand half width was of the order of 300 oersteds. As ν increases the absorption peak is shifted in the direction of higher constant magnetic field strengths; this is shown in the following set of data:

ν in Mc =	48	93	131	160
Magnetic field in oersteds at peak =	250	290	330	360

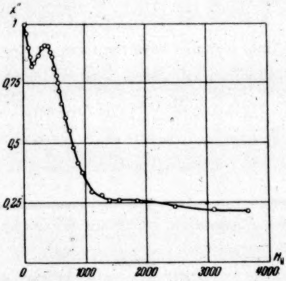

The intensity of the absorption peak compared with absorption at $H = 0$ diminishes with increasing frequency from 10 to 160 Mc. At frequencies of the order of 660 Mc, the shape of the paramagnetic absorption curve differs very little from the usual $\chi''(H_{\parallel})$ curve which is described by Shaposhnikov's formula[2] $\chi'' = (1-F)^2 \rho_s \nu$.

Below 10 Mc, spin-lattice relaxation influences the absorption curve so strongly that a peak is hardly discernible.

This phenomenon is apparently associated with the new form of spin-spin relaxation discovered by DeVrijer and Gorter[3,4] in potassium chrome alum at the temperature of liquid hydrogen. Gorter and his associates[5] later detected this type of relaxation in a number of other materials but again only at very low temperatures. So far as we know the effect has not previously been observed at room temperature.

At the present time the author is using the grid current method in similar investigations of other chromium salts and salts of Mn^{++}, Cu^{++} and Fe^{+++}.

In conclusion I take this opportunity to thank B. M. Kozyrev for guidance and constant assistance.

---

[1] E. K. Zavoiskii, Dissertation, Physical Institute, Academy of Sciences, U.S.S.R., Moscow, 1944.

[2] I. G. Shaposhnikov, Dissertation, Molotov State University, 1949.

[3] F. W. DeVrijer and C. G. Gorter, Physica 14, 617 (1949).

[4] F. W. Vrijer and C. G. Gorter, Physica 18, 549 (1952).

[5] Smits, Derkson, Verstelle and Gorter, Physica 22, 773 (1956).

Translated by I. Emin
148

Electric Monopole Transitions in Nuclei with Odd Mass Numbers

L. K. PEKER AND L. A. SLIV

(Submitted to JETP editor December 17, 1956)
J. Exptl. Theoret. Phys. (U.S.S.R.) 32, 621-622
(March, 1957)

THE non-radiative wholly converted electric monopole $E0$ transitions between two spin zero levels ($0+ \rightarrow 0+$) have been studied well enough only in three cases (see Table 1). However, $E0$ transitions can take place not only between 0-0 levels, but between any two levels with same spin and parity, because in this case the selection rules are satisfied ($\Delta I = 0$, no). The matrix element for an $E0$-transition has the form

$$H_{if} = \langle f \left| \sum_{p} r_p^2 \right| i \rangle = \rho R_0^2, \qquad (1)$$

where R_0 is the nuclear radius and ρ a parameter, which is of the order of unity in the case of a complete overlapping of the initial and final state wave functions. The monopole transitions, more than the others, depend on the structure of the nucleus; their study can therefore give additional information on nuclear models.

An attempt has recently been made[2] to observe $E0$-transitions between two levels $2 \rightarrow 2$ in even-even nuclei. If one measures the internal conversion coefficient (ICC) for the K-shell, a_k and, by an independent method (e.g., from angular correlation), determines the contribution to the radiation of $M1$ and $E2$-transitions, then

$$\alpha_k = T_e / T_\gamma = \varkappa \alpha_2 + (1 + \varkappa) \beta_1 + T_{e0} / T_\gamma. \qquad (2)$$

α_2 and β_1 are the theoretical ICC's for $E2$ and $M1$-transitions respectively, κ is the contribution of $E2$ transition, T_γ is the probability of γ-transition equal to $T_\gamma(M1) + T_\gamma(E2)$ and T_e is the conversion probability. The third term T_{e0}/T_γ determines the part of the electrons involved in the monopole transition.

It follows from the experimental values of the ICC for the $2+ \rightarrow 2+$ transitions in Pt^{192}, Pt^{196} and Hg^{198} nuclei, that the part T_{e0}/T_γ is very small and lies within the limits of the experimental errors; theoretical considerations[2] indicate that this part should be of the order of unity. Such a result has been understood after it has been determined that the spin 2 levels in the considered nuclei have a vibrational character, and that the transitions between them involve a change by unity of the vibrational quantum number ν. This strongly forbids $E0$-transitions and reduces their probability by a factor of about 100. The investigation of $E0$-transitions between levels of other type is made difficult by the necessity of independent measurements of the ICC and of the percentage of $E2$ (or $M1$) transitions, which is a very difficult experimental problem at the present time.

The purpose of the present note is to point out the existence of $E0$-transitions between spin ½ levels ($\frac{1}{2}\pm \rightarrow \frac{1}{2}\pm$) in odd A nuclei. In this case, the spin selection rules rule out the possibility of $E2$-transitions ($\kappa = 0$) and Eq. (2) becomes:

$$T_{e0} / T_\gamma = \alpha_k - \beta_1. \qquad (3)$$

This simplifies the experimental method a great deal, because it suffices to measure only the ICC a_K.

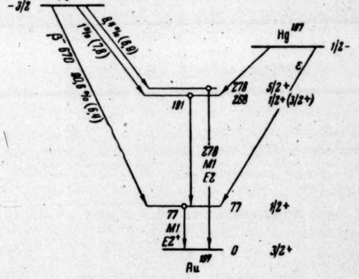

The best investigated is the level scheme of Au^{197} (see Figure). The latest measurement[3] of the ICC for the 191 kev transition gave the value $a_K = 2.5$. If the transition was a pure $M1$, then $a_K = 1.0$; with a mixture of $E2$, the ICC would be still smaller. The possibility of a higher spin contradicts the β-decay character. It remains therefore to assume that the spin of the 268 kev level is ½ and that the 191 kev transition is a mixture $M1 + E0$. Evaluating T_γ for an $M1$-radiation by Moszkowski's formula[4], we obtain from (3) $T_{e0} \approx 4.10^{11}$ sec^{-1}. The corresponding value of ρ is $\rho \approx 0.5$, which is in agreement with the value of ρ obtained from 0+ → 0+ transitions. The table gives a compilation of the data on $E0$-transitions.

It seems of interest to determine the contribution of $E0$-transitions to the conversion spectra of other nuclei, *e.g.* In^{115} and Hg^{199}; there are indications[5] that these nuclei have two spin ½ levels with same parity. One would also like to confirm the results of Potnis *et al.*[3], which we used here.

Nucleus	Type of $E0$-transition		E (Mev)	ρ
C^{12}	0+	0+	·7,68	1/2
O^{16}	0+	0+	6,06	1/2
Ge^{72}	0+	0+	0,69	1/9
Po^{214}	0+	0+	1,42	~1/20
Au^{197}	1/2+	1/2+	0,191	~1/2
Pt^{192}	2+	2+	0,30	⩽1/45
Pt^{196}	2+	2+	0,33	⩽1/34
Hg^{198}	2+	2+	0,68	⩽1/14

---

[1] J. Blatt and V. Weisskopf, *Theoretical nuclear physics.*

[2] E. L. Church and J. Weneser, Phys. Rev. **103**, 1035 (1956); **100**, 943 (1955).

[3] Potnis, Mandeville and Burlew, Phys. Rev. **101**, 753 (1956).

[4] S. A. Moszkowski, *Beta and Gamma-Ray Spectroscopy*, Chapter 13.

[5] B. S. Dzhelepov and L. K. Peker, *Decay Schemes of Radioactive Isotopes*, (Academy of Sciences Press (1957).

Translated by E. S. Troubetzkoy
149

Internal Conversion Coefficient of the 53 kev Gamma-Radiation on the L shell of Th^{230}

A. A. VOROB'EV, V. A. KOROLEV, A. P. KOMAR AND D. M. SELIVERSTON

Leningrad Physico-Technical Institute, Academy of Sciences, USSR

(Submitted to JETP editor December 17, 1956)
J. Exptl. Theoret. Phys. (U.S.S.R.) **32**, 623 (March, 1957)

THE energy of the first excited state of Th^{230} is now determined to be of 52.5 kev[1]. From the data available in the literature, it can be concluded that the conversion coefficient of the 53 kev γ-radiation is large[2].

For the measurement of the conversion coefficient we have used the α-γ coincidence method. An enriched source of U^{234} was used. The α-particles were recorded by an impulse ionization chamber, (the α-spectrum is shown on Fig. 1) the γ-quanta by a scintillation counter with an NaI(Tl) crystal. The γ-spectrum was photographed when in coincidence with the α-particles, which gave an impulse on the output of the multiplier in the interval 17 to 23 volts (Fig. 1), *i.e.*, when in coincidence with the α-particles going to the ground and first excited states of Th^{230}. On Fig. 2, the thin line shows the γ-spectrum photographed without absorption. As it can be seen, the main contribution to the spectrum comes from a 15 kev x-ray. Controlling experiments have shown that this radiation can

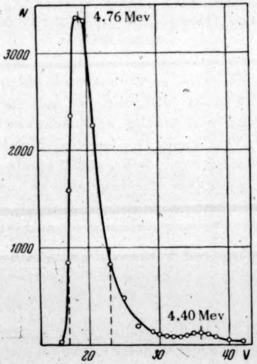

FIG. 1. The volts (V) show the discriminator level.

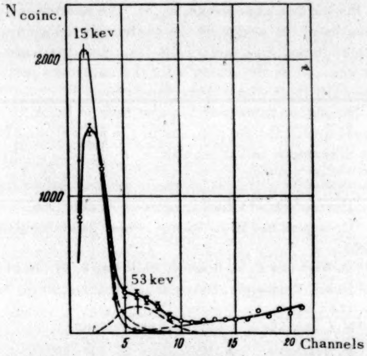

FIG. 2.

be neither the result of an excitation of Th atoms in the recoil process, nor the result of the excitation of the uranium atoms by the α-particles going through the source; it is due only to the internal conversion on the L-shell of Th^{230}. In the experiment, the 53 kev γ-rays have been separated by using 120 μ of Sn as an absorber (thick line on Fig. 2).

The conversion coefficient has been determined from the ratio of the number N_R of Roentgen quanta (without absorber) to the number N_γ of 53 kev γ-quanta, normalized to the same number N_α of recorded α-particles.

The following result is obtained: $N_R/N_\gamma = 130$. The experimental error does not exceed 50%. The extrapolation of the theoretical data gives for the sum of the conversion coefficient on L_{i}, L_{ii}, and L_{iii} shells, depending on the type of transition:

$E1$	$E2$	$E3$	$M1$	$M2$
$<1,0$	170	$>5\cdot 10^3$	~ 25	>500.

The comparison with the experimental result enables one to conclude that the observed radiation is of the electric quadrupole type. The ground state moment of even-even nuclei being equal to zero, and its parity +, the total angular momentum of the first excited state of Th^{230} has to be equal to 2, parity +. The result obtained confirms experimentally the assumption of the rotational character of the level, according to the model of A. Bohr.

---

[1] L. A. Gold'in *et al.*, Academy of Science USSR Session on the Peaceful Use of Atomic Energy (Phys.-Math. Section) p. 226 (1955).

[2] T. Teillac, Compt. rend. **230**, 1056 (1950).

Translated by E. S. Troubetzkoy
150

Level Shift of π-Mesonic Atoms

S. M. BILEN'KII
United Institute for Nuclear Research

(Submitted to JETP editor December 18, 1956)
J. Exptl. Theoret. Phys. (U.S.S.R.) 32, 624 (March 1957)

IN recently completed experiments[1-3], the energy levels of π-mesonic atoms of light elements have been measured. It was found out that the ground state level does not coincide with the energy level obtained by solving the Schrödinger equation in the potential of a point charge, taking into account the corrections for the finite size of the nucleus and the vacuum polarization. Theoretically, this problem has been investigated by Deser *et al.*[4] who obtained an equation expressing the level shift of π-mesonic atoms of light elements in terms of the scattering length of the π-meson on the nucleon; the assumption is made, however, that the scattering amplitude of the π-meson on the nucleus is, for small energies, equal to the sum of the scattering amplitudes on individual nucleons. An attempt to take into account the binding of the nucleons in the nucleus was made by Brueckner[5], but the agreement with experiment is worse than for the results of Deser *et al.*

We will describe the non-electromagnetic interaction between the π-meson and nucleus by a complex V, different from zero in a region of the order of the nuclear dimensions. For a sufficiently light nucleus, we apply the perturbation theory, and obtain the following expression for the shift of the ground state level of the π-mesonic atom:

$$\Delta E = \int \psi_0^* V \psi_0 d\tau \cong {}^4/_3 \, (r_0 / a)^3 \overline{V} Z^3 A, \qquad (1)$$

where A and Z are the atomic weight and charge of the nucleus; $\overline{V}$ is the mean value of the interaction potential; $a = \hbar^2/\mu e^2$, μ is the meson mass; $r_0 = R/A^{1/3}$, R being the nuclear radius. According to this formula, one can determine the product $r_0^3 \overline{V}_R$ from the experimental data on the mesoatomic level shifts. If one takes $r_0 = 1.2 \times 10^{-13}$ cm. then the following values of $\overline{V}_R$ are obtained:

	$r_0^3\overline{V}_R 10^{38}$ Mev. cm³	$\overline{V}_R$, Mev.
Li	2,43	15
Be	1,77	10,3
B^{10}	1,55	9
B^{11}	2,13	12,3
C	1,37	7,9
N	0,99	5,8
O	1,37	7,9
F	1,00	5,8

In this fashion, the potential varies irregularly with the variation of the atomic number A. One does not succeed in explaining such a behavior by the variation of r_0 (it is true that the available data[6] on light nuclei are incomplete and preliminary).

It remains to note that the formula of Deser *et al.* follows from (1) if the potential V is optical and is expressed in terms of the scattering lengths in the following way[7]

$$\left.\begin{aligned} V(r) &= V_0\rho(r), \\ V_0 &= -\frac{3}{2}\left(\frac{\hbar}{\mu c}\right)^2 \mu c^2 \frac{1}{Ar_0^3}\left[\frac{3N+Z}{3}a_3 + \frac{2Z}{3}a_1\right], \end{aligned}\right\} \quad (2)$$

where $\rho(r)$ is the nucleon density in the nucleus, N the number of neutrons, a_1, a_2 the scattering lengths of the meson on the nucleus in the spin states ½ and ³⁄₂. Finally, Eq. (1) yields the same expression as Brueckner's for the imaginary part of the shift (half width of the level).

The author expresses his gratitude to Ia. A. Smorodinskii for the position of the problem and for the discussion of the results.

---

[1] Proceedings of CERN Symposium 2, 417 (1956).

[2] M. Stearns and M. B. Stearns, Phys. Rev. 103, 1534 (1956).

[3] D. West and E. F. Bradley, Phil. Mag 8, 97 (1956).

[4] Deser, Goldberger, Baumann and Thirring, Phys. Rev. 96, 774 (1954).

[5] K A. Brueckner, Phys. Rev. 98, 769 (1955).

[6] R. Hofstadter, Rev. Mod. Phys. 28, 214 (1956).

[7] Frank, Gammel and Watson, Phys. Rev 101, 891 (1956).

Translated by E. S. Troubetzkoy
151

Possibilities of Focussing in a Linear Accelerator With the Aid of Traveling Waves

V. S. TKALICH
Physico-Technical Institute, Academy of Science, USSR

(Submitted to JETP editor December 20, 1956)
J. Exptl. Theoret. Phys. (U.S.S.R.) 32, 625-626
(March 1957)

As is well known, a simultaneous radial and phase stability of the motion of the accelerated particle in a linear accelerator with a traveling wave can be obtained by introducing a periodic unhomogeneity in the wave-guide. This method of alternating-phase focussing was proposed independently by Ia. B. Fainberg[1], by Mullet[2] and by Myron and Good[3] in 1953. In the present note, a modification of this method is proposed: the simultaneous radial and phase stability of heavy particles is obtained by the action of the additional generator on the field of the focussing traveling wave.

In the case considered here, the non-relativistic equations of motion of the accelerated particle have the form

$$\begin{aligned} m\ddot{z} &= eE\left\{I_0(kr)\cos\left(\omega t - \omega\int\frac{dz}{v}\right) + \vartheta I_0(k_1 r)\cos\left(\omega_1 t - \omega_1\int\frac{dz}{v_1}\right)\right\}, \\ m\ddot{r} &= -eE\left\{I_1(kr)\sin\left(\omega t - \omega\int\frac{dz}{v}\right) + \vartheta I_1(k_1 r)\sin\left(\omega_1 t - \omega_1\int\frac{dz}{v_1}\right)\right\}, \end{aligned} \quad (1)$$

where the first term is determined by the action of the accelerating travelling wave, and the second by the focussing wave. The phase velocities of the accelerating and focussing waves are determined by the formulas

$$v = \sqrt{(2eE/m)\cos\varphi_s (z+z_0)},$$

$$v_1 = \sqrt{(2eE/m)\cos\varphi_s (z+z_0+g)}, \quad z_0 = mv_0^2/2eE\cos\varphi_s;$$

where v_0 is the calculated velocity of the injected particles.

Let us use the notation

$$\vartheta = E_1/E, \quad N = \omega_1/\omega, \quad k = \omega/v, \quad k_1 = \omega_1/v_1,$$
$$\lambda = 2\pi c/\omega, \quad \Delta z = z - z_s, \quad \beta = v/c,$$
$$\mu = \beta^3\lambda mc^2/\pi(Ng\cos\varphi_s)^2 eE, \quad \Phi = k[(\Delta z)_{\max} - (\Delta z)_{\min}].$$

We will consider as small the deviations of the nonsynchronous particle from the corresponding synchronous values, as well as the magnitude of the synchronous phase:

$$|kr|,\ |k_1 r|,\ |k\Delta z|,\ |k_1\Delta z|,\ |\varphi_s| \ll 1, \quad (2)$$

The ratio of the amplitudes of the focussing and accelerating waves and the difference in their phase velocities will also be considered as small:

$$\vartheta,\ N\vartheta,\ g,\ (v_1 - v)/v \ll 1. \tag{3}$$

In the approximate formulas reported below, only the lowest-order terms are included.

In order to perform the integrations in (1), we start by solving the equation of motion of a synchronous particle by the method of successive approximations:

$$m\ddot{z}_s = eE\left\{\cos\left(\omega t - \omega\int\frac{dz_s}{v}\right) + \vartheta\cos\left(\omega_1 t - \omega_1\int\frac{dz_s}{v_1}\right)\right\},$$
$$m\ddot{r}_s = 0 \tag{4}$$

with the use of the assumption that

$$(\vartheta/10N)(\beta\lambda/g)^2 \ll eE\lambda/mc^2\beta \ll 1. \tag{5}$$

Using the obtained expression for $z_s = z_s(t)$ and Eq. (4), let us expand Eq. (1) in a series with respect to the deviations of the particle coordinates from the corresponding values of the synchronous particle coordinates. Let us average[4] (over a period of the high frequency perturbation) the linear equations of motion for the deviations. The averaged equations of motion have the form:

$$\ddot{\overline{\Delta z}} + \Omega_z^2\,\overline{\Delta z} = 0, \quad \ddot{\overline{r}} + \Omega_r^2\,\overline{r} = 0;$$
$$\Omega_z^2 = \frac{1}{2}\left(\frac{e\vartheta E}{mg}\right)^2 (t+t_0)^2 - \frac{\omega\varphi_s}{(t+t_0)\cos\varphi_s},\ \Omega_r^2 = \frac{1}{8}\left(\frac{e\vartheta E}{mg}\right)^2 (t+t_0)^2 + \frac{\omega\varphi_s}{2(t+t_0)\cos\varphi_s}; \tag{6}$$
$$t_0 = mv_0/eE\cos\varphi_s.$$

If $\varphi_s = 0$, the solutions of (6) are

$$\overline{\Delta z} = C_1\sqrt{t+t_0}\,J_{1/4}\left\{\frac{e\vartheta E}{2\sqrt{2}\,mg}(t+t_0)^2\right\} + C_2\sqrt{t+t_0}\,J_{-1/4}\left\{\frac{e\vartheta E}{2\sqrt{2}\,mg}(t+t_0)^2\right\},$$
$$\overline{r} = C_1'\sqrt{t+t_0}\,J_{1/4}\left\{\frac{e\vartheta E}{4\sqrt{2}\,mg}(t+t_0)^2\right\} + C_2'\sqrt{t+t_0}\,J_{-1/4}\left\{\frac{e\vartheta E}{4\sqrt{2}\,mg}(t+t_0)^2\right\}.$$

On the other hand, if $\varphi_s \neq 0$, applying the WKB method, we get:

$$\overline{\Delta z} = \frac{C_3}{\sqrt{\Omega_z}}\cos\int_{C_4}^{t}\Omega_z(t')\,dt',$$

$$\overline{r} = \frac{C_3'}{\sqrt{\Omega_r}}\cos\int_{C_4'}^{t}\Omega_r(t')\,dt',$$

where $C_1, C_1', \ldots, C_4'$ are constants determined by the initial conditions. When $\Omega_z^2, \Omega_r^2 > 0$, the solution obtained for $\overline{\Delta z}$ and $\overline{r}$ are oscillating, which corresponds to a simultaneous radial and phase stability of the accelerated particle motion.

If one takes into account the non-linear terms in the equations of motion for the deviations, then one obtains, for the capture angle Φ and for the acceptable velocity spread $(\Delta\beta/\beta)_{\text{acc}}$ the expressions

$$\Phi = 3\,\frac{\mu(N\vartheta)^2 - \varphi_s}{\cos\varphi_s},$$
$$\left(\frac{\Delta\beta}{\beta}\right)_{\text{acc}} = \sqrt{\frac{2eE\lambda}{3\pi mc^2\beta}}\,\frac{[\mu(N\vartheta)^2 - \varphi_s]^{3/2}}{\cos\varphi_s},$$

which are accurate in the absence of resonance in the radial and phase oscillations[5,6].

The author is grateful to Ia. B. Fainberg for valuable discussions.

---

[1] Ia. B. Fainberg, Report # 601, Physico-Technical Institute, Academy of Science, USSR (1953).

[2] L. B. Mullet, AERE-GP/M-147, Harwell, England (1953) [cited in Rev. Sci. Instr. **26**, 220 (1955)].

[3] V. Myron and L. Good, Phys. Rev. **92**, 538 (1953).

[4] N. N. Bogoliubov and Iu. A. Mitropol'skii, *Asymptotic Methods in Non-Linear Oscillations Theory*, Moscow (1955).

[5] Ia. B. Fainberg, Report at the Geneva Conference (June, 1956).

[6] F. M. Nekrasov, Thesis, Kharkov State University (1955).

Translated by E. S. Troubetzkoy
152

Derivation of the Formula for the Cross Section for Formation of High Energy Neutrons in Deuteron-Nuclei Collisions

V. S. ANASTASEVICH

(Submitted to JETP editor December 24, 1956)
J. Exptl. Theoret. Phys. (U.S.S.R.) 32, 626-627
(March, 1957)

SOMEWHAT prior to the appearance of Serber's article,[1] we suggested that the formation of a narrow beam of neutrons upon interaction of high energy deuterons with matter, was due to the stripping of deuterons colliding with atomic nuclei. We derive here the formula for the effective cross section for the formation of neutrons by the stripping reaction; this was set forth in an unpublished report[2].

The formation of a neutron by stripping will of course take place every time that the proton in the deuteron interacts with the nuclear surface, while the neutron is outside the nuclear force radius. Let R be the nuclear radius, and d be average distance between the neutron and the proton of the deuteron. We shall call r the distance between the neuteron and the point at which the *pn* (proton-neutron) line intersects the nucleus. Let θ be the angle between the *x*-axis (the *x*-axis is drawn from the center of the nucleus through the point where the *pn* line intersects the nuclear surface) and the *pn* direction; the cross section for formation of neutrons for given values of θ, r, and $R \gg r$ is then:

$$\sigma_{r\theta} = \pi(\rho^2 - R^2) \approx 2\pi Rr\cos\theta\,,$$
$$\rho^2 = R^2 + r^2 - 2Rr\cos(\pi - \theta) \approx R^2 + 2Rr\cos\theta.$$

The average cross section for neutron formation for a given r and arbitrary θ is:

$$\sigma_r = \frac{1}{2\pi}\int\limits_0^{\Omega\max} \sigma_{r\theta}\,d\Omega \approx \frac{1}{2\pi}\int\limits_0^{\pi/2} 2\pi Rr\cos\theta\, 2\pi\sin\theta d\theta = \pi Rr,$$
$$\Omega_{\max} \approx \pi/2 - (d-r)/2\pi R,$$

where $d\Omega = 2\pi \sin \theta d\theta$ is the solid angle formed by a change in the deuteron direction from $\theta + d\theta$. The average cross section for neuteron formation for arbitrary θ and r is found the formula:

$$\sigma = \frac{1}{d}\int\limits_0^d \sigma_r dr = \frac{\pi}{2}Rd;$$

this is the effective cross section which we were seeking.

---

[1] R. Serber, Phys. Rev 72, 1008 (1947).

[2] V. S. Anastasevich, Otchet Akad. Nauk SSSR (Nov., 1947).

Translated by M. A. Melkanoff
153

Possible Correlations in π-μ-e Decay

L. OKUN' AND A. RUDIK

(Submitted to JETP editor December 24, 1956)
J. Exptl. Theoret. Phys. (U.S.S.R.) 32, 627-628
(March, 1957)

LEE and Yang[1] have recently shown that if parity is violated in π-μ-e decay, there must be correlations between the orientations of the momenta of the μ-mesons and the electrons. We present here the results of computations of such correlations when parity is violated in both the $\pi \to \mu + \nu$ decay and the $\mu \to e + 2\nu$ decay.

The interaction leading to π-meson decay has the form:

$$H_\pi = f\varphi_\pi \overline{\psi}_\nu (1 + \alpha\gamma_5)\psi_\mu. \tag{1}$$

The coefficient α characterizes here the degree of violation of parity conservation. The probability that during the decay of π-meson, a μ-meson will be emitted with momentum **n** and spin **s** is given by

$$\frac{dW_\pi}{d\Omega} = \frac{f^2}{16\pi}\left\{(1 + |\alpha|^2)\left(1 + \frac{m^2 - \mu^2}{m^2 + \mu^2}\right) + (\alpha + \alpha^*)(\mathbf{ns})\right\}$$
$$\times \frac{(m^2 - \mu^2)^2(m^2 + \mu^2)}{m^5} = u_1 + u_2(\mathbf{ns}), \tag{2}$$

where m is the mass of π-meson and μ the mass of the μ-messon. Expression (2) indicates that the μ-meson is longitudinally polarized. It may be shown that if $\alpha = 1$, the μ-meson is completely polarized in the rest system of the μ-meson.

Let us consider now the decay of a μ-meson at rest. The interaction for this process has the form

$$H_\mu = \sum_1^5 g_i(\overline{\psi}_\mu(1 + \alpha_i\gamma_5)O_i\psi_e)(\psi_\nu O_i\psi_\nu). \tag{3}$$

If the two neutrinos which appear during the decay of the μ-meson are identical, then it is well known that $g_2 = g_3 = 0$. Applying Lenard's method[2], one obtains the following expression for the angular distribution of decay electrons:

$$d^2W_\mu/d\Omega d\varepsilon = (2\pi)^{-4}\varepsilon_m^5\varepsilon^2\{(a_1+a_5)(1-\varepsilon)+{}^8/_3a_3(3-\varepsilon) + {}^2/_3(a_2+a_4)(3-2\varepsilon)+[(b_1+b_5)(1-\varepsilon) - {}^8/_3b_3(1+\varepsilon)+{}^2/_3(b_2+b_4)(1-2\varepsilon)](\mathbf{sl})\}, \quad (4)$$

where 1 denotes a unit vector in the direction of the momentum of the electron, and

$$a_i = g_i^2(1+|\alpha_i|^2), \quad b_i = g_i^2(\alpha_i+\alpha_i^*).$$

Integrating the probability (4) over the energy of the electron yields

$$\frac{dW_\mu}{d\Omega} = \frac{\varepsilon_m^5}{(2\pi)^4}\left\{\left(\frac{a_1+a_5}{12}+2a_3+\frac{a_4+a_2}{3}\right) + \left(\frac{b_1+b_5}{12}-\frac{14}{9}b_3-\frac{b_2+b_4}{9}\right)(\mathbf{sl})\right\} = v_1+v_2(\mathbf{sl}). \quad (5)$$

Note that the coefficient α which characterizes the degree of parity violation may be either real (for invariance under time reversal) or purely imaginary (for invariance under charge conjugation). In the latter case, the coefficients u_2 and v_2 are easily seen to be identically equal to zero, and there is no correlation. If α is real, then the correlation between the direction of the momentum of the μ-meson and that of the electron is given by

$$W(\mathbf{l},\mathbf{n}) = \sum_{s_1s_2} W_\pi(\mathbf{ns}_1)\,W_d(\mathbf{s}_1,\mathbf{s}_2)\,W_\mu(\mathbf{s}_2\mathbf{l}). \quad (6)$$

W_π and W_μ are obtained from Eqs. (2) and (5), and $W_d(\mathbf{s}_1, \mathbf{s}_2)$ is the probability for depolarization of the μ-meson as it is slowed down. If the depolarization is small, *i.e.*, if $W_d \sim \delta(\mathbf{s}_1-\mathbf{s}_2)$, Eq. (6) is easily solved:

$$W(\mathbf{ln}) = u_1v_1+u_2v_2(\mathbf{ln}). \quad (7)$$

Note that the effect of parity violation shows up in (7) through the appearance of a scalar quantity (ln), and not a pseudoscalar as is usually the case. This is linked to the fact that parity is violated twice in the process under consideration, during the decay of the π-meson, and during that of the μ-meson.

In conclusion, we remark that experimental observation of this correlation is very difficult due to the fact that strong depolarization takes place during the lifetime of the μ-meson ($\sim 10^{-6}$ sec).

The authors wish to express their appreciation to Acad. L. D. Landau, V. B. Berestetskii and B. L. Ioffe for a discussion of this analysis.

---

[1] T. D. Lee and C. N. Yang, Phys. Rev **104**, 254 (1956).

[2] A. Lenard, Phys. Rev. **90**, 968 (1953).

[3] Ioffe, Okun', and Rudik, J. Exptl. Theoret. Phys. U.S.S.R. **32**, 396 (1957).

Translated by M. A. Melkanoff
154

Polarization in Reverse Reactions

A. I. BAZ'

(Submitted to JETP editor December 27, 1956)
J. Exptl. Theoret. Phys. (U.S.S.R.) 32, 628-630 (March, 1957)

IN this note, we shall demonstrate a relation which holds between the polarization of final particles in forward and reverse reactions. Consider an arbitrary reaction of the form $a + X \to b + Y$, where a, b, X, Y are arbitrary particles of spin ½; we shall assume that the product of the intrinsic parities of the particles before the reaction is the same as the product of the intrinsic parities of the particles formed after the reaction. We shall denote the spin states of the initial and final systems by the components ζ_{sm} of a column vector, where s is the total spin and m its z-component. It may be shown that the amplitude of the final particles has the form

$$\frac{e^{ik_1r}}{r}\frac{\sqrt{\pi}}{ikk_1}\cdot\begin{vmatrix} a-f & c & -d_2 \\ b & g-b & 0 \\ c & f & a & -d_2 \\ d_1 & 0 & d_1 & e\end{vmatrix}\cdot\begin{vmatrix}\zeta_{11}\\ \zeta_{10}\\ \zeta_{1-1}\\ \zeta_{00}\end{vmatrix} = \frac{e^{i\mathbf{k}_1r}}{r}M\cdot\begin{vmatrix}\zeta_{11}\\ \zeta_{10}\\ \zeta_{1-1}\\ \zeta_{00}\end{vmatrix}, \quad (1)$$

where k and k_1 are the wave vectors before and after the reaction, ζ_{sm} is the spin function for the initial state (particles a and X), and the coefficients a, b, c, ... are expressed by means of the elements of the reaction matrix $M_{ls,\,l's'}$ and the scattering angle θ. If we know the operator M, we can solve for the average values of the spin operators of particles b and Y and the reaction cross section $d\sigma$ $d\sigma/do$.

$$\overline{\sigma_i^{(b)}} = \langle\sigma_i^{(b)}\rangle/(d\sigma/(do); \overline{\sigma_i^{(Y)}} = \langle\sigma_i^{(Y)}\rangle/d\sigma/do$$

$$\langle\sigma_i^{(b,\,Y)}\rangle = (k_1/k)\ \mathrm{Sp}\,(M\rho M^+\sigma_i^{(b,\,Y)});$$

$$d\sigma/do = (k_1/k)\,\mathrm{Sp}\,(M\rho M^+). \quad (2)$$

ρ is here the spin density matrix for the initial state, and $i = x, y, z$.

In the center-of-mass system of coordinates (x, y, z)*, we have:

$$d\sigma/do = (d\sigma/do)_0 + P_y\,(d\sigma/do)_y;$$
$$\langle\sigma_y\rangle = \langle\boldsymbol{\sigma}_y\rangle_0 + P_y\langle\boldsymbol{\sigma}_y\rangle_y,\ \langle\boldsymbol{\sigma}_x\rangle = P_x\langle\boldsymbol{\sigma}_x\rangle_x + P_z\langle\boldsymbol{\sigma}_x\rangle_z,$$
$$\langle\boldsymbol{\sigma}_z\rangle = P_x\langle\boldsymbol{\sigma}_z\rangle_x + P_z\langle\boldsymbol{\sigma}_z\rangle_z. \tag{3}$$

where P_i is the polarization component of particles a (particles X are assumed unpolarized), and $(d\sigma/do)_{0,\,y}$ and $\langle\sigma_i\rangle_{x,\,y,\,z}$ are expressible in terms of the coefficients $a, b, c, \ldots$ appearing in formula (1). The polarization of particles b and Y is conveniently expressed in the coordinate system (x', y', z'), wherein the z'-axis is in the direction of motion of particle b, and the y'-axis coincides with the y-axis; The components of the vectors $\langle\boldsymbol{\sigma}^{(b)}\rangle$ and $\langle\boldsymbol{\sigma}^{(Y)}\rangle$ in this system are obtained from the components of these vectors in the system (x, y, z) by applying the usual rules of vector algebra. Their dependence upon the polarization of particle a has the same form as in the (x, y, z) system [see Eq. (3)]. For example,

$$\langle\boldsymbol{\sigma}^{(b)}_{x'}\rangle = P_x[\cos\vartheta\,\langle\boldsymbol{\sigma}^{(b)}_x\rangle_x - \sin\vartheta\,\langle\boldsymbol{\sigma}^{(b)}_z\rangle_x] + P_z$$
$$[\cos\vartheta\,\langle\boldsymbol{\sigma}^{(b)}_x\rangle_z - \sin\vartheta\,\langle\boldsymbol{\sigma}^{(b)}_z\rangle_z] \equiv P_x\langle\boldsymbol{\sigma}^{(b)}_{x'}\rangle_x + P_z\langle\boldsymbol{\sigma}^{(b)}_{x'}\rangle_z.$$

Consider now the reverse reaction $b+Y\rightarrow a+X$. The cross section for this reaction $(d\sigma/do)'$ and the average values of the spin operators for particles a and X may be obtained in exactly the same way as in the reaction $a+X\rightarrow b+Y$. One need only interchange a and X with b and Y in the preceding analysis, and correspondingly change the directions of the coordinate axis (*i.e.*, the z-axis must now be directed along the direction of motion of particle b, the z'-axis along the direction of motion of particle a, etc. ...). Then in all the formulas, $\boldsymbol{\sigma}^{(a)}$ will replace $\boldsymbol{\sigma}^{(b)}$, $\boldsymbol{\sigma}^{(Y)}$ will replace $\boldsymbol{\sigma}^{(X)}$, k_1 will replace k, and some new coefficients $a', b', c', d'_1 \ldots$ will replace $a, b, c, d_1, \ldots$; furthermore the quantities P_i must then be taken as describing the polarization of particle b before the reaction. The coefficients $a', b', c', \ldots$ which describe the reaction $b + Y \rightarrow a + X$ depend upon the elements of the matrix for this reaction, ${}'M^{I}_{ls,\,l's'}$, in exactly the same way as the coefficients $a, b, c, \ldots$ depend upon $M^{I}_{ls,\,l's'}$. Symmetry under time reversal implies [1] that ${}'M^{I}_{ls,\,l's'} = M^{I}_{ls,\,l's'}$ Making use of this relation, and of the explicit form of the elements $a, b, c, \ldots$, it may easily be shown that

$$\begin{gathered} a-a' = \mathfrak{M};\ g-g' = -2\mathfrak{M};\ c-c' = -\mathfrak{M};\ b-b' = -\sqrt{2}\,\mathrm{ctg}\,\vartheta\cdot\mathfrak{M}, \\ f-f' = \sqrt{2}\,\mathrm{ctg}\,\vartheta\cdot\mathfrak{M};\ d_2 = d'_1;\ d_1 = d'_2;\ e' = e, \\ \mathfrak{M} = {}^1/_2\sin^2\vartheta\,[(a-g-c) - \sqrt{2}\,\mathrm{ctg}\,\vartheta\,(b-f)]. \end{gathered} \tag{4}$$

Substituting the expressions obtained from (4) for $a', b', \ldots$ into the formulas for the cross section and the polarization of particles in the reaction $b + Y \rightarrow a + X$, one finds that the cross section and polarization for this reaction are related to the cross section and polarization for the reverse reaction in the following way:

$$\begin{gathered} (d\sigma/do)'_0 = (k/k_1)^2(d\sigma/do)_0;\ \langle\boldsymbol{\sigma}^{(a)}_{y'}\rangle = (k/k_1)^2(d\sigma/do)_y; \\ \langle\boldsymbol{\sigma}^{(X)}_{y'}\rangle_0 = (k/k_1)^2\langle\boldsymbol{\sigma}^{(b)}_{y'}\boldsymbol{\sigma}^{(Y)}_{y'}\rangle_y; \\ \langle\boldsymbol{\sigma}^{(a)}_{y'}\rangle_y = (k/k_1)^2\langle\boldsymbol{\sigma}^{(b)}_{y'}\rangle_y;\ \langle\boldsymbol{\sigma}^{(X)}_{y'}\rangle_y = (k/k_1)^2\langle\boldsymbol{\sigma}^{(Y)}_{y'}\rangle_y; \\ \langle\sigma^{(a)}_{x'}\rangle_x = (k/k_1)^2\langle\boldsymbol{\sigma}^{(b)}_{x'}\rangle_x;\ \langle\boldsymbol{\sigma}^{(a)}_{x'}\rangle_z = -(k/k_1)^2\langle\boldsymbol{\sigma}^{(b)}_{z'}\rangle_x;\ \langle\boldsymbol{\sigma}^{(a)}_{z'}\rangle_z = (k/k_1)^2\langle\boldsymbol{\sigma}^{(b)}_{z'}\rangle_z; \\ \langle\boldsymbol{\sigma}^{(X)}_{x'}\rangle_x = (k/k_1)^2\langle\boldsymbol{\sigma}^{(Y)}_{x'}\rangle^{*}_x;\ \langle\boldsymbol{\sigma}^{(X)}_{x'}\rangle_z = -(k/k_1)^2\langle\boldsymbol{\sigma}^{(Y)}_{z'}\rangle^{*}_x;\ \langle\boldsymbol{\sigma}^{(X)}_{z'}\rangle_z = (k/k_1)^2\langle\boldsymbol{\sigma}^{(Y)}_{z'}\rangle^{*}_z. \end{gathered} \tag{5}$$

The first formula in (5) gives the well known relation between cross sections in the forward and reverse reactions. The second formula in (5) relates the asymmetry of angular distribution in the forward reaction to the polarization in the reverse reaction. Indeed the right-and-left symmetry of the angular distribution in the reaction $a + X \rightarrow b + Y$, $e = P_y\,(d\sigma/do)_y/(d\sigma/do)_0$ (P_y is the polarization component of particle a, perpendicular to the reaction plane), may be found from the second formula in (5) to be equal to

---

* The z-axis is directed along the trajectory of particle a, the x-axis lies in the reaction plane (so that the direction of motion of the particle b corresponds to an azimuthal angle $\varphi = 0$), and the y-axis is perpendicular to the reaction plane.

$$e = P_y^{(a)} \langle \sigma_{y'}^{(a)} \rangle_0 / (d\sigma / do)_0' = P_y \overline{\sigma_{y'}^{(a)}}, \tag{6}$$

where $\overline{\sigma_y^{(a)}}$ is the polarization of particle a in the reaction $b + Y \rightarrow a + X$, when b and Y are unpolarized. In the case of elastic scattering $(a + X \rightarrow a + X)$ equation (6) becomes the well known formula of Wolfenstein.[2] Note that Wolfenstein only proved his theorem for the case where inelastic scattering is absent (he assumed the scattering operator M was unitary). Our demonstration is free of this limitation. The third formula in (5) relates the polarization of particle Y in the reaction $a + X \rightarrow b + Y$ to the correlated polarization in the reverse reaction. The remaining formulas in (5) need no special elucidation except for the formula of line four. The asterisk attached to the brackets $< >$, such as in $<\sigma_x^{(b)}>_x^*$, denotes the fact that it describes the polarization of particle b for the reaction $a + X \rightarrow b + Y$ wherein particle X was polarized in the initial state while particle a was completely unpolarized. The index x attached to the bracket $< >$, refers here to the x-component of polarization of particle X. The rest of the formulas of line four may be interpreted in this way.

In conclusion the author wishes to thank Ia. A. Smorodinskii for a discussion of the results.

---

[1] J. M. Blatt and V. Weisskopf, *Theoretical Nuclear Physics*, John Wiley and Sons, Inc., New York (1952).

[2] L. Wolfenstein and J. Ashkin, Phys. Rev. **85**, 947 (1952).

Translated by M. A. Melkanoff
155

Polarization of Cerenkov Radiation

A. A. SOKOLOV AND IU. M. LOSKUTOV
Moscow State University

(Submitted to JETP editor January 3, 1957)
J. Exptl. Theoret. Phys. (U.S.S.R.) **32**, 630-632
(March, 1957)

IN order to analyze the dependence of Cerenkov radiation upon the spin of the charged particles, we have utilized the method developed in Ref. 1 (see also Ref. 2)., which allows one to solve for the intensities of both linearly and circularly polarized radiation.

When we consider linear polarization, we must resolve the amplitude of the vector potential of the quantized photon field into two mutually perpendicular components in the following fashion:

$$\begin{gathered}\mathbf{a} = \mathbf{a}_2 + \mathbf{a}_3 = \beta_2 q_2 + \beta_3 q_3, \\ \beta_2 = [\varkappa^0 \mathbf{k}^0] / \sqrt{1 - (\varkappa^0 \mathbf{k}^0)}, \quad \beta_3 = [\varkappa^0 \beta_2].\end{gathered} \tag{1}$$

$\boldsymbol{\varkappa}^0 = \boldsymbol{\varkappa}/\varkappa$ is a unit vector which characterizes the motion of the photon and the unit vector $\mathbf{k}^0$ must be assigned some definite direction (in our problem, we shall assume that the vector $\mathbf{k}^0$ is in the direction of the electron motion, *i.e.*, along the z-axis).

In the case of circular polarization the vector potential is resolved into two different components:

$$\begin{gathered}\mathbf{a} = \mathbf{a}_1 + \mathbf{a}_{-1} = \beta_1 q_1 + \beta_{-1} q_{-1}, \\ \sqrt{2}\beta_\lambda = \beta_2 + i\lambda\beta_3, \quad \lambda = 1, -1.\end{gathered} \tag{2}$$

The quantized part of the vector potential appearing in Eq. (1) and (2) must satisfy the relations

$$q_{j'}^+ \, q_j = 0, \quad q_j q_{j'}^+ = \delta_{jj'}, \quad j, j' = 2, 3, 1, -1.$$

In contructing the quantized transverse electromagnetic field in a medium of refractive index $n \, (n = \sqrt{\varepsilon}, \mu = 1)$ (*cf.* Refs. 3 and 4, where the quantum theory of the Cerenkov effect is developed), we find, that the vector potential $\mathbf{A}$ is related to the quantized amplitudes $\mathbf{a}$ (*cf.* Ref. 1 or 2) through the following expression

$$\begin{aligned}\mathbf{A} = L^{-3/2} \sum_{\varkappa} \sqrt{\frac{2\pi c\hbar}{n\varkappa}} & (\mathbf{a} \exp\{-ic(\varkappa t / n) + i\varkappa\mathbf{r}\} \\ & + \mathbf{a}^+ \exp\{ic(\varkappa t / n - i\varkappa\mathbf{r}\}).\end{aligned} \tag{3}$$

We shall choose to write the wave function for a free electron in the form

$$\psi = L^{-3/2} \sum_{\mathbf{k}'} C' b' \exp\{-ic K' t + i\mathbf{k}' \mathbf{r}\}, \tag{4}$$

where $\hbar\mathbf{k}$ is the momentum of the electron, $c\hbar K = c\hbar\sqrt{k^2 + k_0^2}$ the electron energy and $\hbar k_0 / c$ its mass. We shall denote the initial state of the electron by an unprimed symbol and its final state by a primed symbol

Introducing the perturbation energy $U = (e/c)(\mathbf{a}\mathbf{A})$, we must consider the coefficients C' as time-dependent, satisfying the initial condition: $C' = C(k', 0) = \delta_{\mathbf{k}'\mathbf{k}}$.

When solving the Dirac equation (*i.e.*, including electron spin), the ψ-function (4) is given by a four-row matrix. When solving the Klein-Gordon Equation (*i.e.*, for spinless particles), we must limit ourselves to two wave functions assuming

$$b_1 = (2c\hbar K)^{-1/2}, \quad b_2 = (c\hbar K / 2)^{1/2}. \tag{5}$$

In that case the expression for the density becomes $\rho = \psi_1^+ \psi_2 + \psi_2^+ \psi_1$. One then finds the following expression for the radiation intensity per unit legth of electron motion:

$$W^{(s)}_{(j)} = \frac{\hbar\omega}{v}\frac{\partial}{\partial t}\sum_{\mathbf{k}'} C'^+C' = \frac{e^2}{2\pi}\int \frac{c}{nv}\,\delta\left(K - \frac{\varkappa}{n} - K'\right)$$

$$R^{(s)+}_{(j)} R^{(s)}_{(j)} \sin\theta d\theta d\varphi \varkappa^2 d\varkappa, \quad R^{(s)}_{(j)} = b'^+ (\alpha^{(s)} \alpha^+_{(j)})\, b, \tag{6}$$

where v is the electron velocity. The index $s (s = ½;$ $s (s = ½, 0)$ denotes here the spin of the particle, $j (j = 2, 3, +1, -1)$ denotes the polarization of the radiated photons, and θ is the angle between the initial momentum of the electron and that of the radiated photon.

The expression for $\cos\theta$ may be obtained, as usual, from conservation of energy and momentum (*cf.* Ref. 3 and 4):

$$\cos\theta = (1 / \beta n) + (n\omega\hbar / 2cp)(1 - n^{-2}). \tag{7}$$

Taking into account the dependence of n upon the frequency ω and the fact that n tends to unity for large values of ω, radiation is possible if $\beta n(\omega) > 1$, and is cut off at a frequency $\omega = \omega_{\max}$ for which $\cos\theta = 1$.

When solving the Dirac equation, we must replace the $a^{(s)}$ by the well-known Dirac matrices $(a^{(½)} = a)$, while in the case of zero-spin particles we must set $b\,a^{(0)} = b\mathbf{k}/K$ and $b'a^0 = b'\mathbf{k}/K$. The radiation due to zero-spin particles $(s = 0)$, and that due to particles possessing spin, is thus found to be:

$$W^{(0)}_{(j)} = \frac{e^2}{v}\int_0^{\omega_{\max}} \omega\, \frac{(\mathbf{k}\mathbf{a}_{(j)})(\mathbf{k}'\mathbf{a}^+_{(j)})}{nKK'}\, \delta\left(K - \frac{\varkappa}{n} - K'\right)\sin\theta\, d\theta\, \varkappa d\varkappa,$$

$$W^{(1/2)}_{(j)} = \frac{e^2}{v}\int_0^{\omega_{\max}} \omega\left[\frac{(\mathbf{k}\mathbf{a}_{(j)})\,(\mathbf{k}'\mathbf{a}^+_{(j)})}{nKK'} + \frac{1}{2}\left(1 - \frac{k_0^2 + (\mathbf{k}\mathbf{k}')}{KK'}\right)(\mathbf{a}_{(j)}\mathbf{a}^+_{(j)})\right] \tag{8}$$

$$\times\,\delta\left(K - \frac{\varkappa}{n} - K'\right)\sin\theta d\theta \varkappa d\varkappa.$$

In order to take polarization into account, we must apply formulas (10) – (12) of Ref. 1 to eliminate the quantized amplitudes of the vector potential. The intensity of radiation emitted per unit length of a zero-spin particle is then found to be

$$W^{(0)}_{(2)} = 0, \quad W^{(0)}_{(3)} = \frac{e^2}{c^2}\int_0^{\omega_{\max}} \omega\,(1 - \cos^2\theta)\, d\omega, \tag{9}$$

i.e., the radiation will be strongly linearly polarized over the whole range of frequency ω, and the polarization vector (the electric intensity vector for the radiated photons) must be in the plane $(\varkappa\mathbf{k})$.

In the case of radiation due to particles of spin one half, we find

$$W^{(1/2)}_{(2)} = \frac{e^2}{c^2}\int_0^{\omega_{\max}} \omega\,\frac{n^2\omega^2\hbar^2}{4c^2p^2}\left(1 - \frac{1}{n^2}\right)d\omega, \tag{10}$$

$$W^{(1/2)}_{(3)} = W^{(0)}_{(3)} + W^{(1/2)}_{(2)}; \quad W^{(1/2)}_{(-1)} = W^{(1/2)}_{(1)}. \tag{11}$$

Thus it may be seen that in the classical approximation ($\hbar \to 0$), the radiation will be completely linearly polarized just as in the case of zero-spin particles.

The presence of spin leads to an additional unpolarized radiation which does not disappear at the radiation threshold ($E = E_0$). The linearly polarized part of the radiation is missing at threshold, but it grows in proportion to $(E - E_0)$ as the electron energy E $((E - E_0)/E_0 \ll 1)$ grows:

$$W^{(0)}_{(3)} = 2\,\frac{e^2}{c^2}\,\frac{E - E_0}{mc^2}\int_0^{\omega_{\max}} \omega n^2 d\omega. \tag{12}$$

Harding and Henderson[5] state in a brief note that they have observed non-polarized Cerenkov radiation near threshold. However, in view of the small intensity of the unpolarized part of the radiation, proportional to $\hbar^2$, it is difficult to believe that these observations are somehow tied up with spin effects. Still, it should be noted that, due to the wide use use of light counters, experimental technique has reached such a degree of accuracy that it has become possible to observe Cerenkov effects due to single particles.[6]

---

[1] A. A. Sokolov and I. M. Termov, J. Exptl. Theoret. Phys. (U.S.S.R.) 31, 473 (1956); Soviet Phys. JETP 4, 396 (1957).

[2] A. A. Sokolov and A. I. Mukhtarov, Vestn. Moscow State Univ. **8**, 63 (1948).

[3] A. A. Sokolov, Dokl. Akad. Nauk SSSR **28**, 415 (1950); see also A. A. Sokolov and D. D. Ivanenko, *The Quantum Theory of Fields*, Moscow-Lenningrad (1952) p. 222.

[4] V. L. Ginzburg. J. Exptl. Theoret. Phys. (U.S.S.R.) **10**, 589 (1940).

[5] J. M. Harding and J. E. Henderson, Phys. Rev. **74**, 1560 (1948).

[6] I. M. Frank, Izv. Fyz. Nauk **58**, 111 (1956).

Translated by M. A. Melkanoff
156

CONTENTS – *continued*

Letters to the Editor:

Energy Dependence of the Effective Cross Section of Inelastic Scattering of Particles near the Threshold . . . . G. F. Drukarev 496 **32**, 601

Statistical Retardation in Dielectric Breakdown of Solid Dielectrics . . . . E. A. Konorova 497 **32**, 603

The Applicability of the Relation of Detailed Balance for a Cluster of Ions of Stationary Composition . . . . Ia. M. Fogel' 499 **32**, 604

On the Possibility of Observing the Variation of the Chemical Potential of Electrons of a Metal in a Magnetic Field . . . . M. I. Kaganov, I. M. Lifshits and K. D. Sinel'nikov 500 **32**, 605

Natural Line Widths of Microwaves . . . . V. M. Fain 501 **32**, 607

Double Absorption Peaks in Electron Resonance at Saturation . . . . N. S. Garif'ianov 503 **32**, 609

Radiation of a Point Charge Moving Along the Boundary between Two Media . . . . V. E. Pafomov 504 **32**, 610

Temperature Dependence of the Overhauser Effect in Metallic Lithium . . . . N. A. Bekeshko and E. I. Kondorskii 505 **32**, 611

The Character of Nucleonic Forces . . . . A. Z. Dolginov 506 **32**, 612

Photodisintegration of Neon Nuclei . . . . A. P. Komar and I. P. Iavor 508 **32**, 614

Concerning the Lifetime of the Two Forms of the π^0 Meson . . . . A. V. Romankevich 509 **32**, 615

On the Derivation of the Low Equation in the Theory of Meson Scattering . . . . A. M. Brodskii 509 **32**, 616

The Hall Effect in Bismuth Under Pressures up to 30,000 Kg/cm^2 . . . . A. I. Likhter and L. F. Vereshchagin 511 **32**, 618

Hydrodynamic Fluctuations . . . . L. D. Landau and E. M. Lifshitz 512 **32**, 618

Dipole Moment of the HDSe Molecule . . . . V. G. Veselago 513 **32**, 620

Second Relaxation in a Spin System at Room Temperature . . . . P. G. Tishkov 514 **32**, 620

Electric Monopole Transitions in Nuclei with Odd Mass Numbers . . . . L. K. Peker and L. A. Sliv 515 **32**, 621

Internal Conversion Coefficient of the 53 kev Gamma-Radiation on the L shell of Th^{230} . . . A. A. Vorob'ev, V. A. Korolev, A. P. Komar and D. M. Seliverston 516 **32**, 623

Level Shift of π-Mesonic Atoms . . . . S. M. Bilen'kii 517 **32**, 624

Possibilities of Focussing in a Linear Accelerator with the Aid of Traveling Waves . . . . V. S. Tkalich 518 **32**, 625

Derivation of the Formula for the Cross Section for Formation of High Energy Neutrons in Deuteron-Nuclei Collisions . . . . V. S. Anastasevich 520 **32**, 626

Possible Correlations in π-μ-e Decay . . . . L. Okun' and A. Rudik 520 **32**, 627

Polarization in Reverse Reactions . . . . A. I. Baz' 521 **32**, 628

Polarization of Cerenkov Radiation . . . . A. A. Sokolov and Iu. M. Loskutov 523 **32**, 630

SOVIET PHYSICS JETP VOLUME 5, NUMBER 3 OCTOBER, 1957

CONTENTS

Russian Reference

Announcement 345
Grigorii Samuilovich Landsberg 345 32, 409
Spectrum and Positive Excess of the Hard Component in the $(0.3 - 17) \times 10^9$ ev/c Momentum Range at an Altitude of 3250 Meters . . . . A. I. Alikhanian and A. O. Vaisenberg 349 32, 413
Momentum Spectrum of the Cosmic Radiation and the Positive Excess in the $(0.1 - 2.5) \times 10^9$ ev/c Range at an Altitude of 3250 m . . . . . . A. O. Vaisenberg 352 32, 417
Energy and Angular Distribution of Neutrons Emitted in the $Be^9(d, n)B^{10}$ Reaction . . . . A. I. Shpetnyi 357 32, 423
Neutron Emission by Excited RaD Nuclei . . . . A. V. Kogan and L. I. Rusinov 365 32, 432
Elastic and Quasi-Elastic Scattering of 660 Mev Protons by Deuterons G. A. Leksin 371 32, 440
Elastic Scattering of 360 Mev Positive π-mesons by Protons . . . . N. A. Mitin and E. L. Grigor'ev 378 32, 445
Loss of Two Electrons in Single Collisions Between Negative Hydrogen Ions and Molecules of Gases . . . . Ia. M. Fogel', V. A. Ankudinov, and R. E. Slabospitskii 382 32, 453
Energy Spectrum of μ-Mesons in Extensive Atmospheric Cosmic Ray Showers . . . . O. I. Dovzhenko, B. A. Nelepo, and S. I. Nikol'skii 391 32, 463
Heat Capacity of Laminar Lattices at Low Temperatures. . . . . E. S. Itskevich and P. G. Strelkov 394 32, 467
Charge Invariance in Nuclear Reactions. . . . . A. I. Baz' 403 32, 478
The Energy Spectrum of Cascade Electrons in Lead . . . . I. P. Ivanenko 413 32, 491
Characteristic Frequencies and Amplitudes of Free Normal Oscillations in KCl Crystals . . . . T. I. Kucher 418 32, 498
Some Relativistic Properties of the Behavior of Spin-$\frac{1}{2}$ Particles . . . . P. E. Kunin and I. M. Taksar 426 32, 506
On Low-Frequency Oscillations in the Plasmas of Electronegative Gases . . . . M. V. Koniukov 429 32, 510
Contribution to the Theory of Collective Motion of Particles in Quantum Mechanical Systems . . . . V. M. Eleonskii and P. S. Zyrianov 432 32, 515
Electrical, Optical and Elastic Properties of Diamond Type Crystals. I . . . . V. S. Mashkevich and K. B. Tolpygo 435 32, 520
Calculation of the Drift Velocity of Ions in the Electric Field in Their Gas . . . . V. I. Perel' 440 32, 526
Contribution to Field Theory Involving a Cut-Off Factor . . . . D. A. Kirzhnits 445 32, 534
Production of Proton-Antiproton Pairs by High Energy γ-Quanta . . . Iu. A. Vdovin 452 32, 542
On the Absorption of High Energy Nuclear-Active Particles . . . . S. Z. Belen'kii and N. M. Gerasimova 456 32, 547
On the Possibility of Formulating a Meson Theory with Several Fields. . . . . A. D. Galanin 460 32, 552
Skin Effect in Thin Films and Wires . . . . B. M. Bolotovskii 465 32, 559
Concerning Some Possibilities of Formulation of a Relativistically Invariant Theory of Extended Particles . . . . V. S. Barashenkov 470 32, 566
Electron-Loss Probabilities for Multiply-Charged Ions . . . . I. S. Dmitriev 473 32, 570
Inelastic Proton-Proton Scattering . . . . Iu. I. Kulakov 477 32, 576
The Application of the Microcanonical Distribution to the Statistical Theory of Multiple Production of Particles . . . . . . V. B. Magalinskii and Ia. P. Terletskii 483 32, 584
Reconstruction of the Scattering Matrix of a Two-Nucleon System . . . . L. Puzikov, R. Ryndin and Ia. Smorodinskii 489 32, 592

(Contents continued on inside back cover)